

Impacts of emerging contaminants and their ecotoxicological consequences

Edited by

Xuchun Qiu, Yuji Oshima, Kun Chen and Yohei Shimasaki

Coordinated by

Yanhong Shi

Published in

Frontiers in Marine Science



FRONTIERS EBOOK COPYRIGHT STATEMENT

The copyright in the text of individual articles in this ebook is the property of their respective authors or their respective institutions or funders. The copyright in graphics and images within each article may be subject to copyright of other parties. In both cases this is subject to a license granted to Frontiers.

The compilation of articles constituting this ebook is the property of Frontiers.

Each article within this ebook, and the ebook itself, are published under the most recent version of the Creative Commons CC-BY licence. The version current at the date of publication of this ebook is CC-BY 4.0. If the CC-BY licence is updated, the licence granted by Frontiers is automatically updated to the new version.

When exercising any right under the CC-BY licence, Frontiers must be attributed as the original publisher of the article or ebook, as applicable.

Authors have the responsibility of ensuring that any graphics or other materials which are the property of others may be included in the CC-BY licence, but this should be checked before relying on the CC-BY licence to reproduce those materials. Any copyright notices relating to those materials must be complied with.

Copyright and source acknowledgement notices may not be removed and must be displayed in any copy, derivative work or partial copy which includes the elements in question.

All copyright, and all rights therein, are protected by national and international copyright laws. The above represents a summary only. For further information please read Frontiers' Conditions for Website Use and Copyright Statement, and the applicable CC-BY licence.

ISSN 1664-8714
ISBN 978-2-8325-6545-2
DOI 10.3389/978-2-8325-6545-2

Generative AI statement

Any alternative text (Alt text) provided alongside figures in the articles in this ebook has been generated by Frontiers with the support of artificial intelligence and reasonable efforts have been made to ensure accuracy, including review by the authors wherever possible. If you identify any issues, please contact us.

About Frontiers

Frontiers is more than just an open access publisher of scholarly articles: it is a pioneering approach to the world of academia, radically improving the way scholarly research is managed. The grand vision of Frontiers is a world where all people have an equal opportunity to seek, share and generate knowledge. Frontiers provides immediate and permanent online open access to all its publications, but this alone is not enough to realize our grand goals.

Frontiers journal series

The Frontiers journal series is a multi-tier and interdisciplinary set of open-access, online journals, promising a paradigm shift from the current review, selection and dissemination processes in academic publishing. All Frontiers journals are driven by researchers for researchers; therefore, they constitute a service to the scholarly community. At the same time, the *Frontiers journal series* operates on a revolutionary invention, the tiered publishing system, initially addressing specific communities of scholars, and gradually climbing up to broader public understanding, thus serving the interests of the lay society, too.

Dedication to quality

Each Frontiers article is a landmark of the highest quality, thanks to genuinely collaborative interactions between authors and review editors, who include some of the world's best academicians. Research must be certified by peers before entering a stream of knowledge that may eventually reach the public - and shape society; therefore, Frontiers only applies the most rigorous and unbiased reviews. Frontiers revolutionizes research publishing by freely delivering the most outstanding research, evaluated with no bias from both the academic and social point of view. By applying the most advanced information technologies, Frontiers is catapulting scholarly publishing into a new generation.

What are Frontiers Research Topics?

Frontiers Research Topics are very popular trademarks of the *Frontiers journals series*: they are collections of at least ten articles, all centered on a particular subject. With their unique mix of varied contributions from Original Research to Review Articles, Frontiers Research Topics unify the most influential researchers, the latest key findings and historical advances in a hot research area.

Find out more on how to host your own Frontiers Research Topic or contribute to one as an author by contacting the Frontiers editorial office: frontiersin.org/about/contact

Impacts of emerging contaminants and their ecotoxicological consequences

Topic editors

Xuchun Qiu — Jiangsu University, China
Yuji Oshima — Kyushu University, Japan
Kun Chen — Jiangsu University, China
Yohei Shimasaki — Kyushu University, Japan

Topic coordinator

Yanhong Shi — Jiangsu University, China

Citation

Qiu, X., Oshima, Y., Chen, K., Shimasaki, Y., Shi, Y., eds. (2025). *Impacts of emerging contaminants and their ecotoxicological consequences*. Lausanne: Frontiers Media SA. doi: 10.3389/978-2-8325-6545-2

Table of contents

- 05 **Editorial: Impacts of emerging contaminants and their ecotoxicological consequences**
Xuchun Qiu, Kun Chen, Yohei Shimasaki and Yuji Oshima
- 07 **Life cycle exposure to 2-phenylbenzimidazole-5-sulfonic acid disrupts reproductive endocrine system and induces transgenerational adverse effects in zebrafish**
Junyan Tao, Qinyuan Yang, Xiaowei Sun, Linxuan Tian, Yuanzhi Deng, Yumei Wang, Weiwei Wang and Xiaoming Fan
- 18 **Microplastics and heavy metals in the sediment of Songkhla Lagoon: distribution and risk assessment**
Siriporn Pradit, Prakrit Noppradit, Kittiwara Sornplang, Preyanuch Jitkaew, Thawanrat Kobkethawin, Thongchai Nitirutsuwan and Dudsadee Muenhor
- 33 **Ecotoxicological consequences of polystyrene naturally leached in pure, fresh, and saltwater: lethal and nonlethal toxicological responses in *Daphnia magna* and *Artemia salina***
Maranda Esterhuizen, Sang-Ah Lee, Youngsam Kim, Riikka Järvinen and Young Jun Kim
- 42 **Erratum: Ecotoxicological consequences of polystyrene naturally leached in pure, fresh, and saltwater: lethal and nonlethal toxicological responses in *Daphnia magna* and *Artemia salina***
Frontiers Production Office
- 43 **Effects of two typical quinolone antibiotics in the marine environment on *Skeletonema costatum***
Yuxin Lin, Tiejun Li and Yurong Zhang
- 54 **Are microplastics efficient remediation tools for removing the statin Lipitor? A laboratory experiment with meiobenthic nematodes**
Bayan M. Aldraiwish, Maha M. Alaqeel, Nawal Al-Hoshani, Sadin Özdemir, Octavian Pacioglu, Marian Necula, Eduard C. Milea, Amor Hedfi, Hassan A. Rudayni and Fehmi Boufahja
- 66 **Foraminiferal detoxification breakdown induced by fatal levels of TiO₂ nanoparticles**
Yuka Inagaki, Yoshiyuki Ishitani, Akihiro Tame, Katsuyuki Uematsu, Naotaka Tomioka, Takayuki Ushikubo and Yurika Ujiié
- 78 **Trophic transfer of PFAS potentially threatens vulnerable Saunders's gull (*Larus saundersi*) via the food chain in the coastal wetlands of the Yellow Sea, China**
Dini Zhang, Wei Liu, Yu Xin, Xiaoshou Liu, Zhenhua Zhang and Yan Liu

- 89 **A study on the transfer of radionuclides and of the resulting radiation dose assessment for marine organisms on the eastern coast of Yantai city**
Jialin Ni, Dongjun Chen, Zhen Qian, Jing Lin, Feng Lin, Jianda Ji, Dekun Huang and Tao Yu
- 102 **Biological effects of munition left on sunken war ships in the North Sea: a multi-biomarker study using caged blue mussels and fish caught at WWII wreck sites at the Belgian coast**
Franziska Isabell Binder, Lillian Tabea Hannah Bünning, Jennifer Susanne Strehse, Sven Van Haelst, Maarten De Rijcke, Edmund Maser and Matthias Brenner



OPEN ACCESS

EDITED AND REVIEWED BY
Ilaria Corsi,
University of Siena, Italy

*CORRESPONDENCE
Xuchun Qiu
✉ xuchunqiu@ujs.edu.cn

RECEIVED 25 May 2025

ACCEPTED 30 May 2025

PUBLISHED 10 June 2025

CITATION

Qiu X, Chen K, Shimasaki Y and
Oshima Y (2025) Editorial: Impacts
of emerging contaminants and their
ecotoxicological consequences.
Front. Mar. Sci. 12:1634908.
doi: 10.3389/fmars.2025.1634908

COPYRIGHT

© 2025 Qiu, Chen, Shimasaki and Oshima. This
is an open-access article distributed under the
terms of the [Creative Commons Attribution
License \(CC BY\)](#). The use, distribution or
reproduction in other forums is permitted,
provided the original author(s) and the
copyright owner(s) are credited and that the
original publication in this journal is cited, in
accordance with accepted academic
practice. No use, distribution or reproduction
is permitted which does not comply with
these terms.

Editorial: Impacts of emerging contaminants and their ecotoxicological consequences

Xuchun Qiu^{1,2*}, Kun Chen¹, Yohei Shimasaki³ and Yuji Oshima^{3,4}

¹School of the Environment and Safety Engineering, Jiangsu University, Zhenjiang, Jiangsu, China,

²Jiangsu Collaborative Innovation Center of Technology and Material of Water Treatment, Suzhou University of Science and Technology, Suzhou, China, ³Laboratory of Marine Environmental Science, Faculty of Agriculture, Kyushu University, Fukuoka, Japan, ⁴Institute of Nature and Environmental Technology, Kanazawa University, Kanazawa, Japan

KEYWORDS

emerging contaminants, aquatic species, biological responses, toxic mechanisms, ecological consequences

Editorial on the Research Topic

Impacts of emerging contaminants and their ecotoxicological consequences

Emerging Contaminants (ECs) in aquatic ecosystems have garnered global environmental concern with the advancement of detection and monitoring technologies. The increasing number and diversity of ECs have shown multiple impacts on biological systems, biodiversity, and ecosystem function in aquatic environments. Furthermore, adverse effects of ECs, particularly those that occur at environmentally relevant concentrations, may appear only when they co-occur with another stressor. However, knowledge about these impacts on aquatic species is still limited. Therefore, this Research Topic focused on exploring the linkages between exposure to emerging contaminants, the biological responses of aquatic species, and their potential ecological consequences, aiming to enhance our understanding of these critical environmental challenges.

This Research Topic comprises 10 articles covering several aspects of emerging contaminants: the impacts and risk assessment of microplastics and nanoparticles, the toxic mechanisms of PPCPs, and the transfer and amplification of pollutants through the food chain.

For the impacts of microplastics (MPs) and nanoparticles (NPs), [Esterhuizen et al.](#) investigated the ecotoxicological effects of polystyrene (PS) leachates on *Daphnia magna* and *Artemia salina*. Results showed higher mortality in *A. salina* exposed to seawater leachate, and sublethal concentrations triggered elevated antioxidant enzyme activities in both species. The findings underscored the need for monitoring species-specific impacts of MPs and their leachates. [Inagaki et al.](#) investigated the cytotoxic effects of titanium dioxide (TiO₂) NPs on the benthic foraminifer *Ammonia veneta*. The results indicated that TiO₂-NPs at ≥ 5ppm could disrupt the foraminiferal detoxification system.

Studies also provide some new evidence that co-exposure to MPs and chemical contaminants may alter the combined toxicity to aquatic species. [Aldraiwish et al.](#) investigated the multifaceted effects induced by MPs and the statin Lipitor on marine benthic nematodes. Results showed that PVC or Lipitor alone significantly reduced nematode abundance, biomass, and diversity, with higher mortality in microvores and diatom feeders. However, combining PS-MPs with Lipitor attenuated toxicity via physical

adsorption, minimizing negative impacts. The findings suggested PS-MPs as a potential remediation tool by reducing Lipitor bioavailability. Pradit et al. reported the distribution and ecological risks of MPs and heavy metals in sediments of Songkhla Lagoon, Thailand. The results suggested that pollution of MPs and heavy metals exhibited ecological risk factors to both ecosystems and human health, which highlighted the risk of MP-heavy metal co-contamination of aquatic ecosystems.

For the impacts of pharmaceuticals and personal care products (PPCPs), Tao et al. investigated the reproductive consequences of a life cycle exposure to 2-phenylbenzimidazole-5-sulfonic acid (PBSA, an organic UV filter) in zebrafish. Results showed that PBSA exposure could disturb fish reproduction through endocrine-disrupting effects and transgenerational toxicity, emphasizing the necessity for environmental regulations on UV filters. Lin et al. investigated the ecotoxicological effects of quinolone antibiotics (levofloxacin and norfloxacin) on the marine diatom *Skeletonema costatum*, and the results showed that both antibiotics at high concentrations could inhibit algal growth by impairing photosynthesis and inducing oxidative stress.

Studies also suggested that the transfer and amplification of pollutants through the food chain could significantly increase their ecological risks. Zhang et al. analyzed the contamination of 14 per- and polyfluoroalkyl substances (PFAS) in the Saunders's gull (*Larus saundersi*) and its food chain in Yellow Sea coastal wetlands. The results suggested that PFSA could be transferred maternally in *L. saundersi*, with bivalves and polychaetes as the primary contributors to PFAS contamination in food sources. In addition, Ni et al. reported the transfer of radionuclides and radiation dose assessment for marine organisms on the eastern coast of Yantai City. Binder et al. assessed the ecotoxicological impacts of munitions leakage from WWII shipwrecks in the Belgian North Sea using caged blue mussels (*Mytilus edulis*) and fish (*Trisopterus luscus*). Multi-biomarker analysis revealed oxidative stress in mussels and lysosomal membrane destabilization. The findings highlight subcellular toxicity in mussels and underscore the ecological risks of historical munitions in marine environments.

Overall, articles in this Research Topic provide some new insights into the impacts of emerging contaminants and their ecotoxicological consequences. The findings are crucial for the environmental risk assessment of these pollutants. Although there is increasing recognition of the importance of a multi-stressor approach to aquatic ecosystems, there is still a lack of knowledge on this topic, especially regarding the ecological consequences of the combined effects of emerging contaminants and other environmental stresses. Such studies are still needed to achieve a more comprehensive understanding of the potential

ecotoxicological consequences of long-term exposure to emerging contaminants on aquatic species worldwide.

Author contributions

XQ: Writing – review & editing, Writing – original draft. KC: Writing – review & editing. YS: Writing – review & editing. YO: Writing – review & editing.

Funding

The author(s) declare that financial support was received for the research and/or publication of this article. This work was supported by the National Natural Science Foundation of China (Grant No. 32071623).

Acknowledgments

We thank all authors, reviewers, and editors who have contributed to this Research Topic.

Conflict of interest

The authors declare that the research was conducted in the absence of any commercial or financial relationships that could be construed as a potential conflict of interest.

Generative AI statement

The author(s) declare that no Generative AI was used in the creation of this manuscript.

Publisher's note

All claims expressed in this article are solely those of the authors and do not necessarily represent those of their affiliated organizations, or those of the publisher, the editors and the reviewers. Any product that may be evaluated in this article, or claim that may be made by its manufacturer, is not guaranteed or endorsed by the publisher.



OPEN ACCESS

EDITED BY

Xuchun Qiu,
Jiangsu University, China

REVIEWED BY

Mohamed Ahmed Ibrahim Ahmed,
Assiut University, Egypt
Jason T. Magnuson,
University of California, Riverside,
United States

*CORRESPONDENCE

Junyan Tao

✉ junyanwmu@163.com

[†]These authors have contributed equally to this work

RECEIVED 27 August 2023

ACCEPTED 11 October 2023

PUBLISHED 01 November 2023

CITATION

Tao J, Yang Q, Sun X, Tian L, Deng Y, Wang Y, Wang W and Fan X (2023) Life cycle exposure to 2-phenylbenzimidazole-5-sulfonic acid disrupts reproductive endocrine system and induces transgenerational adverse effects in zebrafish.
Front. Mar. Sci. 10:1283816.
doi: 10.3389/fmars.2023.1283816

COPYRIGHT

© 2023 Tao, Yang, Sun, Tian, Deng, Wang, Wang and Fan. This is an open-access article distributed under the terms of the [Creative Commons Attribution License \(CC BY\)](https://creativecommons.org/licenses/by/4.0/). The use, distribution or reproduction in other forums is permitted, provided the original author(s) and the copyright owner(s) are credited and that the original publication in this journal is cited, in accordance with accepted academic practice. No use, distribution or reproduction is permitted which does not comply with these terms.

Life cycle exposure to 2-phenylbenzimidazole-5-sulfonic acid disrupts reproductive endocrine system and induces transgenerational adverse effects in zebrafish

Junyan Tao^{1*†}, Qinyuan Yang^{1†}, Xiaowei Sun¹, Linxuan Tian¹, Yuanzhi Deng², Yumei Wang², Weiwei Wang¹ and Xiaoming Fan³

¹School of Public Health, The Key Laboratory of Environmental Pollution Monitoring and Disease Control, Ministry of Education, Guizhou Medical University, Guiyang, China, ²Clinical Medical College, Guizhou Medical University, Guiyang, China, ³Department of Human Anatomy, School of Basic Medicine, Guilin Medical University, Guangxi Zhuang Autonomous Region, Guilin, China

Global attention has been focused on organic UV filters due to their ubiquity and potential damage to aquatic environment, yet the effects of their life cycle exposure on fish reproduction remain unknown. In the present study, the influence of 2-phenylbenzimidazole-5-sulfonic acid (PBSA) exposure on the reproductive endocrine system of zebrafish was examined, from 6 hours post fertilization (hpf) until 150 days, at levels that near-environmentally relevant (0 to 20 µg/L). Our results showed that exposure to PBSA at 20 µg/L caused a slight decrease in the Gonadosomatic Index (GSI) of female zebrafish in the F0 generation. Furthermore, this exposure had a negatively effect on reproduction, accompanied by delayed oocyte maturation, reduced cumulative egg production and decreased fertilization rate. Additionally, offspring embryos displayed reduced egg diameter at 0.75 hpf, delayed cumulative hatching rate at 60 hpf, and increased deformities rate at 72 hpf, indicating an adverse transgenerational effect. Moreover, PBSA exposure was associated with decreased plasma levels of sex hormones of 17β-estradiol (E2) and 11-ketotestosterone (11-KT), as well as altered the transcriptional profiles of certain genes in the HPG (hypothalamic–pituitary–gonadal) and liver axis. Molecular docking (MD) simulations revealed that specific amino acid residues of PBSA interact with zebrafish estrogen receptors, confirming its xenoestrogenic properties. Therefore, exposure to PBSA during its life cycle can disturb fish reproduction through endocrine disruption, thus necessitating strict environmental regulations for the disposal of UV filters to protect ecological and public health.

KEYWORDS

2-phenylbenzimidazole-5-sulfonic acid, life cycle exposure, reproductive endocrine disruption, sex hormones, HPGL axis, transgenerational effects

1 Introduction

Organic ultraviolet (UV) filters are a type of synthetic chemicals that are designed to protect from radiation, mainly acting as a sunscreen to prevent sunburn and skin cancer. They are also employed in personal care products, such as shampoos and cosmetics, and in industrial processes, including anti-freezing, anti-corrosion, and photo-initiator (Carve et al., 2021). Currently, there are around 55 UV filters approved for usage worldwide (Shaath, 2016), with an annually production of over 10,000 tons (Shaath and Shaath, 2005). Reports have indicated that concentrations of benzophenone-3 (BP3) and 2-ethylhexyl-4-methoxycinnamate (EHMC), two common organic UV filters, have been observed in water sources at levels of up to 3,316 µg/L and 19 µg/L, respectively (Balmer et al., 2005; Mitchelmore et al., 2019; Downs et al., 2022; Scheele et al., 2023). As a result of their widespread use, UV filters are released into the environment through wastewater treatment plants (WWTP) and recreational activities, raising growing concerns about potential environmental and human health risks.

In recent years, 2-phenylbenzimidazole-5-sulfonic acid (PBSA) has been used extensively as an organic UV filter in sunscreens and has been found in many aquatic habitats. For example, the concentration of PBSA ranged from 1.3 to 2.3 ng/L in the north-west Kerch Strain, 1.0 to 170 ng/L in the Baltic Sea, and 4490 ng/L in Australian WWTPs (Orlikowska et al., 2015; O'Malley et al., 2020). The highest concentration of PBSA in water was recorded to be over 13 µg/L in outdoor swimming pools in South Bohemia (Grabicova et al., 2013). Though most UV filters, including PBSA, are present in the environment at low concentrations, they can still have the potential biological activity by targeting certain metabolic, enzymatic or cell signaling pathways (Zhang et al., 2017; Huang et al., 2020; Wang et al., 2021). However, there is limited information available on the toxicological effects and associated risks of PBSA. Only one study showed that exposure to environmentally relevant concentration of PBSA can activate certain P450 cytochromes and alter biochemical parameters and enzyme activities in the fish plasma (Grabicova et al., 2013), indicating its potential to disrupt endocrine function. Given that UV filters are now considered as emerging endocrine disrupting chemicals (EDCs) (Ma et al., 2023; Mustieles et al., 2023; Yan et al., 2023), it is critical to evaluate the potential reproductive endocrine disruption effects of life cycle PBSA exposure and its adverse impacts on the development of offspring in aquatic species.

Zebrafish (*Danio rerio*) has been identified as a suitable model for studying the biological effects of EDCs (Guo et al., 2019; Qian et al., 2020). The hypothalamic-pituitary-gonadal and the liver (HPGL) axis is responsible for regulating reproduction in fish, with hormones such as follicle-stimulating hormone (FSH), luteinizing hormone (LH), 11-ketotestosterone (11-KT), estradiol (E2) and multiple molecular targets influencing gametogenesis and maturation (Mo et al., 2021; Yang et al., 2022). Environmental pollutants that interfere with these hormones in the HPGL axis can have a negative effect on fish reproductive processes, as any disruption of the endocrine system is associated with this axis.

However, the consequences of PBSA exposure on fish reproduction and the growth of their offspring are still not fully understood.

Recently, structure-based molecular docking (MD) simulation has been an essential approach for uncovering the molecular mechanisms and structure-toxicity correlations of toxic substances (Shi et al., 2023; Wu et al., 2023). PBSA may activate the steroid hormone pathway via the formation of a ligand-protein complex with estrogen receptors (er α and er β), utilizing the lock-and-key principle as a mechanism, which provides a novel insight into the mechanisms of toxicity *in vivo*. Therefore, the purpose of this study is to identify the amino acids of steroid hormone receptors that can interact with PBSA and generate binding sites. Additionally, it seeks to evaluate the reproductive endocrine disruption potential of PBSA through cumulative egg production, fertilization rate, gonad histopathology analysis, plasma sex hormones levels and expression levels of genes related to the HPGL axis. Furthermore, it will investigate any adverse transgenerational effects, such as the diameter of embryo, cumulative malformation rate and hatching rate in F1 generation, without continued exposure to PBSA. Finally, it will use *in silico* MD technique to forecast the interaction between PBSA and the estrogen receptors of zebrafish. The results of this study will provide a better understanding of the endocrine-disrupting effects of PBSA on reproduction.

2 Materials and methods

2.1 Adult zebrafish maintenance and spawning

Wild-type AB strain zebrafish were used in this study. Healthy adult zebrafish were raised in tanks with a temperature of 28 ± 1°C, a 14:10 light-dark cycle, and a conductivity of 500-1000 µS/cm. Zebrafish were provided with live *Artemia* (Jiahong Feed Co., Ltd., Tianjin, China) twice daily. The night before spawning, zebrafish were placed in tanks with a 1:1 sex ratio (6 males and 6 females per tank). In the morning, light stimulation was used to induce spawning and the embryos were collected within 30 minutes. The embryos were then rinsed in a solution of 0.8 g NaCl, 0.04 g KCl, 0.00358 g Na₂HPO₄, 0.006 g KH₂PO₄, 0.149 g CaCl₂, 0.246 g MgSO₄ 7H₂O, and 0.35 g NaHCO₃, which had been dissolved in 1 liter of ultrapure water (referred to as 'embryo medium'). Normal fertilized embryos were then selected for subsequent experimentation under a SZX12 dissecting microscope (SOPTOP, China), following the established protocol (Kimmel et al., 1995).

2.2 Chemical stock solutions and embryo exposure protocols

PBSA (2-phenylbenzimidazole-5-sulfonic acid, CAS: 27503-81-7, 96% purity) was acquired from Sigma-Aldrich. A stock solution of 200 µg/mL PBSA was prepared in dimethyl sulfoxide (DMSO), and stored in a cool dark environment (4°C) for further dilution. A

working solution of PBSA was prepared by diluting the stock solution to a 10000-fold concentration prior to the experiment. Initially, 60–80 embryos per dish were cultured in a 90 mm petri dish with 30 mL of exposure medium from 6 to 120 hours post fertilization (hpf). Afterwards they were moved to 1 L plastic tanks with a density of 60 larvae/tank until 1 month old. Finally, they were kept in glass tanks (30 cm length × 20 cm width × 20 cm height) with 10–15 fish/tank in 7 L of water until 5 months old, and three parallel tanks were established for each treatment group. Throughout the entire period, the zebrafish were exposed to 0.01% DMSO (control), 0.2, 2 and 20 µg/L PBSA. All exposure solution was renewed daily to maintain a consistent PBSA concentration during the experiment, and the males and females were housed separately. For this study, the PBSA concentration of 20 µg/L was chosen based on two primary considerations. Firstly, PBSA concentrations in water have been reported to be as high as 13 µg/L in outdoor swimming pools a decade ago, which is likely to have increased due to increased attention to sun protection. Secondly, the preliminary experiment showed no gross morphological deformities at a concentration of less than 20 µg/L in an acute test in adults, and this concentration, which is close to the environmental background values, had a mortality rate of less than 5% in an acute test in embryos. Thus, 20 µg/L was decided upon as the high concentration of PBSA.

2.3 An assessment of growth and reproduction of F0 and the development of F1

Ten males and ten females from each treatment group were randomly chosen, anesthetized with ice, and their body length, weight, and gonad weight were measured. Subsequently, the condition factor ($CF = 100 \times [\text{body weight (g)}/\text{total length}^3 (\text{cm})]$) and gonadosomatic index ($GSI = 100 \times [\text{gonad weight (g)}/\text{body weight (g)}]$) were calculated in order to evaluate the effect of PBSA exposure on growth in F0 zebrafish (Tao et al., 2023).

After a 5-month period of exposure, a 1:1 ratio of fish was paired and spawned in corresponding concentrations of exposure solutions to evaluate the effects of PBSA on reproductive capacity and transgenerational effects. Every morning, the eggs spawned were gathered within 30 minutes of the light being switched on and the cumulative egg number laid in the course of 7 days was recorded. Twenty fertilized eggs were randomly chosen from each group to measure the egg diameter at 0.75 hpf. The fertilization rate of the larvae at 6 hpf, the cumulative hatching rate at 60 and 72 hpf, and the cumulative malformation rate at 72 hpf were evaluated using a SOPTOP SZX12 microscope, as described in our previous article (Sun et al., 2023).

2.4 Gonadal hematoxylin-eosin staining

To investigate the impact of life cycle exposure to PBSA on the gonads of adult zebrafish, histopathological examination of the ovaries and testes was performed. Briefly, after anesthetizing

the zebrafish on ice, intact ovaries and testis were dissected and fixed overnight in 4% paraformaldehyde (Cat. No. P1110, Solarbio, China) at 4°C. The samples were then dehydrated in graded ethanol solutions and embedded in paraffin (Cat. Q/YSQN40-91, Shanghai Huayong Paraffin Co., LTD, China), and sectioned (4 µm). Following this, the sections were stained with hematoxylin (Cat. ZLI-9610, Beijing Zhongshan Jinqiao Biotechnology Co., LTD, China) and eosin (Cat. ZLI-9613, Beijing Zhongshan Jinqiao Biotechnology Co., LTD, China) and imaged using a Shunyu EX20 biological microscope (SOPTOP, China). Subsequently, the digital images acquired were analyzed with Image J (version 1.8.0) (Schneider et al., 2012) and the proportion of different developmental stages of germ cells (Ovary: PG, primary growth; EV, early vitellogenic; MV, midvitellogenic; FG, full growth; Testis: SPG, spermatogonia; SPC, spermatocytes; SPD, spermatids) compared to the total germ cell counts were calculated, following the method described in previous studies (Chen et al., 2022).

2.5 Sex steroid hormone measurement in plasma

After a 5-month period of PBSA exposure, the zebrafish were anesthetized with ice and a 3–5 µL blood sample was taken from each fish's tail using a heparinized microcapillary tube and transferred to a 1.5 mL EP tube. This sample was then centrifuged at 12000 g for 15 minutes at 4°C and the upper layer plasma was placed in a pre-chilled EP tube and stored at –80°C for hormone analysis. To prepare the sample for analysis, 10 µL of the supernatant was diluted to 500 µL with ultrapure water (Cat. R1600, Solarbio, China), followed by the addition of 2 mL of diethyl ether used to extract the diluent twice at 2000 g for 30 minutes at 4°C. The extract was evaporated with the aid of a stream of nitrogen and the residue was then dissolved in 350 µL of ELISA buffer. Plasma from five females or males was collected in one tube with three replicates per treatment group. An enzyme-linked immunosorbent assay (ELISA) kits (Cayman Chemical, USA) was then employed to measure the plasma levels of E2 (No. 501890) and 11-KT (No. 582751) according to the manufacturer's instructions.

2.6 RNA isolation and quantitative real-time PCR

Samples of brains, gonads and livers from each treatment group were collected (Supplementary Figure S1), pooled tissues (3 fish/sex per replicate with 3 replicates) were rinsed two times with ice-cold PBS and homogenized with 1 mL TRIzol reagent (Life Technology, USA) using a hand-held grinder (MY-20, Jingxin, China). Total RNA was then extracted following the manufacturer's instructions and quantified and assessed for purity using a MultiskanTMFC (Thermo, USA). The quality and integrity of the RNA were further verified by measuring the ratio of absorbance value 260:280 between 1.9–2.0 and by 1% agarose gel electrophoresis. cDNA was synthesized using Revert Aid First Stand cDNA Synthesis Kit (Thermo, USA). The PCR reaction mixtures were

composed of 5 μ L of TB Green[®] Permix Ex TaqTM II (Til RNaseH Plus) (TaKaRa, Japan), 0.4 μ L of a 10 μ M forward primer, 0.4 μ L of a 10 μ M reverse primer, 0.8 μ L of cDNA and 3.4 μ L of ddH₂O. The PCR was then conducted using the CFX Connect Real-Time PCR Detection System (Bio-rad, USA). Primers for genes were synthesized by Sangon Biotech Co., Ltd. (Shanghai, China). Their sequences are listed in Table 1 and melting curves for all genes are available in Supplementary Figures S2–S4. The thermal cycling reaction was carried out following standard protocols, with 30 s at 95°C, followed by 40 cycles of 5 s at 95°C and 30 s at 60°C. mRNA expression levels were evaluated in three biological replicates for each treatment group. The housekeeping gene β -actin was employed as the internal reference gene to normalize the expression levels of target genes and the fold change was computed using the $2^{-\Delta\Delta CT}$ equation as described in our previous study (Livak and Schmittgen, 2001; Tao et al., 2020).

2.7 Homology modeling and molecular docking

We utilized the protein models of ER α (PDB ID:6CHW) and ER β (PDB ID:7XVY) for homologous modeling using Discovery Studio 2019 software. To identify suitable template proteins, a BLAST search was conducted in the NCBI protein database to compare the sequences of ER α and ER β . MODELLER was then employed to construct the models based on the selected template proteins. The quality of the models was evaluated using a Ramachandran plot, with 90% of residues within the allowed region being the threshold for deeming the model satisfactory (Chen et al., 2021). Molecular docking was also used to identify the active sites of small molecules that interact with protein structures and estimate binding affinity. Cdocker, a semi-flexible docking mode based on CHARMM, was utilized in this process. The protein model obtained from homologous modeling was

dehydrated and the binding pocket was then defined as the receptor. The 3D structures of BP3 (Benzophenone-3, a typical UV filter), BPA (Bisphenol A, a typical endocrine disruptor) and PBSA from the Pubchem database were used as ligands for molecular docking, which was conducted using the Cdocker module in Discovery Studio 2019. The evaluation of the result was based on Cdocker interaction energies, with higher Cdocker interaction energy indicating greater binding affinity between the protein and the ligand (Rampogu et al., 2019).

2.8 Statistical analysis

Data analysis was conducted for normality and homogeneity of variance through the Kolmogorov-Smirnov and Levene's tests respectively, using GraphPad Prism 8.0 software (GraphPad Inc., USA). Non-paired t-test was utilized to assess the statistical differences between the control and PBSA-treated group for each sex. Two-way ANOVA followed by Sidak's multiple comparisons test was used for all other datasets in terms of body weight, body length, CF and GSI. The results were expressed as the mean \pm standard deviation (SD) and statistical significance was set at $P < 0.05$.

3 Results

3.1 PBSA caused a female-biased decrease in GSI value

To evaluate the effects of long-term exposure to PBSA on the development of fish, we measured the growth index including body weight, body length, CF and GSI after 5 months of exposure. The results showed that there were no significant differences in body weight, body length and CF between the treatment groups and the

TABLE 1 Primer sequence for RT-qPCR in this study.

Gene bank number	Gene	Forward primer	Reverse primer	Amplicon
XM_005156973.4	<i>erβ</i>	CGCTCGGCATGGACAAC	CCCATGCGGTGGAGAGTAAT	80 bp
AF349412	<i>erα</i>	ACTCTACCCATGTACCTAAGG	CGGGTAGTATCCCACTGAAGC	151 bp
NM_181439.4	<i>gnrh2</i>	GGTCTCACGGCTGGTATCCT	TGCCTCGCAGAGCTTCACT	89 bp
NM_182888	<i>gnrh3</i>	TTGGAGGTCAGTCTTTGCCAG	CCTCCATTTACCAACGCTTC	76 bp
NM_205622	<i>lhβ</i>	GAGACGGTATCGGTGAAAA	AACAGTCGGGCAGGTAAATG	178 bp
AY424303	<i>fshβ</i>	GTGCAGGACTATGCTGGACA	AGCTCCCCAGTCTGTGTGT	206 bp
NM_205584	<i>17βhsd</i>	AATAGAGGGCGCTTGTGAGA	TCCAGCACCTTGTCTCCAGG	138 bp
NM_131154	<i>cyp19a1a</i>	TCATCGAGGGCTACAACGTG	GATCCGAACGGCTGGAAGAA	151 bp
NM_212720.2	<i>cyp11b</i>	CTGGGCCACACATCGAGAG	AGCGAACGGCAGAAATCC	171 bp
XM_009296387	<i>vtg1</i>	CTCCCAGTTCATTCAGA	ATGACAACTTCACGCAGA	133 bp
NM_001044913.1	<i>vtg2</i>	TACTTTGGGCACTGATGCAA	AGACTTCGTGAAGCCCAAGA	152 bp
NM_181601	<i>β-actin</i>	AAGCAGGAGTACGATGAGTC	TGGAGTCCTCAGATGCATTG	238 bp

vehicle control group (Figures 1A–C). However, a female-biased reduction in GSI value was observed in the group exposed to a concentration of 20 $\mu\text{g/L}$ PBSA (Figure 1D).

3.2 PBSA hindered the development of the ovary but not the testis

The stages of adult gonadal germ cell development can be used to assess the condition of the gonads. It is possible that exposure to PBSA across the lifespan may have an impact on the normal development of the female zebrafish ovary, we then assessed the proportion of germ cells at different stages in ovaries or testes. Histological examination results indicated that PBSA had a gender-dependent effect on zebrafish germ cells. Specifically, the proportion of primary growth follicles (PG) in the ovaries was significantly increased in only 20 $\mu\text{g/L}$ PBSA group, while the proportions of both mid vitellogenic follicles (MV) and full grown follicles (FG) were decreased in comparison to the control group (Figures 2A, B, other groups not shown). In contrast, PBSA had little impact on the testes (Figures 2C, D). Consequently, we selected the 20 $\mu\text{g/L}$ exposure concentration for the subsequent experiments.

Moreover, we evaluated the reproductive capability in fish by measuring the cumulative egg number per female over the seven-day period and the fertilization rate during spawning. Our results revealed that PBSA exposure significantly reduced the egg number and significantly impeded the fertilization rate (Figures 2E, F).

3.3 PBSA altered morphology index of offspring embryos

The inhibited gonadal development induced by PBSA might be related to the development of offspring embryos. To assess the influence of PBSA on offspring embryos, a study was conducted in which females exposed to PBSA across their lifespan were mated with males. Results showed that the egg diameter of the 0.75 hpf F1 embryos was visibly reduced compared to the vehicle control group (Figures 3A, B). The cumulative hatching rate was delayed at 60 hpf, but restored at 72 hpf (Figure 3C). However, the malformation rate was considerably higher at 72 hpf (Figure 3D), with deformities such as pericardial edema (PE), yolk-sac edema (YSE) and bent spine (BS) observed in F1 (Supplementary Figure S5).

3.4 PBSA disrupted plasma sex steroid hormone levels

To investigate the possibility of endocrine disruption and reproductive dysfunction caused by an imbalance in sex hormones, we tested the plasma sex hormone levels. Results from ELISA analyses revealed that the plasma levels of E2 and 11-KT were significantly decreased in the PBSA exposure group compared to the control group for both male and female zebrafish (Figures 4A, B). Notably, the decrease in E2 and 11-KT levels was more pronounced in females, indicating that PBSA had a greater effect on them.

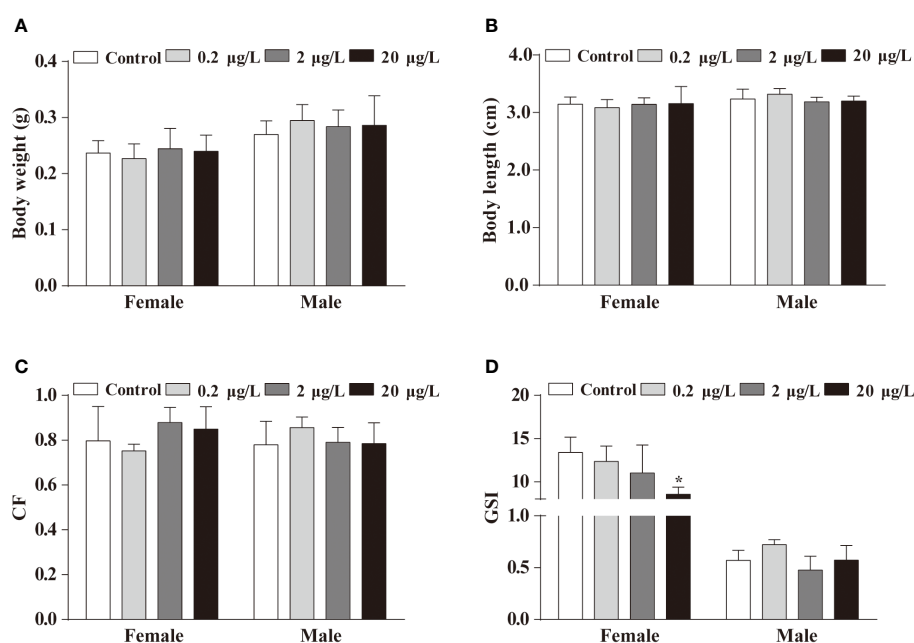


FIGURE 1

Effects of life cycle exposure to PBSA on the growth of adult zebrafish. (A, B) Body weight (A) and body length (B) of adult zebrafish after life cycle exposure to PBSA. (C) Condition factor indices in adult zebrafish. (D) Zebrafish gonadosomatic index. Values plotted are mean \pm SEM. * $P < 0.05$ indicate significant differences between the control and exposure groups.

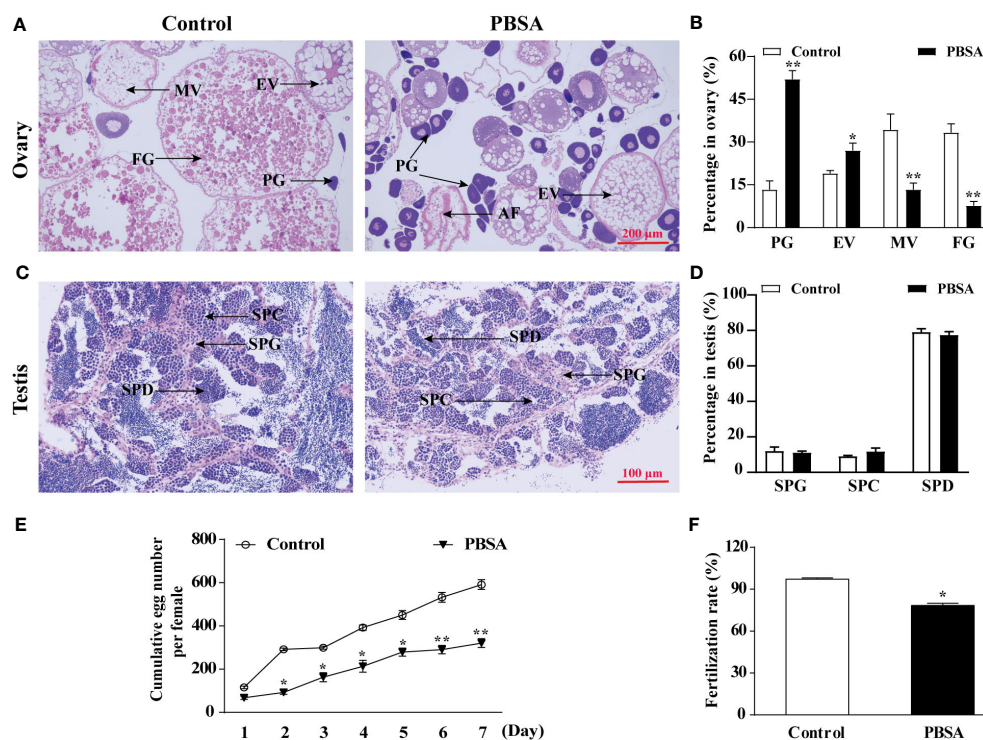


FIGURE 2

Effects of PBSA on reproduction of adult zebrafish. (A) Representative images of ovaries of adult zebrafish stained with hematoxylin-eosin (H&E) (PG, primary growth follicles; EV, early vitellogenic follicles; MV, midvitellogenic follicles; FG, full grown follicles). (B) Percentage of oocyte in ovaries at different stages. (C) Representative images of testis of adult zebrafish stained with H&E (SPG, spermatogonia; SPC, spermatocytes; SPD, spermatids). (D) Percentage of testis cells in testis at different stages. (E) Cumulative egg numbers per female over 7 days after life cycle exposure to PBSA ($n = 3 \times 3$; 3 repeats with 3 female/3 male fish per repeat). (F) Fertilization rate ($n = 3 \times 3$; 3 repeats with 3 female/3 male fish per repeat). Values plotted are mean \pm SD. * $P < 0.05$, and ** $P < 0.01$ indicate significant differences from the vehicle control.

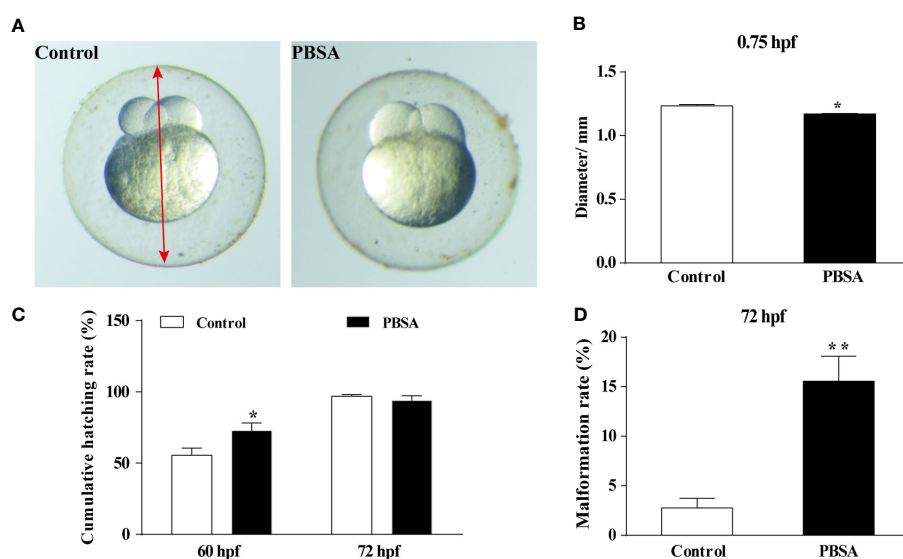


FIGURE 3

Effects of PBSA on the development of embryos in F1 generation. (A) Representative image of F1 generation embryos at 0.75 hpf, with the red arrow denoting the egg diameter. (B) Egg diameter of embryos at 0.75 hpf ($n = 3 \times 20$). (C) Cumulative hatching rate of F1 generation embryos at 60 and 72 hpf ($n = 3 \times 20$). (D) Cumulative malformation rate of F1 generation embryos in 72 hpf ($n = 3 \times 20$). Values plotted are mean \pm SD. * $P < 0.05$, and ** $P < 0.01$ indicate significant differences from the vehicle control.

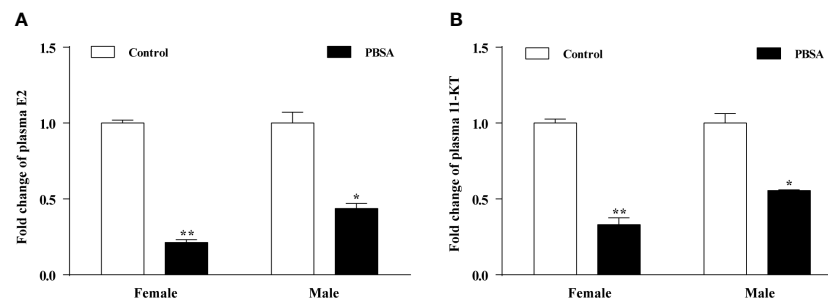


FIGURE 4

Effects of PBSA on the plasma sex steroid hormone levels in adult zebrafish. E2 (A), 11-KT (B). Values plotted are mean \pm SD. * P < 0.05, and ** P < 0.01 indicate significant differences from the vehicle control.

3.5 PBSA altered the expression levels of genes along HPGL axis in zebrafish

We further explored the mechanisms of reproductive impairment in zebrafish caused by PBSA, by measuring the expression levels of selected genes along the HPGL axis in the brain, gonad, and liver of zebrafish after long-term exposure to PBSA (Supplementary Figure S6). In the brain, the expression levels of both *erα* and *erβ* were significantly increased in female zebrafish, whereas *erα* decreased and *erβ* remained unchanged in male zebrafish. Furthermore, *gnrh2* expression was significantly increased in both female and male zebrafish, while *gnrh3*, *lhβ* and *fshβ* expression levels were only increased in female zebrafish, with fewer transcriptional changes observed in males (Figures 5A, B). In the ovary, the expression levels of *17βhsd*, *cyp19a1a* and *cyp11b* were all significantly decreased in the PBSA exposure group compared to the control group (Figure 5C). In the testis, excluding *17βhsd*, the expression levels of the *cyp19a1a* and

cyp11b were significantly decreased in the treatment group (Figure 5D). In the liver, *vtg1* and *vtg2* genes were down-regulated in females but up-regulated in males (Figures 5E, F), demonstrating a gender-dependent response to PBSA exposure.

3.6 Molecular docking analysis

A BLAST comparison of protein sequences in the NCBI database was conducted, which identified sequences with 94.7% sequence identity and similarity in ERα and ERβ respectively, to be used as templates for homologous modelling. Ramachandran analysis of the protein structure revealed that the amount of ERα and ERβ residues in the allowed region was 99.5% (Supplementary Figures S7A, B), indicating that the protein structure was constructed effectively.

The results of the molecular docking and Cdocker interaction energy evaluation of three compounds (BP3, BPA, and PBSA) with

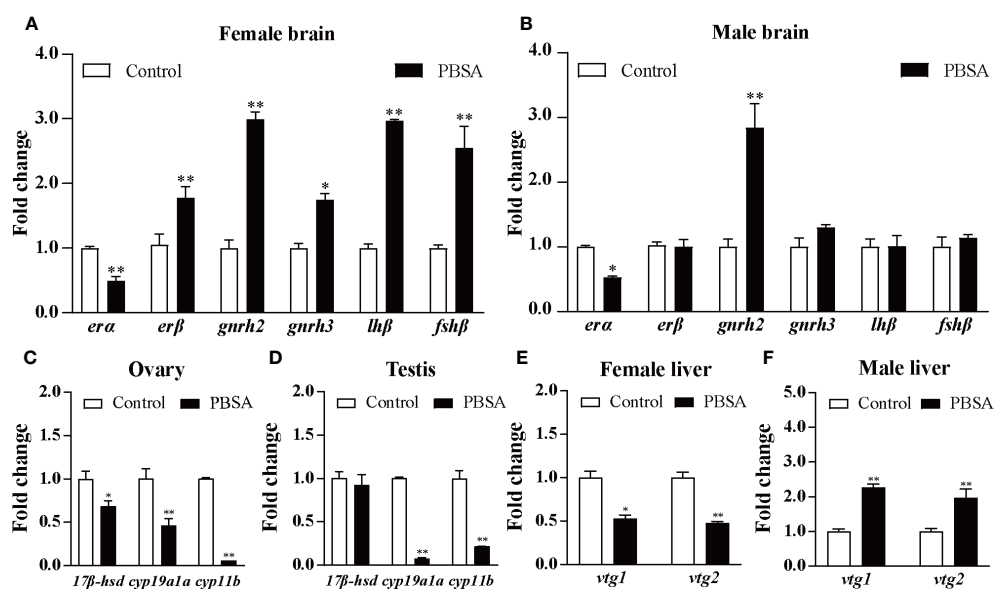


FIGURE 5

Effects of life cycle exposure to PBSA on the expression levels of genes in zebrafish brains (A, B), gonads (C, D), and livers (E, F). Values plotted are mean \pm SD. * P < 0.05 and ** P < 0.01 indicate significant differences from the vehicle control.

both ER α and ER β (as shown in Figures 6A, B; details displayed in Supplementary Figure S8) indicate that BP3 has an interaction energy of 32.84 kcal/mol with ER α and 17.69 kcal/mol with ER β . BPA has an interaction energy of 39 kcal/mol with ER α and 20.43 kcal/mol with ER β , whereas PBSA has an interaction energy of 26.89 kcal/mol with ER α and 12.96 kcal/mol with ER β (Table 2). All three compounds appear to possess similar binding affinities to ER α and ER β . Moreover, other significant parameters such as structure, interacting amino-acid residues number and cdocker energy are also presented in Table 2.

4 Discussion

This study explored the effects of life cycle exposure to PBSA at near-environmentally relevant concentrations on the reproductive potential of zebrafish and the development of their offspring embryos, as well as the possible underlying mechanisms. The finding showed that PBSA inhibited oocyte maturation, decreased the levels of steroid sex hormones in the plasma, reduced fecundity, and caused malformations and growth inhibition in the F1 generation. The changes in the transcriptional profiles of genes in the HPGL axis, along with molecular docking results, provide further insight into the potential mechanisms of PBSA-induced reproductive endocrine disruption. It is suggested that PBSA exposure has a detrimental effect on female fertility and the development of their offspring, which may could lead to a decline in fish populations.

To investigate the potential impacts of life cycle exposure to PBSA on the growth and development of zebrafish, we employed a concentration range (0.2–20 μ g/L) that is near-environmentally relevant. The results indicated that only the highest concentration of PBSA (20 μ g/L) caused a decrease in the GSI of female fish,

suggesting a potential inhibition of ovarian development and reproductive dysfunction in female zebrafish. GSI has been used as an indicator of sexual maturity and reproductive potential in fish (Huang et al., 2019; Quintaneiro et al., 2019). To further investigate this, histological analysis of the ovaries was conducted. The results showed that after exposure to 20 μ g/L of PBSA, the proportion of follicles in the primary growth and early vitellogenic stages was increased, while the full grown follicle was decrease. This ovary inhibition could affect the female reproduction since the ovary is the major reproductive organ for females. Therefore, we evaluated the cumulative egg number and fertilization rate and found that they were significantly lower than the control group, indicating that PBSA is toxic to ovary development and may impede female reproduction. A similar decrease in ovary development and fecundity in fish was observed after exposure to benzophenonic UV filter BP2 and BP3 (Weisbrod et al., 2007; Tao et al., 2023). Further research is needed to uncover and explore the molecular mechanism responsible for ovarian inhibition when exposed to PBSA.

In vertebrates, gonadal development is mainly regulated by the HPG axis, which can control the levels of sex hormones. GnRH from the hypothalamus stimulates the pituitary gland to secrete gonadotropins such as LH and FSH, which then interact with FSH and LH receptors on the gonads to initiate steroidogenesis and gametogenesis (Chen et al., 2022). In our study, life cycle exposure to PBSA was found to decrease the concentration of steroid sex hormones (11-KT, E2) in the plasma, suggesting a disruption of the HPG axis. In the brain, the transcription of *gnrh2*, *lh β* and *fsh β* genes was increased in females, possibly as a result of a negative feedback mechanism to enhance the pituitary's sensitivity and the subsequent secretion of higher levels of gonadotrophins to compensate for the decreased steroid sex hormones after PBSA treatment. Further investigation is needed to gain better

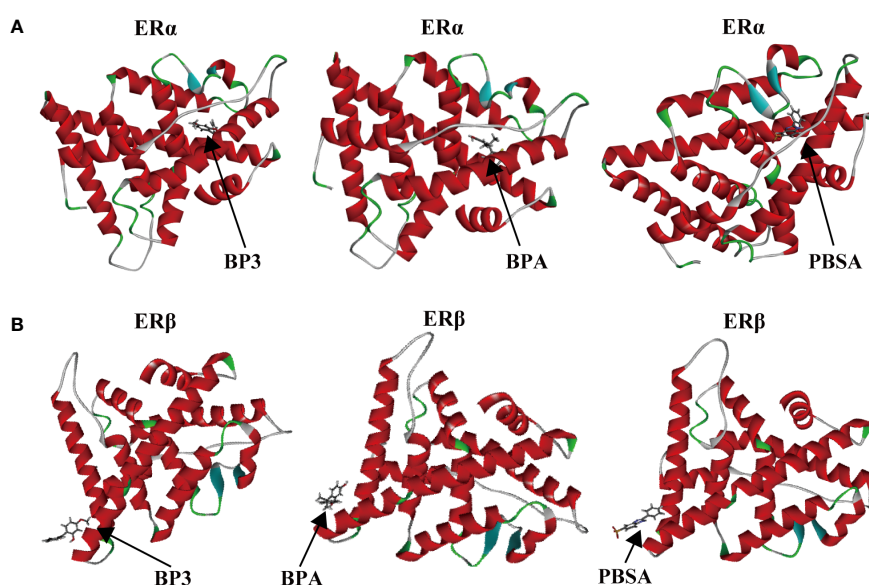





FIGURE 6

Binding modes between chemicals (BP3, BPA, and PBSA) and target proteins (ER α and ER β). BP3-ER α , BPA-ER α , PBSA-ER α (A); BP3-ER β , BPA-ER β , PBSA-ER β (B).

TABLE 2 Binding energy of molecular docking.

Ligand	Structure	Interacting amino-acid residues number		Cdocker energy (kcal/mol)		Cdocker interaction energy (kcal/mol)	
		ER α	ER β	ER α	ER β	ER α	ER β
BP3		19	7	21.90	6.80	32.84	17.69
BPA		19	7	32.83	14.32	39.00	20.43
PBSA		19	6	9.02	0.29	26.89	12.96

understanding of this. In the gonad, the transcription of *17 β hsd*, *cyp19a1a*, and *cyp11b*, which are enzymes responsible for the conversion of cholesterol to testosterone (T), the transformation of T to E2, and the transformation of T to 11-KT respectively (Dang et al., 2015; Yang et al., 2022), were observed to be reduced. This could be the cause of the decrease in plasma 11-KT and E2 levels observed in the PBSA treatments. Furthermore, the decrease of E2 in the treatment group could be partially attributed to the suppression of T. Taken together, the transcription of genes related to reproduction in the HPG axis was suppressed, resulting in a decrease in the levels of E2 and 11-KT. This, in turn, may have hindered gamete maturation and consequently leading to a diminished reproductive capacity of the adult zebrafish.

The elevated expression levels of steroid receptors (ER α and ER β) in females indicated a strong xenoestrogenic behavior of PBSA. To confirm the results, an *in silico* molecular docking of zebrafish estrogen receptors was conducted, which revealed that PBSA had the strongest binding affinity to ER α and ER β , similar to the typical endocrine disruptors BP3 and BPA. This was in agreement with a previous study which found that PPCPs had the strongest binding energies to ER α and ER β (Hamid et al., 2022). Therefore, *in silico* MD has determined that PBSA may act as a xenoestrogen, mimicking the roles of natural ligands and thus disrupting the normal functioning of the HPGL axis.

Fish follicles secrete estradiol, prompting the liver to create the vitellogenin (vtg), a yolk protein, and initiating oocyte maturation and yolk biosynthesis. This yolk is subsequently stored and processed by the maturing oocyte to supply nourishment for the progeny, as described by Brion et al. (Brion et al., 2004; Yuan et al., 2013). The reduction of E2 concentration in the plasma after PBSA exposure may be partially accountable for the decreased expression of the *vtg1* and *vtg2* genes in the livers of females. Taking into account the fact female zebrafish are responsible for supplying the majority of nutrients for the F1 generation embryos (Yang et al., 2022), the inhibition of the *vtg1* and *vtg2* genes in females could impede the growth of the ovary and reduce the quality of eggs. As expected, we did find a reduction in egg diameter, abnormal cumulative hatching rate and an increase in malformation rate in

F1 offspring. The same phenomenon was found in zebrafish after exposure to tribromophenol (TBP) for 120 days at concentrations of 0, 0.3 and 3.0 μ g/L, a significant decrease in *vtg1* and *vtg2* expression was observed in the liver of female zebrafish, leading to an increased rate of malformation, reduced survival, and inhibited growth in their F1 larvae (Deng et al., 2010). Consequently, it can be assumed that the decreased *vtg* gene expression and lower plasma levels of sex hormones in female fish are likely to be responsible for the impaired fertility and inhibited growth of the F1 generation in PBSA treated fish. Further investigation is required to determine the potential molecular mechanism.

5 Conclusion

This study explored the reproductive consequences of a life cycle exposure to PBSA at near-environmentally relevant concentrations in zebrafish. Results showed that PBSA inhibited ovary development, resulting in a decrease in cumulative egg number and an increase in the proportion of primary growth follicles. Histological analysis of the gonads, sex hormones and the expression of HPGL axis related genes, particularly *vtg1* and *vtg2*, revealed that the reproductive endocrine disruption caused by PBSA was predominantly female-biased. This reproductive endocrine disruption caused a decrease in egg diameter at 0.75 hpf, an alteration in cumulative hatching rate at 60 hpf, and an increase in malformation rate at 72 hpf in the F1 generation. Given these adverse effects on the reproductive endocrine systems, PBSA could potentially cause a decrease in fish populations due to impaired reproductive capacity.

Data availability statement

The original contributions presented in the study are included in the article/Supplementary Material. Further inquiries can be directed to the corresponding author.

Ethics statement

The care and use of zebrafish in this study was approved by the Institutional Animal Care and Use Committee of Guizhou Medical University. The studies were conducted in accordance with the local legislation and institutional requirements. Written informed consent was obtained from the owners for the participation of their animals in this study.

Author contributions

JT: Conceptualization, Funding acquisition, Supervision, Writing – review & editing. QY: Conceptualization, Data curation, Formal Analysis, Investigation, Methodology, Writing – original draft. XS: Data curation, Formal Analysis, Investigation, Writing – original draft. LT: Data curation, Methodology, Writing – original draft. YD: Formal Analysis, Methodology, Writing – original draft. YW: Formal Analysis, Methodology, Writing – original draft. WW: Formal Analysis, Methodology, Writing – original draft. XF: Formal Analysis, Methodology, Writing – original draft.

Funding

The author(s) declare financial support was received for the research, authorship, and/or publication of this article. This study was partly supported by the National Natural Science Foundation of

China (No. 22166014), the Science and Technology Program of Guizhou Province (No. ZK [2023] 292), and the Guizhou Education Department Youth Science and Technology Talents Growth Project (No. KY [2021] 175).

Conflict of interest

The authors declare that the research was conducted in the absence of any commercial or financial relationships that could be construed as a potential conflict of interest.

Publisher's note

All claims expressed in this article are solely those of the authors and do not necessarily represent those of their affiliated organizations, or those of the publisher, the editors and the reviewers. Any product that may be evaluated in this article, or claim that may be made by its manufacturer, is not guaranteed or endorsed by the publisher.

Supplementary material

The Supplementary Material for this article can be found online at: <https://www.frontiersin.org/articles/10.3389/fmars.2023.1283816/full#supplementary-material>

References

- Balmer, M. E., Buser, H. R., Muller, M. D., and Poiger, T. (2005). Occurrence of some organic uv filters in wastewater, in surface waters, and in fish from swiss lakes. *Environ. Sci. Technol.* 39 (4), 953–962. doi: 10.1021/es040055r
- Brion, F., Tyler, C. R., Palazzi, X., Laillet, B., Porcher, J. M., Garric, J., et al. (2004). Impacts of 17beta-estradiol, including environmentally relevant concentrations, on reproduction after exposure during embryo-larval-, juvenile- and adult-life stages in zebrafish (*danio rerio*). *Aquat. Toxicol.* 68 (3), 193–217. doi: 10.1016/j.aquatox.2004.01.022
- Carve, M., Allinson, G., Nugegoda, D., and Shimeta, J. (2021). Trends in environmental and toxicity research on organic ultraviolet filters: a scientometric review. *Sci. Total Environ.* 773, 145628. doi: 10.1016/j.scitotenv.2021.145628
- Chen, X., Zheng, J., Zhang, J., Duan, M., Xu, H., Zhao, W., et al. (2022). Exposure to difenconazole induces reproductive toxicity in zebrafish by interfering with gamete maturation and reproductive behavior. *Sci. Total Environ.* 838 (Pt 1), 155610. doi: 10.1016/j.scitotenv.2022.155610
- Chen, Y., Wang, X., Zhai, H., Zhang, Y., and Huang, J. (2021). Identification of potential human ryanodine receptor 1 agonists and molecular mechanisms of natural small-molecule phenols as anxiolytics. *ACS Omega*. 6 (44), 29940–29954. doi: 10.1021/acsomega.1c04468
- Dang, Y., Giesy, J. P., Wang, J., and Liu, C. (2015). Dose-dependent compensation responses of the hypothalamic-pituitary-gonadal-liver axis of zebrafish exposed to the fungicide prochloraz. *Aquat. Toxicol.* 160, 69–75. doi: 10.1016/j.aquatox.2015.01.003
- Deng, J., Liu, C., Yu, L., and Zhou, B. (2010). Chronic exposure to environmental levels of tribromophenol impairs zebrafish reproduction. *Toxicol. Appl. Pharmacol.* 243 (1), 87–95. doi: 10.1016/j.taap.2009.11.016
- Downs, C. A., Bishop, E., Diaz-Cruz, M. S., Haghshenas, S. A., Stien, D., Rodrigues, A., et al. (2022). Oxybenzone contamination from sunscreen pollution and its ecological threat to hanauma bay, oahu, hawaii, U.S.A. *Chemosphere*. 291 (Pt 2), 132880. doi: 10.1016/j.chemosphere.2021.132880
- Grabicova, K., Fedorova, G., Burkina, V., Steinbach, C., Schmidt-Posthaus, H., Zlabek, V., et al. (2013). Presence of uv filters in surface water and the effects of phenylbenzimidazole sulfonic acid on rainbow trout (*oncorhynchus mykiss*) following a chronic toxicity test. *Ecotox. Environ. Safe.* 96, 41–47. doi: 10.1016/j.ecoenv.2013.06.022
- Guo, Y., Chen, L., Wu, J., Hua, J., Yang, L., Wang, Q., et al. (2019). Parental co-exposure to bisphenol a and nano-tio(2) causes thyroid endocrine disruption and developmental neurotoxicity in zebrafish offspring. *Sci. Total Environ.* 650 (Pt 1), 557–565. doi: 10.1016/j.scitotenv.2018.09.007
- Hamid, N., Junaid, M., Manzoor, R., Duan, J. J., Lv, M., Xu, N., et al. (2022). Tissue distribution and endocrine disruption effects of chronic exposure to pharmaceuticals and personal care products mixture at environmentally relevant concentrations in zebrafish. *Aquat. Toxicol.* 242, 106040. doi: 10.1016/j.aquatox.2021.106040
- Huang, X., Li, Y., Wang, T., Liu, H., Shi, J., and Zhang, X. (2020). Evaluation of the oxidative stress status in zebrafish (*danio rerio*) liver induced by three typical organic uv filters (bp-4, paba and pbsa). *Int. J. Environ. Res. Public Health* 17 (2), 651. doi: 10.3390/ijerph17020651
- Huang, Y., Liu, J., Yu, L., Liu, C., and Wang, J. (2019). Gonadal impairment and parental transfer of tris (2-butoxyethyl) phosphate in zebrafish after long-term exposure to environmentally relevant concentrations. *Chemosphere*. 218, 449–457. doi: 10.1016/j.chemosphere.2018.11.139
- Kimmel, C. B., Ballard, W. W., Kimmel, S. R., Ullmann, B., and Schilling, T. F. (1995). Stages of embryonic development of the zebrafish. *Dev. Dyn.* 203 (3), 253–310. doi: 10.1002/aja.1002030302
- Livak, K. J., and Schmittgen, T. D. (2001). Analysis of relative gene expression data using real-time quantitative pcr and the 2(-delta delta c(t)) method. *Methods*. 25 (4), 402–408. doi: 10.1006/meth.2001.1262
- Ma, J., Wang, Z., Qin, C., Wang, T., Hu, X., and Ling, W. (2023). Safety of benzophenone-type uv filters: a mini review focusing on carcinogenicity,

reproductive and developmental toxicity. *Chemosphere*. 326, 138455. doi: 10.1016/j.chemosphere.2023.138455

Mitchellmore, C. L., He, K., Gonsior, M., Hain, E., Heyes, A., Clark, C., et al. (2019). Occurrence and distribution of uv-filters and other anthropogenic contaminants in coastal surface water, sediment, and coral tissue from hawaii. *Sci. Total Environ.* 670, 398–410. doi: 10.1016/j.scitotenv.2019.03.034

Mo, A., Wang, X., Yuan, Y., Liu, C., and Wang, J. (2021). Effects of waterborne exposure to environmentally relevant concentrations of selenite on reproductive function of female zebrafish: a life cycle assessment. *Environ. pollut.* 270, 116237. doi: 10.1016/j.envpol.2020.116237

Mustieles, V., Balogh, R. K., Axelstad, M., Montazeri, P., Marquez, S., Vrijheid, M., et al. (2023). Benzophenone-3: comprehensive review of the toxicological and human evidence with meta-analysis of human biomonitoring studies. *Environ. Int.* 173, 107739. doi: 10.1016/j.envint.2023.107739

O'Malley, E., O'Brien, J. W., Verhagen, R., and Mueller, J. F. (2020). Annual release of selected uv filters via effluent from wastewater treatment plants in Australia. *Chemosphere*. 247, 125887. doi: 10.1016/j.chemosphere.2020.125887

Orlikowska, A., Fisch, K., and Schulz-Bull, D. E. (2015). Organic polar pollutants in surface waters of inland seas. *Mar. pollut. Bull.* 101 (2), 860–866. doi: 10.1016/j.marpolbul.2015.11.018

Qian, L., Qi, S., Zhang, J., Duan, M., Schlenk, D., Jiang, J., et al. (2020). Exposure to boscalid induces reproductive toxicity of zebrafish by gender-specific alterations in steroidogenesis. *Environ. Sci. Technol.* 54 (22), 14275–14287. doi: 10.1021/acs.est.0c02871

Quintaneiro, C., Soares, A., Costa, D., and Monteiro, M. S. (2019). Effects of pcb-77 in adult zebrafish after exposure during early life stages. *J. Environ. Sci. Health Part A-Toxic/Hazard. Subst. Environ. Eng.* 54 (5), 478–483. doi: 10.1080/10934529.2019.1568793

Rampogu, S., Park, C., Ravinder, D., Son, M., Baek, A., Zeb, A., et al. (2019). Pharmacotherapeutics and molecular mechanism of phytochemicals in alleviating hormone-responsive breast cancer. *Oxid. Med. Cell. Longev.* 2019, 5189490. doi: 10.1155/2019/5189490

Scheele, A., Sutter, K., Karatum, O., Danley-Thomson, A. A., and Redfern, L. K. (2023). Environmental impacts of the ultraviolet filter oxybenzone. *Sci. Total Environ.* 863, 160966. doi: 10.1016/j.scitotenv.2022.160966

Schneider, C. A., Rasband, W. S., and Eliceiri, K. W. (2012). Nih image to imagej: 25 years of image analysis. *Nat. Methods* 9 (7), 671–675. doi: 10.1038/nmeth.2089

Shaath, N. A. (2016). *Principles and Practice of Photoprotection* (Switzerland: Springer International Publishing). doi: 10.1007/978-3-319-29382-0

Shaath, N. A., and Shaath, M. (2005). *Sunscreens: Regulations and Commercial Development*. 3rd ed. (Taylor & Francis).

Shi, Q., Yang, H., Chen, Y., Zheng, N., Li, X., Wang, X., et al. (2023). Developmental neurotoxicity of trichlorfon in zebrafish larvae. *Int. J. Mol. Sci.* 24 (13), 11099. doi: 10.3390/ijms241311099

Sun, X., Yang, Q., Jing, M., Jia, X., Tian, L., and Tao, J. (2023). Environmentally relevant concentrations of organic (benzophenone-3) and inorganic (titanium dioxide nanoparticles) uv filters co-exposure induced neurodevelopmental toxicity in zebrafish. *Ecotox. Environ. Safe.* 249, 114343. doi: 10.1016/j.ecoenv.2022.114343

Tao, J., Bai, C., Chen, Y., Zhou, H., Liu, Y., Shi, Q., et al. (2020). Environmental relevant concentrations of benzophenone-3 induced developmental neurotoxicity in zebrafish. *Sci. Total Environ.* 721, 137686. doi: 10.1016/j.scitotenv.2020.137686

Tao, J., Yang, Q., Jing, M., Sun, X., Tian, L., Huang, X., et al. (2023). Embryonic benzophenone-3 exposure inhibited fertility in later-life female zebrafish and altered developmental morphology in offspring embryos. *Environ. Sci. pollut. Res.* 30 (17), 49226–49236. doi: 10.1007/s11356-023-25843-7

Wang, J., Meng, X., Feng, C., Xiao, J., Zhao, X., Xiong, B., et al. (2021). Benzophenone-3 induced abnormal development of enteric nervous system in zebrafish through mapk/erk signaling pathway. *Chemosphere*. 280, 130670. doi: 10.1016/j.chemosphere.2021.130670

Weisbrod, C. J., Kunz, P. Y., Zenker, A. K., and Fent, K. (2007). Effects of the uv filter benzophenone-2 on reproduction in fish. *Toxicol. Appl. Pharmacol.* 225 (3), 255–266. doi: 10.1016/j.taap.2007.08.004

Wu, L., Zeeshan, M., Dang, Y., Zhang, Y. T., Liang, L. X., Huang, J. W., et al. (2023). Maternal transfer of f-53b inhibited neurobehavior in zebrafish offspring larvae and potential mechanisms: dopaminergic dysfunction, eye development defects and disrupted calcium homeostasis. *Sci. Total Environ.* 894, 164838. doi: 10.1016/j.scitotenv.2023.164838

Yan, Y., Guo, F., Liu, K., Ding, R., and Wang, Y. (2023). The effect of endocrine-disrupting chemicals on placental development. *Front. Endocrinol.* 14. doi: 10.3389/fendo.2023.1059854

Yang, R., Wang, X., Wang, J., Chen, P., Liu, Q., Zhong, W., et al. (2022). Insights into the sex-dependent reproductive toxicity of 2-ethylhexyl diphenyl phosphate on zebrafish (danio rerio). *Environ. Int.* 158, 106928. doi: 10.1016/j.envint.2021.106928

Yuan, H. X., Xu, X., Sima, Y. H., and Xu, S. Q. (2013). Reproductive toxicity effects of 4-nonylphenol with known endocrine disrupting effects and induction of vitellogenin gene expression in silkworm, bombyx mori. *Chemosphere*. 93 (2), 263–268. doi: 10.1016/j.chemosphere.2013.04.075

Zhang, Q., Ma, X., Dzakpasu, M., and Wang, X. C. (2017). Evaluation of ecotoxicological effects of benzophenone uv filters: luminescent bacteria toxicity, genotoxicity and hormonal activity. *Ecotox. Environ. Safe.* 142, 338–347. doi: 10.1016/j.ecoenv.2017.04.027



OPEN ACCESS

EDITED BY

Xuchun Qiu,
Jiangsu University, China

REVIEWED BY

Gabriel-Ionut Plavan,
Alexandru Ioan Cuza University, Romania
Mohamed Mohsen,
Jimei University, China
Lingshi Yin,
Hunan University, China

*CORRESPONDENCE

Prakrit Noppradit

✉ prakrit.n@psu.ac.th

RECEIVED 11 September 2023

ACCEPTED 18 December 2023

PUBLISHED 09 January 2024

CITATION

Pradit S, Noppradit P, Sornplang K, Jitkaew P,
Kobkethawin T, Nitirutsuwan T and
Muenhor D (2024) Microplastics and heavy
metals in the sediment of Songkhla Lagoon:
distribution and risk assessment.
Front. Mar. Sci. 10:1292361.
doi: 10.3389/fmars.2023.1292361

COPYRIGHT

© 2024 Pradit, Noppradit, Sornplang, Jitkaew,
Kobkethawin, Nitirutsuwan and Muenhor. This
is an open-access article distributed under the
terms of the [Creative Commons Attribution
License \(CC BY\)](https://creativecommons.org/licenses/by/4.0/). The use, distribution or
reproduction in other forums is permitted,
provided the original author(s) and the
copyright owner(s) are credited and that the
original publication in this journal is cited, in
accordance with accepted academic
practice. No use, distribution or reproduction
is permitted which does not comply with
these terms.

Microplastics and heavy metals in the sediment of Songkhla Lagoon: distribution and risk assessment

Siriporn Pradit^{1,2}, Prakrit Noppradit^{1,2*}, Kittiwara Sornplang^{1,2},
Preyanuch Jitkaew^{1,2}, Thawanrat Kobkethawin³,
Thongchai Nitirutsuwan⁴ and Dudsadee Muenhor^{5,6,7}

¹Marine and Coastal Resources Institute, Faculty of Environmental Management, Songkhla, Thailand,

²Coastal Oceanography and Climate Change Research Center, Faculty of Environmental
Management, Prince of Songkla University, Songkhla, Thailand, ³Center of Excellence in Catalysis for
Bioenergy and Renewable Chemicals (CBRC), Faculty of Science, Chulalongkorn University,
Bangkok, Thailand, ⁴Faculty of Science and Fisheries Technology, Rajamangala University of
Technology Srivijaya, Trang, Thailand, ⁵Faculty of Environmental Management, Prince of Songkla
University, Songkhla, Thailand, ⁶Health Impact Assessment Research Center, Prince of Songkla
University, Songkhla, Thailand, ⁷Center of Excellence on Hazardous Substance Management (HSM),
Bangkok, Thailand

Heavy metal and microplastic (MP) contamination of aquatic systems is a major environmental issue that affects human health globally. Songkhla lagoon, the largest lagoon in Thailand, also faced with the environmental issues. Here, this study reported the occurrence of heavy metal and MP in 10 sites of sediment in the Songkhla lagoon. From the microplastic separation, fibers were found at all stations at 68.24% (15.15 items/g) and fragments were found at 31.76% (7.05 items/g). The highest number of MP particles was found at the area near the mouth of the lagoon (5.4 items/g). The average concentrations (mg/kg) of heavy metal at all sites showed the following trend: Mg (732.54 ± 247.04) > Mn (176.74 ± 83.68) > Zn (29.36 ± 39.47) > Cu (12.31 ± 24.58) > Pb (11.07 ± 7.60) > As (5.64 ± 3.30) > Co (2.90 ± 1.38) > Cd (0.22 ± 0.17). Regarding the overall risk assessment of MPs in lagoon sediment in this study, the risk was categorized as high for the polymer hazard index. The ecological risk index found Cd and As to have high ecological risk. High EF values were observed for As and Cd, which indicated severe enrichment. Based on the I_{geo} calculation, the majority of sampling stations were unpolluted to moderately contaminated (Pb, Zn, Mg, and Co). Furthermore, there was no significant correlation between MPs and heavy metals, except for Zn ($r = 0.697$) and Cu ($r = 0.61$) (both $p < 0.05$). The results of this study might provide valuable data to develop conservation policies for coastal lagoon areas.

KEYWORDS

trace element, marine debris, risk assessment, coastal, organic matter

1 Introduction

Contamination of the ocean by plastic is a global concern due to its negative effects on marine biota. Microplastics (MPs), first defined by Thompson et al. (2004), are plastic particles smaller than 5 mm in length. MPs are widespread in the environment and in living organisms (Browne et al., 2008; Claessens et al., 2011). MPs tend to accumulate pollutants such as organic pollutants and heavy metals (Bayo et al., 2018; Liu et al., 2022), mostly on the surface of seawater because of their density compared to water. This circumstance may contribute to the interaction between these two pollutants whereby heavy metal is attached or adsorbed to the MP surface (Goh et al., 2022). Heavy metals can enter the human body through various routes of exposure including the gastrointestinal tract, inhalation, and skin contact (Alia et al., 2020). Sediments in coastal lagoon ecosystems play an important role as a major site source and sink for aquatic organisms and also for chemical substances. Sediments tend to act as reservoirs for heavy metals in marine environments and release more heavy metals into seawater when local environmental conditions change, for instance, due to changes in salinity, pH, and redox potential. Sediment therefore acts as both a sink and a source of trace metals (Rajeshkumar et al., 2018). Sediment-associated metals pose a direct risk to detrital and deposit-feeding benthic organisms and may also represent long-term sources of contamination to higher tropic levels (Mendil and Uluözlü, 2007). The distribution and accumulation of heavy metals is influenced by sediment texture, mineralogical composition, reduction/oxidation state, adsorption and desorption processes, and physical transport (Buccolieri et al., 2006). The changes in sediment oxidation/reduction state and pH influence the solubility of both metals and nutrients (Miao et al., 2006). To evaluate the potential heavy metal concentration of lagoons of the surface sediments is very important since it represents the current situation. However, sediment in lagoons or in mangrove areas also acts as a sink for MPs (Cordova et al., 2021; Pradit et al., 2022). MPs and heavy metals are typically classified as different types of pollutants, and the interconnection between them is poorly understood (Goh et al., 2022). To enhance the properties of plastics during the polymer production process, heavy metals are mainly used as additives for colorants, flame-retardants, fillers, and stabilizers. The toxic component of plastic particles increases when the metal concentrations in plastic particles are higher than those found in the water column and the bioavailability of heavy metals adsorbed to MPs is also at a high level (Holmes et al., 2012). This is likely to affect aquatic animals and finally influence human health.

Coastal lagoons are widespread along oceanic coasts globally. Many coastal lagoons are among the most productive aquatic ecosystems. Lagoons frequently have high nutrient concentrations due to both riverine fertilizer imports and efficient nutrient recycling between the sediments and the water column (Baeyens et al., 2005). Moreover, some lagoons have recently been converted to receiving reservoirs for various by-products of human activities such as urbanization, industrialization, and agriculture. These substances may affect the health of benthic and water column organisms. Both heavy metals and MPs can build up in the

environment to high levels and can contaminate food chains as a result. It is therefore crucial to assess the risks posed by MPs and heavy metals to attain a comprehensive understanding of the potential dangers associated with the consumption of MPs and heavy metals by biota. Songkhla Lagoon is the biggest coastal lagoon in Thailand, with a rich biodiversity, but there have been few studies on the heavy metals and MPs in this lagoon. Therefore, the objectives of this study are as follows: 1) to determine the levels of MPs, heavy metals (As, Cd, Pb, Cu, Zn, Mg, Co, and Mn), and sediment-related variables (organic matter, grain size, and pH) in surface sediment; and 2) to assess the potential ecological risk of MPs and heavy metals in surface sediment.

2 Materials and methods

2.1 Sample collection and preparation

The study area is the lower part of Songkhla Lagoon, a shallow coastal lagoon that is Asia's second-largest. This lagoon is located in southern Thailand between 7°08' and 7°50' N and 100°07' and 100°37' E. The lower lagoon is connected to the Gulf of Thailand by a 420 m wide and 9.5 m deep waterway (Sirinawin and Sompongchaiyakul, 2005). It is the largest natural lagoon in Thailand, located on the Malay peninsula in southern Thailand. The complex ecosystem confers Songkhla Lagoon with high biodiversity, including birds along with a rare freshwater dolphin population (Irrawaddy dolphins), while also supporting extensive fisheries. Sediment samples were collected by grab sampling at all 10 stations in the lower part of Songkhla Lagoon in December, 2022 (Figure 1). At each station, three replications were performed. Thereafter, the sediment was kept in clean plastic zip-lock bags (around 500 g of wet weight per replicate). Before the experiment, the sediment samples were separated into two parts. For the first part, samples were left to dry in an oven at 50°C for approximately 48 h. These sediments were used for analyses of MPs, heavy metals (As, Cd, Pb, Cu, Zn, Mg, Co, and Mn), and organic matter. The second part was air-dried and kept for grain size analysis.

2.2 Laboratory analysis

2.2.1 Microplastic analysis

The samples (20 g) were weighed and placed in a beaker. The sediment was then treated with 200 mL of saturated sodium chloride (NaCl) and violently agitated with a glass stirrer before being covered with aluminum foil. The NaCl approach is commonly used to remove MPs from sediments (Wang et al., 2020; Chinfak et al., 2021). The sediments in the beaker were left for 30 min. After this period, 100 ml samples from the beaker were filtered using filter net (20 µm), and 100 ml of NaCl was added into the original beaker again, before being left to stand for another 30 min. This step was repeated three times. After the filtering process, the filter net was rinsed with distilled water and transferred into another beaker. Then, 10 ml of ferrous sulfate (FeSO₄) and hydrogen peroxide (H₂O₂) were added to the filtered samples to

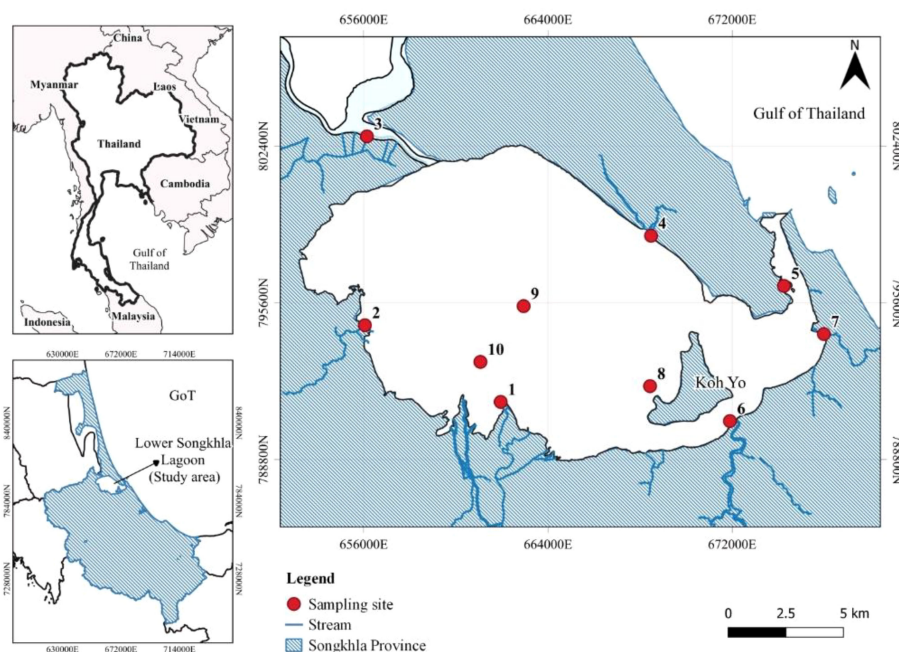


FIGURE 1
Map of the study area and locations of the sampling sites.

digest the organic matter, before covering with aluminum foil and placement on a hot plate for about 1 h for the digestion process. After this period, the filtering process was continued by filtering through GF/C filter paper (1.2 μm), and the filter paper was kept in a Petri dish. After that, all Petri dishes that contained the filter paper were oven-dried at 50°C. The MP particles were then counted and visually observed under a stereomicroscope (Olympus, model SZ61) with a light-emitting diode base. The number of MP particles was recorded, in addition to their color, shape, and size. MPs were divided into three groups: smaller than 500 μm , 500–1000 μm , and larger than 1000 μm . Polymer types of MPs were analyzed using a Fourier transform infrared spectrophotometer (FTIR, Spotlight 200i; Perkin Elmer). Wavelengths in the analysis ranged from 4000 to 400 cm^{-1} . The obtained spectrum was compared to the reference library spectrum of each polymer type.

2.2.2 Heavy metal analysis

Analysis of heavy metals (As, Cd, Pb, Cu, Zn, Mg, Co, and Mn) was carried out by inductively Coupled Plasma Optical Emission Spectrometer (ICP-OES: Perkin Elmer Optima, model 4300 DV), followed the AOAC Official Method (AOAC, 2005). Sediment samples (0.5 g) were placed in a test tube, adding 2 ml of HNO_3 (65%, Merck), and digesting in a water bath at 95°C for approximately 90 min. Then, 0.5 ml of H_2O_2 (30%, Merck) was added and digested for around 30 min in the temperature-controlled water bath, before being allowed to cool at room temperature and filtered through filter paper. The marine sediment-certified reference material was MESS-4. The certified value was within 90% of the analytical value. Three replicates were used to evaluate the efficiency of the analysis. All compounds used

were of analytical grade and all glassware used in the study was submerged in nitric acid overnight (3% HNO_3 , Merck) and then cleaned three times with Milli-Q deionized water before being used.

2.2.3 Sediment characteristic analysis

2.2.3.1 Organic matter

The Walkley-Black method was used to assess the readily oxidizable organic matter content of the sediment samples (Loring and Rantala, 1992). To summarize, dried sediment samples were sieved via a 0.2 mm nonferrous sieve. The dried sediment was then transferred to a 500 mL Erlenmeyer flask. The organic carbon in the sample was then oxidized using 10 mL of 1 N potassium dichromate. To remove the chlorine, a 20 mL mixture of H_2SO_4 and Ag_2SO_4 was added. After 30 min, the mixture was diluted with 200 mL of distilled water. As a catalyst, 10 mL of 85% H_3PO_4 and 0.2 g of NaF were added. The diphenylamine indicator was then added.

2.2.3.2 Sediment grain size analysis

The hydrometer approach was used to analyze particle size (Gee et al., 1986). In brief, around 40 g of air-dried sediment was transferred to a 600 mL beaker and 100 to 150 mL of distilled water was added. Then, to remove organic debris, 30% hydrogen peroxide was continuously applied. The samples were heated on a hot plate at 90°C for 1 h before being incubated in a 105°C oven for 24 h. The silt was then treated with 100 mL of Calgon 5% and 50 mL of distilled water. The samples were sieved using a 63 μm sieve. The filtrate from the sieve was transferred to a 1-L sedimentation cylinder. A plunger was used to scatter the silt in the cylinder, and the density and temperature of the sample were determined

using a hydrometer and a thermometer, respectively. The entire system was allowed to stand for 2 h before the density and temperature were measured again.

2.2.3.3 pH

Measurements of pH of the surface sediments were performed in the field with a combined pH meter (IQ 140 pH). At each station, the pH meter was inserted into the sediment and the value was recorded.

2.3 Data processing and statistical analysis

Statistical analysis was used to calculate the minimum, maximum, mean, and standard deviation using Microsoft Excel. The differences in the number of MP particles among the stations were analyzed by the Kruskal–Wallis method. Pearson's correlation test was performed to determine the relationships between the number of MP particles found in sediment and heavy metal, organic matter, and grain size. A significance level of 0.05 was considered for all analyses.

2.3.1 Microplastic data analysis

2.3.1.1 Polymer hazard index

We examined both the concentration and the chemical composition of MPs in surface sediments to assess the possible hazards of MPs (Xu et al., 2018). The chemical toxicity of certain MP polymer types was taken into account in order to assess the environmental impact (Lithner et al., 2011). The following formula was used to calculate the polymer hazard of MPs (Equation 1):

$$PHI = \sum P_n \times S_n \quad (1)$$

where PHI is the calculated polymer hazard index caused by MP, P_n is the percentage of specific polymer types [polyethylene (PE) score 11; PET score 4] collected at each sampling location, and S_n is the hazard score of the polymer types of MPs derived from a previous study (Lithner et al., 2011).

2.3.2 Heavy metal data analysis

2.3.2.1 Enrichment factor

The sediment enrichment factor (EF) is an important index reflecting the degree of human activity regarding the accumulation of elements in the environment. It is determined by comparing the measured values with those of the control area (Han et al., 2023). Fe is commonly used as a reference element because it is a naturally abundant element (Al-Wabel et al., 2017). The enrichment factors of heavy metals were calculated using Equation (2):

$$EF = (C_n/C_{Fe})_{\text{Sediment}} / (C_i/C_{Fe})_{\text{Background}} \quad (2)$$

where $(C_n/C_{Fe})_{\text{Sediment}}$ is the ratio of the concentration of metal in the sample to the concentration of Fe and $(C_i/C_{Fe})_{\text{Background}}$ is the ratio of the concentration of metal in the background to the concentration of Fe (Bayrakli et al., 2023).

The soil background values of various trace metals in the study area were not available. Thus, the geochemical background values from offshore sediments in the Gulf of Thailand from a previous

study (Taylor and McLennan, 1995) were taken as reference values in this study. The background concentrations were 12,200 µg/g for Fe, 12.7 µg/g for Cu, 15 µg/g for Pb, 104 µg/g for Mn, 10 µg/g for Co, 20 µg/g for Ni, 1.5 µg/g for As, 0.098 µg/g for Cd, 71 µg/g for Zn, and 13,300 µg/g for Mg (Taylor and McLennan, 1995; Shazili et al., 1999). Ekissi et al. (2021) divided contamination into different categories based on EF values: no enrichment ($EF < 1$); minor enrichment ($1 \leq EF \leq 3$); moderate enrichment ($3 \leq EF \leq 5$); moderate to severe enrichment ($5 \leq EF \leq 10$); severe enrichment ($10 \leq EF \leq 25$); very severe enrichment ($25 \leq EF \leq 50$); and extreme enrichment ($EF > 50$) (Ekissi et al., 2021).

2.3.2.2 Geoaccumulation index (I_{geo})

The degree of metal contamination or pollution in the marine environment can be determined using the geoaccumulation index (I_{geo}). The I_{geo} values were calculated as follows (Equation 3):

$$I_{geo} = \log 2C_n / 1.5 \times B_n \quad (3)$$

where C_n is the element concentration in the sediment sample and B_n is the trace metal geochemical background concentration. Due to lithogenic processes in the sediments, the background matrix correlation factor is 1.5 (Dytlow and Gorka-Kostrubiec, 2021). The geoaccumulation index divides sediment quality into seven categories: extremely contaminated ($I_{geo} > 5$); strongly to extremely contaminated ($4 < I_{geo} \leq 5$); strongly contaminated ($3 < I_{geo} \leq 4$); moderately to strongly contaminated ($2 < I_{geo} \leq 3$); moderately contaminated ($1 < I_{geo} \leq 2$); uncontaminated to moderately contaminated ($0 < I_{geo} < 1$); and uncontaminated ($I_{geo} < 0$) (Shirani et al., 2020).

2.3.2.3 Ecological risk index (R_i)

The ecological risk index (R_i) was quantified to assess the degree of potential ecological risks of heavy metals in the surface sediment of Songkhla Lagoon. Many studies have shown that the presence of toxic heavy metals can cause different types of health problems (Tchounwou et al., 2012). The R_i (Equation 4) was calculated according to Equation 4 as the sum of E_i (Equation 5) (Sánchez et al., 2022):

$$R_i = \sum_{i=1}^n E_i \quad (4)$$

$$E_i = T_i \cdot \left(\frac{C_i}{C_o} \right) \quad (5)$$

where R_i is the sum of the possible ecological risk factors for elements in sediments, E_i is the potential ecological risk factor for the elements, and T_i is the toxic response factor for the elements. T_i values reflect the toxicity of the metals. In accordance with a report by Hakanson, the following toxic response factors were used: As = 10, Cd = 30, Pb = 5, Cu = 5, and Zn = 1 (Hakanson, 1980). C_i is the metal concentration of the sediments and C_o is the metal concentration background value. According to the values obtained, R_i was classified as follows: low ($R_i < 150$); moderate ($150 \leq R_i \leq 300$); considerable ($300 \leq R_i \leq 600$); and high ($R_i > 600$).

3 Results and discussion

3.1 Abundance and occurrence of microplastics in sediment

The numbers of MP particles found at 10 stations in the lower Songkhla Lagoon are shown in Figure 2. The highest number of particles was found at station 7 (5.4 items/g), followed by sampling sites 6 (3.2 items/g), 3 (2.85 items/g), 5 (2.3 items/g), 1 (2.1 items/g), 2 (1.85 items/g), 8 (1.25 items/g), 9 (1.2 items/g), and site 4 (1.05 items/g), while the lowest number was found at site 10 (1.00 items/g). The differences in the number of MP particles among the stations were analyzed by the Kruskal–Wallis method, which found that these differences were significant ($p = 0.014$). Several studies of MPs in sediments in different environments in lagoons, lakes, bays, estuaries, coasts, rivers, beaches, and mangroves have found lower amounts than in the present study. Studies of MPs in the Lagoon of Tunisia found 63.8 ± 30.9 items/kg (Wakkaf et al., 2022), while in China 250.4 ± 92.0 items/kg were found (Wei et al., 2022), and in the Colombian Caribbean 0–3.1 items/kg were found (Garcés-Ordóñez et al., 2022). Elsewhere, 54–506 items/kg were found in the Lake of China (Yuan et al., 2019), while another study at the same lake found 244 ± 121 items/kg (Tang et al., 2022). In Thailand, a study on a beach found 0–33 items/kg (Jualaong et al., 2021) and another study on mangrove sediment found 106–180 items/kg (Pradit et al., 2022).

The size and color of the MPs scattered on the surface of the sediment are shown in Figure 3. This study only found fiber and fragment shapes of MPs. Fiber was accumulated in the sediment at different stations, with statistically significant differences among them ($p < 0.01$). In the sediment samples, fibers were found at all sampling sites, which accounted for 68.24% (15.15 items/g) of the

total MP particles, while fragments accounted for 31.76% (7.05 items/g). According to Tukey's HSD grouping, MPs of less than 500 μm were most commonly found among all 10 stations, at a rate of 46.62% (10.35 items/g), followed by those of 500–1000 μm (31.31%, 6.95 items/g) and then those greater than 1000 μm (22.07%, 4.90 items/g). Significant differences in the sizes of MP particles in the sediment were found ($p < 0.01$). The colors of the MPs found on the sediment surface varied. The predominant colors in this study were black (20.50%, 4.55 items/g), blue (31.53%, 6.70 items/g), transparent (23.65%, 5.25 items/g), and other (24.32%, 5.7 items/g). Five polymers were found, namely rayon, PP, polyester, PET, and copolymer, as shown in Figure 4. In the sediment, polyester and PP were found to have the same percentage distribution, which was 33.33%, followed by rayon at 16.67%, PET at 11.11%, and copolymer at 5.56%.

The most widely distributed polymer around the lagoon is polyester. It is common for polyester to be found in both water and sediment. This is similar to the findings in previous studies on MPs in sediment (Alam et al., 2019). Polyester, PET, and PA are important synthetic fibers used to produce synthetic fabrics such as clothing and carpets. Therefore, polyester may be derived from the deterioration of clothing when spun for washing and drying (Śaravanja et al., 2022; Wei et al., 2022). The accumulation of MPs in the environment occurs via waterways, followed by the MPs settling in the sediment over time if left undisturbed. However, in sediment, PP was found to be distributed at the same rate as polyester. The density of PP (0.89–0.92 g/cm^3) was lower than that of water. In general, it was distributed more on the water surface than in the sediment. However, the longevity of this polymer causes it to accumulate and adhere to bacteria, resulting in an increase in the density and speed of sedimentation of MPs (Kershaw et al., 2011). This explains the abundance of PP in

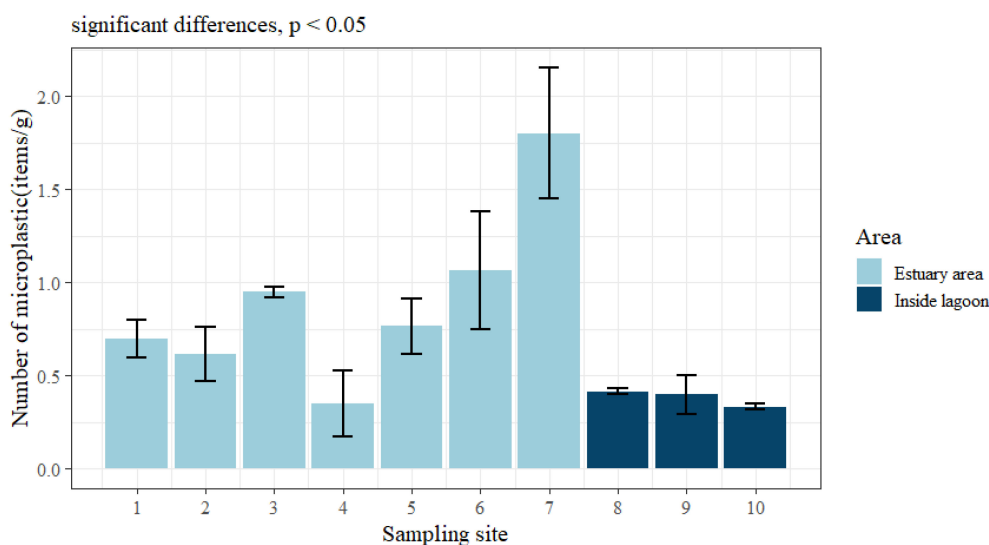


FIGURE 2
Microplastic distribution in the surface sediment at all sampling sites in Songkhla Lagoon.

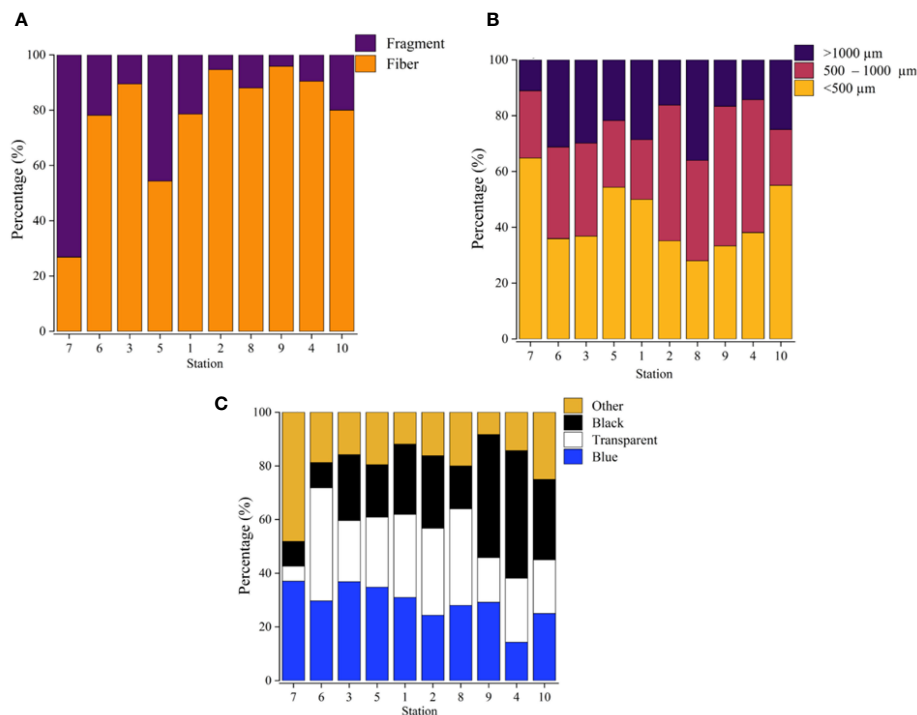


FIGURE 3

Distribution of microplastic characteristics in the surface sediment, classified by (A) shape, (B) size, and (C) color.

sediments, as similarly found in other studies (Yuan et al., 2019; Wakkaf et al., 2022; Wei et al., 2022). The other polymers found, rayon, PET, and copolymer, are all based on fibrous substrates, although fragments were found in smaller proportions. Rayon and PET fibers may be derived from garments and fishing equipment, which are made with rayon and PET that then deteriorate and enter the environment (Neves et al., 2015).

3.2 Relationship between microplastics, grain size, pH, and organic matter in sediment

Data on MPs found in sediment and sediment properties such as grain size (%clay, %silt, and %sand), organic matter (OM), and pH are shown in Table 1 and Figures 5, 6. The results show that clay

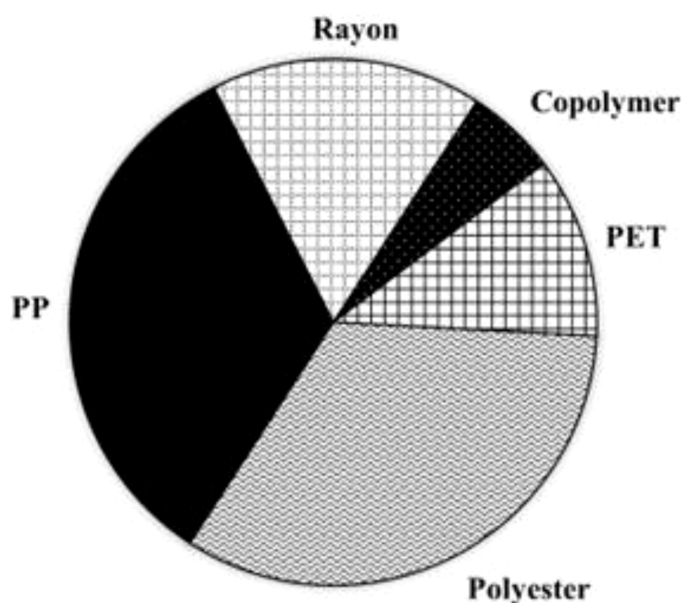


FIGURE 4

Distribution of microplastic polymers in the surface sediment.

deposits were found at stations 3, 5, 8, 9, and 10. Sand was found at sampling sites 1, 2, and 7, and silt at site 4. The pH in the sediment ranged from 7.37 to 9.37. At site 7, the highest amount of organic matter was found at 4.02%. From all 10 sediment sampling sites, it was found that site 7 had the highest organic matter value, which was related to the high MP content in the sediment there. This area also features a still water source with no tidal circulation. The sediment found was black and had a foul odor. The organic matter had completely decomposed into humus and improved the soil structure. This explanation can be linked to why MPs adhere to soil constituents since MPs can attach to mucus secreted by bacteria. In this study, the majority of MPs were less than 500 μm in size. When there is an abundance of organic matter, an abundance of MPs also accumulates in the sediment.

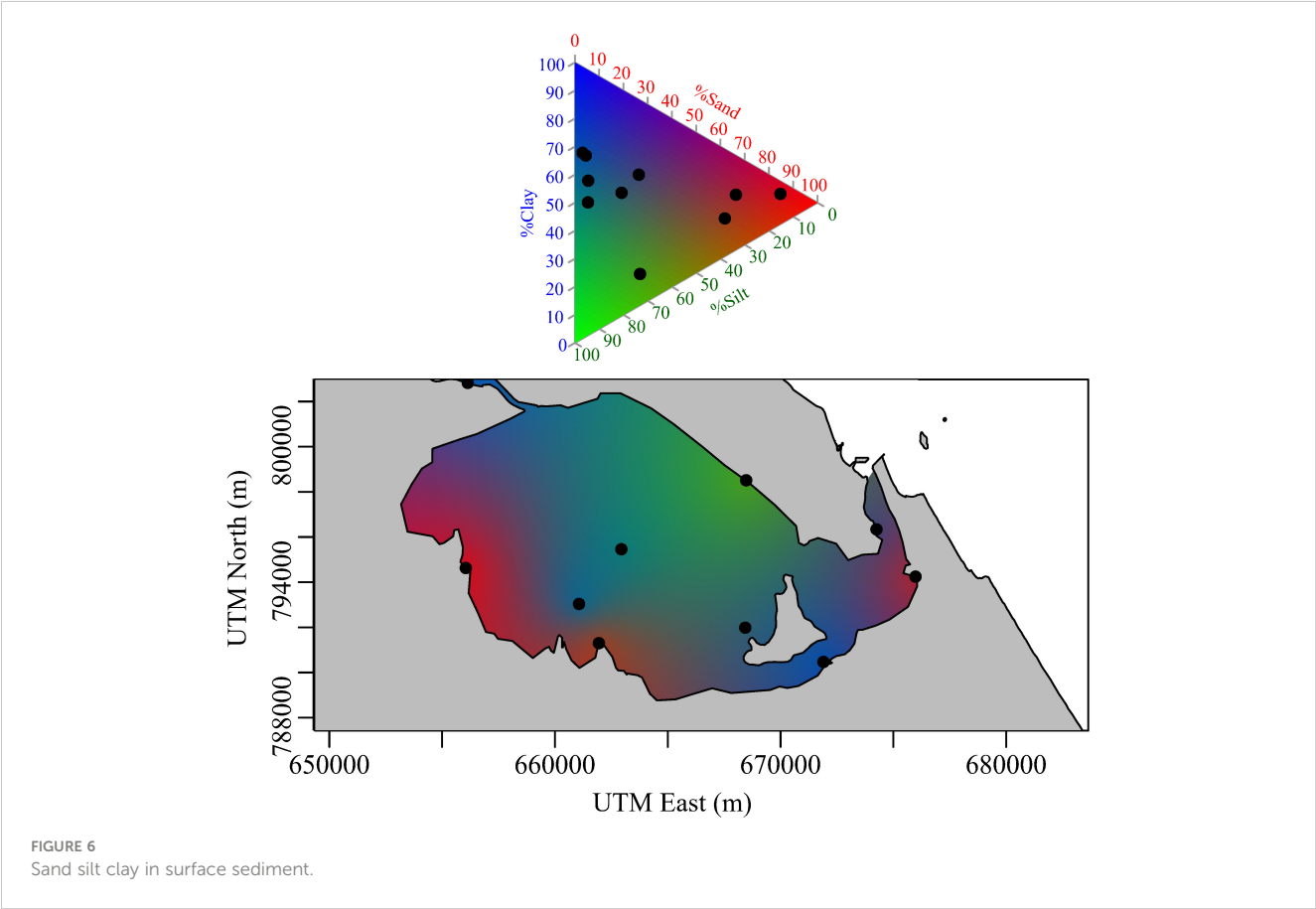
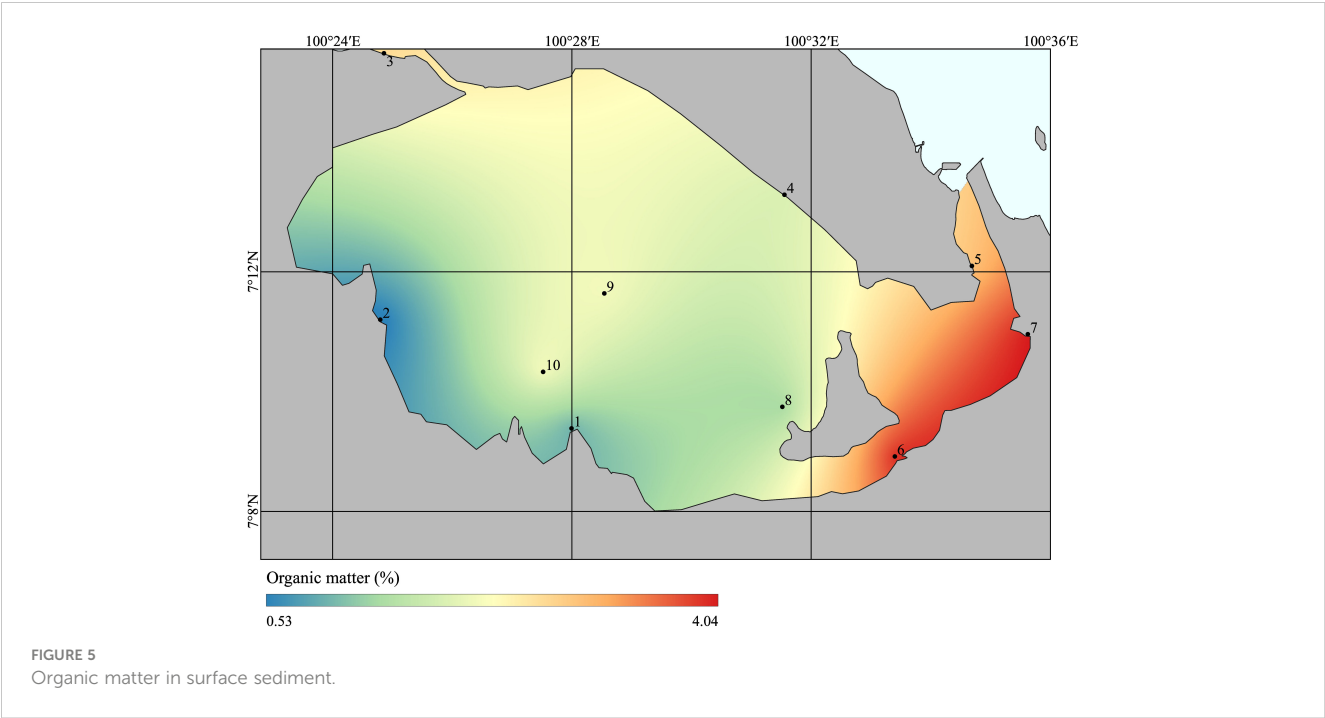
In this study, there was no correlation between MP content and grain size. MP contamination in the soil resulted in a decrease in the stability of the agglomeration and enzymatic activity in the soil due to MP infiltration by reducing the absorption of nutrients into microorganisms and reducing the rate of mineralization in the soil. MPs would have no effect on the stability of soil cohesion without increased organic matter (Liang et al., 2021). The greater the MP contamination, the more difficult it is for soil particles to agglomerate, especially polyester microfibers (Lehmann et al., 2019). After analyzing the relationship between the number of MPs in sediment and sediment properties, no correlation was found between MPs, grain size, and pH. The number of MP particles contaminating the sediment was positively correlated with %OM, according to Pearson's correlation analysis ($r = 0.696$, $p = 0.025$) (Figure 7). Surface lagoon sediment consists of minerals, organic matter, and other minor component. Due to MP and organic matter falling within the same range of density (Tian et al., 2023), MPs and OM would be deposited in the same condition. These MPs can also absorb pollutants (i.e., organic, inorganic, POPs, heavy metal) from sediment or from water on their surfaces. It can be obviously seen that the problem of MPs and marine wastes has a serious adverse impact on the environment, on living organisms, and on human food security as well (Pradit et al., 2020).

3.3 Concentrations of heavy metals in sediment

The concentrations of heavy metals (As, Cd, Pb, Cu, Zn, Mg, Co, and Mn) and their spatial distribution in the study area are summarized in Table 2. The average concentrations (mg/kg) of the trace metals are exhibited the following trend: Mg (732.54 ± 247.04) > Mn (176.74 ± 83.68) > Zn (29.36 ± 39.47) > Cu (12.31 ± 24.58) > Pb (11.07 ± 7.60) > As (5.64 ± 3.30) > Co (2.90 ± 1.38) > Cd (0.22 ± 0.17). The data show that Mg had the highest concentration in the surface sediments, while Cd was minimally accumulated. Mg is an abundant element in the Earth's crust and in sea water, and is transferred from continents to the hydrosphere via the weathering of rock (Guo et al., 2019). The use of fertilizers from agriculture increases the concentrations of trace metals, which can be transferred to the environment and increase harmful effects on aquatic organisms through runoff from agricultural soils to water bodies (Naz et al., 2022; Nakamaru et al., 2023). Moreover, high concentrations of Mn were also found in the study area. This observation is in line with the work of Pradit et al., 2010), who quantified the accumulation of Mn within the upper part of Songkhla Lagoon in 2010. The lagoon receives inputs from aquaculture activities such as shrimp farms and sea bass farms, along with various mining activities (Pradit et al., 2010). The mean heavy metal content in this study was compared with that in other coastal sediments around the world. The average values of As in this study are higher than the mean level reported in the Arabian Gulf, Saudi Arabia, but lower than in Chaohu Lake in China (Fang et al., 2022), Brisbane River in Australia (Duodu et al., 2016), and Badovci Lake in Kosovo (Malsiu et al., 2020). Moreover, the mean concentrations of Cd, Pb, Cu, Zn, and Mn were in the same ranges as in other coastal sediments, such as in the Arabian Gulf of Saudi Arabia, Aqaba, Saudi Arabia, and Chaohu Lake, China. Although the mean concentration of As in this study reflects strong contamination, the concentration of As is still lower than in other countries. However, it is a concern that all of the monitored heavy metals

TABLE 1 Grain size, organic matter, pH, and the number of microplastic particles found in the sediment at each station.

Sampling site	Grain size			OM (%)	pH	MPs in sediment (items/g)
	% Clay	%Silt	%Sand			
1	13.47	24.70	61.83	1.03	7.78	2.10
2	10.77	4.49	84.74	0.46	7.37	1.85
3	71.03	34.03	4.94	2.67	7.68	2.85
4	11.15	61.99	26.86	1.90	7.91	1.05
5	46.64	26.75	26.28	2.95	8.07	2.30
6	66.20	30.63	3.18	3.90	9.31	3.20
7	19.64	13.96	66.40	4.02	8.00	5.40
8	43.91	36.84	19.26	1.42	9.21	1.25
9	47.41	47.19	5.40	2.16	9.37	1.20
10	55.10	39.42	5.48	2.15	8.92	1.00



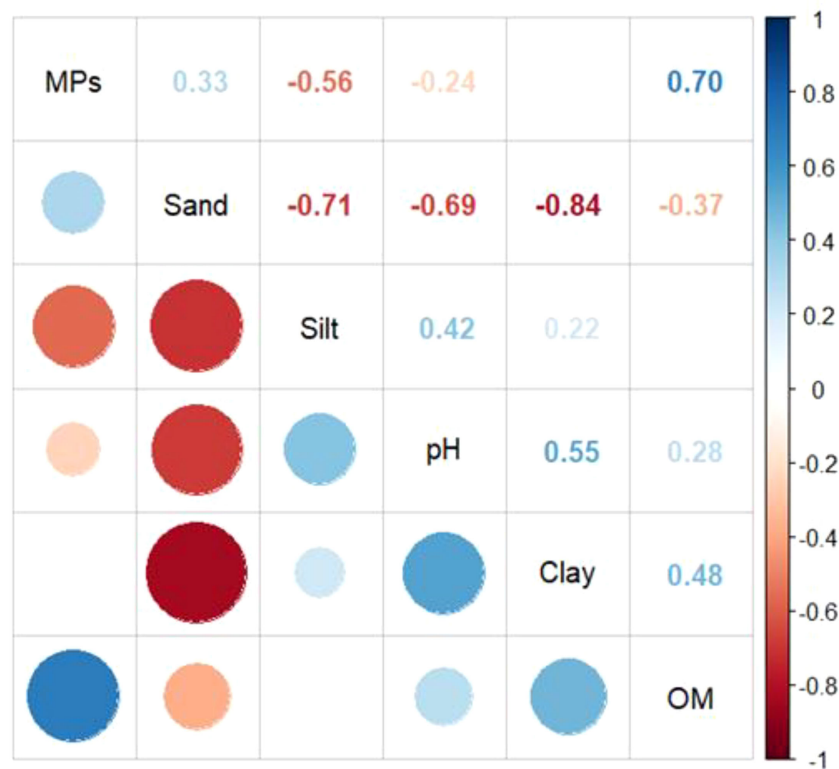


FIGURE 7
Correlations between microplastics, grain size, organic matter, and pH.

exceed the sediment quality standard, so regular monitoring of these variables should be performed.

The spatial distribution of trace metals in surface sediments is an important factor determining the level of pollution of aquatic

environments, which can be affected by natural and anthropogenic factors such as weathering of parent rock, industrial wastewater, transportation, and agriculture (Dong et al., 2023). It was found that most of the trace metals had high concentrations at site 7, especially

TABLE 2 Heavy metal concentrations (mg/kg dry weight) in the surface sediment of Songkhla Lagoon.

Sampling sites	Metal concentration (mg/kg)							
	As	Cd	Pb	Cu	Zn	Mg	Co	Mn
1	4.10 ± 0.41	0.15 ± 0.02	3.54 ± 0.32	3.28 ± 0.70	19.68 ± 1.32	424.25 ± 52.60	2.45 ± 0.14	141.84 ± 38.18
2	1.52 ± 0.26	0.05 ± 0.01	5.70 ± 1.15	2.37 ± 0.52	9.90 ± 2.39	154.45 ± 41.63	0.66 ± 0.10	113.99 ± 22.71
3	5.30 ± 0.29	0.19 ± 0.01	15.77 ± 0.66	5.98 ± 0.51	20.60 ± 1.06	802.22 ± 13.79	3.10 ± 0.43	138.40 ± 39.51
4	1.34 ± 0.13	0.08 ± 0.01	4.44 ± 0.20	3.31 ± 0.17	18.75 ± 0.78	736.25 ± 28.72	2.23 ± 0.24	208.21 ± 39.88
5	5.86 ± 0.10	0.19 ± 0.01	9.44 ± 1.22	9.92 ± 1.71	22.37 ± 0.88	985.23 ± 14.53	2.25 ± 1.08	124.91 ± 28.15
6	7.46 ± 1.13	0.23 ± 0.04	9.29 ± 2.02	7.44 ± 1.29	19.56 ± 4.26	876.43 ± 52.24	2.57 ± 0.42	223.42 ± 46.14
7	5.13 ± 2.87	0.55 ± 0.35	27.98 ± 12.50	73.91 ± 48.67	129.38 ± 75.73	811.79 ± 118.15	1.97 ± 1.04	71.08 ± 39.19
8	13.04 ± 1.16	0.41 ± 0.05	11.45 ± 2.11	5.32 ± 0.62	18.29 ± 2.08	909.17 ± 38.45	5.34 ± 0.42	369.15 ± 17.55
9	6.31 ± 0.39	0.18 ± 0.01	12.44 ± 0.30	5.91 ± 0.21	16.43 ± 0.50	834.00 ± 18.85	4.15 ± 0.13	193.80 ± 9.90
10	6.37 ± 0.19	0.19 ± 0.02	10.61 ± 0.22	5.71 ± 0.12	18.67 ± 0.98	794.59 ± 6.29	4.23 ± 0.15	182.63 ± 7.76
Mean	5.64 ± 3.30	0.22 ± 0.17	11.07 ± 7.60	12.31 ± 24.58	29.36 ± 39.47	732.54 ± 247.04	2.90 ± 1.38	176.74 ± 83.68
Min	1.20	0.04	3.26	1.84	7.15	104.81	0.56	34.43
Max	13.74	0.92	39.02	124.83	206.55	1001.56	5.82	388.90

Pb, Cu, and Zn. Station 7 is connected to Samrong Canal, which receives pollutants from Songkhla City, in addition to agricultural waste from rubber plantations, the parawood industry, and the seafood processing industry (Pradit et al., 2021). It is thus possible that high concentrations of metals are derived from these human activities. This is consistent with previous reports describing how anthropogenic activities such as wastewater discharge, battery disposal, transportation, and agricultural activities can affect metal concentrations (Li et al., 2022; Moldovan et al., 2022). Cu is used as a wood preservative (Lasota et al., 2019), while the parawood industry has rapidly expanded in this area (Sompongchaiyakul and Sirinawin, 2007), indicating that it may be an important source of Cu contamination in sediment. A high concentration of Zn was found in soil at a rubbish tip. In addition, the increase in metal concentrations in outer Songkhla Lagoon may have resulted from hydrological dynamics, and water velocity in particular. However, high concentrations of Mg were found at stations 5, 6, and 7, which are connected to three important canals (U-Tapao, Phawong, and Samrong). These canals receive municipal waste from Songkhla and Hat Yai cities. It is possible that, in these highly productive agricultural areas, ammonium phosphate fertilizers are widely used (Medina et al., 2009).

3.4 Risk assessment

3.4.1 Microplastic risk assessment

MPs with a small particle size are easily consumed by marine animals such as zooplankton (Kosore et al., 2018), fish (Klangnurak and Chunniyom, 2020), and molluscs (Abidli et al., 2019), and have an impact on the health of marine organisms (Sharma and Chatterjee, 2017). A risk assessment of MPs in surface sediment based on PHI, as reported by Ranjani et al. (2021), identified five hazard levels of MP pollution (Table 3). Based on PHL value, the overall risk of MPs in lagoon sediment in this study was categorized as Hazard Level III (high risk). The PHI values calculated in this study are lower than those previously reported in India (Ranjani et al., 2021).

3.4.2 Heavy metal risk assessment

The findings on enrichment factor (EF) and geoaccumulation index (I_{geo}) are shown in Table 4. The EF values of trace metals varied as follows: 4.15–45.89 (mean = 19.06 ± 10.63), 3.63–48.84 (mean = 11.63 ± 9.12), 1.09–13.55 (mean = 3.80 ± 2.58), 0.99–52.04 (mean = 5.09 ± 10.31), 0.98–15.16 (mean = 2.15 ± 2.93), 0.08–0.38 (mean = 0.28 ± 0.09), 0.48–2.69 (mean = 1.46 ± 0.66), and 1.95–17.50 (mean = 8.80 ± 3.89) for As, Cd, Pb, Cu, Zn, Mg, Co, and Mn, respectively. The average EF value of Mg was lower than 1. These values indicate no enrichment at the sampling sites. The Co and Zn average concentrations were in the range of 1–3, indicating minor enrichment. For Pb, it was found in the range of 3–5, indicating moderate enrichment. Cu and Mn were in the range of 5–10, which indicates moderate to severe enrichment. High EF values were observed for As and Cd in the range of 10–25, which indicates severe enrichment. According to Zhang and Liu (2002), crustal materials or natural processes are the primary sources of metal elements with EF between 0.5 and 1.5, whereas anthropogenic activities are the primary source of metal elements with EF greater than 1.5. Based on the I_{geo} calculation, the majority of sampling stations were in unpolluted to moderately contaminated regions (Pb, Zn, Mg, and Co). The average I_{geo} values of Cu and Mn were in the range of 1–2, which showed moderate contamination. Cd showed moderate to strong contamination and As showed strong contamination. As is typically used to distinguish between natural and anthropogenic sources of heavy metals because it is a lithogenic

TABLE 3 Pollution load index and polymer hazard index for microplastic pollution.

PHI	Hazard	Risk category
0–1	I	Minor
1–10	II	Medium
10–100	III	High
100–1000	IV	Danger
>1000	V	Extreme danger

TABLE 4 Enrichment factor (EF) and geoaccumulation index (I_{geo}) value of trace metals.

Metals	Enrichment factor (EF)				Geoaccumulation index (I_{geo})			
	Mean	S.D.	Min	Max	Mean	S.D.	Min	Max
As	19.06	10.63	4.15	45.89	3.83	2.14	0.83	9.23
Cd	11.63	9.12	3.63	48.84	2.33	1.83	0.73	9.80
Pb	3.80	2.58	1.09	13.55	0.76	0.52	0.22	2.72
Cu	5.09	10.31	0.99	52.04	1.02	2.07	0.20	10.52
Zn	2.15	2.93	0.98	15.16	0.43	0.59	0.20	3.04
Mg	0.28	0.09	0.08	0.38	0.06	0.02	0.02	0.08
Co	1.46	0.66	0.48	2.69	0.29	0.13	0.09	0.54
Mn	8.80	3.89	17.50	1.95	1.77	0.78	0.39	3.51

metal that enters the soil through the weathering of rocks (Huang et al., 2020). Human activities, such as agricultural activities, mixed orchard cultivation, use of fertilizers in agriculture, and rubber plantations may contribute to heavy metal deposition, resulting in As content in surface sediment.

The ecological risk index (R_i) values of Pb, Cu, and Zn are 110, 145, and 12, respectively (Figure 8). According to the Hakenson classification, the potential ecological risk indices of Pb, Cu, and Zn are less than 150. This is classified as “low risk”, indicating that these heavy metals will not cause serious damage to the ecology of Songkhla Lagoon. Meanwhile, high R_i values were observed for As (1128) and Cd (2047), being suggestive of high ecological risk. The main contributors to the R_i are the most toxic elements, Cd and As. Cd and As have a long history of accumulation as pollutants and can represent very serious ecological risk factors to both ecosystems and human health.

3.5 Relationship between heavy metals and microplastics

Owing to their connection to additives used or created during the plastic production process, heavy metals, and persistent organic pollutants that exist in the environment, MPs, are frequently referred to as a “cocktail of contaminants” (Rochman, 2015). Metals such as Zn, Pb, Cr, Co, Cd, and Ti are often used as

pigment-based colorants for inorganic polymers (Massos and Turner, 2017). It was observed that the areas where MPs were found most prominently also contained Pb, Cu, and Zn (Figure 9). The relationship between MPs and heavy metals in sediments from this study was calculated using Spearman’s rho correlation analysis, with the results showing that only Zn ($r = 0.697$) and Cu ($r = 0.61$) were strongly positively correlated with MP particle counts ($p < 0.05$). This indicates that the highly concentrated MPs in the sediment were highly contaminated with Zn and Cu, as shown in Figure 10.

3.6 Potential sources of microplastics and heavy metals

According to the sediment data, the lagoon is considerably enriched in trace elements. The waste water is discharged into the river and lagoon. The source of MPs in the lagoon could be from waste from households, paint of fishing boats, and fishing gear (Pradit et al., 2022). These rivers collect urban waste as well as industrial and agricultural waste. The potential sources of heavy metal in the sediment of Songkhla Lagoon (the outer section) include municipal waste from the large and rapidly expanding cities of Songkhla province, as well as agricultural and industrial discharges transported via the U-Taphao canal (Sompongchaiyakul and Sirinawin, 2007; Pradit et al., 2018). As and Cu are employed in the parawood business as wood preservatives near to the lagoon

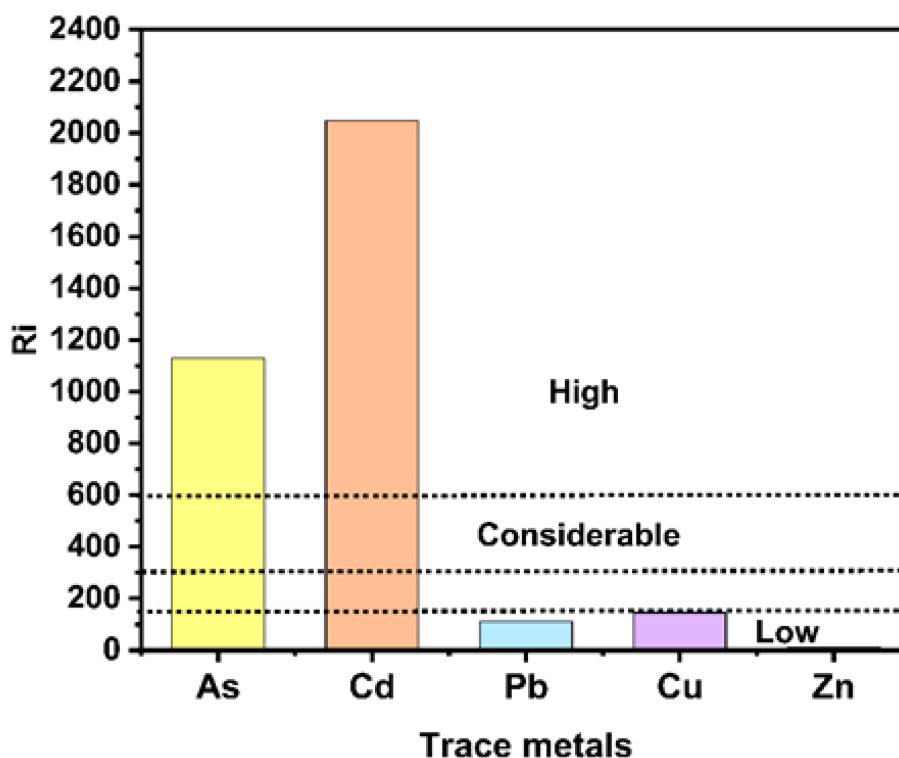


FIGURE 8
Potential ecological risk indices (R_i) of lagoon sediment.

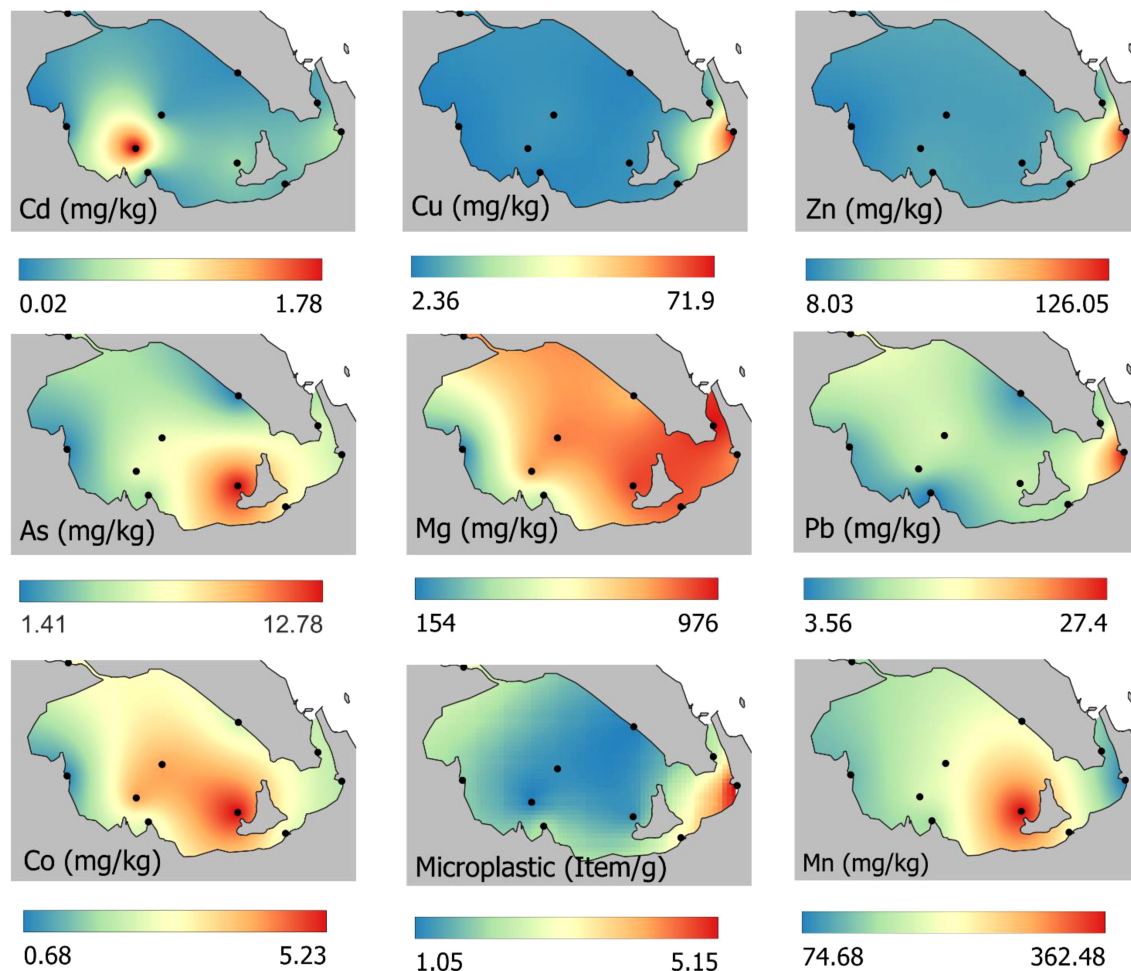


FIGURE 9

Heavy metal (mg/kg dry weight) and microplastic (items/g) distribution in the surface sediment of Songkhla Lagoon.

(Sompongchaiyakul and Sirinawin, 2007). The high levels of As found in the soils at a rubbish tip indicate that runoff from such sites into canals, and abandoned mines near the lagoon, may also be important sources of As (Pradit et al., 2010). Notably, the pH in the sediment increased at the station near the mouth of the lagoon, which was probably due to wastewater from houses flowing into the main rivers. Water from washing clothes with detergent normally has highly alkaline components, such as OH^- , CO_3^{2-} , and HCO_3^- ions of calcium, sodium, magnesium, potassium, and ammonia. These basic conditions from laundry activities can clearly raise the pH in both water and sediment (Pradit et al., 2021). If looking at historical data on heavy metal concentrations in Songkhla Lagoon sediments from 2010 to the present (Table 5), there is a decreasing trend for As and Pb. For MPs in sediments in the lagoon there have been few studies, but the concentration of this study seems to indicate more MPs than the study in 2021. The possible explanation is that the study area in 2021 was in the canal flowing to the lagoon whereas this study area covered a section of the lagoon itself.

3.7 Conclusion

This study reports the occurrence of MPs and heavy metals in the sediment of Songkhla Lagoon, the largest lagoon in Thailand. The area where MPs particularly accumulate is near the mouth of the lagoon, possibly derived from the three main rivers flowing into the lagoon. Risk assessment of MP loading showed that MPs constitute a minor hazard, whereas the polymer hazard index indicated a high hazard. The main contributors to the R_i are the most toxic elements, Cd and As. Cd and As have a long history of accumulation as pollutants and can represent very serious ecological risk factors to both ecosystems and human health. This study only investigated the lower Songkhla Lagoon area. The abundance and distribution of MPs and heavy metals in the lagoon sediment may lead to transfer of toxic chemicals to marine organisms and humans. The study area should be expanded to cover the middle and upper parts of the lagoon, which are the habitat of Irrawaddy dolphins.

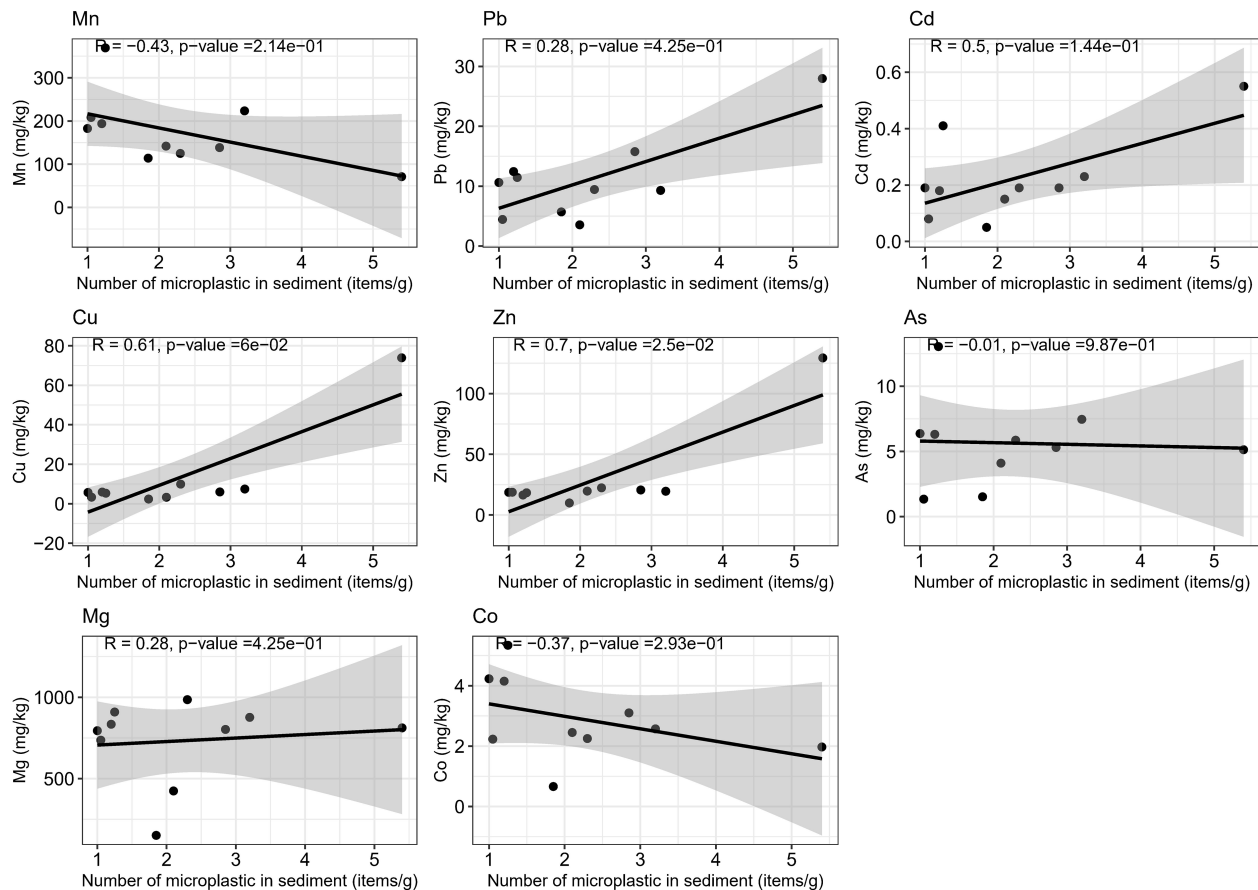


FIGURE 10

Relationship of heavy metals and abundance of microplastics in surface sediment in Songkhla Lagoon.

TABLE 5 The historical information of heavy metal and microplastic concentrations in the sediment of Songkhla Lagoon.

Heavy metals concentrations (mg/kg dry weight)					Concentration microplastic (item/kg)	
	2010	2013	2018	2023	2021	2023
Mn	48.1–1,817	123–846	–	34.43–388.90	106–413	1000–5400
Co	1.3–16.3	5.0–12.6	–	0.56–5.82		
Ni	2.5–21.9	11.0–23.2	–	–		
Cu	1.8–125	8–38	–	1.84–124.83		
Zn	5.4–562	40–198	48.6–126.6	7.15–206.55		
As	0.8–70.7	7–30	20.35–50.5	1.20–13.74		
Cd	0.1–2.4	0.14–0.92	0.076–0.18	0.04–0.92		
Pb	8.2–131	19–39	48.8–78.8	3.26–39.02		
Mg	–	–	–	104.81–1001.56		
Reference	Pradit et al., 2010	Pradit et al., 2013	Pradit et al., 2018	This study	Pradit et al., 2022	This study

Data availability statement

The original contributions presented in the study are included in the article/supplementary material. Further inquiries can be directed to the corresponding author.

Author contributions

SP: Conceptualization, Formal analysis, Funding acquisition, Investigation, Methodology, Project administration, Supervision, Validation, Writing – original draft, Writing – review & editing. PN:

Conceptualization, Funding acquisition, Investigation, Methodology, Software, Writing – review & editing. KS: Investigation, Methodology, Writing – review & editing. PJ: Investigation, Software, Visualization, Writing – review & editing. TK: Software, Visualization, Writing – review & editing. TN: Software, Writing – review & editing. DM: Conceptualization, Funding acquisition, Investigation, Methodology, Writing – review & editing.

Funding

The author(s) declare financial support was received for the research, authorship, and/or publication of this article. This research was supported by the National Science, Research and Innovation Fund (NSRF) and Prince of Songkla University (Grant No. ENV6601203S, Ref.no. 23801).

References

- Abidli, S., Lahbib, Y., and El Menif, N. T. (2019). Microplastics in commercial molluscs from the lagoon of Bizerte (Northern Tunisia). *Mar. Pollut. Bull.* 142, 243–252. doi: 10.1016/j.marpolbul.2019.03.048
- Alam, F. C., Sembiring, E., Muntalif, B. S., and Suendo, V. (2019). Microplastic distribution in surface water and sediment river around slum and industrial area (Case study: ciwalengke river, majalaya district, Indonesia). *Chemosphere* 224, 637–645. doi: 10.1016/j.chemosphere.2019.02.188
- Alia, T. K. A. T. N., Hing, L. S., Sim, S. F., Pradit, P., Ahmad, A., and Ong, M. C. (2020). Comparative study of raw and cooked farmed sea bass (*Lates calcarifer*) in relation to metal content and its estimated human health risk. *Mar. Pollut. Bulletin* 153, 111009. doi: 10.1016/j.marpolbul.2020.111009
- Al-Wabel, M. I., Sallam, A. E.-A. S., Usman, A. R. A., Ahmad, M., El-Naggar, A. H., El-Saeid, M. H., et al. (2017). Trace metal levels, sources, and ecological risk assessment in a densely agricultural area from Saudi Arabia. *Environ. Monit. Assess.* 189, 252. doi: 10.1007/s10661-017-5919-1
- AOAC (2005). "Official methods of analysis of AOAC international 18th Ed.", In: *Metals and Other Elements*, eds. W. Horwitz and G. W. Latimer. (Maryland: Gaithersburg). pp. 46–50.
- Baeyens, W., Leermakers, M., De Gieter, M., Nguyen, H. L., Parmentier, K., Panutrakul, S., et al. (2005). Overview of trace metal contamination in the Scheldt estuary and effect of regulatory measures. *Hydrobiologia* 540, 141–154. doi: 10.1007/s10750-004-7129-4
- Bayo, J., Guillen, M., Olmos, S., Jimenez, P., Sanchez, E., and Roca, M. J. (2018). Microplastics as vector for persistent organic pollutants in urban effluents: The role of polychlorinated biphenyls. *Int. J. Sus. Dev. Plann.* 13, 671–682. doi: 10.2495/SDP-V13-N4-671-682
- Bayraklı, B., Dengiz, O., Özyazıcı, M. A., Koç, Y., Kesim, E., and Türkmen, F. (2023). Assessment of heavy metal concentrations and behavior in cultivated soils under humid-subhumid environmental condition of the Black Sea region. *Geoderma Regional* 32, e00593. doi: 10.1016/j.geodrs.2022.e00593
- Browne, M., Dissanayake, A., Galloway, T. S., Lowe, D. M., and Thompson, R. C. (2008). Ingested microscopic plastic translocates to the circulatory system of the mussel, *Mytilus edulis* (L.). *Environ. Sci. Technol.* 42, 5026–5031. doi: 10.1021/es800249a
- Buccolieri, A., Buccolieri, G., Cardellicchio, N., Atti, A. D., Leo, A. D., and Maci, A. (2006). Heavy metals in marine sediments of Taranto Gulf (Ionian Sea, Southern Italy). *Mar. Chem.* 99, 227–235. doi: 10.1016/j.marchem.2005.09.009
- Chinfak, N., Sompongchaiyakul, P., Charoenpong, C., Shi, H., Yeemin, T., and Zhang, J. (2021). Abundance, composition, and fate of microplastics in water, sediment, and shellfish in the Tapi-Phumduang river system and Bandon bay, Thailand. *Sci. Total. Environ.* 781, 146700. doi: 10.1016/j.scitotenv.2021.146700
- Claessens, M., De Meester, S., Landuyt, L. V., De Clerck, K., and Janssen, C. R. (2011). Occurrence and distribution of microplastics in marine sediments along the Belgian coast. *Mar. Pollut. Bull.* 62, 2199–2204. doi: 10.1016/j.marpolbul.2011.06.030
- Cordova, M. R., Ulumuddin, Y. I., Purbonegoro, T., and Shiomoto, A. (2021). Characterization of microplastics in mangrove sediment of Muara Angke Wildlife Reserve, Indonesia. *Mar. Pollut. Bull.* 163, 112012. doi: 10.1016/j.marpolbul.2021.112012
- Dong, Q., Song, C., Yang, D., Zhao, Y., and Yan, M. (2023). Contamination assessment and origin of soil heavy metals in the Danjiangkou reservoir, China. *Int. J. Environ. Res. Public Health* 20, 3443. doi: 10.3390/ijerph20043443
- Duodu, G. O., Goonetilleke, A., and Ayoko, G. A. (2016). Comparison of pollution indices for the assessment of heavy metal in Brisbane River sediment. *Environ. Pollut.* 219, 1077–1091. doi: 10.1016/j.envpol.2016.09.008
- Dytlow, S., and Gorka-Kostrubiec, B. (2021). Concentration of heavy metals in street dust: an implication of using different geochemical background data in estimating the level of heavy metal pollution. *Environ. Geochem. Health* 43, 521–535. doi: 10.1007/s10653-020-00726-9
- Ekişi, D., Kinimo, K. C., Kamelan, T. M., and Kouamelan, E. P. (2021). Physicochemical characteristics and heavy metals contamination assessment in water and sediment in a tropical hydroelectric dam of sassandra river, côte d'Ivoire. *JH&P* 9, 27–35. doi: 10.12691/jeph-9-2-1
- Fang, T., Yang, K., Wang, H., Fang, H., Liang, Y., Zhao, X., et al. (2022). Trace metals in sediment from Chaohu Lake in China: Bioavailability and probabilistic risk assessment. *Sci. Total. Environ.* 849, 157862. doi: 10.1016/j.scitotenv.2022.157862
- Garcés-Ordóñez, O., Saldarriaga-Vélez, J. F., Espinosa-Díaz, L. F., Patiño, A. D., Cusba, J., Canals, M., et al. (2022). Microplastic pollution in water, sediments and commercial fish species from Ciénaga Grande de Santa Marta lagoon complex, Colombian Caribbean". *Sci. Total. Environ.* 829, 154643. doi: 10.1016/j.scitotenv.2022.154643
- Gee, G. W., and Bauder, J. W. (1986). "Particle-size analysis" in *Methods of Soil Analysis. Part 1. Physical and Mineralogical Methods*, ed. A. Klute (Madison: American Society of Agronomy), 383–411. doi: 10.2136/sssabookser5.1.2ed.c15
- Goh, P. B., Pradit, S., Towatana, P., Khokkatiwong, S., and Ong, M. C. (2022). Laboratory experiment on copper and lead adsorption ability of microplastics. *Sains Malaysiana* 51 (4), 993–1004. doi: 10.17576/jsm-2022-5104-04
- Guo, B., Zhu, X., Dong, A., Yan, B., Shi, G., and Zhao, Z. (2019). Mg isotopic systematics and geochemical applications: A critical review. *J. Asian Earth Sci.* 176, 368–385. doi: 10.1016/j.jseas.2019.03.001
- Hakanson, L. (1980). An ecological risk index for aquatic pollution control: a sedimentological approach. *Water Res.* 14, 975–986. doi: 10.1016/0043-1354(80)90143-8
- Han, Y.-J., Liang, R.-Z., Li, H.-S., Gu, Y.-G., Jiang, S.-J., and Man, X.-T. (2023). Distribution, multi-index assessment, and sources of heavy metals in surface sediments of zhelin bay, a typical mariculture area in southern china. *Toxics* 11 (2), 150. doi: 10.3390/toxics11020150
- Holmes, L. A., Turner, A., and Thompson, R. C. (2012). Adsorption of trace metals to plastic resin pellets in the marine environment. *Environ. Pollut.* 160, 42–48. doi: 10.1016/j.envpol.2011.08.052
- Huang, Z., Liu, C., Zhao, X., Dong, J., and Zheng, B. (2020). Risk assessment of heavy metals in the surface sediment at the drinking water source of the Xiangjiang River in South China. *Environ. Sci. Eur.* 32, 2–9. doi: 10.1186/s12302-020-00305-w
- Jualong, S., Pransilpa, M., Pradit, S., and Towatana, P. (2021). Type and distribution of microplastics in beach sediment along the coast of the Eastern Gulf of Thailand. *J. Mar. Sci. Eng.* 9, 1–12. doi: 10.3390/jmse9121405
- Kershaw, P., Katsuhiko, S., Lee, S., Samseth, J., Woodring, D., and Smith, J. (2011). *Plastic debris in the ocean. UNEP year book.*
- Klangnarak, W., and Chunniyom, S. (2020). Screening for microplastics in marine fish of Thailand: the accumulation of microplastics in the gastrointestinal tract of different foraging preferences. *Environ. Sci. Pollut. Res.* 27, 27161–27168. doi: 10.1007/s11356-020-09147-8

Conflict of interest

The authors declare that the research was conducted in the absence of any commercial or financial relationships that could be construed as a potential conflict of interest.

Publisher's note

All claims expressed in this article are solely those of the authors and do not necessarily represent those of their affiliated organizations, or those of the publisher, the editors and the reviewers. Any product that may be evaluated in this article, or claim that may be made by its manufacturer, is not guaranteed or endorsed by the publisher.

- Kosore, C., Ojwang, L., Maghanga, J., Kamau, J., Kimeli, A., Omukoto, J., et al. (2018). Occurrence and ingestion of microplastics by zooplankton in Kenya's marine environment: first documented evidence. *Afr. J. Mar. Sci.* 40, 225–234. doi: 10.2989/1814232X.2018.1492969
- Lasota, S., Stephan, I., Horn, M. A., Otto, W., and Noll, M. (2019). Copper in wood preservatives delayed wood decomposition and shifted soil fungal but not bacterial community composition. *AEM* 85, e02391–e02318. doi: 10.1128/AEM.02391-18
- Lehmann, A., Fitschen, K., and Rillig, M. C. (2019). Abiotic and biotic factors influencing the effect of microplastic on soil aggregation. *Soil Syst.* 3, 21. doi: 10.3390/soilsystems3010021
- Li, F., Yu, X., Lv, J., Wu, Q., and An, Y. (2022). Assessment of heavy metal pollution in surface sediments of the Chishui River Basin, China. *PLoS One* 17, e0260901. doi: 10.1371/journal.pone.0260901
- Liang, Y., Lehmann, A., Yang, G., Leifheit, E. F., and Rillig, M. C. (2021). Effects of microplastic fibers on soil aggregation and enzyme activities are organic matter dependent. *Front. Environ. Sci.* 9. doi: 10.3389/fenvs.2021.650155
- Lithner, D., Larsson, A., and Dave, G. (2011). Environmental and health hazard ranking and assessment of plastic polymers based on chemical composition. *Sci. Total. Environ.* 409, 3309–3324. doi: 10.1016/j.scitotenv.2011.04.038
- Liu, J., Liu, H., He, D., Zhang, T., Qu, J., Lv, Y., et al. (2022). Comprehensive effects of temperature, salinity, and current velocity on the microplastic abundance in offshore area. *Pol. J. Environ. Stud.* 31, 1727–1736. doi: 10.15244/pjoes/142389
- Loring, D. H., and Rantala, R. T. T. (1992). Manual for the geochemical analyses of marine sediments and suspended particulate matter. *Earth-Sci. Rev.* 32, 235–283. doi: 10.1016/0012-8252(92)90001-A
- Malsiu, S., Shehu, I., Staflov, T., and Faiku, F. (2020). Assessment of heavy metal concentrations with fractionation method in sediments and waters of the Badovci Lake (Kosovo). *JEPH* 2020, 14. doi: 10.1155/2020/3098594
- Massos, A., and Turner, A. (2017). Cadmium, lead and bromine in beached microplastics. *Environ. Pollut.* 227, 139–145. doi: 10.1016/j.envpol.2017.04.034
- Medina, L. C., Sartain, J. B., and Obreza, T. A. (2009). Estimation of release properties of slow-release fertilizer materials. *Horttechnology* 19, 13–15. doi: 10.21273/HORTTECH.19.1.13
- Mendil, D., and Uluözülü, O. D. (2007). Determination of trace metal levels in sediment and five fish species from lakes in Tokat, Turkey. *Food Chem.* 101, 739–745. doi: 10.1016/j.foodchem.2006.01.050
- Miao, S., De Laune, R. D., and Jugsujinda, A. (2006). Influence of sediment redox conditions on release/solubility of metals and nutrients in a Louisiana Mississippi River deltaic plain freshwater lake. *Sci. Total. Environ.* 371, 334–343. doi: 10.1016/j.scitotenv.2006.07.027
- Moldovan, A., Török, A. I., Kovacs, E., Cadar, O., Mirea, I. C., and Micle, V. (2022). Metal contents and pollution indices assessment of surface water, soil, and sediment from the Arieș river basin mining area, Romania. *Sustainability* 14 (13), 8024. doi: 10.3390/su14138024
- Nakamaru, Y. M., Matsuda, R., and Sonoda, T. (2023). Environmental risks of organic fertilizer with increased heavy metals (Cu and Zn) to aquatic ecosystems adjacent to farmland in the northern biosphere of Japan. *Sci. Total. Environ.* 884, 163861. doi: 10.1016/j.scitotenv.2023.163861
- Naz, S., Fazio, F., Habib, S. S., Nawaz, G., Attaullah, S., Ullah, M., et al. (2022). Incidence of heavy metals in the application of fertilizers to crops (Wheat and Rice), a fish (Common carp) Pond and a human health risk assessment. *Sustainability* 14, 13441. doi: 10.3390/su142013441
- Neves, D., Sobral, P., Ferreira, J. L., and Pereira, T. (2015). Ingest of microplastic by commercial fish off the Portuguese Coast. *Mar. Pollut. Bull.* 101, 119–126. doi: 10.1016/j.marpolbul.2015.11.008
- Pradit, S., Gao, Y., Faiboon, A., Baeyens, W., and Leermakers, M. (2013). Application of DET (diffusive equilibrium in thin films) and DGT (diffusive gradients in thin films) techniques in the study of the mobility of sediment-bound metals in the outer section of Songkhla Lake, Southern Thailand. *Environ. Monit. Assessment.* 185 (5), 4207–4220. doi: 10.1007/s10661-012-2862-z
- Pradit, S., Nitiratsuwat, T., Towatana, P., Jualaong, S., Jirajarus, M., Sonrnpang, K., et al. (2020). Marine debris accumulation on the beach in libong, a small island in andaman sea, Thailand. *Appl. Ecol. Environ. Res.* 18 (4), 5461–5474. doi: 10.15666/aer/1804_54615474
- Pradit, S., Noppradit, P., Goh, B. P., Sonrnpang, K., Ong, M. C., and Towatana, P. (2021). Occurrence of microplastics and trace metals in fish and shrimp from Songkhla lake, Thailand during the covid-19 pandemic. *Appl. Ecol. Environ. Res.* 19, 1085–1106. doi: 10.15666/aer/1902_10851106
- Pradit, S., Noppradit, P., Loh, P.-S., Nitiratsuwat, T., Le, T. P. Q., Oeurng, C., et al. (2022). The occurrence of microplastics in sediment cores from two mangrove areas in Southern Thailand. *J. Mar. Sci. Eng.* 10, 418. doi: 10.3390/jmse10030418
- Pradit, S., Shazili, N. A. M., Pattaratumrong, M. S., Chotikarn, P., Kobkeathawin, T., Yucharoen, M., et al. (2018). Accumulation of trace metals in mangrove plant *Sonneratia Caseolaris* in Songkhla Lake, Thailand. *Appl. Ecol. Environ. Res.* 16 (4), 4081–4095. doi: 10.15666/aer/1604_40814095
- Pradit, S., Wattayakorn, G., Angsupanich, S., Baeyens, W., and Leermakers, M. (2010). Distribution of trace elements in sediments and biota of songkhla lake, southern Thailand. *Water Air. Soil Pollut.* 206, 155–174. doi: 10.1007/s11270-009-0093-x
- Rajeshkumar, S., Liu, Y., Zhang, X., Ravikumar, B., Bai, G., and Li, X. (2018). Studies on seasonal pollution of heavy metals in water, sediment, fish and oyster from the Meiliang Bay of Taihu Lake in China. *Chemosphere* 191, 626–638. doi: 10.1016/j.chemosphere.2017.10.078
- Ranjani, M., Veerasingam, S., Venkatachalapathy, R., Mugilarasan, M., Bagaev, A., Mukhanov, V., et al. (2021). Assessment of potential ecological risk of microplastics in the coastal sediments of India: A meta-analysis. *Mar. Pollut. Bull.* 163, 111969. doi: 10.1016/j.marpolbul.2021.111969
- Rochman, C. M. (2015). "The complex mixture, fate and toxicity of chemicals associated with plastic debris in the marine environment" in *Marine Anthropogenic Litter*, eds. M. Bergmann, L. Gutow and M. Klages (Springer, Cham), 117–140. doi: 10.1007/978-3-319-16510-3_5
- Sánchez, E. R. S., Martínez, J. M. E., Morales, M. M., Mendoza, O. T., and Alberich, M. V. E. (2022). Ecological and health risk assessment of potential toxic elements from a mining area (Water and Sediments): The San Juan-Taxco River System, Guerrero, Mexico. *Water* 14, 518. doi: 10.3390/w14040518
- Šaravanja, A., Pušić, T., and Dekanić, T. (2022). Microplastics in wastewater by washing polyester fabrics. *Materials* 15, 2683. doi: 10.3390/ma15072683
- Sharma, S., and Chatterjee, S. (2017). Microplastic pollution, a threat to marine ecosystem and human health: a short review. *Environ. Sci. Pollut. Res.* 24, 21530–21547. doi: 10.1007/s11356-017-9910-8
- Shazili, N. A. M., Rashid, M. K. A., Husain, M. L., Nordin, A., and Ali, S. (1999). "Trace metals in the surface sediments of the South China Sea, area I: Gulf of Thailand and the East Coast of Peninsular Malaysia," in *Proceedings of the first technical seminar on marine fishery resources survey in the south China sea, area I: gulf of Thailand and east coast of peninsular Malaysia*, vol. 1999. (Bangkok, Thailand: Training Department, Southeast Asian Fisheries Development Center), 73–85.
- Shirani, M., Afzali, K. N., Jahan, S., Strezov, V., and Soleimani-Sardo, M. (2020). Pollution and contamination assessment of heavy metals in the sediments of Jazmurian playa in southeast Iran. *Sci. Rep.* 10, 4775. doi: 10.1038/s41598-020-61838-x
- Sirinawin, W., and Sompongchaiyakul, P. (2005). Nondetrital and total metal distribution in core sediments from the U-taphao Canal, Songkhla, Thailand. *Mar. Chem.* 94, 5–16. doi: 10.1016/j.marchem.2004.07.007
- Sompongchaiyakul, P., and Sirinawin, W. (2007). Arsenic, Chromium and Mercury in surface sediment of Songkhla lake system, Thailand. *Asian J. Water Environ. Pollut.* 4, 17–24. doi: 10.1016/j.sbspro.2013.08.456
- Tang, N., Yu, Y., Cai, L., Tan, X., Zhang, L., Huang, Y., et al. (2022). Distribution characteristics and source analysis of microplastics in urban freshwater lakes: A case study in Songkhla lake of Dongguan, China. *Water* 14, 1111. doi: 10.3390/w14071111
- Taylor, S. R., and McLennan, S. M. (1995). The geochemical evolution of the continental crust. *Rev. Geophys.* 33, 241–265. doi: 10.1029/95RG00262
- Tchounwou, P. B., Yedjou, C. G., Patlolla, A. K., and Sutton, D. J. (2012). Heavy metals toxicity and the environment. *NIH. Public Access.* 101, 133–164. doi: 10.1007/978-3-7643-8340-4_6
- Thompson, R. C., Olsen, Y., Mitchell, R. P., Davis, A., Rowland, S. J., John, A. W. G., et al. (2004). Lost at sea: where is all the plastic? *Science* 304, 838. doi: 10.1126/science.1094559
- Tian, X., Yang, M., Guo, Z., Chang, C., Li, J., Guo, Z., et al. (2023). Amount and characteristics of microplastic and organic matter in wind-blown sediment at different heights within the aeolian sand saltation layer. *Environ. Pollut.* 327, 121615. doi: 10.1016/j.envpol.2023.121615
- Wakkaf, T., Zrelli, R. E., Yacoubi, L., Kedzierski, M., Lin, Y.-J., Mansour, L., et al. (2022). Seasonal patterns of microplastics in surface sediments of a Mediterranean lagoon heavily impacted by human activities (Bizerte Lagoon, Northern Tunisia). *Environ. Sci. Pollut. Res.* 29, 76919–76936. doi: 10.1007/s11356-022-21129-6
- Wang, Y., Zou, X., Peng, C., Qiao, S., Wang, T., Yu, W., et al. (2020). Occurrence and distribution of microplastics in surface sediments from the Gulf of Thailand. *Mar. Pollut. Bull.* 152, 110916. doi: 10.1016/j.marpolbul.2020.110916
- Wei, Y., Ma, W., Xu, Q., Sun, C., Wang, X., and Gao, F. (2022). Microplastic distribution and influence factor analysis of seawater and surface sediments in a typical bay with diverse functional areas: A case study in Xincun lagoon, China. *Front. Environ. Sci.* 10. doi: 10.3389/fenvs.2022.829942
- Xu, P., Peng, G., Su, L., Gao, Y., Gao, L., and Li, D. (2018). Microplastic risk assessment in surface waters: A case study in the Changjiang Estuary, China. *Mar. Pollut. Bull.* 133, 647–654. doi: 10.1016/j.marpolbul.2018.06.020
- Yuan, W., Liu, X., Wang, W., Di, M., and Wang, J. (2019). Microplastic abundance, distribution and composition in water, sediments, and wild fish from Poyang lake, China. *Ecotoxicol. Environ. Saf.* 170, 180–187. doi: 10.1016/j.ecoenv.2018.11.126
- Zhang, J., and Liu, C. L. (2002). Riverine composition and estuarine geochemistry of particulate metals in China—weathering features, anthropogenic impact and chemical fluxes. *Estuarine. Estuar. Coast. Shelf. Sci.* 54, 1051–1070. doi: 10.1006/eccc.2001.0879



OPEN ACCESS

EDITED BY

Xuchun Qiu,
Jiangsu University, China

REVIEWED BY

Mohamed Mohsen,
Jimei University, China
Carola Murano,
Anton Dohrn Zoological Station Naples, Italy

*CORRESPONDENCE

Maranda Esterhuizen
✉ maranda.esterhuizen@helsinki.fi

RECEIVED 15 November 2023

ACCEPTED 19 January 2024

PUBLISHED 05 February 2024

CITATION

Esterhuizen M, Lee S-A, Kim Y, Järvinen R
and Kim YJ (2024) Ecotoxicological
consequences of polystyrene naturally
leached in pure, fresh, and saltwater: lethal
and nonlethal toxicological responses in
Daphnia magna and *Artemia salina*.
Front. Mar. Sci. 11:1338872.
doi: 10.3389/fmars.2024.1338872

COPYRIGHT

© 2024 Esterhuizen, Lee, Kim, Järvinen and
Kim. This is an open-access article distributed
under the terms of the [Creative Commons
Attribution License \(CC BY\)](https://creativecommons.org/licenses/by/4.0/). The use,
distribution or reproduction in other forums
is permitted, provided the original author(s)
and the copyright owner(s) are credited and
that the original publication in this journal is
cited, in accordance with accepted academic
practice. No use, distribution or reproduction
is permitted which does not comply with
these terms.

Ecotoxicological consequences of polystyrene naturally leached in pure, fresh, and saltwater: lethal and nonlethal toxicological responses in *Daphnia magna* and *Artemia salina*

Maranda Esterhuizen^{1,2,3,4*}, Sang-Ah Lee^{4,5}, Youngsam Kim^{4,6},
Riikka Järvinen^{1,4} and Young Jun Kim^{4,6}

¹Ecosystems and Environment Research Programme, Faculty of Biological and Environmental Sciences, University of Helsinki, Lahti, Finland, ²Helsinki Institute of Sustainability Science (HELSUS), Helsinki, Finland, ³Clayton H. Riddell Faculty of Environment, Earth, and Resources, University of Manitoba, Winnipeg, MB, Canada, ⁴Korea Institute of Science and Technology Europe (KIST Europe) Forschungsgesellschaft GmbH, Joint Laboratory of Applied Ecotoxicology, Environmental Safety Group, Universität des Saarlandes, Saarbrücken, Germany, ⁵Faculty of Biotechnology, College of Applied Life Sciences, Jeju National University, Jeju, Republic of Korea, ⁶Division of Energy & Environment Technology, University of Science & Technology, Daejeon, Republic of Korea

Polystyrene is widely used in disposable products and is now a ubiquitous plastic pollutant in aquatic environments, where it degrades into smaller particles that leach potentially toxic chemicals. However, knowledge regarding the impacts of plastic leachates remains limited. This study investigates the lethal and nonlethal effects of polystyrene leachate on two ecologically significant aquatic organisms, *Daphnia magna* (water flea) and *Artemia salina* (brine shrimp). Polystyrene leachates were prepared in seawater, freshwater, and sterile, pure water by incubating the material in each of the media under natural conditions for six months. *D. magna* and *A. salina* were exposed to varying concentrations of the leachates under controlled laboratory conditions, monitoring their survival, as well as measuring reactive oxygen species and antioxidant responses as superoxide dismutase and catalase activity. The data show that *A. salina* was more significantly affected with higher mortality observed at lower leachate concentrations, potentially linked to seawater enhancing the leaching of toxic additives. Moreover, at non-lethal concentrations, the antioxidative responses maintained homeostasis in both organisms. Considering the current reported microplastic concentrations in the aquatics and the adequate antioxidative response, leachate from plastic potentially does not pose a severe threat to these organisms. Nevertheless, hydrological characteristics of waterbodies may cause microplastic hotspots, which could significantly concentrate plastics and thus their leachates, necessitating action to reduce the current microplastic pollution level and avoid future surges. This study highlights the ecological significance of polystyrene pollution, emphasizing the need for more comprehensive regulatory measures and the development of sustainable alternatives to polystyrene-based products. The distinct responses of *D. magna*

and *A. salina* imply that the impact of plastic pollution varies among species, necessitating further research to elucidate broader ecological consequences. Understanding how polystyrene leachate affects keystone species provides crucial insights into the overall implications for aquatic ecosystems.

KEYWORDS

aquatic organisms, planktonic organisms, plastic leachate, microplastic, oxidative stress, ecotoxicology

1 Introduction

Plastic pollution is a pressing environmental issue that is garnering merited attention. The growing global distribution of plastic waste in the environment stems from its widespread use and improper disposal (Dahlbo et al., 2018; van Velzen et al., 2019). While studies on the ecotoxicology of plastic and its breakdown products, such as micro- and nanoplastics, are increasing, and the impacts are being better understood (Esterhuizen and Kim, 2022; Samadi et al., 2022), another aspect of this problem, namely the toxicity of leaching chemicals, is being recognised (Lithner et al., 2009; Lithner et al., 2012; Pflugmacher et al., 2020).

Plastic items can leach harmful chemicals into their surroundings (Do et al., 2022). Additives which are not covalently bound to the polymer matrix and residual monomers could migrate into the environment from virgin plastics (Crompton, 1979; Araújo et al., 2002; Lithner et al., 2011; Kwan and Takada, 2016). Over time, when exposed to environmental factors like sunlight and water, plastics can break down and release a cocktail of toxic compounds, including phthalates, bisphenol A (BPA), and polychlorinated biphenyls (PCBs). These compounds are known as additives and are applied during the manufacture of plastics depending on the intended use and properties of the final product (Wiesinger et al., 2021; Do et al., 2022). They play a crucial role in tailoring plastics for specific applications by imparting desirable properties or allowing the retaining of the original plastic properties during moulding (OECD, 2009; Hahladakis et al., 2018). Regularly used additives include plasticisers, flame retardants, thermal stabilisers, photostabilisers, antioxidants, and pigments (Stevens, 1990; Andradý and Rajapakse, 2016).

Various media have been shown to facilitate leaching, including sea- and freshwater (Bridson et al., 2021). Release of additives from plastics was studied by Do et al. (2022). They found that polymer type, surface characteristics, the environment, and time are the main factors influencing leaching. Furthermore, biodegradation, thermal and photodegradation influenced the liberation of additives.

Some additives are known carcinogens, mutagens, and endocrine disruptors, and thus potentially hazardous to many organisms (EBC, 2008; Groh et al., 2019). As plastic and microplastic (MP) pollution has been found globally (Scopetani

et al., 2019; Mammo et al., 2020; Patti et al., 2020; Prabhu et al., 2022), these leached chemicals can contaminate terrestrial and aquatic ecosystems and even enter the food chain, with potentially detrimental effects on the health of both wildlife and humans. Understanding and addressing this facet of plastic pollution is essential for mitigating its far-reaching consequences, especially concerning the toxicity of leachates to native biota.

In addition to intrinsic toxicants that may be liberated, MPs can adsorb and concentrate persistent organic pollutants (POPs, e.g., PCBs and organochlorine pesticides), heavy metals (lead, cadmium, and mercury), and non-plastic pollutants (e.g., polycyclic aromatic hydrocarbons (PAHs)) from the surrounding water (Caruso, 2019). Chemicals that adhere to MP surfaces have been shown to bioaccumulate in organisms that ingest the fragments (Caruso, 2019). Furthermore, microbial biofilms can develop on MPs in the environment, releasing metabolites, enzymes, and other chemicals that have been found to contribute to plastic degradation and, thus, facilitate leaching (Han et al., 2020; Sooriyakumar et al., 2022), which may contribute to toxicity.

Even though several studies have considered the ecotoxicological effects of leachates from plastics (reviewed by Gunaalan et al., 2020), many have used artificial leaching methods and have not considered the effect of factors such as the environment, climate fluctuations, and naturally occurring microbes. Therefore, the present study aimed to investigate the toxicological effects of natural leachate from polystyrene (PS), one of the most detected plastics in the environment (Scopetani et al., 2019; Tian et al., 2023). PS was leached in pure water (MilliQ), freshwater, and seawater for six months outside under environmental conditions and the ecotoxicological effects of the leachate, and dilutions thereof, were investigated in terms of immobility, oxidative stress, and enzymatic antioxidative defence response in *Daphnia magna* (pure and freshwater) and *Artemia salina* (seawater) with acute exposure. Many previous studies regarding MP and leachates were conducted with *D. magna* (Samadi et al., 2022), a recognised model bioindicator organism for evaluating ecotoxicology (Reilly et al., 2023). Likewise, *A. salina* has been suggested as a model species for ecotoxicity assessments (Kalčíková et al., 2012; Albarano et al., 2022). The three media were selected to assess how the properties of a natural media can

influence the toxicity of the leachate, where both fresh- and seawater contained natural microbes and minerals compared to sterile MilliQ water which is both deionized and demineralized. This approach allows the direct comparison of the toxicities of the obtained PS leachates in the various media on keystone bioindicator organisms which have not previously been assessed. Thus, the selection of three distinct media aimed to investigate the impact of natural media properties on leachate toxicity. Both fresh- and seawater, rich in natural microbes and minerals, were compared to sterile MilliQ water, known for its deionized and demineralized composition. This method facilitates a direct comparison of the toxicities exhibited by the obtained PS leachates across different media. The chosen bioindicator organisms, considered keystone species, have not been previously evaluated under these conditions.

2 Materials and methods

2.1 Bioindicator organism cultivation

D. magna ephippia were supplied by MicroBiotests Inc. (Gent, Belgium). Hatching was facilitated under 7000 lux light with a 16-to-8-hour light-to-dark cycle at $20.0 \pm 1.0^\circ\text{C}$ in Elendt M4 medium (OECD, 2004). A population of 15 daphnid individuals was maintained in 1.5 L Elendt M4 medium in a controlled climate incubator. Once a day, the daphnids were with *Chlorella vulgaris* ($\sim 1.5 \times 10^8$ cells/mL), purchased from the Culture Collection of Algae (Cologne University, Essen, Germany), at a density of 0.1–0.2 mg C per individual. Additionally, twice a week, the culture was fed with yeast, cerophyl, and trout chow at a concentration of 0.5 $\mu\text{L/mL}$ (v/v). Offspring were removed daily, and the cultural medium was renewed thrice weekly. The pH and dissolved oxygen content were checked and maintained according to OECD guidelines (OECD, 2004). Interlaboratory tests were performed using potassium dichromate (Sigma-Aldrich, St. Louis, MO, USA) as a reference toxicant. For the present study, neonates were ≤ 24 hours old.

Artemia cysts were purchased from Great Salt Lake Artemia (Utah, USA) and hatched in an artificial seawater medium. This medium was prepared to a salinity of 25 parts per thousand (ppt) by dissolving sodium chloride (Sigma Aldrich, St. Louis, MO, USA) in deionized water. To achieve a pH level above 8, sodium bicarbonate (Sigma Aldrich, St. Louis, MO, USA) was added to the medium. The incubation was carried out in a temperature-controlled environment at $25 \pm 1^\circ\text{C}$, with continuous aeration and an illumination intensity of 3000 lux for 30 hours.

2.2 Consumables

Polystyrene (PS) granules (3–5 mm particle size; product Code: ST31-GL-000111; LS555533; batch C3586) were purchased from Goodfellow (Huntingdon, UK) and ground into smaller fragments employing low-temperature ball milling on a cryomill (Retsch GmbH, Haan, Germany) maintained between -196°C and -100°C using liquid nitrogen. A 50 mL cell and a 2 cm diameter steel ball were used for mechanical cryogenic grinding. A third of the cell was

filled with the plastic material and ground for approximately 30 minutes, with 5 minutes of pre-cooling. The plastic fragments were separated using a Vibratory Sieve shaker AS 300 Control (Retsch GmbH, Haan, Germany) via four sieves with mesh sizes of 100, 63, 45, and 25 μm according to ISO 3310-01 (ISO, 2016) and the size fraction 45 to 63 μm was used for the environmental leaching.

All other consumables were purchased from Sigma Aldrich unless stated otherwise and were of analytical grade.

2.3 Leachate preparation

Seawater and freshwater were collected from the North Sea, Knokke-Heist, Belgium (coordinates: 51.359060, 3.306336) and the Handelsdok Canal in Bruges, Belgium (coordinates: 51.221321, 3.223855), respectively, on the September 9th, 2021, as 100 L grab samples. The pH of the seawater and freshwater measured as 8.1 and 8.08, respectively. In the seawater sample, the salinity and conductivity values were 29.52 ppt and 45.79 $\mu\text{S/cm}$ and the media had a turbidity of 0.27. For the freshwater, the measurements were 2.12 ppt for salinity, 40.51 $\mu\text{S/cm}$ for conductivity, and 0.67 for turbidity respectively. The collected water samples were filtered via vacuum filtration (0.22 μm pore 19.6 cm^2 CA membrane) including a storage Bottle System (Cat. No. 430758, Corning Inc. Corning, US). PS fragments at a concentration of 100 g/L were added to each of the filtered waters (freshwater and seawater), respectively, as well as MilliQ water (pH 7.01) in capped glass vessels ($n = 3$) and placed outside for six months at the premises of KIST Europe in Saarbrücken from October 26, 2021, to April 30, 2022. The chosen PS concentration aligns with previous studies investigating the toxicity of microplastic (MP) leachates (Lithner et al., 2009; Lithner et al., 2012). MilliQ water was used to allow the evaluation of the toxicity of the PS leachate without the influence of ions, minerals, and microbes. The vessels were uncapped and aired daily. The leachate was filtered with a 0.45 μm GHP membrane prior to the exposure experiments to remove all MP. The seawater leachate had a pH of 7.88, salinity of 22.95 ppt, conductivity of 36.75 $\mu\text{S/cm}$ and turbidity of 3.41. Meanwhile, the freshwater leachate showed a pH of 7.69, salinity of 2.01, conductivity of 38.61 $\mu\text{S/cm}$ and turbidity of 1.54, respectively.

2.4 Exposures set up

D. magna neonates (5 organisms per replicate) were exposed to the PS leachate in MilliQ and freshwater, and *A. salina* (5 organisms per replicate) were exposed to the PS leachates in seawater, both at four concentrations (undiluted (100%), 50%, 25% and 10%) for 48 hours in triplicate. The dilutions were prepared in the organism cultivation media stipulated in section 2.2. These acute immobilisation tests were conducted according to the OECD guideline test no. 202 (OECD, 2004). After 12, 24, and 48 hours, immobilisation of each treatment replicate was observed and recorded. Organisms were considered immobile if they did not move after approximately 15 seconds of gentle stirring. The results were expressed as percentage mobility over time.

Based on the initial lethal response toxicity test, an exposure concentration of 50% dilution for *D. magna* and 10% for *A. salina* was selected. These leachate concentration percentages were selected based on the highest concentration that did not result in more than 80% mortality after 24 hours as live organisms were required to assess the physiological non-lethal effects.

For the analysis of the oxidative stress status (reactive oxygen species (ROS) level) and the antioxidative response analysis (catalase (CAT) and superoxide dismutase (SOD) activities), 70 neonate *D. magna* and 200 *A. salina* per replicate ($n = 3$) were exposed to each of the specified dilutions of the leachates for 24 hours against a control consisting only of the exposure media. Thereafter, one-third of the organisms per replicate were collected for ROS analysis, and the other two-thirds were collected for enzyme extraction and antioxidant defence analysis.

2.5 Oxidative stress status and response assays

For the ROS determination, as a measure of the oxidative stress status, one-third of the mobile daphnids were snap-frozen in liquid nitrogen and thoroughly homogenised in 1.0 mL phosphate-buffered saline (PBS), followed by centrifugation at $3,000 \times g$ at 4°C for 10 minutes. Then, 10 μL of supernatant was used to determine the protein content using a bicinchoninic acid kit (Thermo Fisher Scientific, Waltham, MA, USA). ROS levels were assessed by measuring the oxidation product of 2',7'-dichlorofluorescein (DCFDA) with excitation and emission spectra at 495 and 529 nm using the DCFDA/H2DCFDA Cellular ROS Assay Kit (catalogue no. ab113851; Abcam, Cambridge MA, USA) as per the manufacturer's instructions on a high-performance multi-mode microplate reader (SPARK, TECAN, Switzerland) using 20 μL of supernatant from each sample. The fluorescence intensities were normalised by the protein content of each specimen.

For extracting the S9 enzyme fraction, the other two-thirds of the mobile daphnids were snap-frozen in liquid nitrogen and homogenised with a micro-pestle in 20 mM potassium phosphate buffer (pH 7) on ice. Cell debris was removed by centrifugation at $13,000 \times g$ at 4°C for 10 minutes, and the supernatant was used to assess the enzyme activities. The SOD activity was evaluated using the SOD Assay Kit (19160-1KT-F; Sigma-Aldrich, St. Louis, Missouri, USA). CAT (E.C. 1.11.1.6) activity was assayed using hydrogen peroxide as substrate as per Claiborne (1985) on a Tecan Infinite 200 Pro Infinite M Nano+ (Tecan GmbH, Grödig, Austria). Catalase activity was normalised against the protein content, determined as per Bradford (1976), i.e., enzyme activity was calculated as nanokatal per milligram protein.

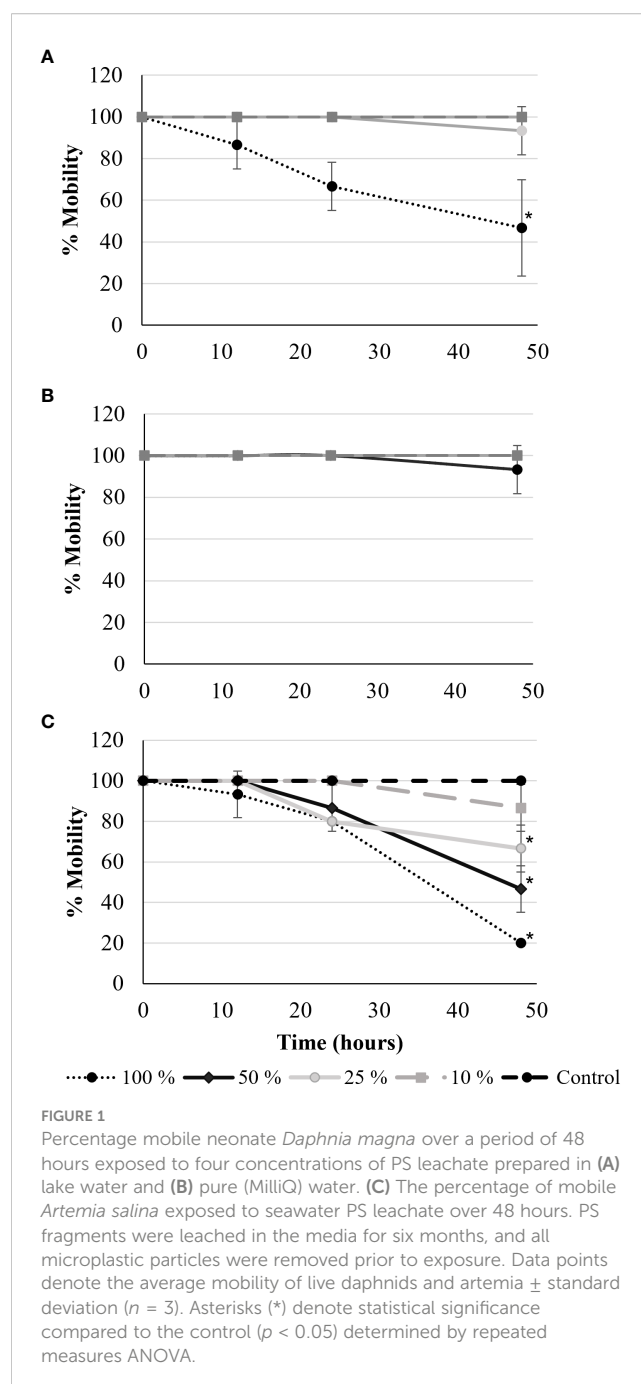
2.6 Statistical analysis

Statistical analysis was performed using IBM® SPSS® Statistics 28.0.0.0 (190) (2021). Descriptive analysis was performed on all data sets, followed by normality and homogeneity analysis. For the analysis of percentage survival over time, a repeated measures

analysis of variance (ANOVA) was performed, followed by Bonferroni posthoc. One-way ANOVA was performed for the antioxidant response data followed by Tukey posthoc tests observing an alpha value of 0.05, indicating statistical significance.

3 Results

D. magna neonates were exposed for 48 h to leachate prepared by incubating PS fragments in freshwater and pure (MilliQ) water, respectively, for 6 months in nature. At the same time, *A. salina* were exposed to leachate prepared by incubating PS-MP in seawater for six months. For neonate *D. magna*, exposed to the PS leachate in



freshwater (Figure 1A), 53.3% fewer neonates were mobile after 48 h of exposure to the undiluted leachate compared to the control ($p = 1.000$). At the same time, exposure to the 10%, 25%, and 50% concentrations of the leachate did not reduce daphnid mobility ($p = 0.001$). However, for neonates exposed to PS-leached in pure water (Figure 1B), mobility was not significantly affected with any of the concentrations of leachate over the 48 h exposure period ($p = 0.596$).

A. salina (Figure 1C) mobility was the most severely affected by the undiluted seawater leachate, with 80.0% of the organisms remaining mobile after 48 h compared to the control ($p < 0.001$). With the 50% and 25% concentrations, the mobility was 53.3% ($p < 0.001$) and 33.3% ($p = 0.001$), respectively. However, with 10% leachate, mobility was not affected ($p = 1.000$).

To evaluate physiological adverse effects in live, healthy organisms, the lowest leachate concentration that exhibited sublethal adverse effects was chosen for further assessment. Specifically, a concentration of 50% leachate was selected for *D. magna*, while for *A. salina*, a concentration of 10% leachate was deemed appropriate. The selection was based on the data obtained in Figure 1.

The cellular ROS concentration relative to the protein content was not elevated after 48 h of exposure to the 50% dilution of the freshwater PS-leachate ($p = 0.116$; Figure 2A). The ROS concentration in the neonates exposed to the 50% diluted pure water PS-leachate for 48 h was increased by 24.2% ($p = 0.022$; Figure 2A). As for *A. salina* after 48 h of exposure to the 10% seawater PS-leached (Figure 2B), the cellular ROS level was statistically equivalent compared to the control ($p = 0.064$).

The SOD activity was significantly elevated in neonate daphnids after 48 h of exposure to both freshwater PS-leachate as well as pure water PS-leachate compared to the control (Figure 3A). With exposure to the freshwater PS-leachate, the SOD activity was increased 104.6% ($p = 0.011$) and 100.3% with exposure to the pure water PS leachate ($p = 0.0140$). The SOD activity in *A. salina* (Figure 3B) was statistically equal to that of the control after 48 h of exposure to the seawater PS leachate ($p = 0.479$).

The CAT activities in neonate daphnids were unchanged relative to the control CAT activity after 48 h of exposure to freshwater as well as pure water PS-leachate ($p = 0.897$; Figure 4A). However, in *A. salina* (Figure 4B), CAT activity was significantly increased by 127.9% ($p = 0.002$).

4 Discussion

The goal of this study was to compare the toxicities of PS leachates prepared in three distinct media, seawater, freshwater, and sterile, pure water (MilliQ). These media were selected to represent the properties of natural water bodies in terms of pH, salinity, conductivity, and turbidity, compared to sterile, deionized, and demineralized water. The leachates produced using the various media resulted in significantly different toxic responses in the bioindicator organisms tested. Notably, PS leachate in MilliQ water was significantly less toxic to *D. magna* compared to PS leachate in freshwater as is evidenced by the immobilization over time. The immobile organisms were not swimming after 15 seconds of agitation. They had all sunken to the bottom of the exposure vessel and their antennae or feeding apparatus showed no movement, which could indicate physiological toxicity leading to death rather than a physical impairment. Additives, which are mostly bound to the MPs by weak dispersion forces (Zhang and Chen, 2014), can leach from plastic materials with fragmentation and degradation accelerating the release of chemicals (Engler, 2012). Since all microplastic fragments were removed before exposure, only leached chemicals could have contributed to the observed immobilization, an established indicator of acute toxicity (OECD, 2004). The additives used in the manufacture of the PS could not be disclosed by the supplier. Nevertheless, several common plastic additives (Smith and Taylor, 2002; Samadi et al., 2022) have been identified as toxic to *D. magna* and other aquatic organisms (Thaysen et al., 2018; Schiavo et al., 2021; Song et al., 2021; Blinova et al., 2023).

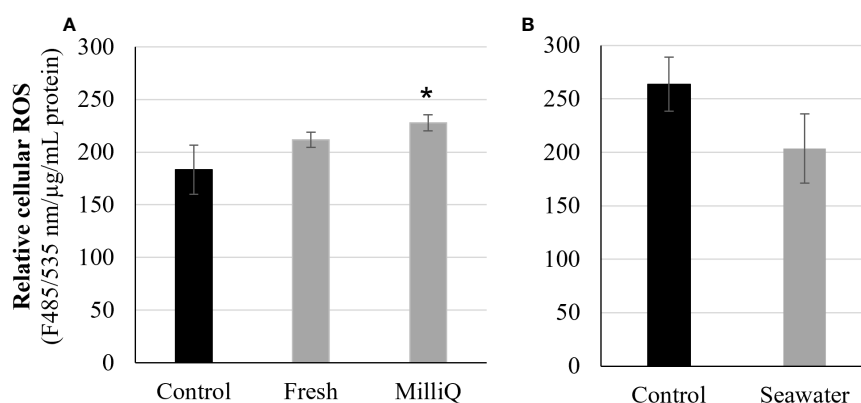


FIGURE 2

Relative cellular reactive oxygen species (ROS) (fluorescence/mg/mL protein) levels in (A) neonate *Daphnia magna* exposed to 50% PS-leachate in freshwater and pure water as well as (B) *Artemia salina* exposed to 10% PS-leachate in seawater after 48 (h) Bars represent the average ROS (fluorescence/mg/mL protein) concentration \pm standard deviation ($n = 3$). Asterisks (*) denote statistical significance compared to the control ($p < 0.05$) determined by one-way ANOVA and Tukey posthoc.

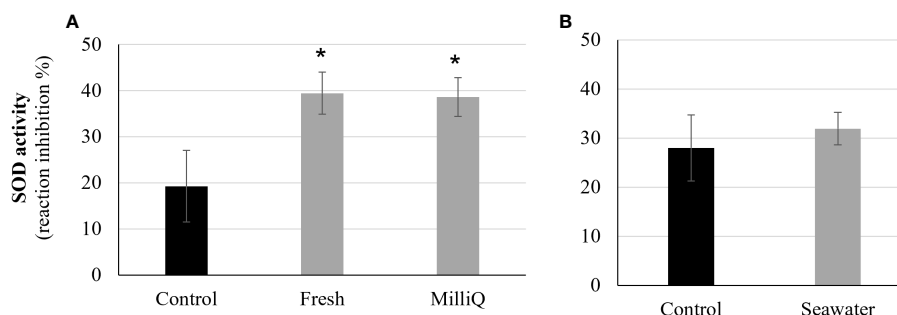


FIGURE 3

Superoxide dismutase (SOD) activity (expressed as percentage inhibition of the coupled reaction) in (A) neonate *Daphnia magna* exposed to 50% PS-leachate in freshwater and pure water as well as (B) *Artemia salina* exposed to 10% PS-leachate in seawater for 48 (h) Bars represent the average SOD activity \pm standard deviation ($n = 3$). Asterisks (*) denote statistical significance compared to the control ($p < 0.05$) determined by one-way ANOVA and Tukey posthoc.

In general, *D. magna* was less susceptible to the PS-leachate. Only the undiluted PS-leachate in freshwater caused significant changes in mobility. Lithner et al. (2012) leached plastics from old electronic products in water for three days at the same concentration as used in the present study (100 g/L). They found that after acute exposure (24 h and 48 h) the leachate was non-toxic to *D. magna*. Furthermore, in 2009, Lithner (2011) reported that leachate prepared from PS (100 g/L) did not cause immobilisation of *D. magna*. However, as deionized water was used, this result concurs with our immobilization findings of daphnids exposed to PS leachate prepared in MilliQ water.

A previous study reported an LD₅₀ of 67 mg/L for 1 μ m PS beads in *D. magna* (Miloloža et al., 2021). Nevertheless, the PS concentration used to prepare the leachate in the present study (100 g/L) far exceeds the highest environmental concentrations reported for PS (Schirrinzi et al., 2019; Scopetani et al., 2019; Badylak et al., 2021) and MP in general. Up to 4650 particles/m³ have been detected in freshwater and 102,000 particles/m³ in coastal waters (Wong et al., 2020; Zhang et al., 2020). A conversion from particles per volume to weight per volume was proposed by Leusch and Ziajahromi (2021). However, this accounts for the specific uniform size of reference particles and the density of a specific polymer. Assuming an average size of 1 μ m and the density of PS (1.05 g/cm³), the environmental concentrations reported may be equivalent

to several orders of magnitude less than the PS concentration used in the present study to prepare the leachate. Thus, leachates from the current level of MP pollution in the environment should not pose a significant threat to *D. magna*. Nevertheless, MP hotspots may form due to water currents, with localized concentrations exceeding millions of particles per litre (Kane et al., 2020), which should be considered in the comprehensive risk assessment of MPs and their leachates in the environment.

A. salina was significantly more affected by the leachate compared to the *D. magna*. This may indicate an overall higher susceptibility, or it could be related to the seawater and associated microbiota facilitating a larger concentration of toxicants to be released from the MP. However, in studies comparing the sensitivities of common bioassay organisms to toxicants, *A. salina* was significantly less susceptible compared to *D. magna* (Minguez et al., 2014). Furthermore, the study by Wang et al. (2019) showed that *Artemia parthenogenetica* was not significantly affected by exposure to various concentrations of PS-MP in terms of survival, growth, or development, irrespective of acute or chronic exposure. In support of this, the study by Sait et al. (2021) demonstrated that salinity facilitates additive leaching.

Due to the mobility and distribution of MP, it has been distributed ubiquitously throughout the global marine environment (Cai et al., 2023; Li et al., 2023; Tian et al., 2023).

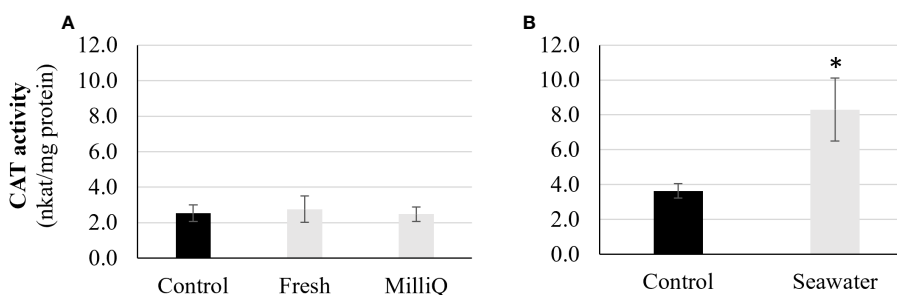


FIGURE 4

Catalase (CAT) activity (nkat/mg protein) in (A) neonate *Daphnia magna* exposed to 50% PS-leachate in freshwater and pure water as well as (B) *Artemia salina* exposed to 10% PS-leachate in seawater for 48 (h) Bars represent the average CAT activity \pm standard deviation ($n = 3$). Asterisks (*) denote statistical significance compared to the control ($p < 0.05$) determined by one-way ANOVA and Tukey posthoc.

Furthermore, in a review by [Wagner et al. \(2014\)](#), they stated that due to specific oceanic hydrology, plastic pollution accumulates in large oceanic gyres (garbage patches), resulting in more MP than zooplankton. Considering this concentration of plastic pollution in oceanic hotspots, together with the significant impact of the leachate observed on *A. salina*, the risk of leachate from pollution in marine environments to zooplankton is of concern and poses a threat to marine ecosystems.

Microbes, including bacteria, algae, and fungi, are recognized for their role in facilitating the degradation of plastics through both enzymatic and nonenzymatic hydrolysis of polymers ([Devi et al., 2016](#); [Amobonye et al., 2021](#)). Even though the collected waters were filtered through a 0.22 µm filter, removing the majority of microbes, some may have passed into the leaching media ([Hahn, 2004](#)). Consequently, the increased toxicity leading to immobilization observed with the leachates in fresh- and seawater, compared to the pure water, could, to some degree, be attributed to microbial action facilitating degradation and allowing more toxicants to be liberated from the plastic material. Furthermore, the potential impact of microbial metabolites, such as exopolysaccharides, on oxidative stress and, consequently, overall toxicity should not be underestimated ([Kavita et al., 2022](#)).

Furthermore, POPs, antibiotics, and heavy metals sorb to plastic debris from the surrounding environment ([Liu et al., 2023](#)). Therefore, as the fresh and seawater were collected from natural sources, POPs may have been present and could have contributed to increased toxicity in addition to leached chemicals. Thus, when assessing the risk of MP and leachate, it is essential to these chemical toxicants and their potential additive or synergistic effects on the overall toxicity.

One of the most common non-lethal endpoints observed as a measure of toxicity is oxidative stress and the corresponding antioxidant responses (consisting of superoxide dismutase (SOD), glutathione peroxidase (GPx), catalase (CAT), glutathione reductase (GR), glutathione-S-transferase (GST) and other low molecular weight scavengers such as glutathione, ascorbate, vitamin E, β-carotene and proteins) which combat cellular damage by maintaining the homeostasis of ROS ([Yu, 1994](#)). Elevated ROS, an indication of oxidative stress, was only observed in daphnids when exposed to the leachate prepared in pure water. However, this was accompanied by a corresponding increase in the SOD activity, which catalysis the conversion of ROS to hydrogen peroxide. Despite CAT not being activated, this daphnid treatment had the lowest corresponding immortality. Thus, hydrogen peroxide generated from SOD may have been made innocuous by other antioxidative enzymes such as peroxidase, glutathione peroxidase or ascorbate peroxidase ([Yu, 1994](#)). In neonates exposed to the leachate prepared in freshwater, ROS homeostasis was maintained as is evident by the still lingering elevated SOD activity. A previous study investigating the effects of PS leachate (50 mg/L) on neonate and adult daphnia found that in neonates ROS was not elevated and SOD activity was not affected but CAT activity was suppressed, with no associated mortality. The authors speculated that the non-enzymatic oxidative stress system may have been involved in maintaining homeostasis. In contrast to *D. magna*'s antioxidant response, the *A. salina*'s catalase activity was elevated after 48 h of exposure indicating its involvement in

maintaining homeostasis and ensuring mobility and survival. This illustrates the vast differences in species' response to toxicants.

In conclusion, the physiological data shows that both indicator organisms' antioxidant response systems could maintain homeostasis at low concentrations of the leachate and considering the currently reported average MP concentrations, leachates from plastic do not pose a severe threat to these organisms. Nevertheless, the potential formation of plastic accumulation points, commonly known as "garbage patches," raises concerns, as these circumstances may lead to elevated concentrations of leachates, potentially resulting in severe adverse effects on native biota, particularly in saline environments.

Data availability statement

The raw data supporting the conclusions of this article will be made available by the authors, without undue reservation.

Ethics statement

The manuscript presents research on animals that do not require ethical approval for their study.

Author contributions

ME: Conceptualization, Data curation, Funding acquisition, Methodology, Project administration, Resources, Supervision, Validation, Visualization, Writing – original draft, Writing – review & editing. S-AL: Conceptualization, Formal analysis, Methodology, Resources, Supervision, Writing – review & editing. YK: Conceptualization, Investigation, Methodology, Supervision, Validation, Writing – review & editing. RJ: Formal analysis, Investigation, Methodology, Writing – review & editing. YJK: Conceptualization, Funding acquisition, Project administration, Supervision, Writing – review & editing.

Funding

The author(s) declare financial support was received for the research, authorship, and/or publication of this article. This work was partly supported by the Nanomaterial Technology Development Program (NRF-2017M3A7B6052455), funded by the South Korean Ministry of Science and the National Research Council of Science & Technology (NST, Global-23-004) grant by the Strategies for Establishing Global Research Networks. The University of Helsinki Library provided open-access funding.

Conflict of interest

ME and RJ were not employed by KIST EU. This is a research institute and we are affiliated via research agreements.

Publisher's note

All claims expressed in this article are solely those of the authors and do not necessarily represent those of their affiliated

organizations, or those of the publisher, the editors and the reviewers. Any product that may be evaluated in this article, or claim that may be made by its manufacturer, is not guaranteed or endorsed by the publisher.

References

- Albarano, L., Ruocco, N., Lofrano, G., Guida, M., and Libralato, G. (2022). Genotoxicity in *Artemia* spp.: An old model with new sensitive endpoints. *Aquat. Toxicol.* 252, 106320. doi: 10.1016/j.aquatox.2022.106320
- Amobonye, A., Bhagwat, P., Singh, S., and Pillai, S. (2021). Plastic biodegradation: Frontline microbes and their enzymes. *Sci. Total Environ.* 759, 143536. doi: 10.1016/j.scitotenv.2020.143536
- Andrady, A. L., and Rajapakse, N. (2016). "Additives and chemicals in plastics," in *Hazardous chemicals associated with plastics in the marine environment, the Handbook of Environmental Chemistry*, vol. 78. Eds. H. Takada and H. Karapanagioti (Cham: Springer), 1–17. doi: 10.1007/698_2016_124
- Araújo, P. H. H., Sayer, C., Giudici, R., and Poço, J. G. R. (2002). Techniques for reducing residual monomer content in polymers: A review. *Polym. Eng. Sci.* 184, 1442–1468. doi: 10.1002/pen.11043
- Badylak, S., Phlips, E., Batich, C., Jackson, M., and Wachnicka, A. (2021). Polystyrene microplastic contamination versus microplankton abundances in two lagoons of the Florida Keys. *Sci. Rep.* 11, 6029. doi: 10.1038/s41598-021-85388-y
- Blinova, I., Lukjanova, A., Vija, H., Mortimer, M., and Heinlaan, M. (2023). Toxicity of plastic additive 1-hydroxycyclohexyl phenyl ketone (1-HCHPK) to freshwater microcrustaceans in natural water. *Water* 15 (18), 3213. doi: 10.3390/w15183213
- Bradford, M. M. (1976). A rapid and sensitive method for the quantitation of microgram quantities of protein utilizing the principle of protein-dye binding. *Anal. Biochem.* 72, 248–254. doi: 10.1006/abio.1976.9999
- Bridson, J. H., Gaugler, E. C., Smith, D. A., Northcott, G. L., and Gaw, S. (2021). Leaching and extraction of additives from plastic pollution to inform environmental risk: a multidisciplinary review of analytical approaches. *J. Hazard. Mater.* 414, 125571. doi: 10.1016/j.jhazmat.2021.125571
- Cai, C., Zhu, L., and Hong, B. (2023). A review of methods for modeling microplastic transport in the marine environments. *Mar. pollut. Bull.* 193, 115136. doi: 10.1016/j.marpolbul.2023.115136
- Caruso, G. (2019). Microplastics as vectors of contaminants. *Mar. pollut. Bull.* 146, 921–924. doi: 10.1016/j.marpolbul.2019.07.052
- Claiborne, A. (1985). "Catalase activity," in *CRC Handbook of Methods for Oxygen Radical Research*. Ed. R. A. Greenwald (Boca Raton: CRC Press), 283–284.
- Crompton, T. R. (1979). *Additive migration from plastics into food. 1st ed* (New York: Pergamon Press).
- Dahlbo, H., Poliakov, V., Mylläri, V., Sahimaa, O., and Anderson, R. (2018). Recycling potential of post-consumer plastic packaging waste in Finland. *Waste Manage.* 71, 52–61. doi: 10.1016/j.wasman.2017.10.033
- Devi, R. S., Kannan, V. R., Natarajan, K., Nivas, D., Kannan, K., Chandru, S., et al. (2016). "The role of microbes in plastic degradation," in *Environmental Waste Management*. Ed. R. Chandra (Boca Raton: CRC Press), 341–370.
- Do, A. T. N., Ha, Y., and Kwon, J. H. (2022). Leaching of microplastic-associated additives in aquatic environments: a critical review. *Environ. pollut.* 305, 119258. doi: 10.1016/j.envpol.2022.119258
- Engler, R. E. (2012). The complex interaction between marine debris and toxic chemicals in the ocean. *Environ. Sci. Technol.* 46 (22), 12302–12315. doi: 10.1021/es3027105
- Esterhuizen, M., and Kim, Y. J. (2022). Effects of polypropylene, polyvinyl chloride, polyethylene terephthalate, polyurethane, high-density polyethylene, and polystyrene microplastic on *Nelumbo nucifera* (Lotus) in water and sediment. *Environ. Sci. pollut. Res.* 29, 17580–17590. doi: 10.1007/s11356-021-17033-0
- European Chemicals Bureau (ECB) (2008) *ESIS – European Chemical Substances Information System*. Available at: <http://ecb.jrc.it/esis/> (Accessed April 12, 2023).
- Groh, K. J., Backhaus, T., Carney-Almroth, B., Geueke, B., Inostroza, P. A., Lennquist, A., et al. (2019). Overview of known plastic packaging-associated chemicals and their hazards. *Sci. Total Environ.* 651, 3253–3268. doi: 10.1016/j.scitotenv.2018.10.015
- Gunaalan, K., Fabbri, E., and Capolupo, M. (2020). The hidden threat of plastic leachates: A critical review on their impacts on aquatic organisms. *Water Res.* 184, 116170. doi: 10.1016/j.watres.2020.116170
- Hahladakis, J. N., Velis, C. A., Weber, R., Iacovidou, E., and Purnell, P. (2018). An overview of chemical additives present in plastics: Migration, release, fate and environmental impact during their use, disposal and recycling. *J. Hazard. Mater.* 344, 179–199. doi: 10.1016/j.jhazmat.2017.10.014
- Hahn, M. W. (2004). Broad diversity of viable bacteria in 'sterile' (0.2 µm) filtered water. *Res. Microbiol.* 155 (8), 688–691. doi: 10.1016/j.resmic.2004.05.003
- Han, Y. N., Wei, M., Han, F., Fang, C., Wang, D., Zhong, Y. J., et al. (2020). Greater biofilm formation and increased biodegradation of polyethylene film by a microbial consortium of *Arthrobacter* sp. and *Streptomyces* sp. *Microorganisms* 8, 1979. doi: 10.3390/microorganisms8121979
- International standards organisation (ISO). (2016). *3310-1: Test Sieves Technical Requirements and Testing—Part 1: Test Sieves of Metal wire Cloth*. Geneva, Switzerland: ISO.
- Kalčíková, G., Zagorc-Končan, J., and Žgajnar Gotvajn, A. (2012). *Artemia salina* acute immobilization test: a possible tool for aquatic ecotoxicity assessment. *Water Sci. Technol.* 66 (4), 903–908. doi: 10.2166/wst.2012.271
- Kane, I. A., Clare, M. A., Miramontes, E., Wogelius, R., Rothwell, J. J., Garreau, P., et al. (2020). Seafloor microplastic hotspots controlled by deep-sea circulation. *Science* 368 (6495), 1140–1145. doi: 10.1126/science.aba589
- Kavitake, D., Veerabhadrapa, B., Sudharshan, S. J., Kandasamy, S., Devi, P. B., Dyavaiah, M., et al. (2022). Oxidative stress alleviating potential of galactan exopolysaccharide from *Weissella confusa* KR780676 in yeast model system. *Sci. Rep.* 12, 1089. doi: 10.1038/s41598-022-05190-2
- Kwan, C. S., and Takada, H. (2016). "Release of additives and monomers from plastic wastes," in *Hazardous chemicals associated with plastics in the marine environment. The Handbook of Environmental Chemistry*, vol. 78. Eds. H. Takada and H. Karapanagioti (Cham: Springer), 51–70. doi: 10.1007/698_2016_122
- Leusch, F. D., and Ziajahromi, S. (2021). Converting mg/L to particles/L: Reconciling the occurrence and toxicity literature on microplastics. *Environ. Sci. Technol.* 55 (17), 11470–11472. doi: 10.1021/acs.est.1c04093
- Li, J., Shan, E., Zhao, J., Teng, J., and Wang, Q. (2023). The factors influencing the vertical transport of microplastics in marine environment: A review. *Sci. Total Environ.* 870, 161893. doi: 10.1016/j.scitotenv.2023.161893
- Lithner, D. (2011). *Environmental and health hazards of chemicals in plastic polymers and products. PhD thesis* (Sweden: University of Gothenburg).
- Lithner, D., Damberg, J., Dave, G., and Larsson, Å. (2009). Leachates from plastic consumer products-screening for toxicity with *Daphnia magna*. *Chemosphere* 74, 1195–1200. doi: 10.1016/j.chemosphere.2008.11.022
- Lithner, D., Halling, M., and Dave, G. (2012). Toxicity of electronic waste leachates to *Daphnia magna*: screening and toxicity identification evaluation of different products, components, and materials. *Arch. Environ. Contam. Toxicol.* 62, 579–588. doi: 10.1007/s00244-011-9729-0
- Lithner, D., Larsson, Å., and Dave, G. (2011). Environmental and health hazard ranking and assessment of plastic polymers based on chemical composition. *Sci. Total Environ.* 409, 3309–3324. doi: 10.1016/j.scitotenv.2011.04.038
- Liu, P., Dai, J., Huang, K., Yang, Z., Zhang, Z., and Guo, X. (2023). Sources of micro (nano) plastics and interaction with co-existing pollutants in wastewater treatment plants. *Crit. Rev. Environ. Sci. Technol.* 53 (7), 865–885. doi: 10.1080/10643389.2022.2095844
- Mammo, F. K., Amoah, I. D., Gani, K. M., Pillay, L., Ratha, S. K., Bux, F., et al. (2020). Microplastics in the environment: Interactions with microbes and chemical contaminants. *Sci. Total Environ.* 743, 140518. doi: 10.1016/j.scitotenv.2020.140518
- Miloloža, M., Kučić Grgić, D., Bolanča, T., Ukić, Š, Cvetnić, M., Očelić Bulatović, V., et al. (2021). Ecotoxicological assessment of microplastics in freshwater sources—A review. *Water* 13 (1), 56. doi: 10.3390/w13010056
- Minguez, L., Di Poi, C., Farcy, E., Ballandonne, C., Benchouala, A., Bojic, C., et al. (2014). Comparison of the sensitivity of seven marine and freshwater bioassays as regards antidepressant toxicity assessment. *Ecotoxicol.* 23, 1744–1754. doi: 10.1007/s10646-014-1339-y
- OECD. (2004). *Daphnia sp. Acute Immobilisation Test*, OECD Guidelines for the Testing of Chemicals, Section 2, OECD Publishing Paris. doi: 10.1787/9789264069947-en
- Organisation for Economic Co-operation and Development (OECD). (2009). *Emission Scenario Document on Plastic Additives: Series on Emission Scenario Documents* (Paris: OECD Environmental Health and Safety Publications No. 3. OECD Environment Directorate). doi: 10.1787/9789264221291-en
- Patti, T. B., Fobert, E. K., Reeves, S. E., and da Silva, K. B. (2020). Spatial distribution of microplastics around an inhabited coral island in the Maldives, Indian Ocean. *Sci. Total Environ.* 748, 141263. doi: 10.1016/j.scitotenv.2020.141263

- Pflugmacher, S., Sulek, A., Mader, H., Heo, J., Noh, J. H., Penttinen, O. P., et al. (2020). The influence of new and artificial aged microplastic and leachates on the germination of *Lepidium sativum* L. *Plants* 9, 339. doi: 10.3390/plants9030339
- Prabhu, P. P., Pan, K., and Krishnan, J. N. (2022). Microplastics: Global occurrence, impact, characteristics and sorting. *Front. Mar. Sci.* 9. doi: 10.3389/fmars.2022.893641
- Reilly, K., Ellis, L. A., Davoudi, H. H., Supian, S., Maia, M. T., Silva, G. H., et al. (2023). *Daphnia* as a model organism to probe biological responses to nanomaterials—from individual to population effects via adverse outcome pathways. *Front. Toxicol.* 5. doi: 10.3389/ftox.2023.1178482
- Sait, S. T., Sørensen, L., Kubowicz, S., Vike-Jonas, K., Gonzalez, S. V., Asimakopoulos, A. G., et al. (2021). Microplastic fibres from synthetic textiles: Environmental degradation and additive chemical content. *Environ. pollut.* 268, 115745. doi: 10.1016/j.envpol.2020.115745
- Samadi, A., Kim, Y., Lee, S. A., Kim, Y. J., and Esterhuizen, M. (2022). Review on the ecotoxicological impacts of plastic pollution on the freshwater invertebrate *Daphnia*. *Environ. Toxicol.* 37, 2615–2638. doi: 10.1002/tox.23623
- Schiavo, S., Oliviero, M., Chiavarini, S., Dumontet, S., and Manzo, S. (2021). Polyethylene, Polystyrene, and Polypropylene leachate impact upon marine microalgae *Dunaliella tertiolecta*. *J. Toxicol. Environ. Health A* 84 (6), 249–260. doi: 10.1080/15287394.2020.1860173
- Schirizzi, G. F., Llorca, M., Seró, R., Moyano, E., Barceló, D., Abad, E., et al. (2019). Trace analysis of polystyrene microplastics in natural waters. *Chemosphere* 236, 124321. doi: 10.1016/j.chemosphere.2019.07.052
- Scopetani, C., Chelazzi, D., Cincinelli, A., and Esterhuizen-Londt, M. (2019). Assessment of microplastic pollution: occurrence and characterisation in Vesijärvi lake and Pikku Vesijärvi pond, Finland. *Environ. Monit. Assess.* 191, 652. doi: 10.1007/s10661-019-7843-z
- Smith, S. H., and Taylor, L. T. (2002). Extraction of various additives from polystyrene and their subsequent analysis. *Chromatographia* 56, 65–169. doi: 10.1007/BF02493206
- Song, J., Na, J., An, D., and Jung, J. (2021). Role of benzophenone-3 additive in chronic toxicity of polyethylene microplastic fragments to *Daphnia magna*. *Sci. Total Environ.* 800, 149638. doi: 10.1016/j.scitotenv.2021.149638
- Sooriyakumar, P., Bolan, N., Kumar, M., Singh, L., Yu, Y., Li, Y., et al. (2022). Biofilm formation and its implications on the properties and fate of microplastics in aquatic environments: a review. *J. Hazard. Mater. Adv.* 6, 100077. doi: 10.1016/j.hazadv.2022.100077
- Stevens, M. P. (1990). *Polymer chemistry* Vol. 2 (New York: Oxford University Press).
- Thaysen, C., Stevack, K., Ruffolo, R., Poirier, D., De Frond, H., De Vera, J., et al. (2018). Leachate from expanded polystyrene cups is toxic to aquatic invertebrates (*Ceriodaphnia dubia*). *Front. Mar. Sci.* 5. doi: 10.3389/fmars.2018.00071
- Tian, W., Song, P., Zhang, H., Duan, X., Wei, Y., Wang, H., et al. (2023). Microplastic materials in the environment: Problem and strategic solutions. *Prog. Mater. Sci.* 132, 101035. doi: 10.1016/j.pmatsci.2022.101035
- van Velzen, E. U. T., Brouwer, M. T., and Feil, A. (2019). Collection behaviour of lightweight packaging waste by individual households and implications for the analysis of collection schemes. *Waste Manage.* 89, 284–293. doi: 10.1016/j.wasman.2019.04.021
- Wagner, M., Scherer, C., Alvarez-Muñoz, D., Brennholt, N., Bourrain, X., Buchinger, S., et al. (2014). Microplastics in freshwater ecosystems: what we know and what we need to know. *Environ. Sci. Eur.* 26 (1), 1–9. doi: 10.1186/s12302-014-0012-7
- Wang, Y., Zhang, D., Zhang, M., Mu, J., Ding, G., Mao, Z., et al. (2019). Effects of ingested polystyrene microplastics on brine shrimp, *Artemia parthenogenetica*. *Environ. pollut.* 244, 715–722. doi: 10.1016/j.envpol.2018.10.024
- Wiesinger, H., Wang, Z., and Hellweg, S. (2021). Deep dive into plastic monomers, additives, and processing aids. *Environ. Sci. Technol.* 55, 9339–9351. doi: 10.1021/acs.est.1c00976
- Wong, J. K. H., Lee, K. K., Tang, K. H. D., and Yap, P.-S. (2020). Microplastics in the freshwater and terrestrial environments: Prevalence, fates, impacts and sustainable solutions. *Sci. Total Environ.* 719, 137512. doi: 10.1016/j.scitotenv.2020.137512
- Yu, B. P. (1994). Cellular defenses against damage from reactive oxygen species. *Physiol. Rev.* 74 (1), 139–162. doi: 10.1152/physrev.1994.74.1.139
- Zhang, X., and Chen, Z. (2014). Observing phthalate leaching from plasticized polymer films at the molecular level. *Langmuir* 30, 17, 4933–4944. doi: 10.1021/la500476u
- Zhang, Y., Kang, S., Allen, S., Allen, D., Gao, T., and Sillanpää, M. (2020). Atmospheric microplastics: A review on current status and perspectives. *Earth-Sci. Rev.* 203, 103118. doi: 10.1016/j.earscirev.2020.103118



OPEN ACCESS

APPROVED BY
Frontiers Editorial Office,
Frontiers Media SA, Switzerland

*CORRESPONDENCE
Frontiers Production Office
✉ production.office@frontiersin.org

RECEIVED 03 July 2024

ACCEPTED 03 July 2024

PUBLISHED 15 July 2024

CITATION

Frontiers Production Office (2024) Erratum:
Ecotoxicological consequences of
polystyrene naturally leached in pure, fresh,
and saltwater: lethal and nonlethal
toxicological responses in *Daphnia magna*
and *Artemia salina*.
Front. Mar. Sci. 11:1458834.
doi: 10.3389/fmars.2024.1458834

COPYRIGHT

© 2024 Frontiers Production Office. This is an
open-access article distributed under the terms
of the [Creative Commons Attribution License](https://creativecommons.org/licenses/by/4.0/)
(CC BY). The use, distribution or reproduction
in other forums is permitted, provided the
original author(s) and the copyright owner(s)
are credited and that the original publication
in this journal is cited, in accordance with
accepted academic practice. No use,
distribution or reproduction is permitted
which does not comply with these terms.

Erratum: Ecotoxicological consequences of polystyrene naturally leached in pure, fresh, and saltwater: lethal and nonlethal toxicological responses in *Daphnia magna* and *Artemia salina*

Frontiers Production Office*

Frontiers Media SA, Lausanne, Switzerland

KEYWORDS

aquatic organisms, planktonic organisms, plastic leachate, microplastic, oxidative stress, ecotoxicology

An Erratum on

[Ecotoxicological consequences of polystyrene naturally leached in pure, fresh, and saltwater: lethal and nonlethal toxicological responses in *Daphnia magna* and *Artemia salina*](#)

By Esterhuizen M, Lee S-A, Kim Y, Järvinen R and Kim YJ (2024). *Front. Mar. Sci.* 11:1338872.
doi: 10.3389/fmars.2024.1338872

Due to a production error, an author's name was incorrectly spelled as "Young Jun".
The correct spelling is "Young Jun Kim".

The publisher apologizes for this mistake.

The original version of this article has been updated.



OPEN ACCESS

EDITED BY

Kun Chen,
Jiangsu University, China

REVIEWED BY

Yao Zheng,
Chinese Academy of Fishery Sciences
(CAFS), China
Futian Li,
Jiangsu Ocean University, China

*CORRESPONDENCE

Yurong Zhang
✉ yurongzhang2008@163.com

RECEIVED 09 November 2023

ACCEPTED 28 February 2024

PUBLISHED 18 March 2024

CITATION

Lin Y, Li T and Zhang Y (2024) Effects of two
typical quinolone antibiotics in the marine
environment on *Skeletonema costatum*.
Front. Mar. Sci. 11:1335582.
doi: 10.3389/fmars.2024.1335582

COPYRIGHT

© 2024 Lin, Li and Zhang. This is an open-
access article distributed under the terms of
the [Creative Commons Attribution License](#)
(CC BY). The use, distribution or reproduction
in other forums is permitted, provided the
original author(s) and the copyright owner(s)
are credited and that the original publication
in this journal is cited, in accordance with
accepted academic practice. No use,
distribution or reproduction is permitted
which does not comply with these terms.

Effects of two typical quinolone antibiotics in the marine environment on *Skeletonema costatum*

Yuxin Lin¹, Tiejun Li² and Yurong Zhang^{2*}

¹School of Fishery, Zhejiang Ocean University, Zhoushan, China, ²Zhejiang Marine Fisheries Research Institute, Key Lab of Mariculture and Enhancement of Zhejiang Province, Zhoushan, China

This study investigated the effects of levofloxacin (LEV) and norfloxacin (NOR) on *Skeletonema costatum*, focusing on cell growth, chlorophyll a (Chla) content, maximal quantum yield of PSII (*Fv/Fm*), protein content, enzyme activities of superoxide dismutase (SOD), glutathione reductase (GR), and glutathione peroxidase (GSH-PX), and the membrane lipid peroxidation product malondialdehyde (MDA) content were conducted to analyze the responses of *S. costatum* under LEV and NOR exposure. Cell growth, Chla content, *Fv/Fm*, protein content, enzyme activities, and MDA content were assessed to elucidate physiological changes. Both LEV and NOR inhibited *S. costatum* growth, except for 10 mg/L NOR, which promoted growth. Algal cells exhibited higher sensitivity to LEV, with 96h-IC₅₀ values of 14.770 mg/L for LEV and 44.250 mg/L for NOR. Low NOR concentration (10 mg/L) increased Chla content, while high antibiotic concentrations (>20 mg/L for LEV, >100 mg/L for NOR) decreased Chla content and *Fv/Fm*, indicating an impact on photosynthesis. Elevated LEV and NOR levels reduced protein and MDA content but increased GR, SOD, and GSH activities, indicating induced oxidative stress. The study provides a comprehensive analysis of LEV and NOR effects on marine microalgae growth and underlying physiological mechanisms, shedding light on potential ecological risks posed by antibiotics in marine ecosystems.

KEYWORDS

levofloxacin, norfloxacin, *Skeletonema costatum*, photosynthesis, antioxidant system

1 Introduction

Antibiotics are extensively employed globally in sectors like animal husbandry, aquaculture, and human healthcare (Zhang et al., 2023). In natural water bodies, the transformation of antibiotics mainly occurs through hydrolysis, photolysis, absorption, adsorption, and biodegradation (Martinez, 2009; Zhang et al., 2020a; Leung et al., 2012). Organisms are unable to fully absorb antibiotics and approximately 90% of antibiotics consumed are excreted by humans and livestock in their original or metabolized form, ultimately entering the environment directly or after wastewater treatment (Huang

et al., 2020). Existing research has confirmed that Antibiotics present in the environment may pose a risk to the health of both humans and animal, as well as ecosystem integrity through the food chain and food web (Huang et al., 2014). Data on antibiotics reported from 2009 to 2022 indicate that in China, antibiotic concentrations have been detected at the micrograms per liter ($\mu\text{g/L}$) level in two-thirds of marine areas, with overall concentrations ranging from 0.04 to 6,800 ng/L (Gao et al., 2023). Quinolone antibiotics have been detected in the seas of Bohai, East China, and South China. Ofloxacin (OFX) and norfloxacin (NOR) are commonly found antibiotics in the Bohai Sea, with concentrations varying between 3 and 5,100 ng/L, 3 and 6,800 ng/L, respectively (Zou et al., 2011). Additionally, in 2017, the highest concentration of NOR, reaching a maximum of 1,990 ng/L, was detected in water samples collected along China's approximately 18,000 km coastline (Lu et al., 2018).

Levofloxacin (LEV) is the levorotatory enantiomer of OFX and is used more widely due to its stronger antibacterial properties compared with OFX. Research on LEV is primarily concentrated within the medical realm (Liou et al., 2016; White et al., 2019), with relatively little research on its effects on microalgae (Pan et al., 2009; Wan et al., 2014). Most research on NOR has focused on clarifying its short-term toxicity to large *Daphnia*, freshwater fish, and freshwater algae (Gonzalez-Pleiter et al., 2013; Liang et al., 2015; Pan et al., 2017; Xiong et al., 2017a; Eluk et al., 2021), with relatively less research on the impacts of NOR on marine microalgae (Aderemi et al., 2018; Dow et al., 2020).

Marine microalgae serve as primary producers within marine aquatic ecosystems, exerting a profound influence on the system's structure and function. The diverse array of microalgae, coupled with their significant primary productivity, profoundly influences the dynamics of the entire aquatic ecosystem (Nie et al., 2013; Wan et al., 2015). Although antibiotics in the marine environment are typically found at low concentrations, they can still affect certain highly sensitive aquatic organisms. As antibiotics accumulate, they may impact the intricate community dynamics within marine ecosystems. Studies have shown that antibiotics affect the photosynthetic capability, cellular reproduction, and algae growth through impeding chloroplast formation, protein synthesis, and damaging to chlorophyll. As a result, the levels of Chla and maximal quantum yield of PSII (*Fv/Fm*) in algal cells are diminished to varying extents (Pinckney et al., 2013; Liu et al., 2018; Mao et al., 2021). Low concentrations of antibiotics may stimulate the expression of genes related to DNA replication, exhibiting a promotive effect (Jiang et al., 2021). This response may differ based on the type of antibiotics or the species of microalgae (Chen and Guo, 2012; Zhang et al., 2021b). The growth and photosynthesis of algal cells are impacted by antibiotics, leading to the production of reactive oxygen species (ROS), which in turn inflict damage upon the cells. During this process, malondialdehyde (MDA) is produced, and its production directly reflects the cell's oxidative stress level (Koussevitzky et al., 2007). To mitigate the harmful effects caused by ROS, algal cells activate antioxidant defense systems, comprising superoxide dismutase (SOD), glutathione reductase (GR) and glutathione peroxidase (GSH-PX) in the antioxidant enzyme system, as well as MDA in the non-enzyme system, to jointly eliminate and regulate the overall ROS

level (Teisseire and Guy, 2000; Sun et al., 2017; Liu et al., 2021). Once ROS is overproduced, it induces oxidative damage, resulting in protein degradation, DNA damage, and lipid peroxidation, ultimately leading to algal cell death (Sies, 1997; Wang et al., 2012; Tang et al., 2016).

S. costatum, a planktonic diatom that is widely distributed in coastal waters around the world, often representing a dominant species in coastal areas (Ma et al., 2023). The current study employed two quinolone antibiotics, LEV and NOR, as target pollutants to investigate the impact of varying concentrations of these antibiotics on *S. costatum*. The biological mechanism of their effect on *S. costatum* was clarified through analyzing the growth, photosystem activity and enzyme activity within algal cells. This study provides a reference for evaluating the potential ecological hazard of antibiotics in marine ecosystems.

2 Materials and methods

2.1 Materials and culture condition

Natural seawater was collected from Changzhi Island in Zhoushan, China (E122°11'03.36", N29°57'27.13"). After being filtered using a nitrocellulose membrane (0.45- μm pore size), and undergoing sterilization via high-pressure steam (120°C, 20 min), the seawater had a salinity of 27 ± 0.5 and a pH value of 8.10 ± 0.01 . *S. costatum* was acquired from Shanghai Guangyu Biotechnological Co., Ltd. (Shanghai, China) and inoculated into a 2,000 mL Erlenmeyer flask filled with 1,000 mL f/2 (+Si) culture medium. The culture was performed at a light intensity of 4,000 lx, following a 12-hour light-on, 12-hour light-off photoperiod, and a constant temperature of $23 \pm 0.1^\circ\text{C}$. The flask underwent regular shaking three times daily.

LEV and NOR were acquired from Shanghai Aladdin Biochemical Technology Co., Ltd. (Shanghai, China). Weighed 0.5g each of LEV and NOR and placed them in separate 50 mL sterilized beakers. Slowly added 0.1mol/L HCl until LEV and NOR were completely dissolved. The consumed amounts of 0.1% HCl were 8 mL and 15 mL, respectively. Transferred the completely dissolved LEV and NOR to 500 mL volumetric flasks and make up to the volume with sterilized seawater. This resulted in a mother liquor concentration of 1g/L. sterilized using the Biosharp vacuum filtration system (Biosharp Life Sciences, Hefei, Anhui, China), and then stored in a 4°C refrigerator. Before utilizing the mother liquor in the experiment, adjusted the pH using 0.1mol/L NaOH.

2.2 Experimental methods

2.2.1 Growth experiment

Cultured microalgae in the logarithmic growth phase growing in sterilized seawater containing f/2 medium and antibiotics were added in certain proportions into 2,000 mL Erlenmeyer flasks to reach a culture volume totaling 1,200 mL. The concentrations of LEV were 0 (blank control), 5, 10, 20, 40, and 60 mg/L. Concentrations of LEV exceeding 20 mg/L were classified as the

high-concentration group. The concentrations of NOR were 0 (blank control), 10, 50, 100, 200, 400 mg/L. Concentrations of NOR over 100 mg/L were considered the high-concentration group. Each concentration was tested three times in replicates. The initial algae density after inoculation was 5×10^5 cells·mL⁻¹. The cultured microalgae were sampled 4 h after inoculation on the first day. After that, the microalgae were sampled regularly every 24 h for 10 days. The algal cells were enumerated utilizing a plankton counting chamber (Zhang et al., 2021b), following the inhibition rate (IR, %) and relative growth rate were calculated. The formula used to calculate the IR (%) is as follows (Equation 1) :

$$IR (\%) = (1 - \frac{Nt}{N0}) \times 100 \%, \quad (1)$$

where $N0$ and Nt represent the density of microalgae at the beginning of the experiment and at day t of the experiment, respectively.

The equation used to determine the relative growth rate (μ) is as follows (Equation 2) (Zhang et al., 2021b):

$$\mu = (\ln Xn - \ln X(n-1)) / (tn - t(n-1)) \quad (2)$$

where μ denotes the relative growth rate, h⁻¹; Xn represents the cell density at time tn ; and $X(n-1)$ is the cell density at time $t(n-1)$ (Zhang et al., 2021b).

2.2.2 Measurement of Fv/Fm and Chla

For each sampling, 20 mL of algae suspension was collected from all treatment groups. Following a 15 min adaptation period, the Fv/Fm were measured utilizing a hand-held chlorophyll fluorometer, AquaPen-C AP-C 100 (Photon Systems Instruments, The Czech Republic). The algae suspension was filtered with a 0.45 μ m nitrocellulose membrane. Subsequently, the filtrate was transferred into a centrifuge tube, followed by the addition of 10 mL of 90% acetone. After incubation at 4°C for 24 hours, the centrifuge tube underwent centrifugation at 3,000 rpm for 10 minutes. Subsequently, the absorbance of the supernatant was assessed at wavelengths of 750, 664, 647, and 630 nm, with 90% acetone serving as the control solution. The Chla content was quantified utilizing the formula (Equation 3) improved by Jeffrey and Humphrey in 1975:

$$pChla = (11.85E664 - 1.54E647 - 0.08E630) \times v / (V \cdot L) \quad (3)$$

where Chla represents the Chla concentration (μ g/L); v signifies the volume of extraction (mL); V represents the actual amount of the seawater sample (L); L represents the cuvette path length in centimeters (cm); and E750, E664, E647, and E630 correspond to the absorbance values at the wavelengths of 750, 664, 647, and 630 nm, respectively.

2.2.3 Measurement of enzyme activity

From each treatment, 50 mL suspension of algae was collected and subsequently centrifuged at 3,000 rpm for 10 minutes. The supernatant was removed, and the precipitated cells were subsequently collected. The protein content, SOD activity, MDA content, GSH-PX activity, and GR activity were quantified by the

corresponding reagent kits (A045-2-2 for protein content, A001-1-2 for SOD, A003-1-3 for MDA, A005-1-2 for GSH-PX, and A062-1-1 for GR) purchased from Nanjing Jiancheng Bioengineering Research Institute (Nanjing, China).

2.3 Data processing

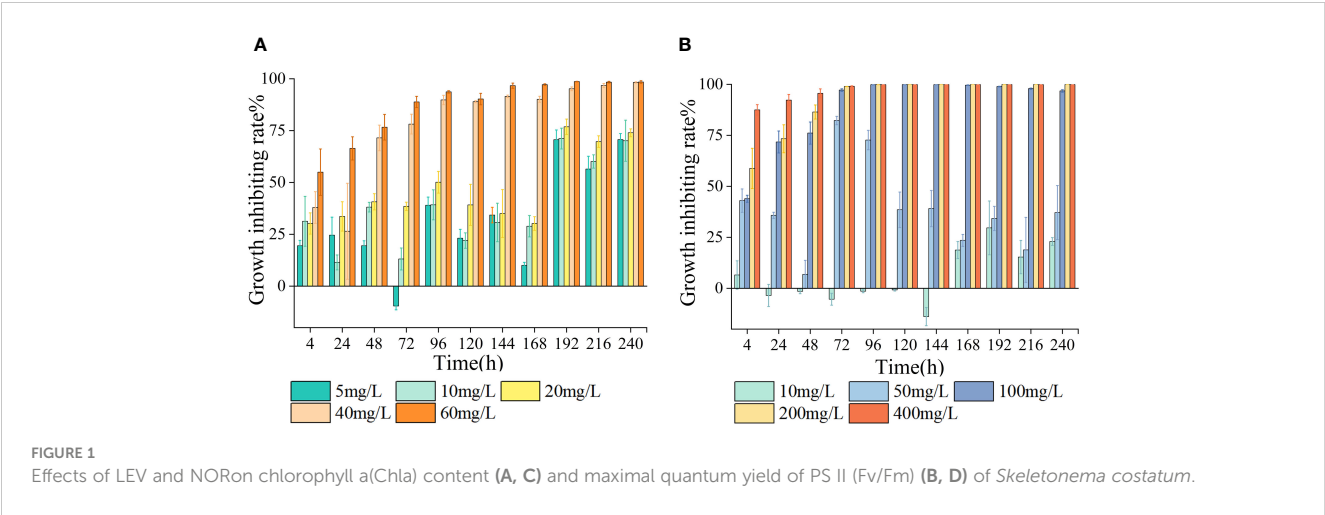
The experimental data were organized and plotted utilizing Origin 9.2. One-way analysis of variance (ANOVA) was conducted using SPSS 26.0.0, with statistical significance defined at $p < 0.05$. Additionally, GraphPad Prism 9.5.0 software was employed to determine the 96-h half-maximal inhibitory concentrations (96h-IC50).

3 Results and analysis

3.1 Effect of antibiotics on microalgae growth

As the treatment duration and antibiotic concentration escalated, the growth of algal cells was increasingly suppressed, showing a clear dose-dependent relationship (Figure 1). In the presence of LEV, the relative growth rate of *S. costatum* exhibited a significant decrease compared to the control group ($p < 0.05$), with a gradual decline observed as the antibiotic concentration increased. During the experimental period, the groups with concentrations including 5, 10, and 20 mg/L initially exhibited higher growth rates before gradually decreasing. In all treatment groups, the relative growth rates became negative after 168 h (Table 1). LEV in all treatment groups exhibited inhibitory effects at 4 h into the experiment. The 40 and 60 mg/L groups both showed inhibition rates exceeding 25%, and the 60 mg/L group displayed significant inhibition ($p < 0.05$) with an inhibition rate of 50.1%. At 72 h, the 5 mg/L group stimulated algal cell growth, whereas the groups treated containing 10 and 20 mg/L exhibited inhibition rates of less than 50%. At 96 h, the 5 mg/L group once again exhibited inhibitory effects, with an inhibition rate of 39.1%, and the 10 mg/L group had an inhibition rate of 39.2%. The high-concentration groups showed significant inhibition ($p < 0.05$), with inhibition rates of 50.1%, 89.7%, and 93.4% for treatments with 20, 40, and 60 mg/L LEV, respectively. At 144 h, the 60 mg/L group had an inhibition rate of 96.6%, and thereafter, the inhibition rate remained relatively stable. After 192 h, the inhibition rates in all treatment groups were greater than 50% (Figure 1).

Under the influence of NOR, the relative growth rate of *S. costatum* exhibited significant differences compared to the control group ($p < 0.05$). In the low-treatment groups, growth resumed after 24 h. However, as the treatment duration increased, the relative growth rates gradually decreased. In groups with treatments exceeding 100 mg/L, the relative growth rates were either zero or negative. After 144 h, all treatment groups exhibited negative relative growth rates (Table 1). At 24 h, the 10 mg/L concentration promoted the growth of algal cells, the 20 mg/L group had an inhibition rate of less than 50%, and the other three



treatment groups all exhibited significant inhibition ($p < 0.05$). At 96 h, the group treated with 5 mg/L exhibited a negative growth rate, and the other four treatment groups all exhibited significant inhibition, with the 50 mg/L group having an inhibition rate of 73%. The inhibition rates gradually decreased thereafter. The high-concentration groups had inhibition rates of 99.8%, 99.9%, and 99.8% for 100, 200, and 400 mg/L NOR, respectively, with

inhibition rates maintaining stability thereafter. At 168 h, the 10 mg/L group showed an increase in the inhibition rate, reaching 23.5% (Figure 2).

LEV exerted stronger inhibitory effects on *S. costatum* compared with NOR. When comparing the growth inhibition rates of the two antibiotics at the same concentration (10 mg/L) under different culture durations, LEV consistently showed higher

TABLE 1 The relative growth rate of *Skeletonema costatum* under the influence of different concentrations of antibiotics(μ) (h^{-1}).

Antibiotic	Concentration (mg/L)	μ (4h-24h)	μ (24h-48h)	μ (48h-72h)	μ (72h-96h)	μ (96h-120h)	μ (120h-144h)	μ (144h-168h)	μ (168h-192h)	μ (192h-216h)	μ (216h-240h)
LEV	0	0.005 $\pm 0.005^*$	0.024 ± 0.002	0.021 ± 0.002	0.012 ± 0.002	0.003 ± 0.004	0.000 ± 0.001	0.003 ± 0.005	0.011 ± 0.004	-0.007 ± 0.003	-0.003 ± 0.002
	5	0.004 $\pm 0.002^*$	0.025 ± 0.002	0.027 ± 0.002	0.001 ± 0.003	0.007 ± 0.004	-0.004 ± 0.001	0.010 ± 0.005	-0.009 ± 0.006	0.001 ± 0.003	-0.010 ± 0.003
	10	0.011 $\pm 0.008^*$	0.018 ± 0.003	0.027 ± 0.003	0.006 ± 0.003	0.008 ± 0.005	-0.004 ± 0.002	0.005 ± 0.002	-0.005 ± 0.002	-0.001 ± 0.003	-0.008 ± 0.006
	20	0.004 $\pm 0.002^*$	0.022 ± 0.002	0.022 ± 0.003	0.008 ± 0.003	0.007 ± 0.004	0.000 ± 0.003	0.006 ± 0.003	-0.009 ± 0.002	-0.002 ± 0.003	-0.005 ± 0.002
	40	0.005 $\pm 0.004^*$	0.010 ± 0.004	0.016 ± 0.003	-0.002 ± 0.001	0.005 ± 0.007	-0.006 ± 0.001	0.007 ± 0.002	-0.002 ± 0.002	-0.014 ± 0.009	-0.013 ± 0.005
	60	0.002 $\pm 0.007^*$	0.013 ± 0.001	0.008 ± 0.006	0.002 ± 0.005	0.010 ± 0.004	-0.021 ± 0.001	0.002 ± 0.002	-0.002 ± 0.001	-0.003 ± 0.003	-0.004 ± 0.003
NOR	0	0.009 $\pm 0.002^*$	0.020 ± 0.003	0.018 ± 0.000	0.032 ± 0.002	0.008 ± 0.001	0.008 ± 0.002	-0.006 ± 0.001	-0.002 ± 0.001	-0.005 ± 0.001	-0.001 ± 0.002
	10	0.010 $\pm 0.003^*$	0.020 ± 0.002	0.019 ± 0.000	0.031 ± 0.003	0.008 ± 0.001	0.011 ± 0.002	-0.012 ± 0.001	-0.005 ± 0.003	-0.002 ± 0.003	-0.002 ± 0.002
	50	0.011 $\pm 0.004^*$	0.026 ± 0.003	0.013 ± 0.001	0.015 ± 0.002	0.020 ± 0.002	0.010 ± 0.001	-0.001 ± 0.001	-0.004 ± 0.001	-0.003 ± 0.001	-0.003 ± 0.002
	100	-0.002 $\pm 0.000^*$	-0.007 ± 0.004	-0.002 ± 0.007	-0.002 ± 0.004	0.000 ± 0.001	0.001 ± 0.001	0.000 ± 0.000	-0.002 ± 0.001	0.000 ± 0.001	0.000 ± 0.002
	200	-0.001 $\pm 0.000^*$	-0.011 ± 0.002	-0.008 ± 0.003	-0.005 ± 0.004	-0.009 ± 0.007	-0.001 ± 0.009	-0.005 ± 0.002	-0.001 ± 0.007	0.001 ± 0.008	0.000 ± 0.002
	400	-0.003 $\pm 0.000^*$	-0.010 ± 0.002	0.012 ± 0.005	-0.005 ± 0.004	-0.007 ± 0.004	-0.001 ± 0.007	-0.007 ± 0.004	0.000 ± 0.001	0.000 ± 0.006	0.000 ± 0.001

*”: Compared with the control, there was significant difference ($p < 0.05$).

inhibition rates than NOR. Based on the dose–response curves obtained through nonlinear fitting for algal cell inhibition rates, the half-maximal inhibitory concentration (IC_{50}) was calculated. The 96h- IC_{50} for LEV was 14.770 mg/L, while the 96h- IC_{50} for NOR was 44.250 mg/L. Therefore, the order of inhibitory effects of these two antibiotics on *S. costatum* was LEV > NOR.

3.2 Effect of antibiotics on the Chla and Fv/Fm

As the concentration of LEV increased, the Chla content gradually decreased compared to the control group (Figure 3). At

24 h, the Chla contents in all treatment groups were lower compared to the control group, with the 40 mg/L and 60 mg/L groups showing significantly decreased Chla levels ($p < 0.05$). After 48 h, the 5 mg/L group showed slightly higher Chla content compared to the control group, while the groups treated with 10, 20, 40, and 60 mg/L all contained significantly lower Chla contents ($p < 0.05$). After 96 h, both the groups treated with 5 mg/L and 10 mg/L showed an upward trend in Chla content, albeit remaining significantly lower than the control group ($p < 0.05$). For Fv/Fm, all treatment groups initially showed an increase followed by a decreasing trend, resulting in lower Fv/Fm values compared to the control group. After 24 h, the 20, 40, and 60 mg/L groups all showed significantly lower Fv/Fm values compared to the control

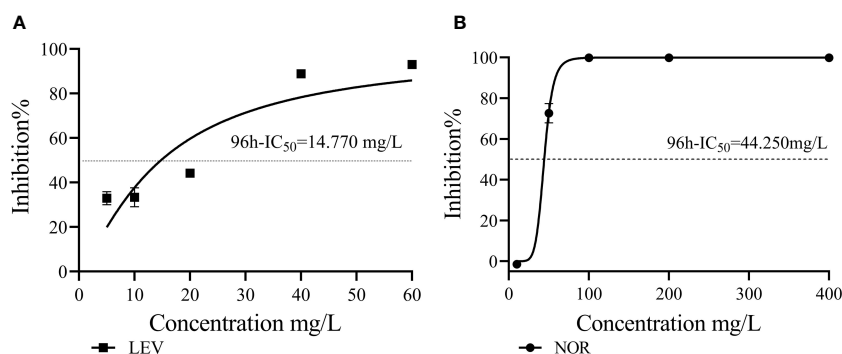


FIGURE 2
The 96h- IC_{50} values of LEV (A) and NOR (B) were compared with that of *Skeletonema costatum*.

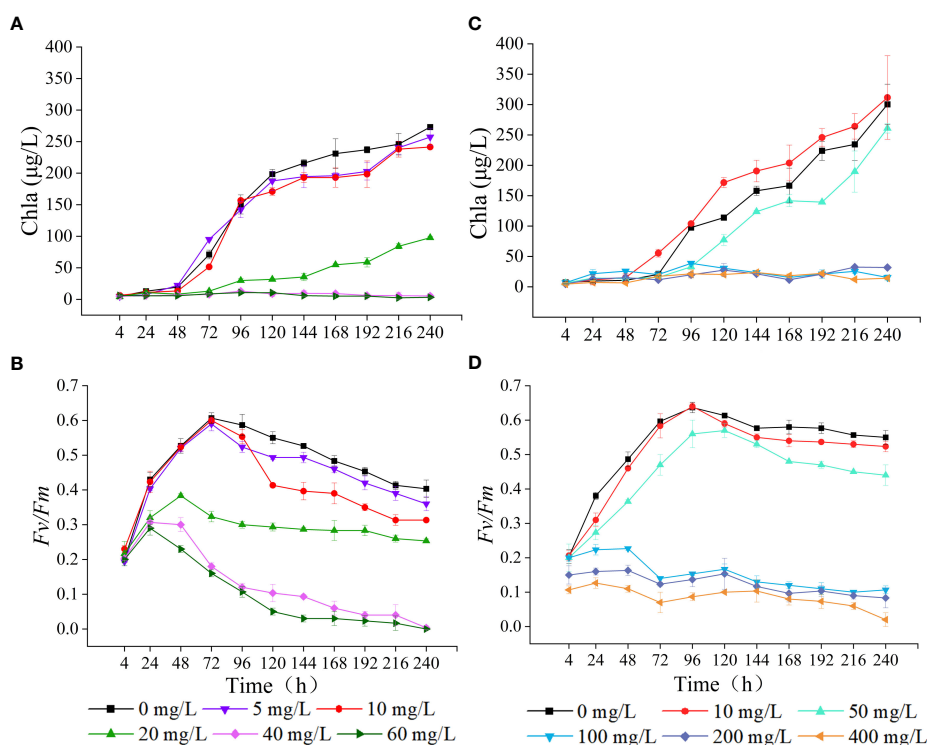


FIGURE 3
Effects of LEV and NOR on chlorophyll a (Chla) content (A, C) and maximal quantum yield of PSII (Fv/Fm) (B, D) of *Skeletonema costatum*.

group ($p < 0.05$). After 96 h, all groups, except for the 5 mg/L group, exhibited significantly lower Fv/Fm values compared to the control group ($p < 0.05$). At 240 h, The Fv/Fm value for the group exposed to 40 mg/L decreased to 0.003 ± 0.006 , and that of the 60 mg/L treatment dropped to zero. The trend observed in Fv/Fm values after 24 h was consistent with that of Chla content.

Under the influence of NOR, the Chla content exhibited a trend of enhancement in low concentrations and decrease in high concentrations (Figure 3). At 24 h, NOR concentrations of 10, 50, 100, and 200 mg/L all had higher Chla content than the control group. After 24 h, Chla gradually increased in the low-concentration group, and at 72 h, the group exposed to 10 mg/L exhibited a markedly elevated Chla content compared to the control group ($p < 0.05$). However, at 96 h, the group treated with 50 mg/L had notably lower Chla content than the untreated group ($p < 0.05$). After 72 h, the Chla content in the groups treated with 100, 200, and 400 mg/L gradually decreased. By 96 h, the Chla content in each group was notably lower compared to the control group ($p < 0.05$). At 4 h, At 4 hours, the Fv/Fm values of the groups treated with 200 mg/L and 400 mg/L were notably lower compared to the control group ($p < 0.05$). After 24 h, the Fv/Fm in all treatment groups gradually increased. The groups exposed to 10 mg/L and 50 mg/L exhibited an initial increase followed by a decreasing trend, with the 10 mg/L group showing relatively small differences compared to the control. The high concentrations all showed significantly lower Chla content compared to the control ($p < 0.05$). After 48 h, the Fv/Fm initially declined in the groups with NOR concentrations above 100 mg/L, and then gradually increased, with the final Fv/Fm values being lower than 0.100. At 240 h, the Fv/Fm value decreased to 0.083 ± 0.029 in the 200 mg/L group, dropped to 0 in the 400 mg/L group, and remained at 0.020 ± 0.020 in the control group.

3.3 Effects of antibiotics on protein content and enzyme activity

In the group exposed to high concentrations of LEV, the protein concentration of algal cells, MDA content, and activities of SOD, GSH-PX, GR were significantly altered compared to the control group. In both the low concentrations and the control group, only the MDA content exhibited a significant difference (Figure 4). Compared to the control, the protein concentration and MDA content in the low concentrations showed a gradual increase, surpassing those of the control group. The MDA levels in the low-concentration group showed a significant increase compared to those in the control group at 96 h ($p < 0.05$) and gradually decreased after reaching the highest value at 120 h. In comparison to the control group, the high-concentration groups exhibited notably lower levels of protein concentration and MDA content at 96 hours and 4 hours, respectively ($p < 0.05$). Compared to the control, the levels of SOD, GR, GSH-PX in all treatment groups initially exhibited an increase followed by a subsequent decrease. As the treatment duration increased, in the low-concentrations the SOD, GR, and GSH-PX activities gradually became notably lower compared to high-concentrations. At 48 h, the 10 and 20 mg/L

groups had significantly higher SOD activity compared to the control ($p < 0.05$). In both low-concentration group and the 20 mg/L group, SOD activity peaked at 72 hours before gradually declining. After 120 h, the SOD activity in both the control group and the low-concentration group significantly decreased compared to the high concentrations, reaching significance at 144 h ($p < 0.05$). At 96 h, the low concentrations exhibited significantly higher GR activity compared to the control group ($p < 0.05$). Similarly, at 120 hours, the high concentrations demonstrated significantly elevated GR activity relative to the control ($p < 0.05$). At 4 h, all treatments exhibited lower GSH-PX compared to the control. However, after 24 h, the GSH-PX activity in all treatments gradually increased, and in the low concentrations it reached the highest value at 72 h. After 96 h, the GSH-PX activity gradually decreased but remained higher compared to the control. In the high concentrations, the activity of GSH-PX peaked at 96 hours, surpassing significantly that of the control group beyond this time point ($p < 0.05$).

Compared to the control group, NOR had a significant impact on the algal cell protein concentration, MDA content, and the activity levels of SOD, GSH-PX, GR (Figure 5). In the low concentrations, there was a gradual increase in protein concentration, which became significantly higher than that of the control group by 168 h ($p < 0.05$). In the high-concentration group, the protein concentration exhibited a significant increase compared to the control group at 24 h ($p < 0.05$), but notably decreased relative to the control group after 96 h ($p < 0.05$). At 240 h, the high-concentration group exhibited a protein concentration merely one-third of that observed in the control group. The MDA content in the low concentrations exhibited an initial increase followed by a subsequent decrease. By 168 h, the MDA content in the 50 mg/L group was notably higher compared to the control ($p < 0.05$). In the high concentrations, the MDA content was notably lower compared to the control group at 4 h ($p < 0.05$) and decreased overall. The activities of SOD, GR, and GSH-PX all initially increased and then decreased. At 4 h, the SOD activities in the 50 mg/L group and the high concentrations were significantly elevated compared to those in the control group ($p < 0.05$). The GR and GSH-PX activities of the low-concentration group were notably elevated compared to those in the control group at 48 h and 72 h, respectively ($p < 0.05$). In the high-concentration group, the GR and GSH-PX levels were elevated compared to those in the control at 120 h and 96 h, respectively ($p < 0.05$).

4 Discussion

4.1 Influence of LEV and NOR on the *S. costatum* growth

Cell density and mean specific growth rate are commonly utilized metrics for quantifying the growth of microalgae (Qian et al., 2018). the calculated inhibition rate can indicate the degree to which microalgae are inhibited under the influence of pollutants (Kurade et al., 2016). In the current study, NOR had dual impacts on *S. costatum*. The 10 mg/L NOR group showed a growth-promoting effect, while the other treatment groups exhibited varying degrees of

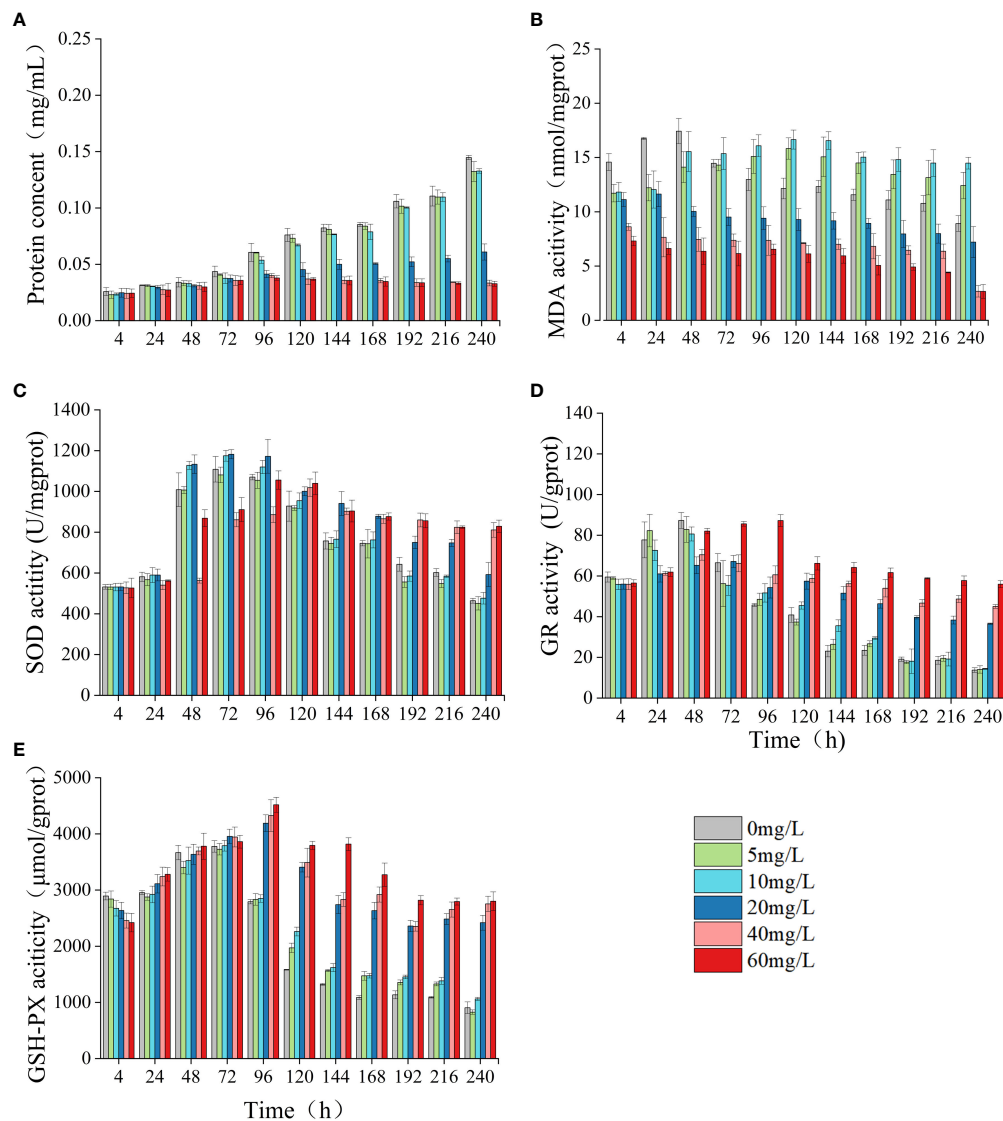


FIGURE 4

Effect of LEV on protein content and antioxidant system of *Skeletonema costatum*. Protein content (A), MDA (B), SOD (C), GR (D) and GSH-PX (E).

inhibition. A previous study showed 1 mg/L of enrofloxacin (ENR) facilitated the growth of *Ourococcus multisporus*, as well as *Micractinium resseri*, but ENR concentrations in excess of 20 mg/L led to different levels of inhibition on *O. multisporus* and *M. resseri* (Xiong et al., 2017a). For moxifloxacin (MOX) and gatifloxacin (GAT), after being used in culture for 48 h, MOX concentrations greater than 5 mg/L significantly inhibited *Chlamydomonas reinhardtii*. Moreover, the inhibitory effects of both MOX and gatifloxacin (GAT) increased with prolonged culture duration (Wan et al., 2022). The presence of antibiotics in marine environments can have a dual impact on microalgae. On one hand, antibiotics may stimulate the growth of microalgae, thereby increasing primary productivity levels. However, on the other hand, they may also contribute to outbreaks of red tide. This phenomenon highlights the complex relationship between antibiotics and marine ecosystems, as they can both enhance and disrupt the delicate balance of primary productivity in the marine.

Through nonlinear fitting, it was determined that the 96h- IC_{50} values for LEV and NOR on algal cells were 14.770 mg/L and 44.250 mg/L, respectively. This finding suggested algal cells were more sensitive to LEV than to NOR. Therefore, algae have varying sensitivities to different antibiotics. Previous studies have shown that *Pseudokirchneriella subcapitata* and *Anabaena subcapitata* are more sensitive to LEV than NOR, with *A. subcapitata* being more sensitive than *P. subcapitata*. The median effective concentration (EC_{50}) values for LEV and NOR in *A. subcapitata* were 4.8 mg/L and 5.6 mg/L, respectively (Gonzalez-Pleite et al., 2013). Other quinolone antibiotics have varying half-maximal inhibitory concentrations on microalgae. For example, for *Selenastrum capricornutum*, ciprofloxacin (CIP) reached EC_{50} at 11.3 mg/L (Magdaleno et al., 2015), for *Chlorella vulgaris*, ENR reached EC_{50} at EC_{50} at 124.5 mg/L (Wang et al., 2019a), and the IC_{50} values were found to be 5.18 mg/L for *Raphidocelis subcapitata* and 10.6 mg/L for *Ankistrodesmus fusiformis* (Carusso et al., 2018).

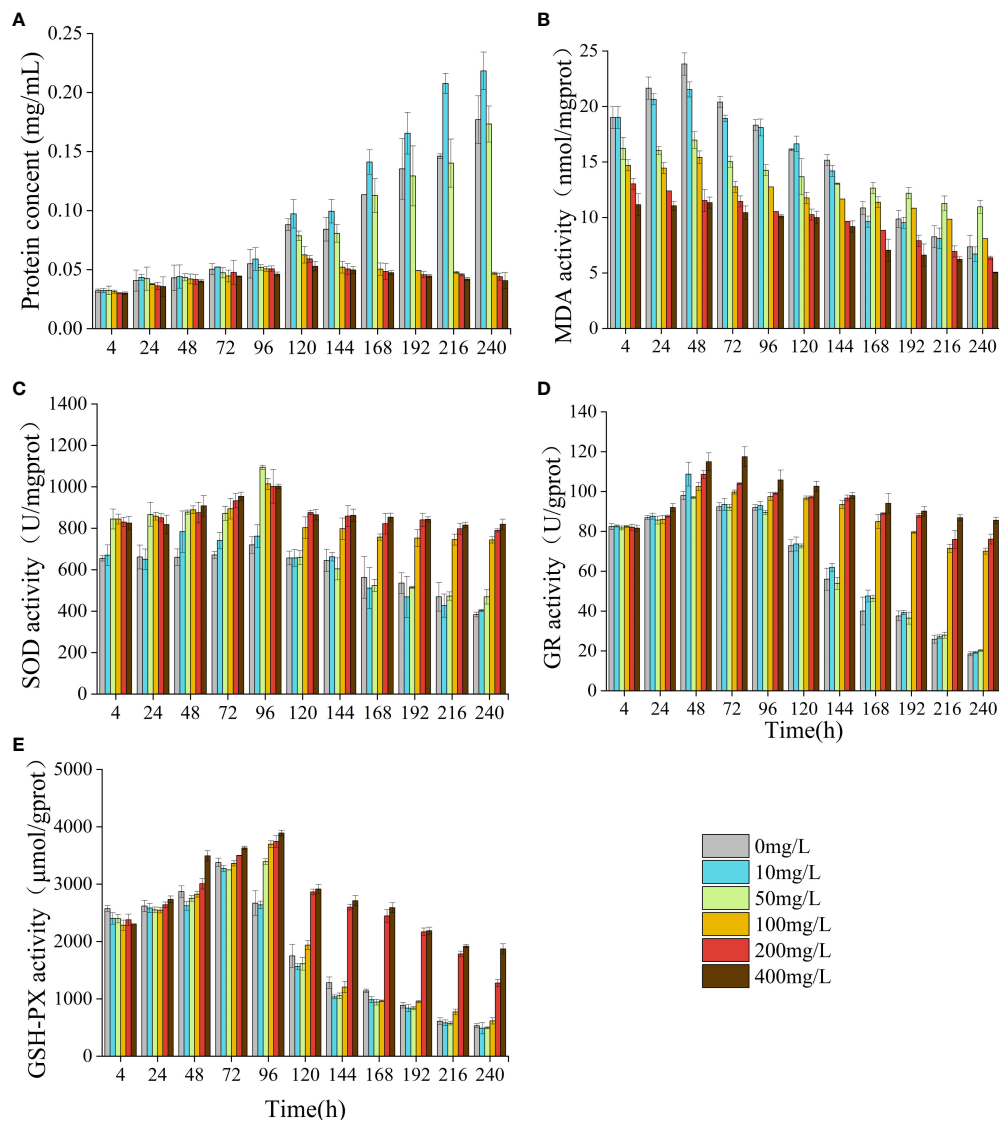


FIGURE 5
Effect of NOR on protein content and antioxidant system of *Skeletonema costatum*. Protein content (A), MDA (B), SOD (C), GR (D) and GSH-PX (E).

4.2 Impact on the Chla and Fv/Fm

Chlorophyll is essential for capturing light, converting it into energy, and facilitating energy transfer within plants. The suppression of algal growth is frequently associated with the adverse effects of toxic substances on chlorophyll synthesis (Koussevitzky et al., 2007; Nie et al., 2008). Previous research have indicated that low-concentration of antibiotics can stimulate an increase in Chla, whereas high-concentration of antibiotics can inhibit Chla and reduce the Fv/Fm (Chen et al., 2020a; Li et al., 2023). Additionally, it has been reported that antibiotics caused the elevation of photosynthetic pigments in algal cells. For example, 60 mg/L and 100 mg/L of CIP resulted in a 38% and 19% elevation, respectively, in chlorophyll content in *Chlamydomonas* cells (Xiong et al., 2017b). It was also found that quinolone antibiotics inhibited the photosynthesis of diatoms (Dow et al., 2020). In this study, the

two antibiotics in the groups exposed to low concentrations caused the gradual increase of the Chla content of microalgae, with the Chla content of the 10 mg/L NOR group consistently surpassing that of the control group after 48 h, while at high concentrations, both antibiotics significantly inhibited the Chla content. Low doses of antibiotics increased the Chla levels possibly because the antibiotics triggered the protective mechanism of algal cells to remove ROS accumulated in chloroplasts and alter some proteins in chloroplasts to delay and reduce the damage to photosynthetic organs (Shinkai et al., 2002; Wan et al., 2014). When antibiotic concentrations exceed the self-regulation range of algal cells, their inhibition effect is strengthened, leading to structural damage in the algal cells. As a result, photosynthesis is negatively affected. Excessive ROS in algal cell membrane lipids disrupt the structure of the microalgal chloroplasts and prevent the localization of chlorophyll, ultimately resulting in the degradation of free

chlorophyll in the chloroplasts, thus inhibiting algal growth and reducing the chlorophyll content (Liu et al., 2011; Wang et al., 2019b).

Maximal quantum yield of PSII (F_v/F_m) is a critical indicator of plant photosynthetic efficiency, particularly under stressful conditions (Krause, 1988). Processes such as the absorption of light, transmission of energy, and initiation of primary photochemical reactions during photosynthesis in microalgae are closely related to changes in the photosynthetic pigments. Therefore, the composition and content of photosynthetic pigments directly determine the efficiency of light energy capture. Under the influence of two low-concentration antibiotics in this study, the F_v/F_m of microalgae exhibited an initial increase followed by a subsequent decrease, whereas the high-concentration group demonstrated markedly lower F_v/F_m values compared to the control group at the 4 h. This result indicated that with an increase in the duration of treatment and antibiotic concentration, the damage to the algal cell photosynthetic system worsened, making normal photosynthesis impossible. Therefore, under the influence of antibiotics, the F_v/F_m values of algal cells vary due to factors such as the treatment duration, antibiotic concentration, and microalgae species (Chen et al., 2020b; Jia et al., 2023; Li et al., 2023).

4.3 Effects on the protein content and enzyme activity

The protein content in algal cells increases in response to external stress to maintain normal cellular growth and metabolic activities (Hu et al., 2019). MDA serves as the ultimate outcome of peroxidation reactions. Its concentration can reflect the extent of microalgae cell membrane damage caused by antibiotics at different concentrations (Ke et al., 2010). In addition, antibiotic-induced oxidative stress in microalgae activates various antioxidant defense systems, such as the SOD and GR of the enzymatic system and the GSH-PX of the non-enzymatic system, all of which can counteract and regulate excessive ROS production (Jubany-Mari et al., 2010; Nie et al., 2013; Guo et al., 2020). Under the influence of low concentrations of LEV and NOR, the protein content of algae cells was significantly elevated compared to the control group. However, exposure to high concentrations resulted in a notable decrease in protein content relative to the control group. This indicated that low concentrations of LEV and NOR stimulated *S. costatum* to increase protein production. The elevation in protein content could stem from a physiological response induced by external stress. This stimulation prompted the metabolic pathways within microalgae cells, thereby protecting important cellular components and biological membranes (Guzmán-Murillo et al., 2007; Hu et al., 2019). In the current study, as the concentration of both antibiotics increased, there was a significant decrease in protein content observed in the high-concentration group. This phenomenon can be attributed to oxidative damage inflicted upon microalgal cells, which triggers the excessive production of reactive oxygen species (ROS) and subsequently leads to protein

oxidation (Xiong et al., 2021). The trend of MDA content mirrored that of protein content, exhibiting a notable rise in MDA levels in the low-concentration LEV group and a gradual increase in the 50 mg/L NOR group compared to the control group, indicating that both antibiotics promoted membrane peroxidation. In contrast, the MDA levels within the high concentrations consistently decreased, suggesting that irreversible damage had been caused to the algal cells. Antibiotics induce oxidative damage to algal cells as the malondialdehyde (MDA) generated by free radicals can cross-link with proteins, phospholipids, and nucleic acids, thereby disrupting DNA synthesis (Zhang et al., 2020b; Hena et al., 2021). Under the respective influence of the two antibiotics, the changes in SOD, GR, and GSH-PX activities in algal cells all demonstrated a pattern of initially increasing followed by decreasing. In the high-concentration group, although there was a decreasing trend with increasing treatment duration, the SOD, GR, and GSH-PX activities remained higher compared to both the control and the low-concentration group. This indicated that as the concentration of antibiotics rise, the activities of SOD and GR were not sufficient to clear the accumulated excess ROS in the algae, and GSH-PX was unable to neutralize the large amount of H_2O_2 produced under stress, inducing an increase in antioxidant activity (Das and Roychoudhury, 2014). The high-concentration group exhibited a higher level of oxidative stress than the low-concentration group. Therefore, in combination with the results regarding the protein and antioxidant systems, both LEV and NOR affected the enzyme activity of *S. costatum*, caused oxidative stress to its cells, and activated its defense system to reduce oxidative damage. Continuous stress disrupted the algal defense system, consequently damaging both the structure and function of algal cells, thereby inhibiting algal growth. This result was consistent with the behavior of algal cells under the influence of other antibiotics and pollutants. For instance, the enzyme activities of SOD, GR, and GSH-PX exhibited significant elevation in *Chlorella* sp., *Microcystis flosaquae*, *C. reinhardtii*, *Scenedesmus obliquus*, and *Merismopedia subcapitata* under the influence of CIP, sulfamethoxazole (SMZ), erythromycin (ERY), polystyrene microplastics, aluminum, and chlorpyrifos (Nie et al., 2013; Wan et al., 2015; Chen et al., 2016; Ameri et al., 2020; Chen et al., 2020b). In addition, under the influence of ENR or benzo[a]pyrene, the MDA content decreased in *O. multisporus* and *Isochrysis zhanjiangensis* (Shen et al., 2016; Xiong et al., 2017a).

5 Conclusion

In this investigation, we explored the impacts of two quinolone antibiotics, LEV and NOR, on *S. costatum*. Through an analysis of their effects on microalgal cell growth, Chl *a* contents, F_v/F_m , protein content, antioxidant enzyme systems (SOD, GR, and GSH-PX), and non-enzymatic system (MDA), it was found that both LEV and NOR inhibited the growth of microalgae, with the cells being more sensitive to LEV. These antibiotics might affect photosynthesis through influencing the algal photosynthetic

system. High doses of LEV and NOR induced significant oxidative stress in microalgae cells. This study provides a comprehensive analysis of the impacts of LEV and NOR on marine microalgae growth and elucidates the underlying physiological mechanisms. These findings significantly contribute to the assessment of ecological risks associated with antibiotics in marine environments, furnishing a theoretical foundation for the development of environmental monitoring and management strategies aimed at controlling antibiotic pollution.

Data availability statement

The original contributions presented in the study are included in the article/supplementary material, further inquiries can be directed to the corresponding author/s.

Author contributions

YL: Data curation, Software, Writing – original draft. TL: Funding acquisition, Resources, Supervision, Writing – review & editing. YZ: Data curation, Methodology, Project administration, Writing – review & editing.

References

- Aderemi, A. O., Novais, S. C., Lemos, M. F. L., Alves, L. M., Hunter, C., and Pahl, O. (2018). Oxidative stress responses and cellular energy allocation changes in microalgae following exposure to widely used human antibiotics. *Aquat. Toxicol.* 203, 130–139. doi: 10.1016/j.aquatox.2018.08.008
- Ameri, M., Baron-Sola, A., Khavari-Nejad, R. A., Soltani, N., Najafi, F., Bagheri, A., et al. (2020). Aluminium triggers oxidative stress and antioxidant response in the microalgae *Scenedesmus* sp. *J. Plant Physiol.* 246–247, 153114. doi: 10.1016/j.jplph.2020.153114
- Carusso, S., Juarez, A. B., Moretton, J., and Magdaleno, A. (2018). Effects of three veterinary antibiotics and their binary mixtures on two green alga species. *Chemosphere* 194, 821–827. doi: 10.1016/j.chemosphere.2017.12.047
- Chen, J. Q., and Guo, R. X. (2012). Access the toxic effect of the antibiotic cefradine and its UV light degradation products on two freshwater algae. *J. Hazard. Mater.* 209–210, 520–523. doi: 10.1016/j.jhazmat.2012.01.041
- Chen, S., Chen, M., Wang, Z., Qiu, W., Wang, J., Shen, Y., et al. (2016). Toxicological effects of chlorpyrifos on growth, enzyme activity and chlorophyll a synthesis of freshwater microalgae. *Environ. Toxicol. Pharmacol.* 45, 179–186. doi: 10.1016/j.etap.2016.05.032
- Chen, S., Zhang, W., Li, J., Yuan, M., Zhang, J., Xu, F., et al. (2020a). Ecotoxicological effects of sulfonamides and fluoroquinolones and their removal by a green alga (*Chlorella vulgaris*) and a cyanobacterium (*Chrysochloris ovalsporum*). *Environ. Pollut.* 263, 114554. doi: 10.1016/j.envpol.2020.114554
- Chen, S., Wang, L., Feng, W., Yuan, M., Li, J., Xu, H., et al. (2020b). Sulfonamides-induced oxidative stress in freshwater microalga *Chlorella vulgaris*: Evaluation of growth, photosynthesis, antioxidants, ultrastructure, and nucleic acids. *Sci. Rep.* 10, 8243. doi: 10.1038/s41598-020-65219-2
- Das, K., and Roychoudhury, A. (2014). Reactive oxygen species (ROS) and response of antioxidants as ROS-scavengers during environmental stress in plants. *Front. Environ. Sci.* 2. doi: 10.3389/fenvs.2014.00053
- Dow, L., Stock, F., Peltekis, A., Szamosvari, D., Prothiwa, M., Lapointe, A., et al. (2020). The multifaceted inhibitory effects of an alkylquinolone on the diatom *Phaeodactylum tricornutum*. *Chembiochem* 21, 1206–1216. doi: 10.1002/cbic.201900612
- Eluk, D., Nagel, O., Gagneten, A., Reno, U., and Althaus, R. (2021). Toxicity of fluoroquinolones on the cladoceran *Daphnia magna*. *Water Environ. Res.* 93, 2914–2930. doi: 10.1002/wer.1631
- Gao, H., Li, B., and Yao, Z. (2023). Advances in research on the presence and environmental behavior of antibiotics in the marine environment. *Environ. Chem.* 42, 779–791. doi: 10.7524/j.issn.0254-6108.2022103107
- Gonzalez-Pleiter, M., Gonzalo, S., Rodea-Palomares, I., Leganes, F., Rosal, R., Boltes, K., et al. (2013). Toxicity of five antibiotics and their mixtures towards photosynthetic aquatic organisms: implications for environmental risk assessment. *Water Res.* 47, 2050–2064. doi: 10.1016/j.watres.2013.01.020
- Guo, J., Peng, J., Lei, Y., Kanerva, M., Li, Q., Song, J., et al. (2020). Comparison of oxidative stress induced by clarithromycin in two freshwater microalgae *Raphidocelis subcapitata* and *Chlorella vulgaris*. *Aquat. Toxicol.* 219, 105376. doi: 10.1016/j.aquatox.2019.105376
- Guzmán-Murillo, M. A., López-Bolaños, C. C., Ledesma-Verdejo, T., Roldan-Libenson, G., Cadena-Roa, M. A., and Ascencio, F. (2007). Effects of fertilizer-based culture media on the production of exocellular polysaccharides and cellular superoxide dismutase by *Phaeodactylum tricornutum* (Bohlin). *J. Appl. Phycol.* 19, 33–41. doi: 10.1007/s10811-006-9108-9
- Hena, S., Gutierrez, L., and Croué, J. P. (2021). Removal of pharmaceutical and personal care products (PPCPs) from wastewater using microalgae: A review. *J. Hazard. Mater.* 403, 124041. doi: 10.1016/j.jhazmat.2020.124041
- Hu, H., Zhou, Q., Li, X., Lou, W., Du, C., Teng, Q., et al. (2019). Phytoremediation of anaerobically digested swine wastewater contaminated by oxytetracycline via *Lemna aquinoctialis*: Nutrient removal, growth characteristics and degradation pathways. *Bioresour. Technol.* 291, 121853. doi: 10.1016/j.biortech.2019.121853
- Huang, F., An, Z., Moran, M. J., and Liu, F. (2020). Recognition of typical antibiotic residues in environmental media related to groundwater in China, (2009–2019). *J. Hazard. Mater.* 399, 122813. doi: 10.1016/j.jhazmat.2020.122813
- Huang, D. J., Hou, J. H., Kuo, T. F., and Lai, H. T. (2014). Toxicity of the veterinary sulfonamide antibiotic sulfamonomethoxine to five aquatic organisms. *Environ. Toxicol. Pharmacol.* 38, 874–880. doi: 10.1016/j.etap.2014.09.006
- Jeffrey, S. W., and Humphrey, G. F. (1975). New spectrophotometric equations for determining chlorophylls a, b, c1 and c2 in higher plants, Algae and Natural Phytoplankton. *Biochimie und Physiologie der Pflanzen* 167, 191–194. doi: 10.1016/S0015-3796(17)30778-3
- Jia, Y., Lu, J., Wang, M., Qin, W., Chen, B., Xu, H., et al. (2023). Algicidal bacteria in phycosphere regulate free-living Symbiodinium fate via triggering oxidative stress and photosynthetic system damage. *Ecotoxicol. Environ. Saf.* 263, 115369. doi: 10.1016/j.ecoenv.2023.115369
- Jiang, Y., Liu, Y., and Zhang, J. (2021). Mechanisms for the stimulatory effects of a five-component mixture of antibiotics in *Microcystis aeruginosa* at transcriptomic and proteomic levels. *J. Hazard. Mater.* 406, 124722. doi: 10.1016/j.jhazmat.2020.124722

Funding

The author(s) declare financial support was received for the research, authorship, and/or publication of this article. This work was supported by the Zhejiang Provincial Natural Science Foundation of China for Distinguished Young Scientists under grant No. LR21C190001.

Conflict of interest

The authors declare that the research was conducted in the absence of any commercial or financial relationships that could be construed as a potential conflict of interest.

Publisher's note

All claims expressed in this article are solely those of the authors and do not necessarily represent those of their affiliated organizations, or those of the publisher, the editors and the reviewers. Any product that may be evaluated in this article, or claim that may be made by its manufacturer, is not guaranteed or endorsed by the publisher.

- Jubany-Mari, T., Munné-Bosch, S., and Alegre, L. (2010). Redox regulation of water stress responses in field-grown plants. Role of hydrogen peroxide and ascorbate. *Plant Physiol. Biochem.* 48, 351–358. doi: 10.1016/j.plaphy.2010.01.021
- Ke, L., Luo, L., Wang, P., Luan, T., and Tam, N. F. Y. (2010). Effects of metals on biosorption and biodegradation of mixed polycyclic aromatic hydrocarbons by a freshwater green alga *Selenastrum capricornutum*. *Bioresour. Technol.* 101, 6950–6961. doi: 10.1016/j.biortech.2010.04.011
- Koussevitzky, S., Stanne, T. M., Peto, C. A., Giap, T., Sjgren, L. L. E., Zhao, Y., et al. (2007). An Arabidopsis thaliana virescent mutant reveals a role for ClpR1 in plastid development. *Plant Mol. Biol.* 63, 85–96. doi: 10.1007/s11103-006-9074-2
- Krause, G. H. (1988). Photoinhibition of photosynthesis. An evaluation of damaging and protective mechanisms. *Physiol. Plant* 74, 566–574. doi: 10.1111/j.1399-3054.1988.tb02020.x
- Kurade, M. B., Kim, J. R., Govindwar, S. P., and Jeon, B.-H. (2016). Insights into microalgae mediated biodegradation of diazinon by *Chlorella vulgaris*: Microalgal tolerance to xenobiotic pollutants and metabolism. *Algal Res.* 20, 126–134. doi: 10.1016/j.algal.2016.10.003
- Leung, H. W., Minh, T. B., Murphy, M. B., Lam, J. C. W., So, M. K., Martin, M., et al. (2012). Distribution, fate and risk assessment of antibiotics in sewage treatment plants in Hong Kong, South China. *Environ. Int.* 42, 1–9. doi: 10.1016/j.envint.2011.03.004
- Li, Z., Gao, X., Bao, J., Li, S., Wang, X., Li, Z., et al. (2023). Evaluation of growth and antioxidant responses of freshwater microalgae *Chlorella sorokiniana* and *Scenedesmus dimorphus* under exposure of moxifloxacin. *Sci. Total Environ.* 858, 159788. doi: 10.1016/j.scitotenv.2022.159788
- Liang, X., Wang, L., Ou, R., Nie, X., Yang, Y. F., Wang, F., et al. (2015). Effects of norfloxacin on hepatic genes expression of P450 isoforms (CYP1A and CYP3A), GST and P-glycoprotein (Pgp) in Swordtail fish (*Xiphophorus helleri*). *Ecotoxicology* 24, 1566–1573. doi: 10.1007/s10646-015-1457-1
- Liou, J. M., Bair, M. J., Chen, C. C., Lee, Y. C., Chen, M. J., Chen, C. C., et al. (2016). Levofloxacin Sequential Therapy vs Levofloxacin Triple Therapy in the Second-Line Treatment of *Helicobacter pylori*: A Randomized Trial. *Am. J. Gastroenterol.* 111, 381–387. doi: 10.1038/ajg.2015.439
- Liu, Y., Gu, Y., Lou, Y., and Wang, G. (2021). Response mechanisms of domoic acid in *Pseudo-nitzschia multiseries* under copper stress. *Environ. pollut.* 272, 115578. doi: 10.1016/j.envpol.2020.115578
- Liu, B., Liu, W., Nie, X., Guan, C., Yang, Y., Wang, Z., et al. (2011). Growth response and toxic effects of three antibiotics on *Selenastrum capricornutum* evaluated by photosynthetic rate and chlorophyll biosynthesis. *J. Environ. Sci. (China)* 23, 1558–1563. doi: 10.1016/S1001-0742(10)60608-0
- Liu, L., Wu, W., Zhang, J., Lv, P., Xu, L., and Yan, Y. (2018). Progress of research on the toxicology of antibiotic pollution in aquatic organisms. *Acta Ecol. Sin.* 38, 36–41. doi: 10.1016/j.chnaes.2018.01.006
- Lu, J., Wu, J., Zhang, C., Zhang, Y., Lin, Y., and Luo, Y. (2018). Occurrence, distribution, and ecological-health risks of selected antibiotics in coastal waters along the coastline of China. *Sci. Total Environ.* 644, 1469–1476. doi: 10.1016/j.scitotenv.2018.07.096
- Ma, Q., Chen, L., and Zhang, L. (2023). Effects of phosphate on the toxicity and bioaccumulation of arsenate in marine diatom *Skeletonema costatum*. *Sci. Total Environ.* 857, 159566. doi: 10.1016/j.scitotenv.2022.159566
- Magdaleno, A., Saenz, M. E., Juarez, A. B., and Moretton, J. (2015). Effects of six antibiotics and their binary mixtures on growth of *Pseudokirchneriella subcapitata*. *Ecotoxicol. Environ. Saf.* 113, 72–78. doi: 10.1016/j.ecoenv.2014.11.021
- Mao, Y., Yu, Y., Ma, Z., Li, H., Yu, W., Cao, L., et al. (2021). Azithromycin induces dual effects on microalgae: Roles of photosynthetic damage and oxidative stress. *Ecotoxicol. Environ. Saf.* 222, 112496. doi: 10.1016/j.ecoenv.2021.112496
- Martinez, J. L. (2009). Environmental pollution by antibiotics and by antibiotic resistance determinants. *Environ. pollut.* 157, 2893–2902. doi: 10.1016/j.envpol.2009.05.051
- Nie, X. P., Liu, B. Y., Yu, H. J., Liu, W. Q., and Yang, Y. F. (2013). Toxic effects of erythromycin, ciprofloxacin and sulfamethoxazole exposure to the antioxidant system in *Pseudokirchneriella subcapitata*. *Environ. pollut.* 172, 23–32. doi: 10.1016/j.envpol.2012.08.013
- Nie, X., Wang, X., Chen, J., Zitko, V., and An, T. (2008). Response of the freshwater alga *Chlorella vulgaris* to trichloroisocyanuric acid and ciprofloxacin. *Environ. Toxicol.* 27, 168–173. doi: 10.1897/07-028.1
- Pan, Y., Liu, C., Li, F., Zhou, C., Yan, S., Dong, J., et al. (2017). Norfloxacin disrupts *Daphnia magna* induced colony formation in *Scenedesmus quadricauda* and facilitates grazing. *Ecol. Eng.* 102, 255–261. doi: 10.1016/j.ecoleng.2017.02.037
- Pan, X., Zhang, D., Chen, X., Mu, G., Li, L., and Bao, A. (2009). Effects of levofloxacin hydrochloride on photosystem II activity and heterogeneity of *Synechocystis* sp. *Chemosphere* 77, 413–418. doi: 10.1016/j.chemosphere.2009.06.051
- Pinckney, J. L., Hagenbuch, I. M., Long, R. A., and Lovell, C. R. (2013). Sublethal effects of the antibiotic tylosin on estuarine benthic microalgal communities. *Mar. pollut. Bull.* 68, 8–12. doi: 10.1016/j.marpolbul.2013.01.006
- Qian, L., Qi, S., Cao, F., Zhang, J., Zhao, F., Li, C., et al. (2018). Toxic effects of boscalid on the growth, photosynthesis, antioxidant system and metabolism of *Chlorella vulgaris*. *Environ. Pollut.* 242, 171–181. doi: 10.1016/j.envpol.2018.06.055
- Shen, C., Miao, J., Li, Y., and Pan, L. (2016). Effect of benzo[a]pyrene on detoxification and the activity of antioxidant enzymes of marine microalgae. *J. Ocean Univ. China* 15, 303–310. doi: 10.1007/s11802-016-2771-9
- Shinkai, K., Mohrs, M., and Locksley, R. M. (2002). Helper T cells regulate type-2 innate immunity in vivo. *Nature* 420, 825–829. doi: 10.1038/nature01202
- Sies, H. (1997). Oxidative stress: oxidants and antioxidants. *Exp. Physiol.* 82, 291–295. doi: 10.1113/expphysiol.1997.sp004024
- Sun, M., Lin, H., Guo, W., Zhao, F., and Li, J. (2017). Bioaccumulation and biodegradation of sulfamethazine in *Chlorella pyrenoidosa*. *J. Ocean Univ. China* 16, 1167–1174. doi: 10.1007/s11802-017-3367-8
- Tang, S., Yin, H., Chen, S., Peng, H., Chang, J., Liu, Z., et al. (2016). Aerobic degradation of BDE-209 by *Enterococcus casseliflavus*: Isolation, identification and cell changes during degradation process. *J. Hazard. Mater.* 308, 335–342. doi: 10.1016/j.jhazmat.2016.01.062
- Teisseire, H., and Guy, V. (2000). Copper-induced changes in antioxidant enzymes activities in fronds of duckweed (*Lemna minor*). *Plant Sci.* 153, 65–72. doi: 10.1016/S0168-9452(99)00257-5
- Wan, J., Guo, P., Peng, X., and Wen, K. (2015). Effect of erythromycin exposure on the growth, antioxidant system and photosynthesis of *Microcystis flos-aquae*. *J. Hazard. Mater.* 283, 778–786. doi: 10.1016/j.jhazmat.2014.10.026
- Wan, J., Guo, P., and Zhang, S. (2014). Response of the cyanobacterium *Microcystis flos-aquae* to levofloxacin. *Environ. Sci. pollut. Res. Int.* 21, 3858–3865. doi: 10.1007/s11356-013-2340-3
- Wan, L., Wu, Y., Zhang, Y., and Zhang, W. (2022). Toxicity, biodegradation of moxifloxacin and gatifloxacin on *Chlamydomonas reinhardtii* and their metabolic fate. *Ecotoxicol. Environ. Saf.* 240, 113711. doi: 10.1016/j.ecoenv.2022.113711
- Wang, C., Dong, D., Zhang, L., Song, Z., Hua, X., and Guo, Z. (2019b). Response of freshwater biofilms to antibiotic florfenicol and ofloxacin stress: role of extracellular polymeric substances. *Int. J. Environ. Res.* 16, 715. doi: 10.3390/ijerph16050715
- Wang, Z. H., Nie, X. P., Yue, W. J., and Li, X. (2012). Physiological responses of three marine microalgae exposed to cypermethrin. *Environ. Toxicol.* 27, 563–572. doi: 10.1002/tox.20678
- Wang, G., Zhang, Q., Li, J., Chen, X., Lang, Q., and Kuang, S. (2019a). Combined effects of erythromycin and enrofloxacin on antioxidant enzymes and photosynthesis-related gene transcription in *Chlorella vulgaris*. *Aquat. Toxicol.* 212, 138–145. doi: 10.1016/j.aquatox.2019.05.004
- White, M., Lenzi, K., Dutcher, L. S., Saw, S., Morgan, S. C., Binkley, S., et al. (2019). 124. Impact of levofloxacin MIC on outcomes with levofloxacin step-down therapy in enterobacteriaceae bloodstream infections. *Open Forum Infect. Dis.* 6, S10. doi: 10.1093/ofid/ofz360.199
- Xiong, Q., Hu, L. X., Liu, Y. S., Zhao, J. L., He, L. Y., and Ying, G. G. (2021). Microalgae-based technology for antibiotics removal: From mechanisms to application of innovational hybrid systems. *Environ. Int.* 155, 106594. doi: 10.1016/j.envint.2021.106594
- Xiong, J. Q., Kurade, M. B., and Jeon, B. H. (2017a). Ecotoxicological effects of enrofloxacin and its removal by monoculture of microalgal species and their consortium. *Environ. pollut.* 226, 486–493. doi: 10.1016/j.envpol.2017.04.044
- Xiong, J. Q., Kurade, M. B., Kim, J. R., Roh, H. S., and Jeon, B. H. (2017b). Ciprofloxacin toxicity and its co-metabolic removal by a freshwater microalga *Chlamydomonas mexicana*. *J. Hazard. Mater.* 323, 212–219. doi: 10.1016/j.jhazmat.2016.04.073
- Zhang, Y., He, D., Chang, F., Dang, C., and Fu, J. (2021a). Combined effects of sulfamethoxazole and erythromycin on a freshwater microalga, *Raphidocelis subcapitata*: toxicity and oxidative stress. *Antibiotics (Basel)* 10, 576. doi: 10.3390/antibiotics10050576
- Zhang, Y., Li, M., Chang, F., Yi, M., Ge, H., Fu, J., et al. (2023). The distinct resistance mechanisms of cyanobacteria and green algae to sulfamethoxazole and its implications for environmental risk assessment. *Sci. Total Environ.* 854, 158723. doi: 10.1016/j.scitotenv.2022.158723
- Zhang, L., Shen, L., Qin, S., Cui, J., and Liu, Y. (2020a). Quinolones antibiotics in the Baiyangdian Lake, China: Occurrence, distribution, predicted no-effect concentrations (PNECs) and ecological risks by three methods. *Environ. pollut.* 256, 113458. doi: 10.1016/j.envpol.2019.113458
- Zhang, Y., Xu, N., and Li, Y. (2021b). Effect of the extracts of *Sargassum fusiforme* on red tide microalgae in East China sea. *Front. Mar. Sci.* 2021. doi: 10.3389/fmars.2021.628095
- Zhang, Y., Zhang, X., Guo, R., Zhang, Q., Cao, X., Suranjana, M., et al. (2020b). Effects of florfenicol on growth, photosynthesis and antioxidant system of the non-target organism *Isochrysis galbana*. *Comp. Biochem. Physiol. C Toxicol. Pharmacol.* 233, 108764. doi: 10.1016/j.cbpc.2020.108764
- Zou, S., Xu, W., Zhang, R., Tang, J., Chen, Y., and Zhang, G. (2011). Occurrence and distribution of antibiotics in coastal water of the Bohai Bay, China: Impacts of river discharge and aquaculture activities. *Environ. pollut.* 159, 2913–2920. doi: 10.1016/j.envpol.2011.04.037



OPEN ACCESS

EDITED BY

Yohei Shimasaki,
Kyushu University, Japan

REVIEWED BY

Gabriel-Ionut Plavan,
Alexandru Ioan Cuza University, Romania
Mohamed Nejib Daly Yahia,
Qatar University, Qatar

*CORRESPONDENCE

Fehmi Boufahja

✉ faboufahja@imamu.edu.sa

[†]These authors have contributed equally to this work

RECEIVED 23 February 2024

ACCEPTED 29 April 2024

PUBLISHED 21 May 2024

CITATION

Aldraiwish BM, Alaqeel MM, Al-Hoshani N, Özdemir S, Pacioglu O, Necula M, Milea EC, Hedfi A, Rudayni HA and Boufahja F (2024) Are microplastics efficient remediation tools for removing the statin Lipitor? A laboratory experiment with meiobenthic nematodes. *Front. Mar. Sci.* 11:1390700. doi: 10.3389/fmars.2024.1390700

COPYRIGHT

© 2024 Aldraiwish, Alaqeel, Al-Hoshani, Özdemir, Pacioglu, Necula, Milea, Hedfi, Rudayni and Boufahja. This is an open-access article distributed under the terms of the [Creative Commons Attribution License \(CC BY\)](https://creativecommons.org/licenses/by/4.0/). The use, distribution or reproduction in other forums is permitted, provided the original author(s) and the copyright owner(s) are credited and that the original publication in this journal is cited, in accordance with accepted academic practice. No use, distribution or reproduction is permitted which does not comply with these terms.

Are microplastics efficient remediation tools for removing the statin Lipitor? A laboratory experiment with meiobenthic nematodes

Bayan M. Aldraiwish^{1†}, Maha M. Alaqeel^{1†}, Nawal Al-Hoshani², Sadin Özdemir³, Octavian Pacioglu⁴, Marian Necula⁴, Eduard C. Milea⁴, Amor Hedfi⁵, Hassan A. Rudayni¹ and Fehmi Boufahja^{1*}

¹Biology Department, College of Science, Imam Mohammad Ibn Saud Islamic University (IMSIU), Riyadh, Saudi Arabia, ²Department of Biology, College of Science, Princess Nourah Bint Abdulrahman University, Riyadh, Saudi Arabia, ³Food Processing Programme Technical Science Vocational School Mersin University, Mersin, Türkiye, ⁴Department of Bioinformatics, National Institute of Research and Development for Biological Sciences, Bucharest, Romania, ⁵LR01ES14 Laboratory of Environment Biomonitoring, Coastal Ecology and Ecotoxicology Unit, Faculty of Sciences of Bizerte, University of Carthage, Zarzouna, Tunisia

Introduction: The current experiment investigated the multifaceted effects induced by microplastics and the statin Lipitor on marine benthic nematodes.

Methods: The nematodes were exposed to a single polystyrene and polyvinyl chlorides (both at 1 mg.kg⁻¹ Dry Weight) and two Lipitor concentrations (0.1 and 1 mg.l⁻¹), as well as to a mixture of both types of pollutants, for 30 days.

Results: The results highlighted a significant decrease in the abundance, individual biomass, and diversity of nematodes directly with the addition of polyvinyl chlorides and/or Lipitor. These treatments induced a greater mortality rate among microvores and diatom feeders compared to other feeding types of nematodes.

Discussion: The nematofauna underwent a strong restructuring phase following exposure to microplastics and Lipitor when added alone, leading to the disappearance of sensitive species and their replacement by more tolerant taxa. The toxicity of Lipitor is attenuated by the physical bonding with polystyrene when added to a mixture and has no negative effect on marine nematode species.

KEYWORDS

polystyrene, polyvinyl chloride, Lipitor, meiofauna, ecotoxicity

1 Introduction

Population growth and urbanization take place in many parts of the world, often accompanied by the local development of industry and technological advances, with detrimental effects on the environment (Avio et al., 2015). Various abiotic components, such as the atmosphere, water, soil, and sediments become the end recipients of traditional and emerging pollutants, with a negative impact on their ecological status (Menchaca et al., 2014).

One of the most widespread types of emergent contaminants of current concern comprises by- and end products of the plastic material industry (Abuwatfa et al., 2021). Two common types of plastics are Polyvinyl chlorides (hereafter PVC) and Polystyrene (hereafter PS). PVCs comprise cheap, easy-to-shape, and lightweight plastics. In recent history, the PVCs replaced traditional materials in various economic domains, but their efficient recycling remains a major challenge (Zhao et al., 2021). Besides, there are also a growing number of technical and economic issues associated with this, hindering progress in this field. The waste recycling technology improved the polymer market industry, but there is still room for improvement (Lange, 2021). Various types of common polymers, such as vinyl, are inherently difficult to recycle and to be transformed into an environmentally friendly end product. Thiolactones are a cleavable common additive used in the chemical degradation and recovery technology of vinyl polymers and produced another well-known free-radical polymer, polystyrene. PSs of variable molecular mass (i.e. 20–300 kDa) and randomly incorporated thioester backbone linkages (i.e. 2.5–55 mol %) are selectively depolymerized to produce well-defined thiol-terminated fragments (i.e. below 10 kDa). These fragments are suitable for efficient oxidative depolymerization, which produces recovered PS in good yields (i.e. 80–95%) with similar molecular mass (Wei et al., 2019).

Besides various end products of the plastic industry, another human activity with a detrimental impact on the environment is the drug industry. More recently, a particular drug type, called statins with a more special focus on Lipitor, caught the attention of specialists (Chow et al., 2010; Jaramillo-Madrid et al., 2020). Several countries with high development rates experienced during the past decade the occurrence of obesity and cardiovascular diseases. The frequency of occurrence of these human issues was proved to be reduced by Lipitor, a common lipid-modifying statin drug, which exerts multiple effects on lipoprotein metabolism and remains up to date the number-one-sold statin of all time.

It is known that large quantities of drugs and microplastics end up in the benthic marine areas and are transferred back to humans by bioaccumulation and biomagnification processes. The multifaceted detrimental effects induced by these xenobiotics on biota remain largely unknown and are insufficiently documented. In the current study, we have explored the impact that Lipitor and microplastics (PVC and PS) have on marine meiofauna, with far-reaching practical applications. The current bioassay aimed to fill the knowledge gap about meiofauna because of their lower use as ecological indicators compared to macrofauna (Borja et al., 2000). The current study supports, however, that utilizing these tiny organisms could be just as

effective or potentially more beneficial and effective, thanks to their multi-species responsiveness, abundant availability, and constrained requirements for sampling (Semprucci et al., 2015). Yet, there remains an ongoing discussion regarding the possession of meiobenthic nematodes of traits that distinguish them as one of the most prosperous multicellular organisms on Earth, thriving in environments with very difficult circumstances (Sapir, 2021). Indeed, these worms form the lower part of marine food webs and comprise very abundant (up to 23 million per m²) and diverse invertebrates (~9000 species were described based on morphological traits) (Nemys, 2024). Global species richness of marine nematodes was even proposed based on the progress of DNA barcoding, being estimated between ~50,000 and one million or more (Ridall and Ingels, 2021). Numerous experimental studies have demonstrated that nematodes have an interesting potential as bioindicative tools in laboratory bioassays due to several characteristics, particularly their small size (generally 1–5 mm in length at the adult stage) and brief lifespans (weeks to months) (Moreno et al., 2011). Numerous studies made thus it possible to obtain ecotoxicological information that covers a large sensitivity/tolerance spectrum for nematodes against stress agents (Hägerbäumer et al., 2015).

The current work aimed to assess the ecotoxicological impact of three emergent contaminants, two microplastic types (i.e. PVC and PS) and Lipitor, on meiobenthic nematodes, by using single and mixture applications. The results obtained will be particularly useful with the goals of testing if one or both categories of microplastics could be used as remediators for statins' contaminated sediments based on outcomes of treatment combinations.

2 Materials and methods

A graphic representation of steps, experimental design, and type of analyses are given in Figure 1. Details of all schematic steps are presented hereafter.

2.1 Collection site and laboratory processing

Sediments were collected early in the morning (7 A.M.) of November 27, 2022, at a coastal site (37°15'07.34" N, 9°56'26.75" E) situated in the upper infralittoral domain of Bizerte Bay, Tunisia. Such a collection timing was chosen on purpose to avoid the vertical migration of nematodes to deeper sediment strata away from heat after sunrise (Wakkaf et al., 2020). The samples were taken from the upper 5 cm of the sediment layer with the aid of Plexiglass hand cores (inner diameter of 3.6 cm, section of 10 cm²). Coull and Chandler (1992) noted that the majority of meiobenthic organisms are found in the top substrate layers. The collection site was chosen following the recommendations of Boufahja (2010) and Hedfi et al (Hedfi et al., 2013, 2021), who classified it as pristine and with a highly diverse meiofauna community. Four abiotic parameters were measured at the sediment-water interface: the water depth, which

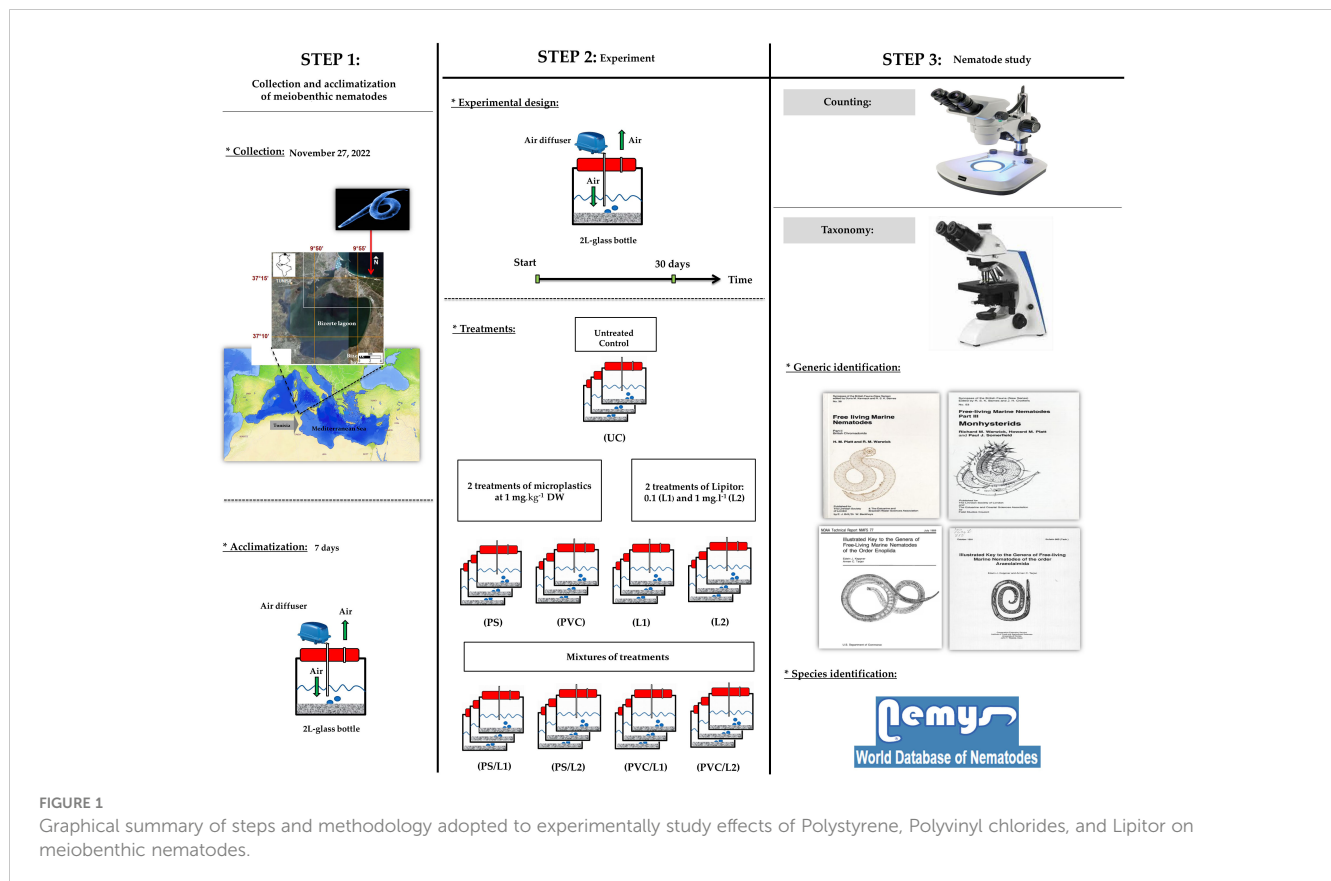


FIGURE 1

Graphical summary of steps and methodology adopted to experimentally study effects of Polystyrene, Polyvinyl chlorides, and Lipitor on meiobenthic nematodes.

was measured with a pendulum, salinity, and temperature, measured with a Thermo-Salinometer Model WTW LF 196 (Weilheim, Germany) and dissolved oxygen concentrations with a WTW Oxi 330/SET, WTW, Weilheim (Germany) Model Oximeter.

In the laboratory, aliquots of sediment were sieved (63 μm mesh size) and then dried at 45°C (Buchanan, 1971). Cumulative curves were plotted afterward to measure the mean grain size of the coarse fraction (Buchanan, 1971). Additional aliquots, of equal volumes, were used to quantify the total organic matter content by the mass loss method (450°C, 6 h) (Fabiano and Danovaro, 1994), and water content, after drying the sediment at 45°C until constant mass (Boufahja et al., 2011).

2.2 Sediment contamination and experimental setup

Following Schratzberger et al. (2004), some of the collected sediment was made azoic by repeated (three times) freezing (-20°C) and thawing (12 h/48 h). Following the removal of coarser particles (small rocks and microalgal debris) by sieving (1 mm), the remaining sediment was allowed to acclimatize for a week to adapt the meiofauna to the experimental conditions (darkness, 4°C) (Bellakhal et al., 2023).

Two types of microplastics were considered in this experiment: polystyrene and polyvinyl chloride. Spheres of PS microplastics measuring 10 μm in size and with a density of 1.05 g cm⁻³ were purchased from PolyScience, Europe (Fluoresbrite YG magnetic microspheres, Hirschberg an der Bergstraße, Germany, excitation:

441 nm, emission: 486 nm). These microplastics were previously identified and microscopically described by Weber et al. (2021). A high molecular weight PVC (MW = 48,000 g. mol⁻¹, 16 mmol of Cl.g⁻¹, 99%) was also acquired from Fluka. These microplastics consist of round particles that are smaller than 40 μm in diameter.

The amounts of PVC and PS to be introduced in the experimental units were chosen based on works of Hedfi et al. (2022) and Bellakhal et al. (2023), respectively. Based on these authors, a concentration of 1 mg.kg⁻¹ Dry Weight 'DW' of microplastics will be not ecotoxic for meiobenthic nematodes in the case of PS, but with no known effect for PVC. The experiment lasted for 30 days (Essid et al., 2021) after applying eight treatments: polystyrene (PS: 1 mg.kg⁻¹ DW), Polyvinyl chloride (PVC: 1 mg.kg⁻¹ DW), and Lipitor (L1: 0.1 mg.l⁻¹ and L2: 1 mg.l⁻¹), and their mixtures (PS/L1, PS/L2, PVC/L1, and PVC/L2). The control nematodes were topped up with only filtered seawater (0.7 μm pore-size Glas Microfibre GF/F, Whatman, Allouche et al., 2022) without the addition of Lipitor or microplastics.

2.3 Nematode study

The method of levigation-decantation-sieving (40 μm and 1 mm) was first applied to extract the meiobenthos, following Vitiello and Dinot (1979). Only the fraction coarser than 40 μm sieve was kept in 4% neutral formalin, and Rose Bengal (0.2 g.l⁻¹) was added to better distinguish the pink-colored organisms from inert background material (Guo et al., 2001). Afterward, the

meiobenthic nematodes were sorted with the aid of a 50x stereomicroscope (Wild-M3B type) with the aid of a tiled Dollfus tank (200 squares of 5 mm², Hedfi et al., 2022). One hundred nematodes were then picked from each microcosm (Ishak et al., 2022) and mounted on microscope slides as described by Seinhorst (1959). The worms were identified to genus level with a Nikon DS-Fi2 camera coupled to a Nikon microscope (Image Software NIS Elements Analysis Version 4.0 Nikon 4.00.07–build 787–64 bit) based on the generic keys of Platt and Warwick (1983, 1988), Warwick et al. (1998) and Keppner and Tarjan (Keppner and Tarjan, 1989, 1991, 1994, 1999). Morphological descriptions of the species were downloaded from the NeMys database (Nemys, 2024). Four community-based qualitative tools were considered, namely: the Species number (S), Margalef's species richness (d), Shannon-Wiener's Index (H'), and Pielou's Evenness (J').

Two functional traits were distinguished for each nematode genus (Schratzberger et al., 2007): feeding type and tail shape. Following Wieser (1953), four trophic groups were separated: the selective deposit feeders (1A), which are mainly microcores, non-selective deposit feeders (1B) that consume detritus, the epistratum feeders (2A) that feed on benthic diatoms, and the omnivores-carnivores (2B) that prey on smaller meiobenthic invertebrates. Moreover, four tail shapes were discriminated according to Thistle et al. (1995): conical (co), clavate/conico-cylindrical (cla), elongated/filiform (e/f), and short/rounded (s/r).

2.4 Statistical processing

Data were tested for normality (i.e. Kolmogorov-Smirnov test) and equality of variances (i.e. Bartlett test) to satisfy the normal distribution and *log*-transformed afterward when necessary. Six univariate metrics were measured for each microcosm: abundance, individual biomass, number of species (S), Margalef's species richness (d), Shannon-Weaner index (H'), and Pielou's evenness (J'). One-way analysis of variance (ANOVA) and Tukey's HSD (Honestly Significant Difference) tests were performed using STATISTICA v.8 software to detect significant global and for multiple comparisons, respectively. Several multivariate analyses were also performed using PRIMER v.5 package (Plymouth Routines in Multivariate Ecological Research) (see Clarke, 1993; Clarke and Gorley, 2001). First, a similarity matrix was constructed based on single-linkage Bray-Curtis similarity scores obtained from square-root transformed nematode abundances. Subsequently, hierarchical cluster analysis

(hereinafter referred to as CA) and non-metric multidimensional scaling (hereinafter referred to as nMDS) sorting were applied. Analysis of similarity (ANOSIM) was necessary to identify significant taxonomic or functional differences, followed by SIMPER analysis (SIMilarity PERcentages) to determine the contribution of taxa or functional groups to ~50% to the average difference between treatments (Clarke, 1993; Mahmoudi et al., 2005).

3 Results

3.1 Abiotic features of the collection site

In-situ dissolved oxygen concentration was 12.6 mg.l⁻¹ at 50 cm of water column, whereas the temperature and salinity were 14°C and 38.4 PSU, respectively. The sediments were coarse (> 63 µm, 87.23 ± 4.11%) and the mean grain size was 0.56 ± 0.09%. Finally, the total organic matter and water content of sediment were 2.5 ± 0.21% and 36.7 ± 2.19%, respectively.

3.2 Abundance and individual biomass of nematodes

Table 1 showed significant fluctuations in terms of abundances and individual biomass of meiobenthic nematodes. Thus, a maximum of 1239 ± 37 individuals and 2.23 ± 0.11 µg DW distinguished discernibly nematodes of the control community UC from those of all the other ones. It should be said that the maximum differences were found between the assemblage UC and those exposed to PVC, L1, and L2, for both abundance and individual biomass (Tukey's HSD test: *p* < 0.0001).

3.3 Taxonomic census and community composition of nematodes

At the end of the bioassay, the free-living marine nematodes comprised 7 orders, 18 families, 23 genera, and 27 species (Tables 2, 3). The most diverse families were Xyalidae (S = 6), Cyatholaimidae (S = 3), Oncholaimidae (S = 2), and Comesomatidae (S = 2). The remaining 14 families comprised just one species (Table 2). The control UC was populated by 27 species, whereas the treatments comprised as follows: PS - 22

TABLE 1 Abundance and individual biomass of meiobenthic nematodes exposed to the control treatment (UC) and those enriched with Polystyrene (PS), polyvinyl chlorides (PVC), Lipitor (L1 and L2), and their mixtures (PS/L1, PS/L2, PVC/L1, and PVC/L2).

Treatments	UC	PS	PVC	L1	L2	PS/L1	PS/L2	PVC/L1	PVC/L2
Abundance (individuals)	1239 (37)	826 (82) *	198 (45) ****	221 (51) ****	172 (24) ****	988 (79) *	817 (64) *	472 (36) **	363 (45) **
Individual biomass (µg Dry Weight)	2.23 (0.11)	1.25 (0.10) **	0.68 (0.22) ****	0.44 (0.07) ****	0.33 (0.02) ****	1.05 (0.25) ***	1.03 (0.08) ***	0.81 (0.16) ****	0.90 (0.24) ****

Stars next to values indicate significant differences with controls (Tukey's HSD test): *p* < 0.05 (*), *p* < 0.01 (**), *p* < 0.001 (***), and *p* < 0.0001 (****).

TABLE 2 Alphabetical listing of nematode taxa from microcosms spiked or not with Polyvinyl chlorides, polystyrene, and/or Lipitor and their taxonomic nomenclature and classification, feeding types (FG), and tail shapes (TS).

Order	Family	Genus	Species	Nomenclature	FG	TS
Enoplida	Tripyloididae	<i>Bathylaimus</i>	sp.	Cobb, 1894	2B	co
Desmoscolecida	Cyartonematidae	<i>Cyartonema</i>	<i>germanicum</i>	Juario, 1972	1A	co
Monhysterida	Xyalidae	<i>Daptonema</i>	<i>fallax</i>	(Lorenzen, 1972) Lorenzen, 1977	1B	co
Monhysterida	Xyalidae	<i>Daptonema</i>	<i>normandicum</i>	(de Man, 1890) Lorenzen, 1977	1B	cla
Monhysterida	Xyalidae	<i>Daptonema</i>	<i>trabeculosum</i>	Schneider, 1906	1B	cla
Enoplida	Thoracostomopsidae	<i>Enoploilaimus</i>	<i>longicaudatus</i>	(Southern, 1914) Filipjev, 1921	2B	cla
Enoplida	Oxystominidae	<i>Halalaimus</i>	<i>gracilis</i>	de Man, 1888	1A	e/f
Plectida	Leptolaimidae	<i>Halaphanolaimus</i>	sp.	Southern, 1914	1A	co
Chromadorida	Cyatholaimidae	<i>Longicyatholaimus</i>	<i>longicaudatus</i>	(de Man, 1876) Micoletzky, 1924	2A	e/f
Chromadorida	Cyatholaimidae	<i>Maryllynna</i>	<i>puncticaudata</i>	Boufahja and Beyrem, 2014	2A	e/f
Chromadorida	Cyatholaimidae	<i>Maryllynna</i>	<i>steckhoveni</i>	(Wieser, 1954) Hopper, 1977	2A	e/f
Enoplida	Oncholaimidae	<i>Metoncholaimus</i>	<i>pristiurus</i>	(Zur Strassen, 1894) Filipjev, 1918	2B	cla
Desmodorida	Microlaimidae	<i>Microlaimus</i>	<i>honestus</i>	de Man, 1922	2A	co
Araeolaimida	Axonolaimidae	<i>Odontophora</i>	<i>wieseri</i>	Luc and De Coninck, 1959	1B	co
Enoplida	Oncholaimidae	<i>Oncholaimellus</i>	<i>calvadocicus</i>	de Man, 1890	2B	cla
Monhysterida	Xyalidae	<i>Paramonohystera</i>	<i>proteus</i>	Wieser, 1956	1B	cla
Monhysterida	Sphaerolaimidae	<i>Parasphaerolaimus</i>	<i>paradoxus</i>	Ditlevsen, 1918	2B	cla
Enoplida	Phanodermatidae	<i>Phanoderma</i>	sp.	Bastian, 1865	2A	co
Chromadorida	Chromadoridae	<i>Prochromadorella</i>	<i>longicaudata</i>	(Kreis, 1929) Lorenzen, 1972	2A	co
Araeolaimida	Comesomatidae	<i>Sabatieria</i>	<i>splendens</i>	(Hopper, 1967)	1B	cla
Araeolaimida	Comesomatidae	<i>Sabatieria</i>	<i>punctata</i>	(Kreis, 1924)	1B	cla
Desmodorida	Desmodoridae	<i>Spirinia</i>	<i>parasitifera</i>	(Bastian, 1865) Gerlach, 1963	2A	co
Chromadorida	Selachinematidae	<i>Synonchiella</i>	<i>edax</i>	Aissa and Vitiello, 1977	2B	co
Enoplida	Ironidae	<i>Thalassironus</i>	<i>britannicus</i>	de Man, 1889	2B	co
Monhysterida	Xyalidae	<i>Theristus</i>	<i>modicus</i>	Wieser, 1956	1B	co
Enoplida	Enchelidiidae	<i>Thoonchus</i>	<i>inermis</i>	Gerlach, 1953	2B	cla
Monhysterida	Xyalidae	<i>Valvaelaimus</i>	<i>maior</i>	(Gerlach, 1956) Lorenzen, 1977	1B	co

species, PVC - 20 species, L1 - 22 species, L2 - 21 species, PS/L1 - 26 species, PS/L2 - 26 species, PVC/L1 - 25 species, PVC/L2 - 19 species.

In control treatments, the nematofauna was co-dominated (5% ≤, Engelmann (1978)) by seven taxa, as follows: *Metoncholaimus pristiurus* (12 ± 2.40%), *Longicyatholaimus longicaudatus* (10.22 ± 1.67%), *Maryllynna puncticaudata* (6.66 ± 1.33%), *Phanoderma* sp. (6 ± 1.3%), *Prochromadorella longicaudata* (5.7 ± 0.76), *M. steckhoveni* (5.55 ± 1.53%), and *Microlaimus honestus* (5.11 ± 1.67%).

The changes observed in the nematode diversity in treatments are graphically representation in Figure 2. The communities comprising the lower number of species were the treatments exposed to Polyvinyl chlorides (PVC) and Lipitor (L1 and L2). The rest of the treatments were associated with higher taxonomic diversity, statistically not different from controls (Tukey-HSD test:

p -values > 0.05, Figure 2). In contrast, the metrics H' and/or d were significantly lower in PVC, L1, and L2 compared to UC (Tukey-HSD test: p -values < 0.01, Figure 2). The Pielou's Evenness did not differ among treatments (1-ANOVA: p -values = 0.7135, Figure 2).

The Hierarchical Cluster Analysis and the nMDS orientation based on the Bray-Curtis similarity matrix, revealed at the cutoff at ~70%, a similar two-dimensional pattern of the nematode assemblages (Figure 3). The nematofauna was divided into three groups. The first group belonged to treatments exposed to PVC and PVC/L2 and was located on the top left of Figure 3. The second group comprised the nematodes exposed to UC, PS/L1, and PS/L2 and was located at the bottom of Figure 3. The third group was exposed to PVC/L1, L1, L2, and PS and was located at the top right of Figure 3. This clustering was also closely supported by the

TABLE 3 Relative abundances (%) of the free-living nematode species identified in the control treatment (UC) and those enriched with Polystyrene (PS), polyvinyl chlorides (PVC), Lipitor (L1 and L2), and their mixtures (PS/L1, PS/L2, PVC/L1, and PVC/L2).

Treatments	UC	PS	PVC	L1	L2	PS/L1	PS/L2	PVC/L1	PVC/L2
<i>Bathylaimus</i> sp.	1.33 (0.66)	6.00 (2.65)	2.00 (0.00)	4.33 (1.53)	4.67 (0.58)	1.00 (0.00)	2.33 (1.53)	2.00 (0.00)	3.00 (1.00)
<i>Cyartonea germanicum</i>	4.66 (1.76)		1.33 (1.53)			5.00 (2.65)	3.67 (1.15)	0.00 (0.00)	2.00 (2.00)
<i>Daptonema fallax</i>	1.11 (0.38)	3.67 (2.52)	3.33 (3.21)	3.00 (2.65)	4.67 (4.16)	1.00 (0.00)	1.67 (0.58)	2.00 (2.00)	
<i>Daptonema normanicum</i>	0.44 (0.76)		3.67 (2.31)			0.33 (0.58)			
<i>Daptonema trabeculosum</i>	0.88 (0.38)	4.00 (0.00)	9.00 (2.65)	6.33 (0.58)	6.33 (0.58)	4.00 (2.00)	1.33 (0.58)	4.67 (1.15)	5.00 (1.00)
<i>Enoplolaimus longicaudatus</i>	4.44 (2.5)	4.00 (0.00)	10.00 (1.00)	6 (3)	6.67 (1.53)	6.00 (1.00)	2.67 (2.89)	10.33 (2.31)	7.00 (0.00)
<i>Halalaimus gracilis</i>	3.33 (1.76)	7.67 (0.58)	3.00 (0.00)	5.67 (0.58)	5.33 (1.53)	4.33 (3.06)	2.00 (1.00)	4.00 (0.00)	1.67 (1.53)
<i>Longicyatholaimus longicaudatus</i>	10.22 (1.67)	4.00 (2.65)	3.67 (3.06)	3.67 (2.08)	1.67 (1.53)	8.67 (2.52)	9.00 (3.00)	2.00 (2.00)	1.67 (1.53)
<i>Metoncholaimus pristiurus</i>	12 (2.40)					6.67 (2.31)	7.00 (2.65)	1.00 (1.00)	
<i>Marylynna puncticaudata</i>	6.66 (1.33)	2.00 (1.00)	2.67 (2.08)	2.33 (2.52)	4.67 (2.31)	6.00 (2.65)	5.33 (0.58)	2.33 (2.08)	3.33 (0.58)
<i>Marylynna steckhoveni</i>	5.55 (1.53)	5.33 (4.04)		4.00 (1.73)	4.67 (1.53)	6.67 (0.58)	5.33 (2.31)	3.67 (0.58)	1.33 (2.31)
<i>Microilaimus honestus</i>	5.11 (1.67)	6.67 (2.31)	2.00 (0.00)	4.33 (0.58)	4.33 (0.58)	1.67 (1.15)	2.00 (1.00)	2.67 (1.15)	2.67 (0.58)
<i>Odontophora wieseri</i>	4.66 (1.15)	1.00 (0.00)	2.67 (2.89)	2.33 (0.58)	2.33 (0.58)	4.67 (2.52)	4.33 (2.08)	2.00 (1.00)	2.33 (0.58)
<i>Oncholaimellus calvadocicus</i>	1.11 (1.38)	5.33 (0.58)	1.00 (0.00)	6.00 (1.73)	8.00 (2.65)	4.00 (1.73)	3.67 (2.08)	6.67 (1.15)	4.67 (1.15)
<i>Halaphanolaimus</i> sp.	4.66 (1.15)	7.33 (0.58)	3.00 (0.00)	5.67 (0.58)	6.67 (1.15)	2.00 (0.00)	3.00 (2.00)	4.00 (0.00)	5.00 (1.00)
<i>Paramonohystera proteus</i>	0.44 (0.76)	5 (2.65)					0.33 (0.58)		
<i>Parasphaerolaimus paradoxus</i>	4.88 (3.67)		2.67 (0.58)	1 (1.73)		3.67 (2.08)	3.67 (1.15)	1.67 (1.53)	5.67 (2.52)
<i>Phanoderma</i> sp.	6 (1.33)	3 (3)		2 (3.46)	4.67 (0.58)	5.67 (2.31)	6 (2)	3 (2.65)	
<i>Prochromadorella longicaudata</i>	5.77 (0.76)	4.67 (3.06)		5.33 (2.52)	7.33 (2.08)	6.67 (2.31)	5.33 (2.52)	3.67 (1.53)	
<i>Synonchiella edax</i>	2.66 (0.66)	7.67 (0.58)	10.67 (0.58)	8.67 (3.21)	6 (1.73)	7.67 (1.15)	10.33 (1.53)	10.67 (2.08)	13.67 (1.15)
<i>Sabatiera splendens</i>	1.55 (1.01)	3.33 (1.53)	6 (3.61)	1 (1.73)	0.67 (1.15)	2 (1.73)	4 (0.00)	3.67 (2.08)	7 (3)
<i>Spirinia parasitifera</i>	3.77 (1.38)	6.33 (0.58)	11.33 (1.15)	6.33 (1.53)	6(1)	7.33 (0.58)	7 (3)	6.33 (1.53)	11.67 (2.52)
<i>Sabatieria punctata</i>	1.55 (1.01)	0.33 (0.58)	5.33 (4.04)			1.33 (0.58)	1.67 (0.58)	1 (1.73)	5 (2.65)
<i>Thalassironus britannicus</i>	3.77 (2.14)	4 (1)	14 (2.65)	7 (1.73)	5.67 (1.53)	5.33 (1.53)	2 (1)	4.67 (0.58)	11 (1)
<i>Theristus modicus</i>	1.55 (1.67)	6 (1)		5 (0.2.65)	4 (1)	1 (0.00)	1.67 (0.58)	6.33 (3.06)	3 (3)
<i>Thoonchus inermis</i>	1.33 (0.66)	2.67 (1.53)		7.67 (1.53)	5 (1.73)	0.33 (0.53)	1 (0.00)	7 (1)	
<i>Valvaelaimus maior</i>	0.44 (0.76)		2.67 (2.08)	1.67 (2.89)	1.33 (1.15)	0.33 (0.58)	1.67 (2.08)	4.67 (1.53)	
Species number	24.33 (1.53)	21 (1)	19.67 (0.58)	18.67 (1.15)	19.33 (1.15)	24 (0)	25 (1)	21.33 (1.15)	17.33 (0.58)

dissimilarity values, which linked treatments to controls (Table 4). Overall, based on the ANOSIM outcomes and dissimilarity values compared to controls (Table 4), the treatments followed the ranking PS/L2 < PS/L1 < L2 < PS < PVC/L1 < L1 < PVC/L2 < PVC. The

minimum values of the *R*-statistics were observed also for PS/L2 (0.889) and PS/L1 (0.926); all the remaining treatments had a value of 1. SIMPER results (Table 4) supported also the overall nMDS outcomes, by specifying the contributions of taxa to ~50% of

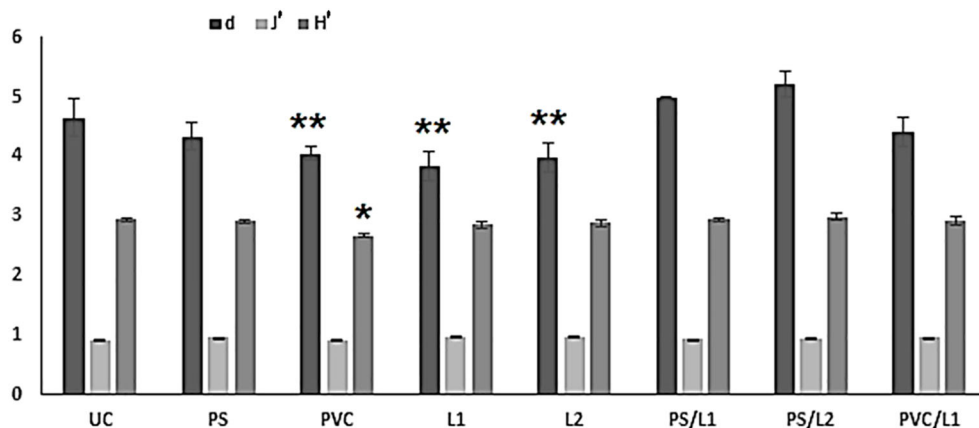


FIGURE 2

Graphical summary of univariate taxonomic indices of the control microcosms (UC) and those enriched with polystyrene (PS), Polyvinyl chlorides (PVC), Lipitor (L1 and L2) and their mixtures (PS/L1, PS/L2, PVC/L1, and PVC/L2). d = Margalef's Species Richness, J' = Pielou's evenness, H' = Shannon-Wiener index. The stars indicate the significant differences compared to the controls UC (* $p < 0.05$; ** $p < 0.01$; Tukey's HSD test, log-transformed data).

dissimilarities among assemblages exposed to PS, PVC, and L and control treatments, as follows:

- The first pattern: the abundances of three species were significantly reduced at PS: *L. longicaudatus*, *M. puncticaudata*, and *Odontophora wieseri* (Table 4). The following species were deleted: *M. pristiurus*, *Cyartonema germanicum*, and *Parasphaerolaimus paradoxus*.
- The second pattern: the abundances of three species were significantly reduced at PVC: *L. longicaudatus*, *C. germanicum*, and *M. puncticaudata* (Table 4). The following species were deleted: *M. pristiurus*, *Phanoderma* sp., *P. longicaudata*, and *M. puncticaudata*.
- The third pattern: the abundances of one species were significantly reduced at L1 and L2: *L. longicaudatus* (Table 4). The following species were deleted: *M. pristiurus*, *C. germanicum*, and *S. punctata*, but the *P. paradoxus* in L1 declined and in L2 disappeared.
- The fourth taxonomic pattern was apparent in the remaining mixtures: PS/L1, PS/L2, PVC/L1, and PVC/L2. *M. pristiurus* declined in all mixtures, except for PVC/L2, from where it disappeared. *L. longicaudatus* declined in all treatments.

4 Discussion

The current experiment aimed to assess the separate and combined effects of PS, PVC, and Lipitor on meiobenthic nematodes. A comparable magnitude of the negative impact of PVC, L1, and L2 was significantly found on the abundance, individual biomass, and taxonomic diversity at the end of the current experiment. The microcosms with the highest concentrations of PVC microplastics and Lipitor were significantly less populated, and less rich in large

individuals and species compared to controls and all the rest of the assemblages. The species *L. longicaudatus* (2A) and *C. germanicum* (1A) appeared to be sensitive, whereas *Daptonema trabeculosum* (1B) and *Oncholaimellus calvadocicus* (2B) were tolerant/opportunistic for PCV and Lipitor, respectively. The special case of the omnivore-carnivore *M. pristiurus*, which appeared extremely sensitive to both types of pollutants, could be related to the fact that most specimens collected were juveniles, so at a vulnerable stage of their life.

The suggested sensitivity of nematodes to both Lipitor and PVC could also be related to the feeding mode, given that the communities from all treatments comprised a low frequency of epistratum feeders (or diatom consumers) and microvores. Thus, it was deduced that the thresholds were reached as low as 1 mg.l^{-1} of Lipitor and 1 mg.kg^{-1} of PVC. The scientific literature on the uptake and toxicity of statins and PVC by diatoms and microbes seems to support the above findings. According to Wang et al. (2020), PVC microplastics negatively impact marine diatoms in a manner that correlates with the dosage, leading to a decrease in chlorophyll levels, hindering photosynthesis, and causing harm to algal cells. Moreover, they indicated that PVC microplastics that have been exposed to UV light are more harmful than new PVC microplastics, causing harm to the growth and chlorophyll levels of freshwater algae *Chlamydomonas reinhardtii*. Overall, it appears that exposure to microplastics PVC has a detrimental impact on the growth of freshwater algae by particularly hindering the photosynthesis process (Wu et al., 2019).

On the other hand, Zhao et al. (2021) mentioned that PVC microplastics play a crucial role in the transportation and spread of pathogenic bacteria and resistance genes in sewage, aiding in the dissemination of antibiotics and heavy metals. Indeed, PVC microplastics have a detrimental effect on the anaerobic digestion of waste-activated sludge due to the release of toxic bisphenol-A, resulting in inhibitory impacts on the processes of hydrolysis-acidification and methanation (Wei et al., 2019). Moreover, as reported Dai et al. (2020), this type of microplastics inhibits nitrogen removal and promotes antibiotic resistance gene propagation.

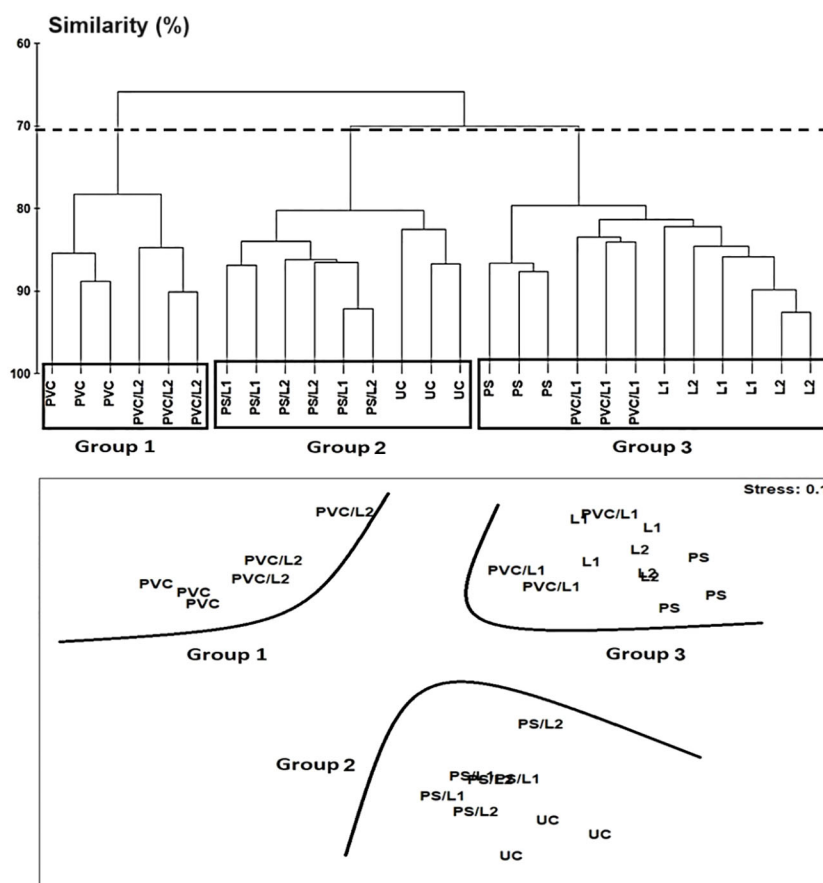


FIGURE 3

Above: Hierarchical Cluster Analysis (single linkage Bray-Curtis similarity values) of nematode assemblages based on square-root transformed abundances of species from a nematofauna the control nematode assemblage (UC) and those enriched with polystyrene (PS), Polyvinyl chlorides (PVC), Lipitor (L1 and L2) and their mixtures (PS/L1, PS/L2, PVC/L1, and PVC/L2) where groups are separated by fixing the cutoff at ~70% of Bray-Curtis similarity, as shown by the dotted horizontal line. Below: non-metric Multidimensional Scaling (nMDS) 2D plot based on Bray-Curtis similarity.

As mentioned above, significant toxicity was also observed after exposure to Lipitor for both algae (Jaramillo-Madrid et al., 2020) and microorganisms (Chow et al., 2010; Ting et al., 2016), suggesting at least a negative indirect impact of statins on feeding-type nematodes 2A and 1A. Indeed, it is known that these drugs have antimicrobial effects on a range of oral microorganisms, such as periodontal pathogens and bacterial species resistant to viruses and fungi (Ting et al., 2016). Also, treating diatoms with statins is known to block the enzymes 3-hydroxy-3-methyl glutaryl CoA reductase and disrupt the metabolism of isoprenoids, leading to a reduction in total sterol content (Jaramillo-Madrid et al., 2020).

By the end of the experiment, two feeding groups seem to have been favored: the non-selective deposit feeders (1B) and omnivore-carnivores (2B). The explanation could be related to the toxicity of PVC and Lipitor on sensitive nematodes, mostly appurtenant to feeding groups made with microvores and epistrate-consumers. The nematodes 1B and 2B may have ingested detritus comprising corpses of decomposing prey 1A and 2A. This feeding mode is common for 1B nematodes (Wieser, 1953), and facultative for 2B, the latter becoming omnivorous if necessary (Moens and Vincx, 1997).

Another functional aspect is likely to have played an important role in the current experiment: the tail shape. The worms with elongated and conical tails were disadvantaged in the presence of both pollutants (i.e. PVC and Lipitor). It could be hypothesized that the movements of the elongated morphotype were hampered by the gluey nature of the organically enriched substrate with decomposing bodies. The worms with conical caudal shape proved to be more sensitive to pollution because of their larger support lateral contact surface and, as a consequence, the lower jumping potential, associated with the frequency and speediness, leading overall to longer exposure time to pollution. An additional potential explanation for such a pattern would also be the possibility of corpses acting as glue themselves, therefore binding the worms with higher leaning surfaces in their caudal part (co).

The mixture of polystyrene and Lipitor had a less toxic impact on meiobenthic nematodes when combined compared to their individual effects. The abundance, individual biomass, and taxonomic diversity of nematodes in treatments PS/L1 and PS/L2 were comparable to control. Such an effect could be related to an antagonist interaction between the two xenobiotics. Particularly, the nMDS ordination showed different clustering between PVC/L2 and

TABLE 4 Analysis of Similarity (ANOSIM) and SIMPER (Similarity Percentage) procedures based on taxonomic composition between the control nematode assemblage (UC) and those enriched with polystyrene (PS), Polyvinyl chlorides (PVC), Lipitor (L), and their mixtures (PS/L1, PS/L2, PVC/L1, and PVC/L2).

Comparisons	ANOSIM		SIMER	
	<i>R</i> -statistics	<i>p</i> -value	AD (%)	Species
UC vs. PS	1	0.01	31.54	<i>Metoncholaimus pristiurus</i> (13.36%) \emptyset <i>Cyartonema germanicum</i> (8.24%) \emptyset <i>Parasphaerolaimus paradoxus</i> (8.06%) \emptyset <i>Longicyatholaimus longicaudatus</i> (6.34%) – <i>Maryllynna puncticaudata</i> (5.59%) – <i>Parmonohystera proteus</i> (5.37%) + <i>Odontophora wieseri</i> (5.15%) –
UC vs. PVC	1	0.01	40.28	<i>Metoncholaimus pristiurus</i> (10.82%) \emptyset <i>Phanoderma</i> sp. (7.65%) \emptyset <i>Prochromadorella longicaudata</i> (7.52%) \emptyset <i>Maryllynna steckhoveni</i> (7.34%) \emptyset <i>Daptonema trabeculosum</i> (4.70%) + <i>Longicyatholaimus longicaudatus</i> (5.41%) – <i>Cyartonema germanicum</i> (4.34%) – <i>Maryllynna puncticaudata</i> (4.10%) –
UC vs. L1	1	0.01	33.43	<i>Metoncholaimus pristiurs</i> (12.83%) \emptyset <i>Cyartonna germanicum</i> (7.91%) \emptyset <i>Phanoderma</i> sp. (6.62%) – <i>Parasphaerolaimus paradoxus</i> (6.22%) – <i>Longicyatholaimus longicaudatus</i> (6.19%) – <i>Maryllynna puncticaudata</i> (5.87%) – <i>Sabtieria punctata</i> (4.46%) \emptyset
UC vs. L2	1	0.01	31.12	<i>Metoncholaimus pristiurs</i> (13.67%) \emptyset <i>Cyartonna germanicum</i> (8.42%) \emptyset <i>Oncholaimellus calvadocicus</i> (5.82%) + <i>Parasphaerolaimus paradoxus</i> (8.24%) \emptyset <i>Longicyatholaimus longicaudatus</i> (9.26%) – <i>Sabtieria punctata</i> (4.76%) \emptyset
UC vs. PS/L1	0.889	0.01	20.02	<i>Metoncholaimus pristiurus</i> (8.21%) – <i>Parasphaerolaimus paradoxus</i> (4.83%) – <i>Oncholaimellus calvadocicus</i> (5.34%) + <i>Halaphanolaimus</i> sp. (5.95%) – <i>Thoonchus inermis</i> (5.15%) – <i>Microlaimus honestus</i> (7.33%) – <i>Longicyatholaimus longicaudatus</i> (4.82%) – <i>Enoplolaimus longicaudatus</i> (5.77%) – <i>Theristus modicus</i> (4.33%) –

The values in parentheses indicate the relative contributions of nematode species participating at about 50% of the average dissimilarity between the reference nematofauna and those exposed to the different treatments. More abundant (+); less abundant (–); steady relative abundance (st); elimination (\emptyset). Average dissimilarity (AD). Significant differences at *p*-values < 0.05.

PS/L2 groups. The former treatment appears to have had a higher toxicity on meiobenthic nematodes compared to the latter. Thus, it could be evoked that the polystyrene was able to neutralize the toxicity of Lipitor and a plausible explanation for the similarity in abundances and species richness among PS/L1 and PS/L2 treatments and control, with just 19.5% dissimilarity. Following the rationale highlighted by [Wakkaf et al. \(2020\)](#) and [Hedfi et al. \(2022\)](#), the occurrence of aggregates of polystyrene and Lipitor on sediment particles seems to distance the latter pollutant away from nematodes ([Figure 4](#)). Therefore, these aggregates may comprise the substrate itself, making it coarser and reducing at least in part the availability of toxicant compounds for nematodes. This agglutination may also affect their bioavailability, by reducing the cuticular uptake rate by nematodes, as naturally larger aggregates are less efficiently internalized.

Overall, two objectives appeared behind the current work: (1) determining the threshold related to the exposure to Lipitor, and (2) testing PS beads as a potential remediation tool for reducing sediment contamination with statins. However, despite the results found are promising, it will be very difficult to obtain governmental authorization to spill microplastics in contaminated areas with Lipitor. As perspectives, more engineering studies should be designed to give more details on how and by using which amount and size of polystyrene particles will be added to contaminated sediments.

5 Conclusion

Meiobenthic nematodes are known to be one the most abundant and diverse groups of invertebrates from marine

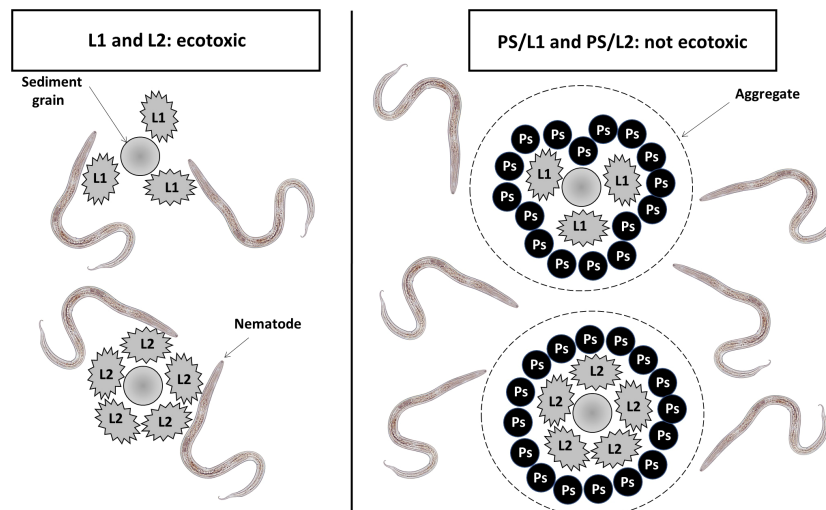


FIGURE 4

Graphical representation showing the hypothetical behavior of Lipitor ($L1 = 0.1 \text{ mg.l}^{-1}$, $L2 = 1 \text{ mg.l}^{-1}$) in the presence of polystyrene particles ($PS = 1 \text{ mg.kg}^{-1}$ Dry Weight).

benthic areas. Despite numerous published studies using these worms as bioindicators and models in ecotoxicology, no work has focused up to date on the toxic impact of microplastic and Lipitor on marine benthic meiofauna. The results of the current experiment identified important interactions between these types of xenobiotics and the abundances, individual biomasses, and taxonomic traits of nematodes, particularly at concentrations of 1 mg.kg^{-1} DW of PVC and Lipitor ($L1$ (0.1 mg.l^{-1}) and $L2$ (1 mg.l^{-1})). A potential list of sensitive (i.e. 1A and 2A) and tolerant/opportunistic (i.e. 1B and 2B) taxa for each type of tested xenobiotic was suggested. However, the nematodes exposed particularly to PS/ $L1$ and PS/ $L2$ treatments were not significantly affected. The interactions between Lipitor and complexing polystyrene can serve as a depollution method to protect living organisms. It is essential to further explore the link between both types of contaminants to mitigate the ecotoxicological risks and for governmental policy purposes. The results obtained in the current study encourage the use of polystyrene for cleaning subtidal marine areas of Lipitor and statins in general, due to its strong adsorbent and electromagnetic power, but also lightness, which makes the collection of contaminated microplastic particles floating on the water easier.

Data availability statement

The raw data supporting the conclusions of this article will be made available by the authors, without undue reservation.

Ethics statement

The manuscript presents research on animals that do not require ethical approval for their study.

Author contributions

BA: Writing – original draft, Software, Formal analysis, Funding acquisition. MA: Writing – original draft, Software, Funding acquisition, Formal analysis. NA-H: Writing – review & editing, Methodology, Investigation, Conceptualization, Software, Formal analysis. SÖ: Writing – original draft, Funding acquisition, Writing – review & editing. OP: Supervision, Software, Resources, Data curation, Conceptualization, Writing – review & editing. MN: Visualization, Validation, Project administration, Writing – review & editing, Software, Resources, Data curation. EM: Investigation, Conceptualization, Writing – review & editing, Validation, Software. AH: Writing – original draft, Supervision, Formal analysis, Data curation, Writing – review & editing, Software. HR: Project administration, Funding acquisition, Conceptualization, Writing – review & editing, Formal analysis, Data curation. FB: Writing – original draft, Validation, Supervision, Writing – review & editing, Funding acquisition, Conceptualization.

Funding

The authors declare financial support was received for the research, authorship, and/or publication of this article. This work was supported and funded by the Deanship of Scientific Research at Imam Mohammad Ibn Saud Islamic University (IMSIU) (grant number IMSIU-RP23071).

Conflict of interest

The authors declare that the research was conducted in the absence of any commercial or financial relationships that could be construed as a potential conflict of interest.

Publisher's note

All claims expressed in this article are solely those of the authors and do not necessarily represent those of their affiliated

organizations, or those of the publisher, the editors and the reviewers. Any product that may be evaluated in this article, or claim that may be made by its manufacturer, is not guaranteed or endorsed by the publisher.

References

- Abuwatfa, W. H., Dana, A., Al-Othman, A., Halalsheh, N., and Tawalbeh, M. (2021). Insights into the removal of microplastics from water using biochar in the era of COVID-19: a mini review. *Case Stud. Chem. Environ. Eng.* 4, 100151. doi: 10.1016/j.csee.2021.100151
- Allouche, M., Ishak, S., Ben Ali, M., Hedfi, A., Almalki, M., Karachle, P. K., et al. (2022). Molecular interactions of polyvinyl chloride microplastics and beta-blockers (diltiazem and bisoprolol) and their effects on marine meiofauna: combined *in vivo* and modeling study. *J. Hazard. Mat.* 431, 128609. doi: 10.1016/j.jhazmat.2022.128609
- Avio, C. G., Gorb, S., Milan, M., Benedetti, M., Fattorini, D., d'Errico, G., et al. (2015). Pollutants bioavailability and toxicological risk from microplastics to marine mussels. *Environ. pollut.* 198, 211–222. doi: 10.1016/j.envpol.2014.12.021
- Bellakhal, M., Ishak, S., Al-Hoshani, N., Qurtam, A. A., Al-Zahrani, M., Pacioglou, O., et al. (2023). The multifaceted effects of fluoranthene and polystyrene on the taxonomic composition and associated functional traits of marine meiofauna, by using single and mixture applications. *Mar. pollut. Bull.* 194, 115390. doi: 10.1016/j.marpolbul.2023.115390
- Borja, A., Franco, J., and Pérez, V. (2000). A marine biotic index to establish the ecological quality of soft bottom benthos within European estuarine and coastal environments. *Mar. pollut. Bull.* 40, 1100–1114. doi: 10.1016/S0025-326X(00)00061-8
- Boufahja, F. (2010). Approches communautaires et populationnelles de biosurveillance du milieu marin chez les nématodes libres (lagune et baie de Bizerte, Tunisie). PhD thesis in Biological Sciences, Faculty of Sciences of Bizerte (Tunisia: University of Carthage), 300.
- Boufahja, F., Hedfi, A., Amorri, J., Aissa, P., Beyrem, H., and Mahmoudi, E. (2011). Examination of the bioindicator potential of *Oncholaimus campylocercoides* (Nematoda, Oncholaimidae) from Bizerte bay (Tunisia). *Ecol. Indic.* 11, 1139–1148. doi: 10.1016/j.ecolind.2010.12.014
- Buchanan, J. B. (1971). "Measurement of the physical and chemical environment: Sediments," in *Methods for the Study of Marine Benthos. International Biological Programme Handbook No. 16*. Eds. N. A. Holme and A. D. McIntyre (Blackwell Scientific Publications, Oxford), 334 pp.
- Chow, O., Köckritz-Blickweide, M., Bright, A., Hensler, M., Zinkernagel, A., Cogen, A., et al. (2010). Statins enhance formation of phagocyte extracellular traps. *Cell Host Microbe* 8, 445–454. doi: 10.1016/j.chom.2010.10.005
- Clarke, K. R. (1993). Non-parametric multivariate analyses of changes in community structure. *Austral. Ecol.* 18, 117–143. doi: 10.1111/j.1442-9993.1993.tb00438.x
- Clarke, K. R., and Gorley, R. N. (2001). *PRIMER v5: User Manual/Tutorial* (Polymouth, UK: PRIMER-E), 91 p.
- Coull, B. C., and Chandler, G. T. (1992). Pollution and meiofauna: field, laboratory and mesocosm studies. *Oceanogr. Mar. Biol.* 30, 191–271.
- Dai, H., Gao, J., Wang, Z., Zhao, Y., and Zhang, D. (2020). Behavior of nitrogen, phosphorus and antibiotic resistance genes under polyvinyl chloride microplastics pressures in an aerobic granular sludge system. *J. Clean. Prod.* 256, 120402. doi: 10.1016/j.jclepro.2020.120402
- Engelmann, H. D. (1978). Zur dominanzklassifizierung von bodenarthropoden. *Pedobiologia* 18, 378–380. doi: 10.1016/S0031-4056(23)00612-1
- Essid, N., Faiza, M., Hedfi, A., Almalki, M., Urkmez, D., and Boufahja, F. (2021). Toxicity of synthetic Endocrine Disrupting Compounds on meiofauna: Estradiol benzoate as a case study. *Environ. pollut.* 286, 117300. doi: 10.1016/j.envpol.2021.117300
- Fabiano, M., and Danovaro, R. (1994). Composition of organic matter in sediment facing a river estuary (Tyrrhenian Sea): relationships with bacteria and microphytobenthic biomass. *Hydrobiologia* 277, 71–84. doi: 10.1007/BF00016755
- Guo, Y., Somerfield, P. J., Warwick, R. M., and Zhang, Z. (2001). Large-scale patterns in the community structure and biodiversity of free-living nematodes in the Bohai Sea, China. *J. Mar. Biol. Assoc.* 81, 755–763. doi: 10.1017/S0025315401004568
- Hägerbäumer, A., Höss, S., Heininger, P., and Trautspurger, W. (2015). Experimental studies with nematodes in ecotoxicology: an overview. *J. Nematol.* 47 (1), 11–27.
- Hedfi, A., Ben Ali, M., Korkobi, M., Allouche, M., Harrath, A. H., Beyrem, H., et al. (2022). The exposure to polyvinyl chloride microplastics and chrysene induces multiple changes in the structure and functionality of marine meiobenthic communities. *J. Hazard. Mat.* 436, 12916. doi: 10.1016/j.jhazmat.2022.12916
- Hedfi, A., Ben Ali, M., Noureldeen, A., Darwish, H., Mahmoudi, E., Plävan, G., et al. (2021). Effects of benzo(a)pyrene on meiobenthic assemblage and biochemical biomarkers in an *Oncholaimus campylocercoides* (Nematoda) microcosm. *Environ. Sci. pollut. Res.* 29, 16529–16548. doi: 10.1007/s11356-021-16885-w
- Hedfi, A., Boufahja, F., Ben Ali, M., Aissa, P., Mahmoudi, E., and Beyrem, H. (2013). Do trace metals (chromium, copper and nickel) influence toxicity of diesel fuel for free-living marine nematodes? *Environ. Sci. pollut. Res.* 20, 3760–3770. doi: 10.1007/s11356-012-1305-2
- Ishak, S., Allouche, M., Nasri, A., Harrath, A. H., Alwasel, S., Plavan, G., et al. (2022). The antidepressants amitriptyline and paroxetine induce changes in the structure and functional traits of marine nematodes. *Sustainability* 14, 6100. doi: 10.3390/su14106100
- Jaramillo-Madrid, A. C., Abbriano, R., Ashworth, J., Fabris, M., Pernice, M., and Ralph, P. J. (2020). Overexpression of key sterol pathway enzymes in two model marine diatoms alters sterol profiles in *Phaeodactylum tricornutum*. *Pharmaceuticals* 13, 481. doi: 10.3390/ph13120481
- Keppner, E. J., and Tarjan, A. C. (1989). *Illustrated key to the genera of free living marine nematodes of the order Enoplida* Vol. 77 (USA: U.S. Department of Commerce. NOAA Technical Report NMFS), 1–26.
- Keppner, E. J., and Tarjan, A. C. (1991). *Illustrated key to the genera of free-living marine nematodes of the order Araeolaimida* Vol. 885 (USA: Corporate Extension service. Institute of Federal Agricultural Sciences. University of Florida. Technical Bulletin), 1–18.
- Keppner, E. J., and Tarjan, A. C. (1994). *Illustrated key to the genera of free-living marine nematodes of the Microlaimoidea and Desmodoroidea* (Nematoda, Chromadorida: Chromadorina) Vol. 890 (USA: University of Florida, Institute of Food and Agricultural Sciences. Technical Bulletin), 1–17.
- Keppner, E. J., and Tarjan, A. C. (1999). *Illustrated key to the genera of free-living marine nematodes in the Superfamily Chromadoroidea - Exclusive of the Chromadoridae*. Extension Publication EENY-82 (USA: University of Florida), 39.
- Lange, J.-P. (2021). Managing plastic waste-sorting, recycling, disposal, and product redesign. *ACS Sustain. Chem. Eng.* 9, 15722–15738. doi: 10.1021/acssuschemeng.1c05013
- Mahmoudi, E., Essid, N., Beyrem, H., Hedfi, A., Boufahja, F., Vitiello, P., et al. (2005). Effects of hydrocarbon contamination on a free-living marine nematode community: results from microcosm experiments. *Mar. pollut. Bull.* 50, 1197–1204. doi: 10.1016/j.marpolbul.2005.04.018
- Menchaca, I., Rodriguez, J. G., Borja, A., Jesus Belzunce-Segarra, M., Franco, J., Garmendia, J. M., et al. (2014). Determination of polychlorinated biphenyl and polycyclic aromatic hydrocarbon marine regional sediment quality guidelines with the European water framework directive. *Chem. Ecol.* 30, 693–700. doi: 10.1080/02757540.2014.917175
- Moens, T., and Vincx, M. (1997). Observations on the feeding ecology of estuarine nematodes. *J. Mar. Biol. Ass. U. K.* 77, 211–227. doi: 10.1017/S0025315400033889
- Moreno, M., Semprucci, F., Vezzulli, L., Balsamo, M., Fabiano, M., and Albertelli, G. (2011). The use of nematodes in assessing ecological quality status in the Mediterranean coastal ecosystems. *Ecol. Indic.* 11, 328–336. doi: 10.1016/j.ecolind.2010.05.011
- Nemys (2024) *Nemys: World Database of Nematodes*. Available online at: <https://nemys.ugent.be>.
- Platt, H. M., and Warwick, R. M. (1983). *Free-living Marine Nematodes. Part I. British Enoploids*. (London, UK: Cambridge University), 307.
- Platt, H. M., and Warwick, R. M. (1988). *Free-living marine nematodes. Part II. British Chromadorids. Synopsis of the British fauna (New Series)*. No. 38: E.J. Brill/W. Backhuys, Leiden.
- Ridall, A., and Ingels, J. (2021). Suitability of free-living marine nematodes as bioindicators: status and future considerations. *Front. Mar. Sci.* 8, 685327. doi: 10.3389/fmars.2021.685327
- Sapir, A. (2021). Why are nematodes so successful extremophiles? *Commun. Integr. Biol.* 14, 24–26. doi: 10.1080/19420889.2021.1884343
- Schratzberger, M., Warr, K. J., and Rogers, S. I. (2007). Functional diversity of nematode communities in the southwestern North Sea. *Mar. Environ. Res.* 63, 368–389. doi: 10.1016/j.marenvres.2006.10.006
- Schratzberger, M., Whomersley, P., Warr, K., Bolam, S. G., and Rees, H. L. (2004). Colonisation of various types of sediment by estuarine nematodes via lateral infanal migration: a laboratory study. *Mar. Biol.* 145, 69–78. doi: 10.1007/s00227-004-1302-1
- Seinhorst, J. W. (1959). A rapid method for the transfer of nematodes from fixative to anhydrous glycerin. *Nematologica* 4, 67–69.
- Semprucci, F., Losi, V., and Moreno, M. (2015). A review of Italian research on free-living marine nematodes and the future perspectives on their use as Ecological Indicators (EcoInds). *Mediterr. Mar. Sci.* 16, 352. doi: 10.12681/mms.1072

- Thistle, D., Lamshead, P. J. D., and Sherman, K. M. (1995). Nematode tail-shape groups respond to environmental differences in the deep sea. *Vie Milieu* 45, 107–115.
- Ting, M., Whitaker, E., and Albandar, J. (2016). Systematic review of the *in vitro* effects of statins on oral and perioral microorganisms. *Eur. J. Oral. Sci.* 124, 4–10. doi: 10.1111/eos.12239
- Vitiello, P., and Dinat, A. (1979). Définition et échantillonnage du méiobenthos. *Rapp. Commun. Int. Expl. Sci. Mer. Médit.* 25, 279–283.
- Wakkaf, T., Allouche, M., Harrath, A. H., Mansour, L., Alwasel, S., Ansari, K. G. M. T., et al. (2020). The individual and combined effects of cadmium, Polyvinyl chloride (PVC) microplastics and their polyalkylamines modified forms on meiobenthic features in a microcosm. *Environ. pollut.* 266, 115263. doi: 10.1016/j.envpol.2020.115263
- Wang, S., Wang, Y., Liang, Y., Cao, W., Sun, C., Ju, P., et al. (2020). The interactions between microplastic polyvinyl chloride and marine diatoms: Physiological, morphological, and growth effects. *Ecotoxicol. Environ. Saf.* 203, 111000. doi: 10.1016/j.ecoenv.2020.111000
- Warwick, R., Platt, H., Somerfield, P., and Shrewsbury, U. K. (1998). Free-living marine nematodes. *Part III. British Monhysterida*.
- Weber, A., von Randow, M., Voigt, A.-L., von der Au, M., Fischer, E., Meermann, B., et al. (2021). Ingestion and toxicity of microplastics in the freshwater gastropod *Lymnaea stagnalis*: no microplastic-induced effects alone or in combination with copper. *Chemosphere* 263, 128040. doi: 10.1016/j.chemosphere.2020.128040
- Wei, W., Huang, Q., Sun, J., Wang, J., Wu, S., and Ni, B. (2019). Polyvinyl chloride microplastics affect methane production from the anaerobic digestion of waste activated sludge through leaching toxic bisphenol-A. *Environ. Sci. Technol.* 53, 2509–2517. doi: 10.1021/acs.est.8b07069
- Wieser, W. (1953). Die Beziehung zwischen Mundhchen-gestalt, Ernährungsweise und Vorkommen beifreilbenden marinen Nematoden. *Ark. Zoop. Ser.* 2, 439–484.
- Wu, Y., Guo, P., Zhang, X., Zhang, Y., Xie, S., and Deng, J. (2019). Effect of microplastics exposure on the photosynthesis system of freshwater algae. *J. Hazard. Mat.* 374, 219–227. doi: 10.1016/j.jhazmat.2019.04.039
- Zhao, Y., Gao, J., Wang, Z., Dai, H., and Wang, Y. (2021). Responses of bacterial communities and resistance genes on microplastics to antibiotics and heavy metals in sewage environment. *J. Hazard. Mat.* 402, 123550. doi: 10.1016/j.jhazmat.2020.123550



OPEN ACCESS

EDITED BY

Xuchun Qiu,
Jiangsu University, China

REVIEWED BY

Praxedes Natalia Muñoz,
Catholic University of the North, Chile
Fabrizio Frontalini,
University of Urbino Carlo Bo, Italy

*CORRESPONDENCE

Yurika Ujiie

✉ yujiie@kochi-u.ac.jp

†PRESENT ADDRESS

Yuka Inagaki,
Graduate School of Integrated Arts and
Sciences, Kochi University, Kochi, Japan

RECEIVED 03 February 2024

ACCEPTED 17 June 2024

PUBLISHED 01 July 2024

CITATION

Inagaki Y, Ishitani Y, Tame A, Uematsu K,
Tomioka N, Ushikubo T and Ujiie Y (2024)
Foraminiferal detoxification breakdown
induced by fatal levels of TiO₂ nanoparticles.
Front. Mar. Sci. 11:1381247.
doi: 10.3389/fmars.2024.1381247

COPYRIGHT

© 2024 Inagaki, Ishitani, Tame, Uematsu,
Tomioka, Ushikubo and Ujiie. This is an open-
access article distributed under the terms of
the [Creative Commons Attribution License
\(CC BY\)](https://creativecommons.org/licenses/by/4.0/). The use, distribution or reproduction
in other forums is permitted, provided the
original author(s) and the copyright owner(s)
are credited and that the original publication
in this journal is cited, in accordance with
accepted academic practice. No use,
distribution or reproduction is permitted
which does not comply with these terms.

Foraminiferal detoxification breakdown induced by fatal levels of TiO₂ nanoparticles

Yuka Inagaki^{1†}, Yoshiyuki Ishitani², Akihiro Tame³,
Katsuyuki Uematsu⁴, Naotaka Tomioka⁵,
Takayuki Ushikubo⁵ and Yurika Ujiie^{1,6*}

¹Department of Biology, Kochi University, Kochi, Japan, ²Institute for Extra-Cutting-Edge Science and Technology Avant-garde Research (X-star), Japan Agency for Marine-Earth Science and Technology (JAMSTEC), Yokosuka, Japan, ³School of Medical Sciences, University of Fukui, Fukui, Japan,

⁴Department of Marine and Earth Sciences, Marine Works Japan Ltd, Yokosuka, Japan, ⁵Kochi Institute for Core Sample Research, X-Star, JAMSTEC, Nankoku, Japan, ⁶Marine Core Research Institute, Kochi University, Nankoku, Japan

The increase discharge of titanium dioxide (TiO₂) nanoparticles, derived from engineered material waste, exerts a detrimental impact on both the marine ecosystem and public health. The cytotoxicity of TiO₂ nanoparticles on marine organisms should be imperatively understood to tackle the urgent concern for the well-being of marine life. Various concentrations of TiO₂ nanoparticles have proven to reach fatal levels in aquatic organisms, requiring a deeper exploration of cytotoxicity. Notably, certain benthic foraminifers, such as *Ammonia veneta*, have been identified as capable of incorporating TiO₂ nanoparticles into vesicles. However, these organisms exhibit a detoxification mechanism through exocytosis, as indicated by previous transcriptomic inferences. This presents the advantage of assessing the tolerance of foraminifers to TiO₂ nanoparticles as pollutants and investigating the long-term effects of cytotoxicity. In this study, we scrutinized the distribution of TiO₂ nanoparticles within cells and the growth rates of individuals in seawater media containing 1, 5, 10, and 50 ppm TiO₂ nanoparticles, comparing the results with a control group over a 5-week period, utilizing *A. veneta* stain. Transmission electron microscopy observations consistently revealed high concentrations of TiO₂ nanoparticles in vesicles, and their expulsion from cells was evident even with exposure to 5 ppm TiO₂ nanoparticles. Under the control and 1 ppm TiO₂ conditions, foraminifers increased their cell volume by adding a calcification chamber to their tests every 1 or 2 days. However, the 5-week culturing experiments demonstrated that foraminifers gradually ceased growing under 5 ppm TiO₂ nanoparticle exposure and exhibited no growth at > 10 ppm concentrations, despite an ample food supply. Consequently, these findings with *A. veneta* suggest that the foraminiferal detoxification system could be disrupted by concentrations exceeding 5 ppm of TiO₂ nanoparticles. The toxic effect of TiO₂ nanoparticles on meiofauna, such as benthic foraminifers, have been poorly understood, though these organisms play an important role in the marine ecosystem. Environmental accumulation of TiO₂

nanoparticles on the coast has already exceeded twenty times more than foraminiferal detoxification level. Future studies focusing on toxic mechanism of TiO₂ nanoparticles are crucial to prevent the breakdown of the marine ecosystem through accelerating discharge of TiO₂ nanoparticles into the ocean.

KEYWORDS

cytotoxicity, detoxification, foraminifera, TiO₂ NPs, fatal level

1 Introduction

Titanium dioxide nanoparticles (TiO₂ NPs) stand as the second most widely employed engineered nanomaterial globally, owing to their advantageous physicochemical properties, notably their photocatalytic capability for the oxidative decomposition of organic matter (Zheng and Nowack, 2021). In recent years, these nanoparticles have found application in sunscreen filters, replacing oxybenzone and octinoxate, to safeguard marine ecosystems (Ammendolia et al., 2022). The escalating demand for TiO₂ NPs has led to the discharge of manufacturing waste into the environment—specifically, soil and groundwater—eventually culminating in the ocean as the ultimate repository. NPs commonly form aggregates in water and sink down to the bottom (Boxall et al., 2007). Indeed, the accumulation of TiO₂ NPs on European coasts was projected to reach up to 123 ppm in 2020, and the current trend indicates an acceleration (Sun et al., 2016; Zheng and Nowack, 2021). This accumulation in the marine environment raises concerns due to its toxicity to aquatic organisms (Moore, 2006; Farré et al., 2009; Delay and Frimmel, 2012; Matranga and Corsi, 2012). Particularly, aggregated nanoparticles are accumulated in the sediments and interacted with sediment-dwelling organisms due to their low mobility (Farré et al., 2009). Experimental studies have previously demonstrated the toxicity of TiO₂ NPs to aquatic organisms, particularly microalgae and macroorganisms (Menard et al., 2011; Minetto et al., 2014; Luo et al., 2020). These studies have assessed the toxic effects through cell stress assays, revealing a Median Effect Concentration (EC₅₀) of 35.3 ppm for algae and a Median Lethal Concentration (LC₅₀) of 5.5–20,000 ppm for *Daphnia magna*. Given the observed variability in lethal effects among organisms in exposure experiments with viability examinations, it becomes imperative to extend studies to benthos, encompassing not only macro or microfauna but also benthic foraminifers, to comprehensively understand the impact of TiO₂ NPs on marine ecosystems.

Benthic foraminifers, ubiquitous unicellular meiofauna on the seafloor, particularly in coastal areas (Culver and Buzas, 1999), serve as biomonitoring targets to assess the effects of NPs on marine environments (Ciacci et al., 2019). Foraminifers construct a test using calcium carbonate, sediment particles, or an organic membrane (Goldstein, 1999), with the test growing larger by

adding chambers. Recent studies utilizing single-cell transcriptome analysis and cellular observations from a time-course experiment with the benthic foraminifers *Ammonia* species exposed to 1 ppm TiO₂ NPs for 24 hours have elucidated the cytotoxic mechanism of TiO₂ NPs (Ciacci et al., 2019; Ishitani et al., 2023). Transcriptome analysis with *Ammonia veneta* successfully unveiled the metabolic pathway associated with TiO₂ NPs toxicity and its time-series changes (Ishitani et al., 2023). Foraminifers demonstrated phagocytosis of TiO₂ NPs into their cells, manifesting stress indicators such as the production of reactive oxygen species (ROS) and peroxidized lipids. Intriguingly, they exhibited detoxification, wherein aggregated TiO₂ NPs were encapsulated in ceramide and expelled as waste within 24 hours. This unique detoxification system enables foraminifers to survive in polluted environments, though the long-term cytotoxicity remains unknown. Furthermore, the limitation of TiO₂ NPs concentration that regulates foraminiferal growth or lethality has been never examined. In the other experiments with unicellular diatom, their EC₅₀ and LC₅₀ are ~10 and ~70 ppm of TiO₂ NPs, which are ~20–30 nm in diameter (Hartmann et al., 2010; Clément et al., 2013). Understanding such limitation becomes crucial in light of the rapid accumulation of TiO₂ NPs in marine environments in recent times.

In this study, we investigated the threshold limits of TiO₂ NPs concentrations for the survival of the benthic foraminifer *A. veneta*. The foraminifer was cultured for five weeks with exposures to 1, 5, 10, and 50 ppm TiO₂ NPs, and the potential for long-term survival was assessed based on individual growth rates, evaluated through the increased number of chambers, and the distribution of intracellular TiO₂ NPs. Our investigations suggest that foraminiferal growth is gradually inhibited in rising of TiO₂ NPs concentration most likely due to the breakdown of detoxification.

2 Materials and methods

2.1 TiO₂ NPs – source, characterization, and preparation

AEROXIDE®TiO₂, a mixture of rutile and anatase crystals with a nominal diameter of 25 nm (Evonik, Germany), was utilized in the

present study. The stock suspension (1000 mg/L) of TiO₂ NPs was prepared using AEROXIDE®TiO₂ powder in Milli-Q water and sonicated using an NR-50M ultrasonic homogenizer (Microtec, Japan) at 50 W for 60 min with 2 s on/off cycles placed in ice to prevent aggregation. Stock suspensions were shielded from light and stored at -20°C. For each experiment, the thawed stock suspension was similarly sonicated for approximately 60 min to disperse the TiO₂ particles, which tend to clump due to their cohesive nature, bringing them to a particle size of 25 nm. The resulting dispersion was diluted with artificial sea water (ASW), which was filtered through a 0.2µm mesh membrane filter (ADVANTEC®, Japan) of 35ppt Coral Pro Salt (Red Sea, USA) in Milli-Q water, according to the experimental conditions.

2.2 Culture experiments of foraminiferal strain *Ammonia veneta*

The study employed specimens derived from the culture strain *A. veneta* (Ishitani et al., 2023), which has been maintained in ASW at 23°C under a 12:12 hour light/dark cycle with weekly feedings of fresh *Dunaliella salina* (NIES-2257). This species forms a calcium carbonate test, which is sequentially increased by the maturity phase prior to reproduction. Adult (ca. 10 chambers) specimens of *A. veneta* showing reticulopodia extension and activity were randomly selected from subcultures, and three individuals were transferred to each petri dish (Aznor Petri Dish ø55 × 17 mm Azwan, Japan) containing 10 mL of either TiO₂ NPs seawater medium or ASW (control). For each medium condition, three replicated petri dishes were prepared and incubated at 23°C under a 12:12 h light/dark cycle for five weeks. All cultures per experiment were run in parallel.

Four different experimental conditions were set for TiO₂ NPs concentrations, as well as the frequency of medium changes, feeding frequency, and amount of food (Table 1). In both culture experiments 1 and 2, TiO₂ NPs seawater media were set up at 1, 10, and 50 ppm, in addition to the control. The frequency of medium changes differed between culture experiments 1 and 2: once a week in Experiment 1 and twice a week in Experiment 2. At each time, 80 µL of food was added to each petri dish. In culture experiment 3, TiO₂ NPs seawater media were set up at 1, 5, and 10 ppm, in addition to the control, with weekly medium changes and with feeding 40 µL of food and increased feeding to a total of 80 µL per week through addition of 20 µL food every few days. Culture experiment 4 involved TiO₂ NPs seawater media at 5 and 10 ppm, in addition to the control, with weekly medium changes with 80 µL of food and increased feeding to a total of

160 µL per week through addition of 40 µL food every few days. In experiments 2 and 4, the number of feedings and the amount of food were increased to keep double the amount of fresh *D. salina* in the petri dishes per week (Table 1).

At the beginning of culture experiments, we photographed each individual using an inverted research microscope (IX73 Olympus, Japan) with a microscope digital camera (DS-Ri2 Nikon Japan) and assigned an individual identification number. We photographed each of all studied individual weekly to check for signs of life or death, regarding the observations: extension and movement of reticulopodia and the movement of the individual to escape from light emission of the inverted microscope for a few minutes. Specimens, which lacked these three observation points, were categorized as dead. Individual growth was evaluated by the number of chamber increases from the previous week.

We firstly tested normality and variances for total numbers of increased chambers for five weeks at each culture experimental condition with Kolmogorov-Smirnov and F test in R v.4.0.2 (R Core Team, 2021), respectively. According to the normality and variances, we conducted the Student-t and Man-Whitney-U tests in R v.4.0.2. The *p* values of multiple comparisons were adjusted with the Bonferroni correction.

2.3 Culture experiment of *Dunaliella salina*

We independently conducted a culture experiment of *D. salina*, a food source for foraminifers, to examine cell divisions in TiO₂ NPs seawater medium. We prepared seven replicates for each of the 10 mL culture media with 1, 5, and 10 ppm TiO₂ NPs and ASW (control) in petri dishes and added 80 µL of *D. salina* to each of the 28 dishes. During the 6-day culture experiments under the same conditions as foraminiferal experiments, we examined the cell density of *D. salina* in each of the four different media daily. All 10 mL medium was transferred into a 15 mL centrifuge tube, and the petri dish was rinsed with 3 mL ASW to recover all remaining cells. After centrifugation at 3,300 rpm for 10 min at 23°C using a micro high-speed centrifuge (CF 16RX II Hitachi, Japan), the pellet of *D. salina* and TiO₂ NPs was suspended with 30 µL of ASW and transferred to a 1.5 ml tube. We immediately added 0.5% xanthan gum solution to a final concentration of 0.01% to inhibit the motility of *D. salina*. Three replicates were made, each of which was mounted with 10 µL of cell suspension to a cell counter (AS ONE, Japan). Following the manufacturer's protocol of the cell counter, we counted the number of cells derived from the control

TABLE 1 Conditions of foraminiferal culture experiments.

	TiO ₂ NPs concentration (ppm)	Frequency of medium change (per week)	Frequency of feeding (per week)	Feeding volume for each time (µL)	Total volume of food per week (µL)
Experiment 1	1, 10, 50	1	1	80	80
Experiment 2	1, 10, 50	2	2	80, 80	160
Experiment 3	1, 5, 10	1	3	40, 20, 20	80
Experiment 4	5, 10	1	3	80, 40, 40	160

and 1 ppm samples using a stereomicroscope (SMZ18 Nikon, Japan) equipped with an inclined-angle lens tube. As TiO₂ NPs aggregations in the 5 and 10 ppm overlapped on *D. salina* and avoided observation, we captured the autofluorescence of *D. salina* with a digital camera (DS-Ri2 Nikon, Japan) using fluorescence observation (U-HGLGPS Olympus Japan, Excitation filter: BP530-550, Barrier filter: BA575IF) equipped with an inverted research microscope (IX73 Olympus, Japan) and counted the cell numbers.

2.4 Scanning electron microscope observation of foraminiferal tests

We used six specimens: two for control and four for the 10 ppm TiO₂ NPs treatment. Two out of four 10 ppm TiO₂ NPs treated specimens formed a new chamber during the culture experiment, while the other two showed no growth. Each test was cleaned with a brush in water and dried in air. These tests were placed on carbon tape and glued to a stage where carbon deposition was performed with the carbon coater (JEE-420 JEOL, Japan). The surface structure and element analysis of foraminiferal tests were conducted with a field emission SEM equipped with an energy dispersive X-ray spectrometer (EF-SEM-EDS) (JSM-6500F JEOL, Japan).

2.5 Transmission electron microscope observation of cells

Ammonia veneta specimens, cultured in the 5 ppm TiO₂ NPs medium, were fixed with 2.5% glutaraldehyde in filtered artificial sea water (FASW) for longer than 24 hours at 4°C. The fixed specimens were embedded in 1% aqueous agarose and then decalcified with 0.2% EGTA in 0.81 mol/L aqueous sucrose solution (pH 7.0) for several days. The specimens were rinsed with FASW, then postfixed with 2% osmium tetroxide in FASW for 2 hours at 4°C, dehydrated in a graded ethanol series, and embedded in epoxy resin (Quetol 651). Ultrathin sections (100 nm for observation and 200 nm for analysis) were cut using a diamond knife on an Ultracut S ultramicrotome (Leica Reichert, Germany), stained with 2% aqueous uranyl acetate and lead staining solution (0.3% lead nitrate and 0.3% lead acetate), and examined using TEM equipped with an energy dispersive X-ray spectrometer (TEM-EDS) (FEI Tecnai G2 20, USA) operated at 200 kV. Elemental mapping was performed in scanning TEM (STEM) mode.

3 Results

3.1 Cell observation and viability of *Ammonia veneta*

Living specimens of *A. veneta* are filled with cytoplasm inside the test and extend fine reticulopodia radially from the aperture and pores of the test to capture food particles in their surroundings (Figure 1). In 1 ppm TiO₂ NPs seawater medium, TiO₂ NPs aggregate up to ~2 µm within 24 hours and accumulate with

other wastes on the bottom (Ishitani et al., 2023). TiO₂ NPs is aggregating faster in high TiO₂ NPs concentration: over 1 µm in hydrodynamic diameter within 1 hour in 5 and 10 ppm TiO₂ NPs seawater and over 15 µm in 50 ppm TiO₂ NPs seawater (Morelli et al., 2018; Reyes et al., 2021; Palmeira-Pinto et al., 2023). These aggregates visibly settled at the bottom of the petri dish as brownish substances during the culture experiment with TiO₂ NPs seawater media (Figure 1). However, these depositions were not observed in the surrounding areas of living *A. veneta*, particularly around the reticulopodia extensions (Figure 1). At the onset of the culture experiment, all studied specimens extended fine reticulopodia. In the control and 1 ppm TiO₂ NPs seawater medium, specimens showed reticulopodia activity and also added new chambers and grew cytoplasm, which typically filled the interior of the test. Under TiO₂ NPs seawater media concentrations greater than 10 ppm, reticulopodia were retracted, and cytoplasm continuously shrank (Figures 2A–D). After reduction of cytoplasm, any reticulopodia activity and movement of specimens were not observed. In these conditions, aggregations containing TiO₂ NPs were observed around foraminiferal specimens.

Holes appeared on the surface of the tests in some specimens exposed to TiO₂ NPs seawater media concentrations higher than 10 ppm (Figure 3). After a 5-week experiment, additional holes were observed on the umbilical side of the test.

3.2 Foraminifera culture experiments

In Experiment 1, control specimens increased by an average of ~2 chambers every week, reaching a total of ~9 chambers over five weeks (Figure 4A; Supplementary Table S1). One out of nine

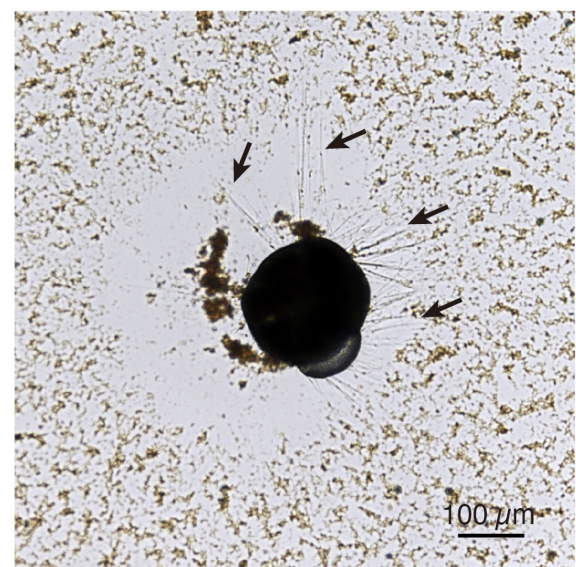


FIGURE 1
Living *Ammonia veneta* specimen in 10 ppm TiO₂ medium. The dark part is cytoplasm inside the test. Fine fibrous reticulopodia, as shown by black arrows, are extended from the cytoplasm in all directions. The brown substance is an aggregation of TiO₂ NPs.

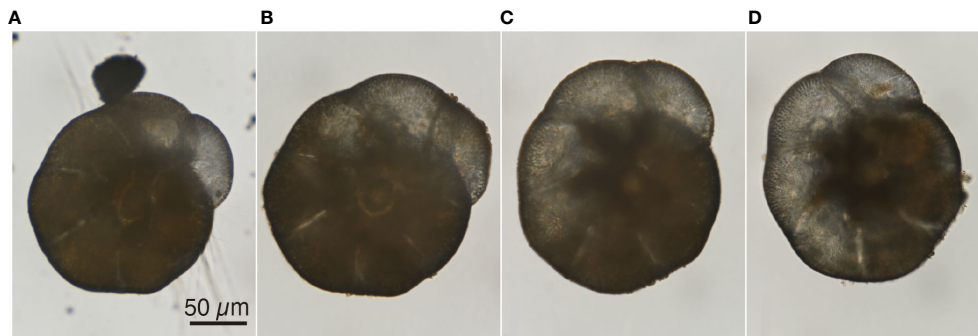


FIGURE 2

Light microscopy images of an *Ammonia veneta* specimen exposed to 10 ppm TiO_2 medium for four weeks. (A) Reticulopodia were extended from the cytoplasm at the onset of experiment. (B) There were no reticulopodia, and cytoplasm was reduced after a week. (C) Cytoplasm was retracted from the previous week. (D) Cytoplasm completely shrank in the fourth week.

control specimens reproduced in the third week. By the end of the 5-week experiment, three specimens had reproduced clones, forming an average of ~20 chambers during their entire lifespan. In the 1 ppm TiO_2 treatment, eight out of nine specimens increased by ~1 chamber per week, although five specimens died after 3 and 5 weeks, respectively. In the 10 ppm TiO_2 treatment, six out of nine specimens increased by ~1 chamber per week, but all specimens ceased growth by the third week and died by the fourth week. In the 50 ppm TiO_2 treatment, only one specimen increased by 1 chamber in the first week, but all specimens died by the fourth week. The total number of increased chambers over the 5-week experiment showed a significant difference between the control specimens and the 10 and 50 ppm TiO_2 treated specimens (Figure 4B).

In Experiments 2, all specimens, both in the control and the 1 ppm TiO_2 treatment, increased by 6–8 chambers over 5 weeks

(Figure 5A; Supplementary Table S1). During the experiment, four and five specimens reproduced clones in the control and the 1 ppm TiO_2 treatment, respectively. However, in both the 10 and 50 ppm TiO_2 treatments, all specimens showed no growth and died by the fourth week. The total number of increased chambers over the 5-week experiment was the same between the control and the 1 ppm TiO_2 treated specimens, but there were significant differences between the controls and the 10 and 50 ppm TiO_2 treatments (Figure 5B).

In Experiment 3, all specimens, both in the control and the 1 ppm TiO_2 treatment, increased by ~8 chambers over 5 weeks (Figure 6A; Supplementary Table S1). During this experiment, one specimen reproduced clones in each of the control and the 1 ppm TiO_2 treatments, but some specimens died. In the 5 ppm TiO_2 treatment, three out of nine specimens increased by ~1 chamber per week, but all had stopped growing and died by the third week. In the 10 ppm TiO_2 treatment, all individuals showed no growth and died by the third week. The total number of increased chambers over the 5-week experiment was the same between the control and the 1 ppm TiO_2 treated specimens, but there were significant differences between the controls and the 5 and 10 ppm TiO_2 treatments (Figure 6B).

In Experiment 4, eight out of nine control specimens increased by ~8 chambers over 5 weeks (Figure 7A; Supplementary Table S1). At the end of the experiment, three specimens reproduced clones. In the 5 ppm TiO_2 treatment, four out of nine specimens increased by ~1 chamber per week, but they stopped growing by the third week and all died by the fifth week. In the 10 ppm TiO_2 treatment, only two specimens increased by one chamber in the first week, but all individuals died by the third week. The total number of increased chambers over the 5-week experiment showed significant differences between the controls and the 5 and 10 ppm TiO_2 treatments, as well as those of Experiment 3 (Figure 7B).

3.3 Surface structure of *Ammonia veneta* test

Morphological differences between control and 10 ppm TiO_2 treated specimens were observed on the surface of the tests, but



FIGURE 3

Light microscopy image of the umbilical side of an *Ammonia veneta* specimen exposed to 50 ppm TiO_2 medium for five weeks. Three big holes were opened on the surface of the test, as shown by the black arrows.

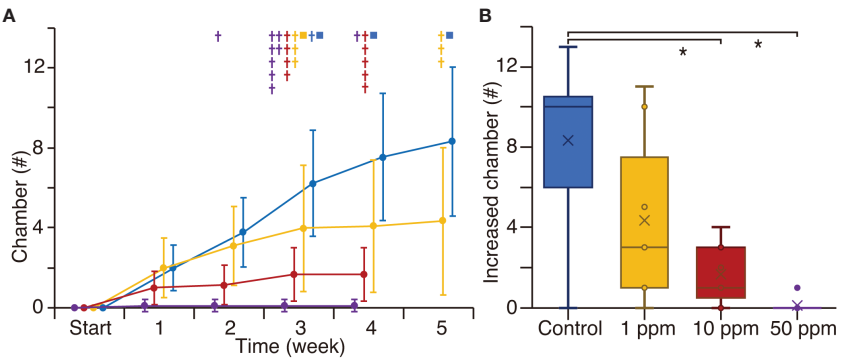


FIGURE 4
The number of increased chambers in culture experiment 1. Blue, yellow, red, and purple colors show the control, 1 ppm, 10 ppm, and 50 ppm TiO_2 treatments, respectively. **(A)** The average of additional numbers of chambers every week during the 5-week experiment. Crosses indicate dead specimen and squares show clonal reproduction. **(B)** Box plot of the number of increased chambers for five weeks. Asterisks show significant differences ($p < 0.0125$ with the Bonferroni correction).

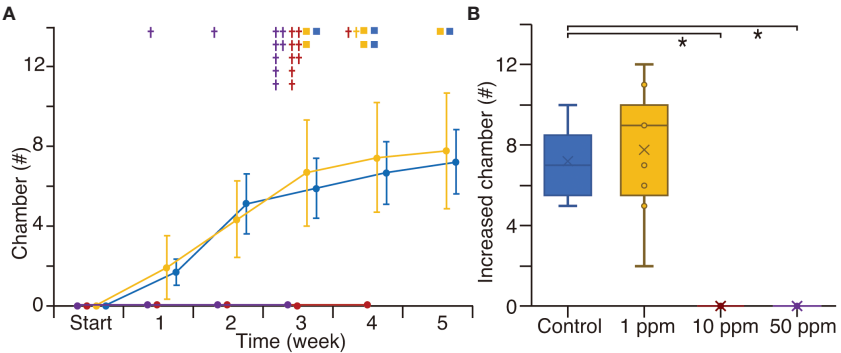


FIGURE 5
The number of increased chambers in the culture experiment 2. The manner of plots is the same as the in [Figure 4](#).

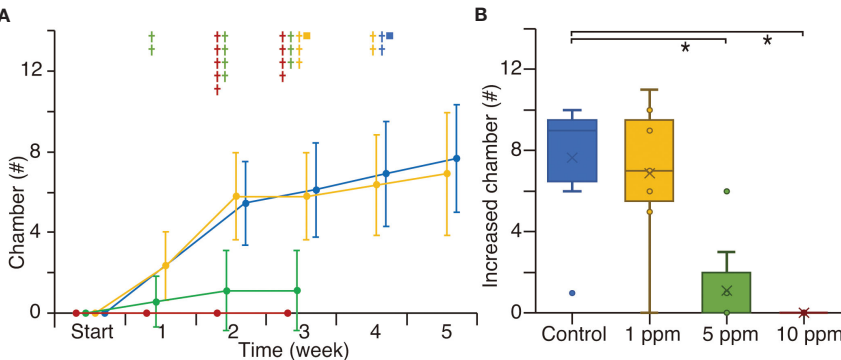


FIGURE 6
The number of increased chambers in the culture experiment 3. Green color indicates the 5 ppm TiO_2 treatment. The other manners of plots are same as [Figure 4](#). The control data for the first week was absent.

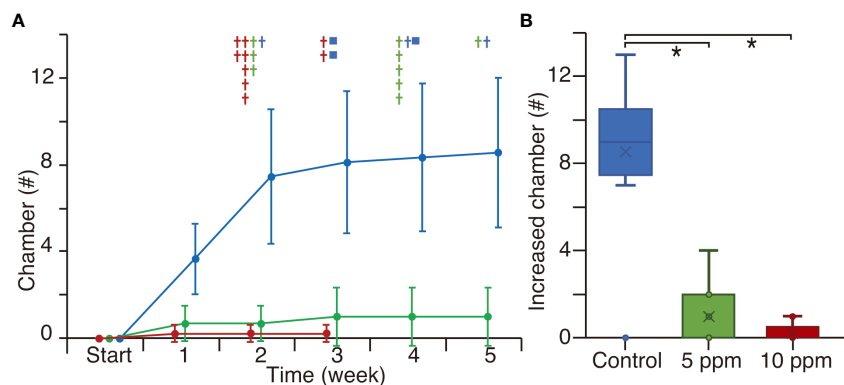


FIGURE 7

The number of increased chambers in culture experiment 4. Blue, green, and red show the control, 5 ppm, and 10 ppm TiO_2 treatments, respectively. The other manners of plots are the same as in Figure 4. Significant differences are $p < 0.0167$ with the Bonferroni correction.

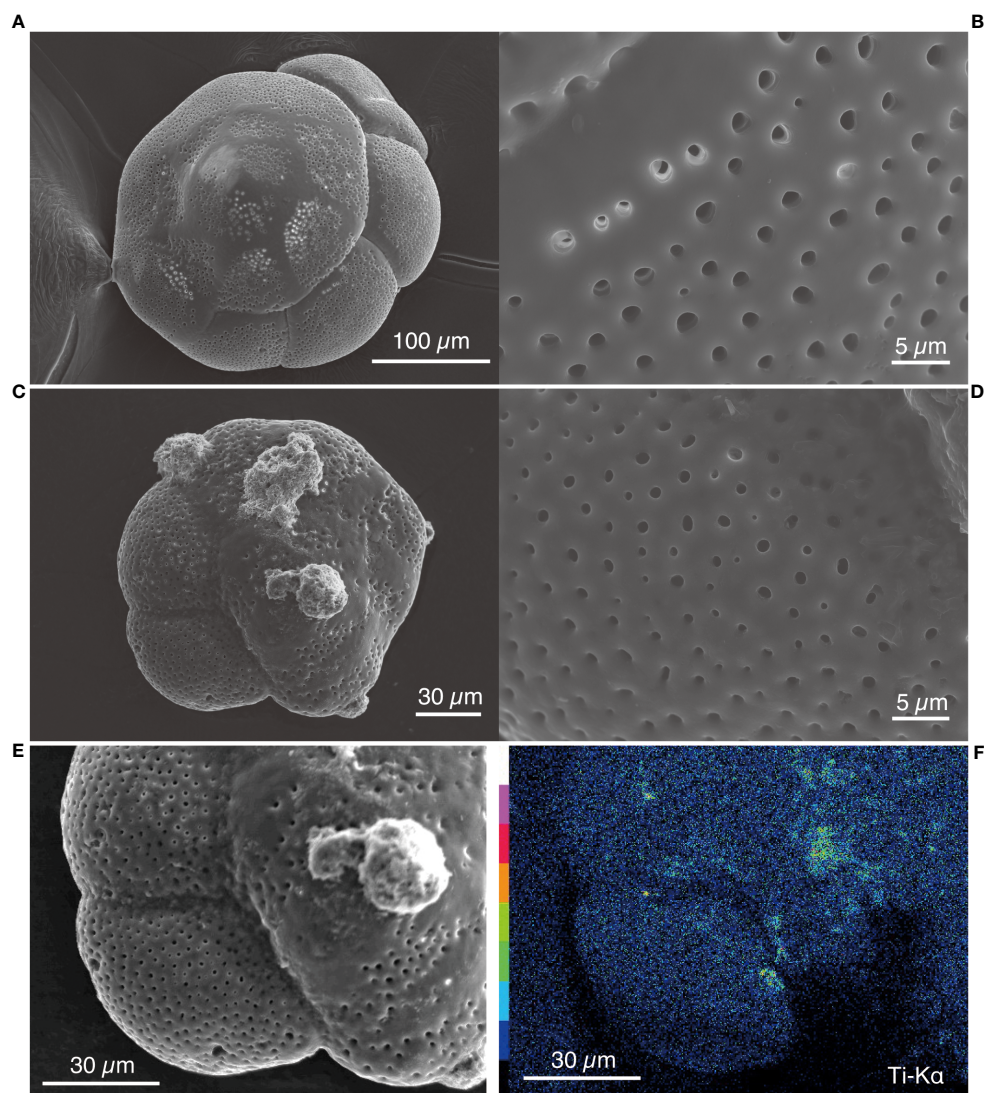


FIGURE 8

SEM images and EDS elemental map. (A) SEM image of the control specimen. (B) The surface test structure of the control specimen. (C) SEM image of a specimen cultured in 10 ppm TiO_2 seawater medium. (D) The surface test structure of the 10 ppm TiO_2 treated specimen. (E) SEM image around a last chamber, which was formed during a culture experiment in 10 ppm TiO_2 medium. (F) EDS elemental map showed the distribution of titanium on the surface of the test (E).

pores were clearly opened on both specimens (Figures 8A–D; Supplementary Figure S1). The test surface was smooth on control specimens but slightly rough on 10 ppm TiO₂ treated specimens (Figures 8B, D). Moreover, some adhesive materials were observed on the test surface of TiO₂ treated specimens, even when cleaned with brushes. These adhesive materials were often observed from the 10 ppm TiO₂ treated specimens, which showed no growth during the culture experiment (Supplementary Figure S1). The SEM-EDS mapping showed a trace amount of titanium from adhesive materials and on the surface of the test but not covering the aperture and pores of the test (Figures 8E, F).

3.4 Increase of *Dunaliella salina* cell density

Time-series changes in *D. salina* cell density were recorded for each culture condition, including control and 1, 5, and 10 ppm TiO₂ seawater media, over a 6-day period. In the control, *D. salina* cell density continuously increased for four days, reaching a stationary phase thereafter (Figure 9). Over the 6-day experiment, the cell density was approximately 10 times higher than the initial density. In the 1 ppm TiO₂ seawater medium, cell density started a slow increase by the second day, significantly rising afterward and reaching a level comparable to the control by the fifth day. However, in the 5 and 10 ppm TiO₂ seawater media, cell densities slightly increased but remained at 2000 cells/mL throughout the experiment. By the end of the experiment, cell densities in the 5 and 10 ppm TiO₂ seawater media were less than half of those in the control and the 1 ppm seawater medium.

3.5 TiO₂ NPs in *Ammonia veneta* cell

Angular-shaped grains with distinct contours were observed in vesicles distributed in the latest three chambers by TEM observations (Figures 10A–C; Supplementary Figure S2). These

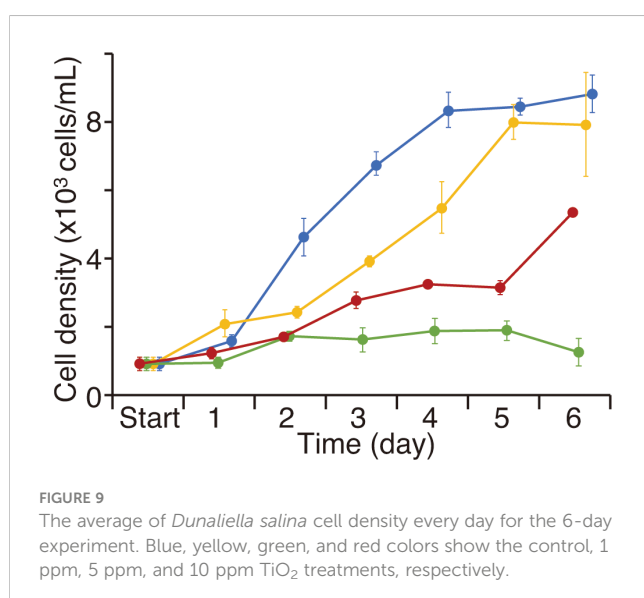
grains, several tens of nanometers in size, exhibited a darker contrast than the surrounding organics and resin, indicating a heavier and more electronically dense element. STEM-EDS analysis detected titanium X-ray peaks from these angular grains (Figures 10D–F), but no titanium peaks were detected from the background (Figures 10G, H). Additionally, STEM-EDS mapping identified abundant titanium-bearing grains in the vesicles, each tens of nanometers in size (Figures 11A, B).

Aggregates of angular grains covered with light-contrast materials were found along the cell, relevant to the surface of the decalcified test (Figure 12A). STEM-EDS analysis detected titanium X-ray peaks from these grains, as well as those in vesicles (Figure 12B), while no titanium peaks were detected from the background (Figure 12C).

4 Discussion

We successfully demonstrated the viability of the clonally reproduced strain of the foraminifer based on the activity of the reticulopodia and chamber formation under microscopic observation (Figures 1–3). *Ammonia veneta* mostly survived for the first three weeks under TiO₂ NPs-containing media, even at high TiO₂ NPs concentrations exceeding 10 ppm (Figures 4–7). TiO₂ NPs did not physically impede the extension of reticulopodia by covering the pores and aperture on the test, as shown by the SEM image (Figures 8C, D). Few TiO₂ NPs were observed in the adhesive materials and on the test surface of 10 ppm-treated specimens (Figures 8E, F). The adhesive materials were often found on the shell surface of the 10 ppm-treated specimens, which stopped reticulopodia activity in the early stage of culture experiments and had no growth of chamber (Supplementary Figure S1). Aggregated TiO₂ NPs might be attached to the shell surface, when reticulopodia did not extend covering over the shell. Although TiO₂ NPs did not physically prevent the extension of reticulopodia, specimens in high concentrations of TiO₂ medium over 5 ppm exhibited no extended reticulopodia and shrunk cytoplasm without chamber formation, leading to their demise (Figures 2, 4–7). The control and 1 ppm TiO₂ treated specimens showed a gradual increase in chambers up to ~20 in total until the reproduction stage. The methods for counting new chambers in addition to reticulopodia activity have been validated to estimate foraminiferal viability and health in response to anthropogenic pollution (Ben-Eliahu et al., 2020; Losada Ros et al., 2020). Our observation based on the test and cytoplasm including reticulopodia is consistent with the trend of chamber increase over time and is useful for estimating the viability and health of foraminifers.

All four foraminiferal culture experiments showed that the control specimens increased by ~8 chambers and grew into maturity from the young form with ~10 chambers during five weeks (Figures 4–7). The specimens exposed to 1 ppm TiO₂ medium showed a slightly low growth rate in Experiment 1, though there was no significant difference from the controls (Figure 4B). When we modified feeding frequency and amount of food in Experiments 2 and 3, the growth rate in 1 ppm TiO₂ treatment was the same as the controls, and some specimens



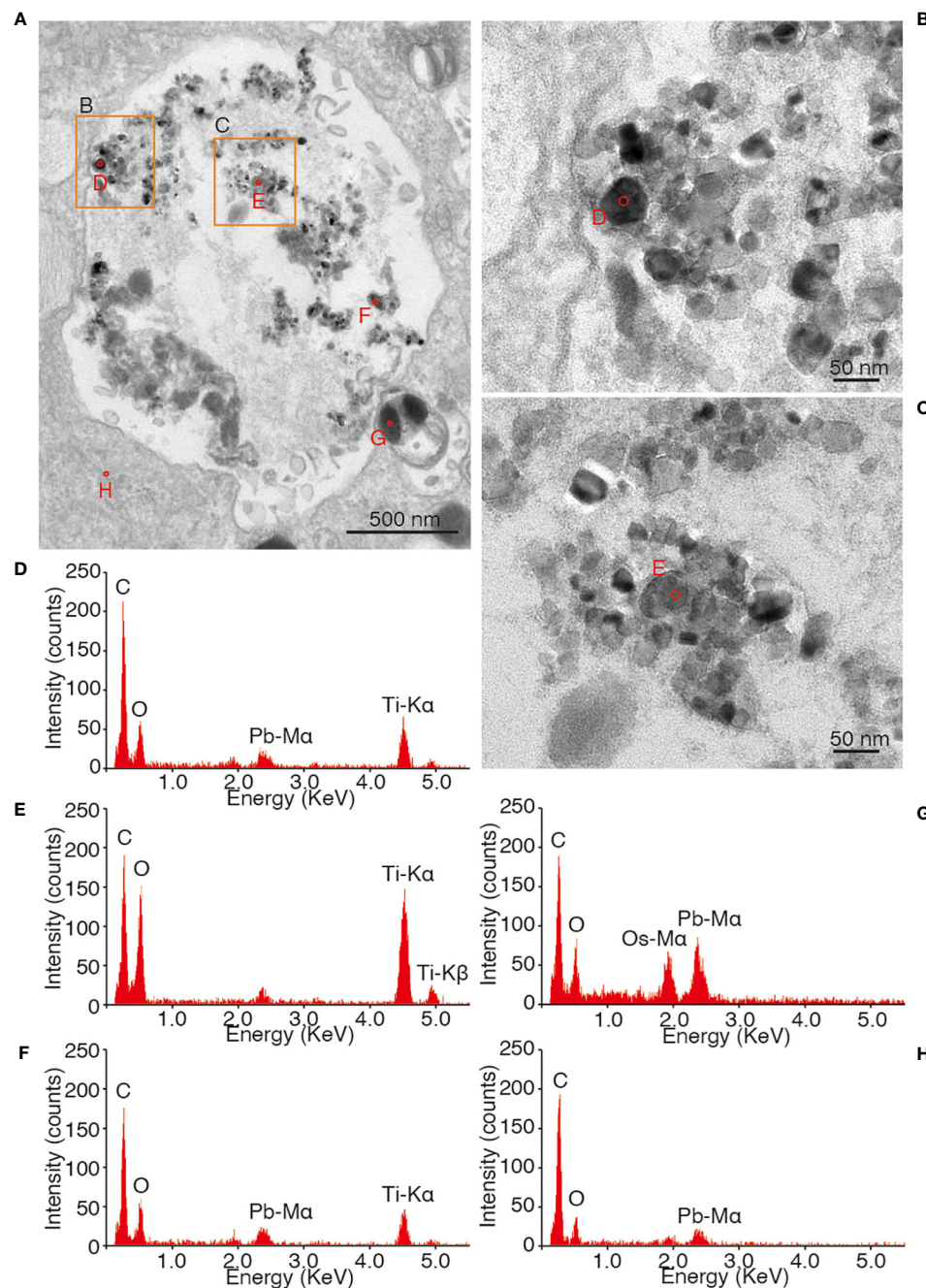


FIGURE 10

Sectioning images and EDS qualitative spectra of the vesicle, which was placed in the second last chamber of *Ammonia veneta* cultured in a 5 ppm TiO_2 seawater medium. The images are contrast-inverted transmission electron micrographs for better visualization of microstructure. (A) Heavier and electronic dense grains in dark color were distributed in the vesicle. Orange squares correspond to (B, C). Red circles show the spots for EDS analysis. (B, C) Heavier and electronic dense grains were ~50 nm in size with an angular shape. (D–H) Qualitative spectra of EDS analysis at each of the five spots shown in (A). (D–F) are associated with small angular grains, (G) shows an electronic dense body, and (H) places the cytosol as a background.

reproduced clones (Figures 5B, 6B). The foraminiferal life cycle has been maintained under a 1 ppm TiO_2 NPs-contained condition, in congruence with the long-term culturing experiment of the previous study (Ishitani et al., 2023). However, the specimens exposed to high TiO_2 NPs concentrations greater than 10 ppm died without growth for four weeks, despite increases of feeding frequency and food volume (Figures 4–7). This indicates that 10

ppm TiO_2 NPs concentration is fatal for foraminifers. Furthermore, we found hole-opening on the test surface of specimens exposed to 10 and 50 ppm TiO_2 media during the experiments (Figure 3). It is thought that foraminifers melt their own tests under conditions of strong stress (Buzas-Stephens and Buzas, 2005), suggesting that high TiO_2 NPs concentrations lead foraminifers to strong stress conditions and cell death.

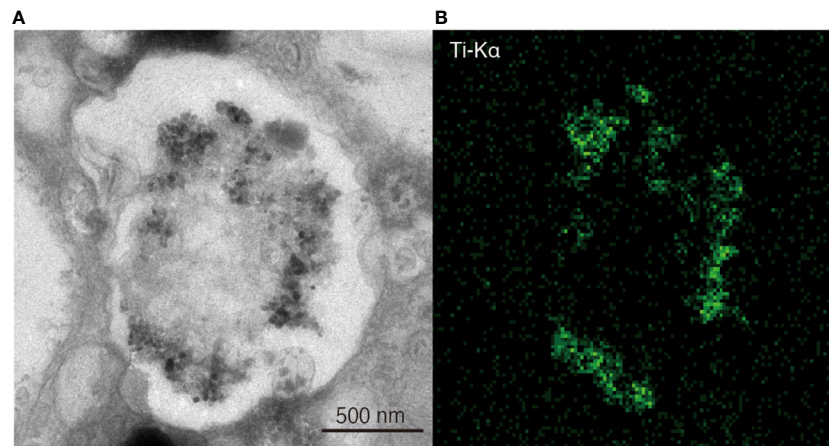


FIGURE 11

Sectioning images and EDS elemental map of the vesicle, which placed in the second last chamber of *Ammonia veneta* cultured in 5 ppm TiO_2 seawater medium. (A) Contrast-inverted TEM image of vesicle. (B) Distribution of titanium with green color by the EDS elemental map in the same area of the TEM image.

In Experiment 3, most specimens stopped growing in 5 ppm TiO_2 medium during the 5-week experiments (Figure 6A). This is possibly caused by a lack of food, *D. salina*. The culture experiment with *D. salina* in TiO_2 media showed that the cell densities of *D. salina* in the 5 and 10 ppm TiO_2 media were lower than half of those in the control and the 1 ppm TiO_2 medium for six days (Figure 9). This result has indicated that the feeding volume in Experiment 3 could not be enough for foraminiferal specimens. However, *A. veneta* specimens stopped growing in 5 ppm TiO_2 medium, even though we increased food volume in Experiment 4 (Figure 7A). Therefore, feeding is not a direct cause to prevent growth of

foraminifers. The growth of some microalgae is suppressed in media with metallic NPs as well as TiO_2 NPs because of physicochemical effects such as inhibition of photosynthesis by packed TiO_2 NPs aggregation and oxidative stress, which damage the cell membrane (Chen et al., 2012; Li et al., 2015; Wang et al., 2016; Ghazaei and Shariati, 2020). The studied specimens have extended reticulopodia at any concentration of TiO_2 treatments and seem to take surroundings including TiO_2 NPs via protoplasmic streaming of reticulopodia without organismal selection (Figure 1). TEM observation of *A. veneta* cells derived from 5 ppm TiO_2 treatment congruently demonstrates uptake of TiO_2 NPs into

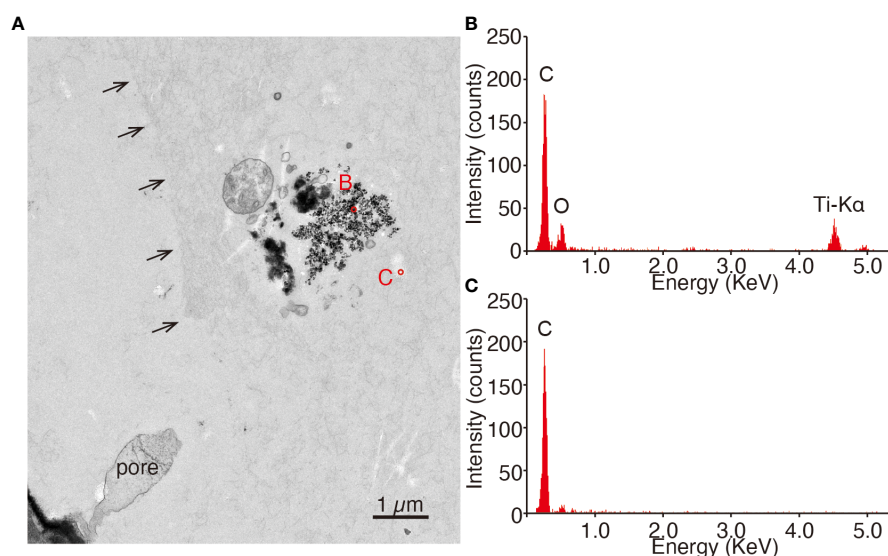


FIGURE 12

Sectioning images and EDS qualitative spectra of expelled materials placed outside of the decalcified test. (A) Contrast-inverted TEM images. The structure of the pore, as shown by the black arrows, remained. Electronically dense grains were distributed near the pore. Circles show the spot of EDS analysis. (B, C) Qualitative spectra of EDS analysis at the spot shown in (A). (B) is associated with a small angular grain, and (C) is a background.

vesicles (Figures 10A–C, 12B). These specimens could take TiO₂ NPs via phagocytosis because of fast aggregation of TiO₂ NPs in high concentrations more than 5 ppm (Morelli et al., 2018; Reyes et al., 2021; Palmeira-Pinto et al., 2023). This is congruent with the previous transcriptomic study, which estimated uptake of TiO₂ NPs via endocytosis or phagocytosis based on the metabolic pathway in 1 ppm TiO₂ treatment (Ishitani et al., 2023). This previous study showed that captured TiO₂ NPs induce the Fenton reaction in vesicles, resulting in ROS production, though such TiO₂ NPs are encapsulated in ceramide and these capsules are expelled from the cell as mucus after 24 hours (Ishitani et al., 2023). The light-contrast materials, including titanium, around the test could be leftovers of waste excreted by foraminifers (Figure 12B). These observations suggest that the foraminiferal metabolic system is acting even in high concentrations of TiO₂ NPs at least 5 ppm condition. This could be caused by two possibilities: a) ROS production is accelerated due to regulation of genes related to stress or releasing toxic substances, and b) overexpression of genes related to releasing toxic substances inhibits cell growth leading to cell death. Future studies will be required to examine the functional changes of detoxification under high TiO₂ NPs concentration environments.

The lethal level of our studied organism, *A. veneta*, is lower than that of microalgae such as green algae and diatoms and those of microorganisms, whose EC₅₀ and LC₅₀ were applicable at concentrations higher than 10 ppm TiO₂ NPs (Menard et al., 2011; Minetto et al., 2014). Our results suggest that the previous examination for EC₅₀ and LC₅₀ could be underestimated than the actual effect of TiO₂ NPs concentration on marine organisms. The previous studies have used different types of TiO₂ NPs: rutile and anatase types with different size ranging from ~10 to ~100 nm. Such material specificity provides different surface charge and other physical characteristics leading to various toxicities reported as cell death by rutile type, while cell necrosis and cell membrane damage by anatase type (Kose et al., 2020). It is still unclear what processes in the metabolic system are affected by the physical characteristics of TiO₂ NPs leading to toxicity. Our study, conducted with same type and size of TiO₂ NPs as those of the transcriptome study (Ishitani et al., 2023), presented that foraminiferal detoxification is possibly disturbed by overdose (> 5 ppm) of TiO₂ NPs. Toxic mechanisms are likely changed associating with concentration of nanoparticles shown by this study, as well as size of nanoparticles. Understanding of both cellular and metabolic mechanisms is important to unveil toxic effects of nanoparticles on various organisms in sets of nanoparticle types. The concentration around 5 ppm of TiO₂ NPs, a limit of foraminiferal detoxification, is much lower than ~120 ppm potentially accumulated on European coasts (Sun et al., 2016; Zheng and Nowack, 2021), though nanoparticle pollution has been invisibly but certainly spread out over marine environment. Considering sedimentation of nanoparticles after aggregation, benthic fauna is dominantly exposed to pollutants. Long-term experiments are crucial to examine an extended cytotoxicity of marine organisms including meiofauna as happen in nature. These studies will help to estimate toxic tolerance of marine organisms to nanoparticles for sustaining marine ecosystem under a harmful impact of nanoparticles pollution.

5 Conclusions

This study succeeded to conduct long-term culture experiments based on the exposure of a marine foraminiferal strain, *A. veneta*, to 1, 5, 10, and 50 ppm TiO₂ NPs. This species had been known to have a detoxification mechanism for TiO₂ NPs by the previous transcriptome analysis. Our TEM observations showed that these foraminifers took TiO₂ NPs into vesicles and ejected some of them even at 5 ppm TiO₂ NPs exposure. However, foraminifers stopped growing in the early stage of 5-week culture experiments under 5 ppm TiO₂ NPs exposure despite the availability of food. These findings indicate that the foraminiferal detoxification system could be disrupted by over 5 ppm TiO₂ NPs. The demand for TiO₂ NPs has grown and their concentration is estimated at up to 120 ppm around the European coast nowadays. Such acceleration of discharging TiO₂ NPs to the ocean could moderate the foraminiferal detoxification ability leading a breakdown of marine ecosystem, because meio-benthos such as foraminifers play an important role for marine food chain. Future studies will be required to examine toxic mechanisms of various marine organisms, for understanding an effect of nanoparticles to the entire marine ecosystem including meiofauna.

Data availability statement

The datasets presented in this study can be found in online repositories. The names of the repository/repositories and accession number(s) can be found in the article/Supplementary Material.

Ethics statement

The manuscript presents research on animals that do not require ethical approval for their study.

Author contributions

YIn: Writing – original draft, Methodology, Investigation, Data curation, Conceptualization. YIs: Writing – original draft, Resources, Investigation. AT: Writing – review & editing, Investigation. KU: Writing – review & editing, Investigation. NT: Writing – review & editing, Investigation. TU: Writing – review & editing, Investigation. YU: Writing – original draft, Project administration, Funding acquisition, Conceptualization.

Funding

The author(s) declare financial support was received for the research, authorship, and/or publication of this article. This work is supported by ESPEC Foundation for Global Environment Research and Technology and Japan Society for the Promotion of Science (JSPS) grant (20H02016).

Acknowledgments

We thank M. Kakimoto, K. Kukita, I. Ikuma, and K. Miura from Kochi University for their help with the culture experiments.

Conflict of interest

Author KU was employed by Marine Works Japan Ltd.

The remaining authors declare that the research was conducted in the absence of any commercial or financial relationships that could be construed as a potential conflict of interest.

Publisher's note

All claims expressed in this article are solely those of the authors and do not necessarily represent those of their affiliated

organizations, or those of the publisher, the editors and the reviewers. Any product that may be evaluated in this article, or claim that may be made by its manufacturer, is not guaranteed or endorsed by the publisher.

Supplementary material

The Supplementary Material for this article can be found online at: <https://www.frontiersin.org/articles/10.3389/fmars.2024.1381247/full#supplementary-material>

SUPPLEMENTARY FIGURE 1

SEM images and EDS analyses of control and 10 ppm TiO₂ treated specimens.

SUPPLEMENTARY FIGURE 2

TEM images of vesicles in a 5 ppm TiO₂ treated specimen.

SUPPLEMENTARY TABLE 1

The number of increased chambers in foraminiferal culture experiments 1–4.

References

- Ammendolia, C., Hofkirchner, C., Plener, J., Bussi eres, A., Schneider, M. J., Young, J., et al. (2022). Non-operative treatment for lumbar spinal stenosis with neurogenic claudication: an updated systematic review. *BMJ Open* 12, e057724. doi: 10.1136/bmjopen-2021-057724
- Ben-Eliahu, N., Herut, B., Rahav, E., and Abramovich, S. (2020). Shell growth of large benthic foraminifera under heavy metals pollution: Implications for geochemical monitoring of coastal environments. *Int. J. Environ. Res. Public Health* 17, 3741. doi: 10.3390/ijerph17103741
- Boxall, A. B., Tiede, K., and Chaudhry, Q. (2007). Engineered nanomaterials in soils and water: how do they behave and could they pose a risk to human health? *Nanomed. (Lond.)* 2, 919–927. doi: 10.2217/17435889.2.6.919
- Buzas-Stephens, P., and Buzas, M. A. (2005). Population dynamics and dissolution of foraminifera in Nueces Bay, Texas. *J. Foraminiferal Res.* 35, 248–258. doi: 10.2113/35.3.248
- Chen, L., Zhou, L., Liu, Y., Deng, S., Wu, H., and Wang, G. (2012). Toxicological effects of nanometer titanium dioxide (nano-TiO₂) on *Chlamydomonas reinhardtii*. *Ecotoxicol. Environ. Saf.* 84, 155–162. doi: 10.1016/j.ecoenv.2012.07.019
- Ciacchi, C., Grimmelmont, M. V., Corsi, I., Bergami, E., Curzi, D., Burini, D., et al. (2019). Nanoparticle-biological interactions in a marine benthic foraminifer. *Sci. Rep.* 9, 19441. doi: 10.1038/s41598-019-56037-2
- Cl ement, L., Hurel, C., and Marmier, N. (2013). Toxicity of TiO₂ nanoparticles to cladocerans, algae, rotifers and plants - effects of size and crystalline structure. *Chemosphere* 90, 1083–1090. doi: 10.1016/j.chemosphere.2012.09.013
- Culver, S. J., and Buzas, M. A. (1999). "Biogeography of neritic benthic foraminifera." in *Modern Foraminifera*, eds. K. Barun and G. Sen (Dordrecht: Springer Netherlands). doi: 10.1007/0-306-48104-9_6
- Delay, M., and Frimmel, F. H. (2012). Nanoparticles in aquatic systems. *Anal. Bioanal. Chem.* 402, 583–592. doi: 10.1007/s00216-011-5443-z
- Farr , M., Gajda-Schrantz, K., Kantiani, L., and Barcel , D. (2009). Ecotoxicity and analysis of nanomaterials in the aquatic environment. *Anal. Bioanal. Chem.* 393, 81–95. doi: 10.1007/s00216-008-2458-1
- Ghazaei, F., and Shariati, M. (2020). Effects of titanium nanoparticles on the photosynthesis, respiration, and physiological parameters in *Dunaliella salina* and *Dunaliella tertiolecta*. *Protoplasma* 257, 75–88. doi: 10.1007/s00709-019-01420-z
- Goldstein, S. T. (1999). "Foraminifera: A biological overview," in *Modern Foraminifera*, eds. K. Barun and G. Sen (Dordrecht: Springer Netherlands). doi: 10.1007/0-306-48104-9_3
- Hartmann, N. B., Von der Kammer, F., Hofmann, T., Baalousha, M., Ottofuelling, S., and Baun, A. (2010). Algal testing of titanium dioxide nanoparticles - testing considerations, inhibitory effects and modification of cadmium bioavailability. *Toxicology* 269, 190–197. doi: 10.1016/j.tox.2009.08.008
- Ishitani, Y., Ciacchi, C., Uji , Y., Tame, A., Tiboni, M., Tanifuji, G., et al. (2023). Fascinating strategies of marine benthic organisms to cope with emerging pollutant: Titanium dioxide nanoparticles. *Environ. Pollut.* 330, 121538. doi: 10.1016/j.envpol.2023.121538
- Kose, O., Tomatis, M., Leclerc, L., Belblidia, N. B., Hochepped, J. F., Turci, F., et al. (2020). Impact of the physicochemical features of TiO₂ nanoparticles on their *in vitro* toxicity. *Chem. Res. Toxicol.* 33, 2324–2337. doi: 10.1021/acs.chemrestox.0c00106
- Li, F., Liang, Z., Zheng, X., Zhao, W., Wu, M., and Wang, Z. (2015). Toxicity of nano-TiO₂ on algae and the site of reactive oxygen species production. *Aquat. Toxicol.* 158, 1–13. doi: 10.1016/j.aquatox.2014.10.014
- Losada Ros, M. T., Al-Enezi, E., Cesarini, E., Canonico, B., Bucci, C., Alves Martins, M. V., et al. (2020). Assessing the cadmium effects on the benthic foraminifer *Ammonia cf. parkinsoniana*: An acute toxicity test. *Water* 12, 1018. doi: 10.3390/w12041018
- Luo, Z., Li, Z., Xie, Z., Sokolova, I. M., Song, L., Peijnenburg, W. J. G. M., et al. (2020). Rethinking nano-TiO₂ safety: overview of toxic effects in humans and aquatic animals. *Small* 16, e2002019. doi: 10.1002/sml.202002019
- Matranga, V., and Corsi, I. (2012). Toxic effects of engineered nanoparticles in the marine environment: model organisms and molecular approaches. *Mar. Environ. Res.* 76, 32–40. doi: 10.1016/j.marenvres.2012.01.006
- Menard, A., Drobne, D., and Jemec, A. (2011). Ecotoxicity of nanosized TiO₂. Review of *in vivo* data. *Environ. Pollut.* 159, 677–684. doi: 10.1016/j.envpol.2010.11.027
- Minetto, D., Libralato, G., and Ghirardini, A. V. (2014). Ecotoxicity of engineered TiO₂ nanoparticles to saltwater organisms: an overview. *Environ. Int.* 66, 18–27. doi: 10.1016/j.envint.2014.01.012
- Moore, M. N. (2006). Do nanoparticles present ecotoxicological risks for the health of the aquatic environment? *Environ. Int.* 32, 967–976. doi: 10.1016/j.envint.2006.06.014
- Morelli, E., Gabellieri, E., Bonomini, A., Tognotti, D., Grassi, G., and Corsi, I. (2018). TiO₂ nanoparticles in seawater: Aggregation and interactions with the green alga *Dunaliella tertiolecta*. *Ecotoxicol. Environ. Saf.* 148, 184–193. doi: 10.1016/j.ecoenv.2017.10.024
- Palmeira-Pinto, L., Emerenciano, A. K., Bergami, E., Joviano, W. R., Rosa, A. R., Neves, C. L., et al. (2023). Alterations induced by titanium dioxide nanoparticles (nano-TiO₂) in fertilization and embryonic and larval development of the tropical sea urchin *Lytechinus variegatus*. *Mar. Environ. Res.* 188, 106016. doi: 10.1016/j.marenvres.2023.106016
- R Core Team (2021). *R: A language and environment for statistical computing* (Vienna, Austria: R Foundation for Statistical Computing). Available at: <https://www.R-project.org/>.
- Reyes, J. P., Lagdameo, J. D., Celorico, J. R., Almeda, R. A., Peralta, M. M., and Basilia, B. A. (2021). Aquatic toxicity studies of titanium dioxide and silver nanoparticles using *Artemia franciscana* Nauplii and *Daphnia magna*. *Mater. Sci. Eng. A* 11, 107–113. doi: 10.17265/2161-6213/2021.10-12.001
- Sun, T. Y., Bornh ft, N. A., Hungerb hler, K., and Nowack, B. (2016). Dynamic probabilistic modeling of environmental emissions of engineered nanomaterials. *Environ. Sci. Technol.* 50, 4701–4711. doi: 10.1021/acs.est.5b05828
- Wang, Y., Zhu, X., Lao, Y., Lv, X., Tao, Y., Huang, B., et al. (2016). TiO₂ nanoparticles in the marine environment: Physical effects responsible for the toxicity on algae *Phaeodactylum tricornutum*. *Sci. Total Environ.* 565, 818–826. doi: 10.1016/j.scitotenv.2016.03.164
- Zheng, Y., and Nowack, B. (2021). Size-specific, dynamic, probabilistic material flow analysis of titanium dioxide releases into the environment. *Environ. Sci. Technol.* 55, 2392–2402. doi: 10.1021/acs.est.0c07446



OPEN ACCESS

EDITED BY
Kun Chen,
Jiangsu University, China

REVIEWED BY
Dario Savoca,
University of Palermo, Italy
Jill Awkerman,
United States Environmental Protection
Agency (EPA), United States

*CORRESPONDENCE

Wei Liu
✉ lw_ecology@163.com
Yan Liu
✉ liuyan@nies.org

†These authors have contributed equally to this work

RECEIVED 19 July 2024

ACCEPTED 18 September 2024

PUBLISHED 04 October 2024

CITATION

Zhang D, Liu W, Xin Y, Liu X, Zhang Z and Liu Y (2024) Trophic transfer of PFAS potentially threatens vulnerable Saunders's gull (*Larus saundersi*) via the food chain in the coastal wetlands of the Yellow Sea, China. *Front. Mar. Sci.* 11:1467022. doi: 10.3389/fmars.2024.1467022

COPYRIGHT

© 2024 Zhang, Liu, Xin, Liu, Zhang and Liu. This is an open-access article distributed under the terms of the [Creative Commons Attribution License \(CC BY\)](https://creativecommons.org/licenses/by/4.0/). The use, distribution or reproduction in other forums is permitted, provided the original author(s) and the copyright owner(s) are credited and that the original publication in this journal is cited, in accordance with accepted academic practice. No use, distribution or reproduction is permitted which does not comply with these terms.

Trophic transfer of PFAS potentially threatens vulnerable Saunders's gull (*Larus saundersi*) via the food chain in the coastal wetlands of the Yellow Sea, China

Dini Zhang^{1,2†}, Wei Liu^{1,2,3*†}, Yu Xin⁴, Xiaoshou Liu³, Zhenhua Zhang^{1,2} and Yan Liu^{1,2*}

¹State Environmental Protection Key Laboratory of Biodiversity and Biosafety, Ministry of Ecology and Environment of China, Nanjing, China, ²Nanjing Institute of Environmental Sciences, Ministry of Ecology and Environment of China, Nanjing, China, ³Institute of Evolution and Marine Biodiversity, Ocean University of China, Qingdao, China, ⁴Department of Ecological Monitoring, Nantong Environmental Monitoring Centre of Jiangsu Province, Nantong, China

Perfluoroalkyl and polyfluoroalkyl substances (PFAS) have been extensively documented as posing significant health risks to human populations. However, there is a lack of research of their impact on endangered species, which significantly affects the effectiveness of conservation efforts and maintenance of these populations. In this study, we examined the levels of PFAS pollution in adults and juveniles of the vulnerable Saunders's gull (*Larus saundersi*), along with their various food sources using ultra high-performance liquid chromatography-tandem mass spectrometry and Ecopath model. Long-chain PFAS, predominantly composed of perfluorooctanoic acid (accounting for 51.4% of the total), were identified as the main pollutants in the gull, its food, and the environment. Saunders's gulls showed significant bioaccumulation and magnification of PFAS, with contamination levels significantly above those recorded in other species. Mean PFAS levels between juveniles (904.26 ng/g wet weight) and adults (407.40 ng/g wet weight) revealed a significant disparity, indicating that PFAS pollution may severely threaten these birds. Among the food sources analyzed, bivalves and polychaetes emerged as the primary contributors to PFAS contamination in Saunders's gulls, with high transfer efficiency. The fundamental cause of PFAS pollution in benthic organisms and the gulls appears to be baseline environmental pollution, which was highly consistent across all examined pollutant types. Moreover, chemical plants close to breeding areas may cause severe environmental pollution, threatening organisms at various trophic levels through the food web. We suggest enhancing the pollution monitoring of important biological habitats for timely prediction and early warning of chemical risks. Additionally, ecological restoration of key habitats should be strengthened to ensure the effectiveness of biodiversity conservation.

KEYWORDS

shorebirds, food web, PFAS, pollution, threatened species

1 Introduction

As portrayed in Rachel Carson's book *Silent Spring*, large amounts of chemical pollutants deposited in the environment seriously threaten ecosystem health and human well-being, while precipitating a sharp decline in biodiversity (Jaureguiberry et al., 2022; Sylvester et al., 2023). Some emerging pollutants such as persistent organic pollutants have been detected in many terrestrial or aquatic organisms, including the common dolphins (*Delphinus delphi*), Cod (*Gadus morhua*) and white-tailed sea eagles (*Haliaeetus albicilla*), which have significantly hindered the effectiveness of biodiversity conservation efforts (Kannan et al., 2002; Falandysz et al., 2007). Hence, Target 7 of the Kunming-Montreal Global Biodiversity Framework was established to mitigate pollution risks and minimize the adverse impact of pollution from all sources to levels that are not detrimental to biodiversity and ecosystem functions and services, taking into account their cumulative effects, by 2030 (<https://www.cbd.int/doc/c/e6d3/cd1d/daf663719a03902a9b116c34/cop-15-l-25-en.pdf>). The Stockholm Convention entered into force in 2004 with the aim of reducing or eliminating persistent organic pollutant emissions and protecting human health and the environment from these pollutants (<https://chm.pops.int/TheConvention/ConferenceoftheParties/ReportsandDecisions/tabid/208/ctl/Download/mid/6863/Default.aspx?id=101&ObjID=7671>). In spite of these multiple and ambitious international agreements that have been established over several decades, the degradation of ecosystems and the consequent decline in biodiversity persist, with some instances even showing an acceleration.

PFAS are emerging pollutants of considerable relevance with characteristics of biotoxicity, environmental persistence, and bioaccumulation (Evich et al., 2022). PFAS are anthropogenic substances that contain high-energy carbon-fluorine covalent bonds (C-F), which have been produced and widely used in industrial and civilian applications, including the production of clothing, blankets, and electroplating, for over 50 years (Dickman and Aga, 2022). Recent studies and reports have found that PFAS are widespread in drinking water, air, soil, foods, food packaging materials, wild organisms, and has a potential risk of biomagnification in the food chain (Wee and Aris, 2023). The existence of PFAS in organisms is of particular concern given the demonstrated harmful effects to health, including impacts on the reproductive system and immune function (Bach et al., 2015; Stein et al., 2016). In addition to humans, many endangered wildlife species suffer from PFAS contamination. Cui et al. (2019) presented the initial findings regarding the presence of PFAS in

the blood and dietary sources of two endangered primate species, the golden snub-nosed monkey (*Rhinopithecus roxellana*) and Francois' leaf monkey (*Trachypithecus francoisi*). Since PFAS are enriched in living organisms through the food chain or food web, species at higher trophic levels will have higher levels of contamination, representing a threat to wildlife survival and population continuation. Most current PFAS exposure research has focused on some special taxa such as seabirds and raptors (Colomer-Vidal et al., 2022; Sun et al., 2022), as important indicator species of environmental change, whereas related studies on shorebirds that are highly dependent on wetland habitats are rather limited (Ma et al., 2022). Given that environmental pollution is one of the most important drivers of the rapid decline of shorebird populations, lack of knowledge of the current status of their PFAS occurrence is not conducive to the conservation of endangered species such as *Eurynorhynchus pygmeus*, *Larus saundersi*, and *Tringa guttifer* (Murray et al., 2018; Ma et al., 2023). For example, concentrations of Perfluorooctane sulfonate (PFOS) in the whole eggs of herring gulls (*Larus argentatus*) from two coastal areas in northern Norway were found to have increased significantly by a factor of nearly two between 1983 and 2003, which then leveled off in 2003 (Verreault et al., 2007). *Charadrius alexandrinus* in China are widely exposed to the pollution stress from PFAS, and PFAS concentrations in adult and juvenile birds have reached dangerous levels (Sun et al., 2023). Thus, there is a huge gap concerning the biodiversity conservation and pollution abatement of threatened and vulnerable shorebirds.

Chemical pollution, especially PFAS pollution, has received relatively less attention as a contributing factor to global biodiversity loss compared to other factors (Sonne et al., 2023). China's chemical industry has been the largest in the world in view of revenue since 2011, especially mainly distributed in some coastal provinces, such as Jiangsu and Shandong (Chen and Reniers, 2020). Due to these sites of chemical industry usually were selected in the undeveloped area with extensive natural habitats, it would formulate a nonnegligible threat on biodiversity and ecosystem health. Not addressing these pollution effects may significantly compromise the effectiveness of biodiversity conservation efforts. Therefore, to fill this gap, we focused on the endangered shorebird species Saunders's gull (*Larus saundersi*) in the wetland along the coast of Jiangsu, and analyzed the transfer of PFAS from substrates to foods and to birds to explore the threat of these pollutants from the adult to juvenile stage. The vast wetland along the coast of Jiangsu supports a large flock of migratory, wintering, and breeding birds with abundant food and suitable habitats. Some endangered bird species are highly dependent on this coastal mudflat, including the spoon-billed sandpiper, Nordmann's greenshank, and the black-faced spoonbill (Yang et al., 2020). Saunders's gull (*Larus saundersi*) is classified as "vulnerable" on the International Union for Conservation of Nature (IUCN) Red List (<https://www.iucnredlist.org/species/22694436/132551327>), which fed mainly on small fish, crustaceans, and polychaete worms (<https://birdsoftheworld.org/bow/species/aukul2/cur/introduction>), breeds in eastern mainland China, and sporadically at sites on the south-west coast of South Korea. Saunders's gull faces endangerment due to habitat loss primarily caused by the diminishing stretches of

Abbreviations: PFAS, perfluoroalkyl and polyfluoroalkyl substances; PFCAs, perfluorocarboxylic acids; PFSA, perfluoroalkanesulfonic acids; PFBA, perfluorobutanoic acid; PFBS, perfluoro-1-butane sulfonic acid; PFDA, perfluorodecanoic acid; PFDoDA, perfluorododecanoic acid; PFDS, perfluoro-1-decanesulfonate; PFHpA, perfluoroheptanoic acid; PFHxA, perfluorohexanoic acid; PFHxS, perfluoro-1-hexane sulfonic acid; PFNA, perfluorononanoic acid; PFOS, perfluorooctanesulfonic acid; PFPeA, perfluoro-n-pentanoic acid; PFUnDA, perfluoroundecanoic acid; PFOA, perfluorooctanoic acid; PFTeDA, perfluorotetradecanoic acid.

common seepweed habitat in the study area and adjacent regions (Jiang et al., 2010). This study area thus plays a vital role in the migration, breeding, and conservation of Saunders's gull.

The results would serve as a theoretical foundation for bird protection and pollution abatement in the biodiversity hotspot. Overall, our work on PFAS pollution in bird habitats can provide not only a scientific basis for the protection of important bird species and data support for the transfer of PFAS in the food chain, but can further offer a reference to facilitate evaluations of the pollution and inform strategies for appropriate habitat management.

2 Material and methods

2.1 Sample collection

In the breeding period (April to August) of 2022, eight fresh carcasses of Saunders's gull (hereinafter "gull") were collected on the coast of Xiaoyangkou in Nantong, Jiangsu, China, where there was a chemical plant nearby (Figure 1), including five adult individuals and three juvenile individuals. Highly putrefied carcasses were discarded because of the potential environmental pollution. We dissected these carcasses to obtain chest muscle samples. To determine the content of PFAS in the food of the

gull, sediment samples and three types of macrobenthos were collected in these gridded sampling sites in April 2022 (Figure 1), including clamworm (*Perinereis nuntia*), bivalve (*Meretrix meretrix*), and shrimp (*Acetes chinensis*). Macrofauna were collected from 9 sampling sites (Figure 1). In the selected sites, the coastal habitat was quantitatively sampled four times each to the sediment depth of 30 cm using a quadrat (25 cm × 25 cm). A 0.5-mm mesh was utilized to sieve the invertebrate samples in the foraging area, including clamworms, bivalves, shrimps, and sediment samples. All samples underwent lyophilization, homogenization, and storage at −20°C until analysis. Sample collection adhered to national ethical guidelines (Animal management regulations, Order No. 2 of the State Science and Technology Commission, China, 1988), and the collection of carcass samples due to natural causes was given its approval by Jiangsu Wildlife Protection Station (Approval [2017] No. 14).

2.2 Sample pretreatment and analysis

Samples underwent extraction procedures according to the methods outlined by Wang et al. (2021), which are elaborated in detail in the supplementary information (refer to Supplementary Figure S1). The solutions were centrifuged for 3 minutes at 10000 rpm and filtered through a 0.22 µm membrane as a final step before

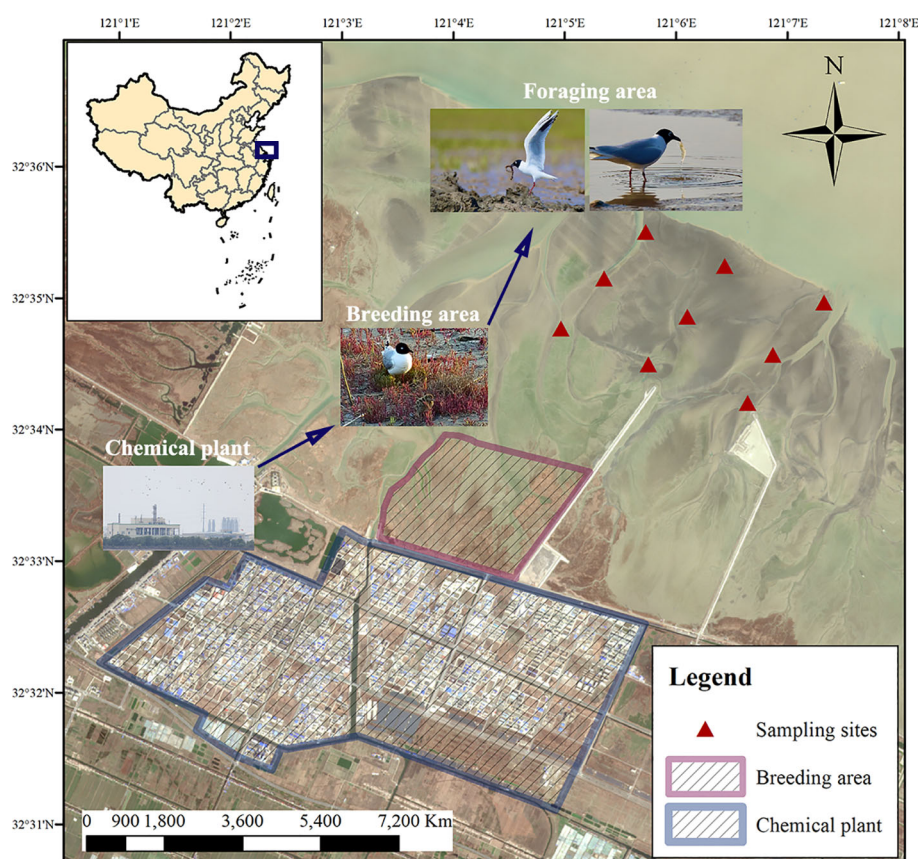


FIGURE 1
Location of study area and sampling point in the Yellow Sea mudflat.

being analyzed using ultra high-performance liquid chromatography (UHPLC)-tandem mass spectrometry (MS/MS). Target PFAS tested encompassed perfluorobutanoic acid (PFBA), perfluoro-n-pentanoic acid (PFPeA), perfluorohexanoic acid (PFHxA), perfluoroheptanoic acid (PFHpA), perfluorooctanoic acid (PFOA), perfluorononanoic acid (PFNA), perfluorodecanoic acid (PFDA), perfluoroundecanoic acid (PFUnDA), perfluorododecanoic acid (PFDoDA), perfluorotetradecanoic acid (PFTeDA), perfluoro-1-butane sulfonic acid (PFBS), perfluoro-1-hexane sulfonic acid (PFHxS), perfluorooctanesulfonic acid (PFOS) and perfluoro-1-decanesulfonate (PFDS). The four chemical compounds (PFBA, PFPeA, PFHxA, PFBS) were classified into the short-chain group based on their carbon content, while the remaining compounds belonged to the long-chain category. The UHPLC-ESIMS/MS conditions and instrument parameters are provided in [Supplementary Table S1](#). The native and mass-labeled PFAS standards used in this study were consistent with those utilized in a prior study (Wang et al., 2021). Multi-reaction monitoring mode was used for quantitative analysis, and [Supplementary Table S2](#) lists the ideal MS/MS parameters for the 14 PFAS along with nine surrogate standards. Acquisition and processing of quantitative data from samples and internal calibration standards were made easier by the Analyst software (AB SCIEX, v1.6).

2.3 Quality assurance and control

Prior to use, all laboratory equipment and solvents underwent testing to prevent contamination. To minimize potential laboratory background pollution, two extraction blanks were processed for each batch, yielding undetectable levels of PFAS. The LOQs were assessed as 10 times the standard deviation of the blank samples fortified at 10 ng/g w.w (Wang et al., 2021). The limit of detection (LOD) and the limit of quantification (LOQ) in samples were 0.01–0.05 ng/g and 0.03–0.15 ng/g respectively. Recovery (RE) was calculated for each analyte using the ratio between the actual calculated values of matrix spike sample and spiked values of samples according to the formula: $RE\% = (\text{actual calculated values} / \text{spiked values}) \times 100\%$. Matrix spike recovery was performed with 3 ng/g contamination levels for five sample matrix from the reference site. Matrix spike recoveries of target compounds ranged from 72.98% to 121.63% for five sample matrix with the relative standard deviation (RSD) values ranged between 0.79% to 19.96% ([Supplementary Table S3](#)).

2.4 Data analysis

Statistical analyses were conducted for PFAS compounds with detection frequencies exceeding 50%; in cases where the PFAS concentration was less than the LOQ, the value of LOQ/2 was utilized in the calculations. T-tests were employed to compare concentrations between juvenile and adult gull group, with statistical significance set at $p < 0.05$. Statistical analyses,

including principal components and visualizations of the results were performed using SPSS 22 (IBM Co, Armonk, NY, USA), OriginPro 2023b (Origin Lab Corporation), and R software. According to previous research on Saunders's gull (Wang et al., 2017), the isotope values from sediment samples, invertebrate, and bird samples were acquired. The biomass data of invertebrates and birds in the study area were obtained from Wang et al. (2019) ([Supplementary Table S4](#)). We employed the Ecopath model within Ecopath with Ecosim (EwE model) (Christensen and Walters, 2004) and followed the methodology outlined by Walters and Christensen (2018) to integrate biomass, contaminant concentrations, and production (on a logarithmic scale) as chemical tracers of the food web structure. The EwE model uses a series of linear equations to describe the balance of energy flow or material flow in each functional group of the ecosystem, and makes the whole ecosystem reach equilibrium by establishing a food web, so as to obtain a static equilibrium model of the ecosystem at a given time, and the basic equations used to balance each functional group are:

$$B_i \left(\frac{P}{B} \right)_i EE_i - \sum_j \left(\frac{Q}{B} \right)_j DC_{ji} - Y_i - BA_i - E_i = 0$$

where: for functional group i , P is its production; B is its biomass (which can be expressed in terms of wet weight, dry weight, energy, nutrient content such as C, N); EE is its Ecotrophic Efficiency (EE), which is usually less than 1; Q is the proportion of food consumed by the predator; and; EE is its ecotrophic efficiency (EE), which is usually less than 1; Q is the proportion of food consumed by the predator; and BA_i is the bioaccumulation rate of functional group i ; DC is an $n \times m$ food matrix (where n is the number of predators and m is the number of baits) describing the predator-prey relationship between functional groups; DC_{ji} is the proportion of bait i in the diet of predator j ; Y_i is the amount of catch; E_i is the net migration rate (emigration minus immigration; in the present model, all functional groups live in the same ecosystem and E_i is 0).

According to the principle of functional group setting in the model, sediment samples, shrimp, clam, bivalve and Saunders' gull were classified into five ecological functional groups in this study. According to the analysis of structure and energy flow among 20 functional groups in the study area (Wang et al., 2019), we obtained the biomass (B), P/B coefficient, Q/B coefficient of each functional group in this study and other parameters ([Supplementary Table S4](#)). The ecological trophic conversion efficiency (EE) refers to the conversion efficiency of the production volume of the functional group, which is a more difficult parameter to obtain, and the model set it as an unknown parameter, which was derived from other parameters by debugging the model. Based on the previous research on the diet of Saunders' gull on the coast of the Yellow Sea (Wang et al., 2017), the food composition matrix from prey (sediment samples, shrimp, clam, bivalve) to predator (Saunders's gull) was obtained ([Supplementary Table S5](#)). After inputting these model parameters, the fractional trophic level was generated, integrating energy flow and food composition, as well as the ecotrophic efficiency.

3 Results

3.1 Detection rate and concentrations of PFAS

The results of testing 14 PFAS in five samples showed that PFOA, PFBA, PFUnDA, PFDA, PFNA, PFOS, and PFHxS had higher detection rates than the remaining PFAS tested (57.17–100%). The organisms exhibited varying concentrations of PFAS compounds, with PFOA being the most prevalent at 51.4% (mean proportion) of the total PFAS concentration, followed by PFBA (16%), PFOS (15.2%), PFUnDA (5.4%), PFNA (4.6%), PFDA (2.6%), and PFDoDA (1.4%). Lower detection rates (2.22–42%) were found for PEDoDA, PFHpA, PETeDA, PFPeA, PFHxA, PFBS, and PFDS. The average detection frequency of long-chain PFAS (50.35%) was higher than that of short-chain PFAS (32%).

3.2 Differentiation of PFAS between adults and juveniles

All 14 PFAS detected in the juvenile ($n = 3$) and adult ($n = 5$) gull chest muscle are presented in [Figure 2](#); [Supplementary Table S6](#); the concentrations of only PFBS and PFDS were below the LOD of the analytical method. In comparison to adult gulls (mean: 407.40 ng/g ww), juvenile gulls exhibited significantly higher concentrations of total PFAS levels in their chest muscles (mean: 904.26 ng/g ww), highlighting a notable disparity. Additionally, the levels of total PFSA in the chest muscles of juvenile gulls (mean: 399.49 ng/g ww) were markedly elevated compared to those in adults (mean: 18.90 ng/g ww; $p < 0.05$). The differences in the levels of PFUnDA, PFDA, PFDoDA, and PFOS between the two groups

were significant ($p < 0.05$), with concentration ranges of 41.47–134.75, 23.62–82.32, 10.59–31.60, and 187.49–732.05 ng/g ww, respectively, in juvenile gulls, and not detected–6.31, not detected–8.07, not detected–13.18, and 0.62–57.78 ng/g ww, respectively, in adult gulls.

3.3 Comparison of PFAS in gulls and their food

PFAS concentrations varied across the organisms collected from the mudflat in the Yellow Sea, ranging from 9.42 ng/g ww (shrimp) to 593.72 ng/g ww (gull chest muscle). Total concentrations of PFAS in the samples followed the sequence gull > clamworm > bivalve > shrimp (refer to [Supplementary Table S7](#); [Figure 3](#)), potentially indicative of variations in their bioaccumulative capacities, environmental surroundings, physiology, and dietary preferences. Regardless of taxa, PFOA, PFBA, and PFOS emerged as the predominant substances detected in the organisms. Their respective concentration ranges were 0.47–677.44, not detected–517.70, and 23.5–682 ng/g ww. Notably, the highest levels of PFAS residues were found in the chest muscle of gulls (ranging from 11.82–677.44 ng/g ww). Previous studies with sampling locations distributed in coastal wetlands such as the North Pacific and Arctic Ocean detected a PFOS content in bird muscles in the range of 0.8–65.8 ng/g, which is much lower than the range detected in the present study ([Supplementary Table S8](#)).

The sediment samples exhibited total PFAS concentrations ranging from 0.05 to 9.10 ng/g, aligning closely with earlier findings in the Yellow Sea ([Zhong et al., 2021](#)), yet notably lower than the levels detected in organisms. Only PFOA, PFBA, and PFOS were above the LOD among the analyzed PFAS at the

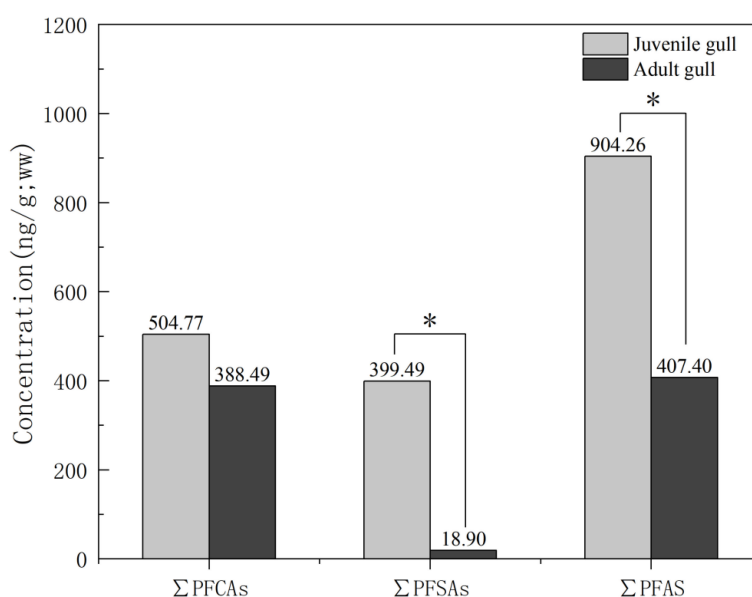


FIGURE 2

Concentrations of Σ PFCAs, Σ PFSA and Σ PFAS in chest muscle from juvenile and adult. * indicated $p < 0.05$. Juvenile gull ($n=3$) and adult gull ($n=5$).

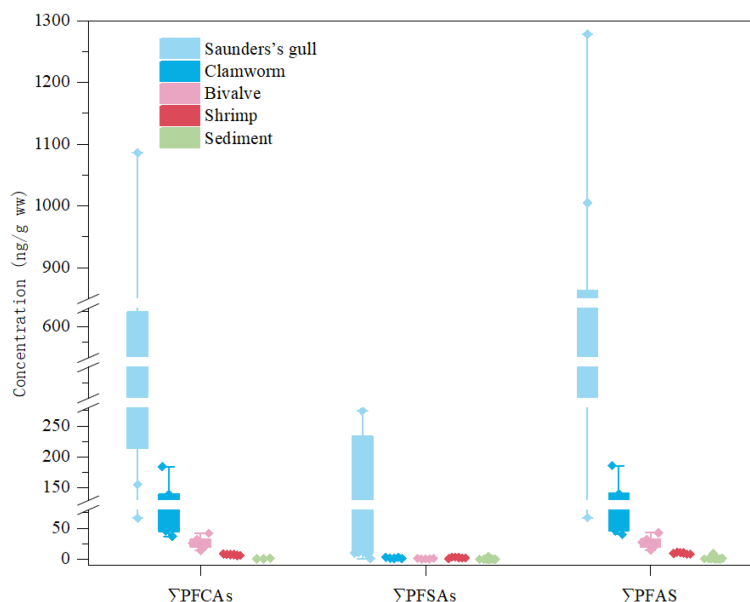


FIGURE 3

Box plot of concentrations of Σ PFCAs, Σ PFASs and Σ PFAS in Saunders's gull (n=8), clamworm, bivalve, shrimp and sediment samples.

concentrations of PFOA (0.92 ng/g), PFOS (0.44 ng/g) and PFBA (0.27 ng/g), respectively (Supplementary Table S7).

3.4 Trophic transfer and bioaccumulation of PFAS

The Sankey diagram revealed the correlation among different creatures, the type and characteristic of PFAS (Figure 4A). The types of PAFS in gulls was more abundant than sediment and invertebrates. Most of PFAS existing in gulls and invertebrates were clustered into long-chain group, and only five types of short-chain PFAS were detected. A principal component analysis was used to assess the connections between the 14 PFAS response signals and five different kinds of samples (Figure 4B). The combined contribution rate of the first two principal components (PC1 and PC2) to the total variation in PFAS levels was 63.11% (Supplementary Table S7), which was highly reliable for explaining the composition of PFAS. Meanwhile, PFNA, PFOA, PFDA, PFHpA, PFDoDA, PFUnDA, PFOS had higher contribution for grouping and describing the PFAS in the study area (Supplementary Figure S2; Figure 4B). PFBS and PFDS were negatively correlated with PC1 and PC2, indicating that these two indicators were not detected or had lower detection values in each group. Other 12 indicators were positively correlated with these two components. The bivalve, shrimp, and sediment groups showed good intragroup repeatability and high similarity in the sample data, whereas the gull group was more dispersed and differed from the other clusters, consistent with the results shown in Supplementary Table S8.

The predicted trophic and bioaccumulation networks for Saunders's gulls are shown in Supplementary Table S4 and visually displayed in Figure 5. According to the analysis of the biomass networks, the model grouped the nutrient flows of the

system into seven frictional trophic levels (Figure 5A). The energy flow pathways for black-billed gulls were dominated by a grazing food chain, i.e. sediment-shellfish-shrimp-Saunders's gulls, or sediment-shellfish-Saunders's gulls (Figure 5A). Mussels and clams are the main food sources for black-billed gulls. Similar to the energy transfer, PFAS showed similar transfer characteristics in the food chain of Saunders's gulls. The most prevalent groups in terms of fluxes and biomass are those that occupy lower trophic levels. Trophic levels and biomass values showed a negative correlation. In comparison, as trophic levels increased, so did the bioaccumulation values of PFAS. As a result, a biomagnification phenomenon was observed, as the network plot illustrates (Figure 5B). Notably, the estimated PFAS values in clamworm were higher than those in the other food sources for the gull.

4 Discussion

4.1 PFAS concentrations and composition profiles in organisms and the sediment

This results showed that the highest levels of PFAS (11.82–677.44 ng/g) were detected in the gull muscle, which were higher than those previously reported for other seabird species elsewhere (Supplementary Table S9) (Olivero-Verbel et al., 2006; Haukås et al., 2007; Chu et al., 2015; Chen et al., 2018; Robuck et al., 2021). The main detected species of PFAS in endangered gulls in China's offshore regions were PFOA (Juvenile mean = 234.19 ng/g; Adult mean = 144.11 ng/g) and PFOS (Juvenile mean = 398.03 ng/g; Adult mean = 16.13 ng/g), which is aligning with our research outcomes. Previous reports indicated the lowest visible adverse effect level of PFOS was 100 ng/g of egg weight (Molina et al., 2006). Furthermore, a significant reduction in hatchability was

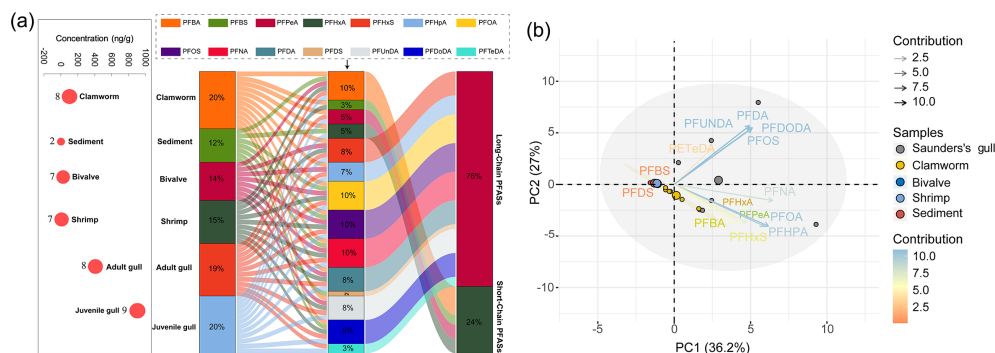


FIGURE 4

The Sankey diagram of PFAS at different trophic levels (A). The left pink circle represents the concentration of PFAS in different sectors in (A). In the Sanger plot, Color lines and numbers represent the flow between different parts. The size of the histogram of different components indicates the percentage of concentration and the value (%) represents the proportion associated with each measure. Principal component analysis (PCA)-based correlation biplots of pollutant concentrations (14 PFAS) in samples (B). The closer the straight line of arrows in the figure is to the outer circle, the larger the impact of the factor. The bluer and darker the color of the straight line, the greater the contribution of the factor. The size of the circle indicates the relative concentration of PFAS in individuals of that species. Saunders's gull ($n=8$), clamworm ($n=5$), bivalve ($n=5$), shrimp ($n=6$) and sediment ($n=9$).

observed in chicken (*Gallus domesticus*) embryos injected with 0.1 μg of PFOS per gram of egg, a concentration representative of environmentally relevant exposures (Molina et al., 2006).

In addition, the alternative PFBA was also detected at high concentrations, in line with the shifting trend in the production and use of PFAS in the coastal cities of eastern China from the traditional long-chain PFAS to the newer short-chain PFAS (Mahoney et al., 2022). The detection of high concentrations of PFOS, PFOA and PFBA in all samples can be attributed to the persistent nature of these compounds and their elevated environmental concentrations. This underscores the significant biomagnification potential of PFAS. The concentration pattern of PFAS in target species can be influenced by various biological factors such as size/age, feeding ecology, migration, and biotransformation. Accumulation of PFAS in seabirds may stem from compound retention; however, this phenomenon may also arise from the ability of PFAS to biotransform and eliminate other less persistent nature (Haukås et al., 2007).

4.2 Differences in PFAS enrichment levels between juvenile and adult gulls

In this study, it was observed that total PFAS muscle concentrations were significantly higher in juvenile gulls compared to adult gulls, particularly for long-chain PFAS such as c11-PFUnDA, c10-PFDA, c12-PFDoDA, and c8-PFOS. The toxic effects of PFOS and/or PFOA in juveniles may surpass those observed in adults, potentially leading to oxidative stress, disruptions in endocrine and metabolic processes, reduced hatching success or weight gain, and even mortality (Costantini et al., 2019). Some prior investigations have examined potential differences in PFAS concentrations between juvenile and adult animals. For instance, Buytaert et al. (2023) found no discernible difference in PFAS plasma concentrations between juvenile and adult great tits. Conversely, in mallards (*Anas platyrhynchos*), PFOS concentrations were observed to increase with age (Newsted et al., 2006). Bustnes et al. (2013) reported a positive correlation between

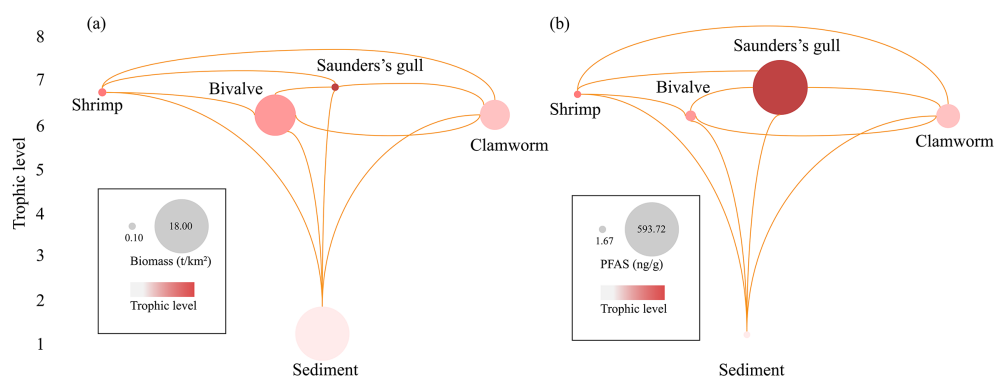


FIGURE 5

Estimated networks of trophic level and energy flow of Saunders's gull biomass (A) and PFAS bioaccumulation (B). Nodes represent functional groups with size proportional to the biomass content (t/km^2) (A) or PFAS concentration (ng/g) (B). Lines depict feeding connections, illustrating the flow of biomass (A) and contaminants (B) from prey to predator. (A, B) have the same fractional thermodynamic level, indicated by the left number.

PFAS levels and age in goshawks (*Accipiter gentilis*) and white-tailed eagle (*Haliaeetus albicilla*) nestlings, with PFOS plasma concentrations showing a marked increase over time. Furthermore, Dauwe et al. found that, given the mobility and wide range of adult great tits, they may cover a greater region around the source of pollution and may be negatively impacted by local PFOS contamination, as suggested by the high levels of PFOS found in them. Great tit nestlings mostly eat food that has been obtained nearby the nesting site, therefore the PFOS concentrations in the nestlings more closely represent local pollution than the concentrations detected in the adults (Dauwe et al., 2007). Nevertheless, the limited sample size in our study constrains our ability to make definitive conclusions regarding these age-related differences. In addition, Ricolfi et al. (2024) found through meta-analysis that wild birds exhibit maternal to offspring transfer of perfluorinated compounds, and found that the concentration of PFAS in offspring was 41% higher than that in the mother. In this study, the total concentration of PFAS in juvenile birds was more than 50% higher than that in adult birds, indicating the possibility of maternal metastasis.

4.3 Transfer of PFAS in the food chain

Previous research has found that organisms higher in the food chain contain significantly higher concentrations of PFAS than those lower in the food chain, indicating the biomagnification effects of PFAS (Evich et al., 2022). Huang et al. (2022) conducted research to examine the presence and transfer dynamics of PFOS and short-chain PFBA within a typical terrestrial food chain, focusing on the plant-pika-eagle ecosystem in the Nam Co Basin of the Tibetan Plateau. Their findings revealed varying concentrations of PFOS and PFBA across different components of the food chain, showcasing a notable biomagnification trend. Grønnestad et al. (2019) conducted a study to analyze the presence, distribution, and biomagnification tendencies of PFOS in the soil, earthworms (*Eisenia fetida*), and voles (*Myodes glareolus*) within a ski resort situated in Wittenham. The results showed that the biomagnification factor of PFOS was greater than 1, but the concentration levels at higher trophic levels (such as top predators) might be much higher (Grønnestad et al., 2019). Ali et al. (2021) conducted a study to explore how PFAS uptake and fate are influenced by both abiotic factors (water, snow, sediment) and biotic factors (zooplankton, benthos, fish, crabs, gulls) in the marine ecosystem of an Arctic fjord near Longyearbyen (Svalbard, Arctic Norway). The concentration of PFAS increased with the trophic level from plankton to polychaetes, crabs, fish liver, and seagull liver (Ali et al., 2021).

Wetlands play a crucial role in ecosystem equilibrium, biodiversity conservation, and the preservation of endangered species. PFAS can have significant impacts on high ecological niche predators through bio-magnification, which may indirectly affect other species through the food chain. Saunders's gull, as the species of focus selected for this study, is an important component of the wetland ecosystem, and the accumulation of PFAS in its body may have a knock-on effect on the entire ecosystem. For example, as

a bio-indicator species, the health and reproductive status of gulls can reflect the overall "health" of the marine environment (Rajpar et al., 2018). Therefore, this pollution may not only affect the gulls themselves but also other species in the ecosystem where they are located.

Our results indicate that the concentrations of PFAS in the pectoral muscles of gulls are much higher than those in their food sources (clamworm, shrimp, and shellfish) and sediment in their habitats. This difference may be related to biological amplification, where the concentration of pollutants in organisms increases with the increase of nutrient levels in the food chain. As a high trophic level organism, the accumulation level of PFAS in gulls is particularly noteworthy. These findings reveal the transmission pathways of PFAS in the food chain and their accumulation characteristics in different ecological environments (Routti et al., 2015). In addition, the physiological characteristics and lifestyle habits of different biological species may also have an impact on the accumulation of PFAS (Ding et al., 2020).

The distribution of PFAS in environmental matrices is also influenced by various factors, including biological species, habitat characteristics, and pollution sources. For example, the distribution of PFAS in wetland ecosystems may be related to local industrial activities and pollution discharge (Zhong et al., 2021). This finding emphasizes the importance of gaining an in-depth understanding of the distribution patterns of PFAS in different environmental matrices, especially in developing effective environmental protection and pollution prevention strategies.

Overall, this study provides an important perspective for understanding the behavior of PFAS in the food chain and different environmental matrices. This is of great significance for evaluating the potential impact of PFAS on biodiversity and developing effective management measures for PFAS pollution. In addition, this work also provides a scientific basis for future environmental monitoring and ecological risk assessment.

4.4 Policy implications and habitat management

Based on this study, we identified several environmental problems in the coastal areas of China, including a high number of chemical enterprise parks along the coast, the lack of effective treatment measures for PFAS, and the low concern for PFAS in organisms (especially endangered species). Therefore, drawing from the findings of this study, we suggest the following recommendations.

First, formulation and improvement of relevant regulations are necessary. It is crucial to strengthen the development and refinement of legal frameworks, particularly those pertaining to environmental protection in specific areas. This includes integrating international conventions such as the Stockholm Convention to establish stricter and more detailed environmental regulations that cater to the unique environmental issues and ecological characteristics of the local region. For instance, specific provisions should be made at the local level for the protection of coastal wetlands, establishment of industrial emission standards, and regulation of pollutants. Moreover, these regulations should be

routinely updated to address evolving environmental challenges and emerging contaminants.

Second, there is a need for timely monitoring of factory hazardous waste discharges. Strengthening the surveillance of discharge points at chemical plants is a vital strategy for controlling environmental pollution. This approach should encompass not only traditional chemical monitoring methods but also biological monitoring techniques such as using benthic organisms and birds as bio-indicators to assess environmental health. Biological monitoring offers direct insights into how pollution impacts ecosystems, aiding in the identification and tracking of pollution sources. Additionally, this enhances transparency in the discharge practices of chemical factories and raises public awareness about environmental pollution.

Third, further exploration and implementation of innovative environmental management technologies are required. By combining membrane technology and bioremediation, we can effectively filter and isolate pollutants, thereby naturally reducing the concentration of contaminants in the environment. These technologies are versatile, as they are applicable not only to water purification but also to soil remediation and air purification (Giorno, 2022), playing a crucial role in diminishing toxic substances in the environment. The development of bioremediation techniques is particularly vital for use in areas of critical biodiversity. These methods can minimize secondary pollution during the treatment process and offer significant means for managing pollution in protected areas and heritage sites.

Finally, the management of wetland protected areas and research on new types of pollutants will need to be strengthened. In particular, the scientific and systematic nature of wetland protected area management should be strengthened. This includes comprehensive research on wetland ecosystems and the development and implementation of scientific management plans to balance urbanization and ecological protection. To further our understanding of the effects of these contaminants, more study should be done on novel pollutant classes including PFAS. At the same time, public awareness of environmental protection and biodiversity conservation should be raised through public education and publicity campaigns to promote the participation of the whole society in environmental protection.

5 Conclusion

In this study, we detected the levels of 14 PFAS in Saunders's gull and food chain samples collected from the Yellow Sea beach wetlands adjacent to the chemical plant. The concentrations of PFAS in gulls were greater than those previously reported for other local shore birds and varied considerably among individuals. The total PFSA level was significantly higher in the muscles of juvenile gulls than in adult gulls, suggesting that PFSA are transferred maternally and re-exposed through food after hatching. Total PFSA concentrations in all biological samples gradually increased when moving up the food chain, confirming PFSA food chain amplification. Long-chain PFOA, PFOS, and short-chain PFBA

emerged as the primary substances found across multiple organisms, confirming the environmental persistence of long-chain PFAS and signaling a gradual transition in China's PFAS production towards short-chain alternatives. It is important to acknowledge that we collected a limited sample size of Saunders's gull and did not establish a toxicity reference value or lowest visible adverse effect level for the gull muscle, which could potentially constrain the interpretation of individual toxicity or biological/ecological impacts. Consequently, additional studies should be conducted to map these thresholds.

Data availability statement

The raw data supporting the conclusions of this article will be made available by the authors, without undue reservation.

Ethics statement

The animal study was approved by Jiangsu Wildlife Protection Station. The study was conducted in accordance with the local legislation and institutional requirements.

Author contributions

DZ: Data curation, Formal analysis, Writing – original draft. WL: Conceptualization, Data curation, Investigation, Writing – original draft. YX: Data curation, Investigation, Writing – original draft. XL: Supervision, Writing – review & editing. ZZ: Data curation, Formal analysis, Writing – original draft. YL: Supervision, Writing – review & editing.

Funding

The author(s) declare financial support was received for the research, authorship, and/or publication of this article. This work was supported by the Open Research Fund from Biodiversity Investigation, Observation, and Assessment Program of the Ministry of Ecology and Environment of China, State Environmental Protection Key Laboratory of Biodiversity and Biosafety, the National Natural Science Foundation of China (grant number 41961144022), and the Open Research Fund from Key laboratory of Marine Ecosystem Dynamic of the Ministry of Natural Resources of China (grant number CEEES2023010).

Conflict of interest

The authors declare that the research was conducted in the absence of any commercial or financial relationships that could be construed as a potential conflict of interest.

The author(s) declared that they were an editorial board member of Frontiers, at the time of submission. This had no impact on the peer review process and the final decision.

Publisher's note

All claims expressed in this article are solely those of the authors and do not necessarily represent those of their affiliated organizations, or those of the publisher, the editors and the

reviewers. Any product that may be evaluated in this article, or claim that may be made by its manufacturer, is not guaranteed or endorsed by the publisher.

Supplementary material

The Supplementary Material for this article can be found online at: <https://www.frontiersin.org/articles/10.3389/fmars.2024.1467022/full#supplementary-material>

References

- Ali, A. M., Langberg, H. A., Hale, S. E., Kallenborn, R., Hartz, W. F., Mortensen, Å.K., et al. (2021). The fate of poly- and perfluoroalkyl substances in a marine food web influenced by land-based sources in the Norwegian Arctic. *Environ. Sci. Process Impacts*. 23, 588–604. doi: 10.1039/d0em00510j
- Bach, C. C., Bech, B. H., Brix, N., Nohr, E. A., Bonde, J. P. E., and Henriksen, T. B. (2015). Perfluoroalkyl and polyfluoroalkyl substances and human fetal growth: a systematic review. *Crit. Rev. Toxicol.* 45, 53–67. doi: 10.3109/10408444.2014.952400
- Bustnes, J. O., Bårdsen, B. J., Herzke, D., Johnsen, T. V., Eulaers, I., Ballesteros, M., et al. (2013). Plasma concentrations of organohalogenated pollutants in predatory bird nestlings: associations to growth rate and dietary tracers. *Environ. Toxicol. Chem.* 32, 2520–2527. doi: 10.1002/etc.2329
- Buytaert, J., Eens, M., Elgawad, H. A., Bervoets, L., Beemster, G., and Groffen, T. (2023). Associations between PFAS concentrations and the oxidative status in a free-living songbird (*Parus major*) near a fluorochemical facility. *Environ. pollut.* 335, 122304. doi: 10.1016/j.envpol.2023.122304
- Chen, C., and Reniers, G. (2020). Chemical industry in China: The current status, safety problems, and pathways for future sustainable development. *Saf. Sci.* 128, 104741. doi: 10.1016/j.ssci.2020.104741
- Chen, H., Han, J., Cheng, J., Sun, R., Wang, X., Han, G., et al. (2018). Distribution, bioaccumulation and trophic transfer of chlorinated polyfluoroalkyl ether sulfonic acids in the marine food web of Bohai, China. *Environ. pollut.* 241, 504–510. doi: 10.1016/j.envpol.2018.05.087
- Christensen, V., and Walters, C. J. (2004). Ecopath with Ecosim: methods, capabilities and limitations. *Ecol. Model.* 172, 109–139. doi: 10.1016/j.ecolmodel.2003.09.003
- Chu, S., Wang, J., Leong, G., Woodward, L. A., Letcher, R. J., and Li, Q. X. (2015). Perfluoroalkyl sulfonates and carboxylic acids in liver, muscle and adipose tissues of black-footed albatross (*Phoebastria nigripes*) from Midway Island, North Pacific Ocean. *Chemosphere* 138, 60–66. doi: 10.1016/j.chemosphere.2015.05.043
- Colomer-Vidal, P., Bertolero, A., Alcaraz, C., Garreta-Lara, E., Santos, F. J., and Lacorte, S. (2022). Distribution and ten-year temporal trends, (2009–2018) of perfluoroalkyl substances in gull eggs from Spanish breeding colonies. *Environ. pollut.* 293, 118555. doi: 10.1016/j.envpol.2021.118555
- Costantini, D., Blévin, P., Herzke, D., Moe, B., Gabrielsen, G. W., Bustnes, J. O., et al. (2019). Higher plasma oxidative damage and lower plasma antioxidant defences in an Arctic seabird exposed to longer perfluoroalkyl acids. *Environ. Res.* 168, 278–285. doi: 10.1016/j.envres.2018.10.003
- Cui, Q., Shi, F., Pan, Y., Zhang, H., and Dai, J. (2019). Per- and polyfluoroalkyl substances (PFASs) in the blood of two colobine monkey species from China: Occurrence and exposure pathways. *Sci. Total Environ.* 674, 524–531. doi: 10.1016/j.scitotenv.2019.04.118
- Dauwe, T., Van de Vijver, K., De Coen, W., and Eens, M. (2007). PFOS levels in the blood and liver of a small insectivorous songbird near a fluorochemical plant. *Environ. Int.* 33, 357–361. doi: 10.1016/j.envint.2006.11.014
- Dickman, R. A., and Aga, D. S. (2022). A review of recent studies on toxicity, sequestration, and degradation of per- and polyfluoroalkyl substances (PFAS). *J. Hazard Mater.* 436, 129120. doi: 10.1016/j.jhazmat.2022.129120
- Ding, N., Harlow, S. D., Randolph, J. F. Jr., Loch-Carusio, R., and Park, S. K. (2020). Perfluoroalkyl and polyfluoroalkyl substances (PFAS) and their effects on the ovary. *Hum. Reprod. Update* 26, 724–752. doi: 10.1093/humupd/dmaa018
- Evich, M. G., Davis, M. J. B., McCord, J. P., Acrey, B., Awkerman, J. A., Knappe, D. R. U., et al. (2022). Per- and polyfluoroalkyl substances in the environment. *Science* 375, eabg9065. doi: 10.1126/science.abg9065
- Falandysz, J., Taniyasu, S., Yamashita, N., Rostkowski, P., Zalewski, K., and Kannan, K. (2007). Perfluorinated compounds in some terrestrial and aquatic wildlife species from Poland. *J. Environ. Sci. Health A Tox Hazard Subst Environ. Eng.* 42, 715–719. doi: 10.1080/10934520701304369
- Giorno, L. (2022). Membranes that filter and destroy pollutants. *Nat. Nanotechnol.* 17, 334–335. doi: 10.1038/s41565-021-01064-2
- Gronnestad, R., Vázquez, B. P., Arukwe, A., Jaspers, V. L. B., Jenssen, B. M., Karimi, M., et al. (2019). Levels, patterns, and biomagnification potential of perfluoroalkyl substances in a terrestrial food chain in a nordic skiing area. *Environ. Sci. Technol.* 53, 13390–13397. doi: 10.1021/acs.est.9b02533
- Haukås, M., Berger, U., Hop, H., Gulliksen, B., and Gabrielsen, G. W. (2007). Bioaccumulation of per- and polyfluorinated alkyl substances (PFAS) in selected species from the Barents Sea food web. *Environ. pollut.* 148, 360–371. doi: 10.1016/j.envpol.2006.09.021
- Huang, K., Li, Y., Bu, D., Fu, J., Wang, M., Zhou, W., et al. (2022). Trophic magnification of short-chain per- and polyfluoroalkyl substances in a terrestrial food chain from the Tibetan Plateau. *Environ. Sci. Technol. Lett.* 9, 147–152. doi: 10.1021/acs.estlett.1c01009
- Jaureguiberry, P., Titeux, N., Wiemers, M., Bowler, D. E., Coscieme, L., Golden, A. S., et al. (2022). The direct drivers of recent global anthropogenic biodiversity loss. *Sci. Adv.* 8, eabm9982. doi: 10.1126/sciadv.abm9982
- Jiang, H. X., Hou, Y. Q., Chu, G. Z., Qian, F. W., Wang, H., Zhang, G. G., et al. (2010). Breeding population dynamics and habitat transition of Saunders's Gull *Larus saundersi* in Yancheng National Nature Reserve, China. *Bird Conserv. Int.* 20, 13–24. doi: 10.1017/S0959270910000017
- Kannan, K., Corsolini, S., Falandysz, J., Oehme, G., Focardi, S., and Giesy, J. P. (2002). Perfluorooctanesulfonate and related fluorinated hydrocarbons in marine mammals, fishes, and birds from coasts of the Baltic and the Mediterranean Seas. *Environ. Sci. Technol.* 36, 3210–3216. doi: 10.1021/es020519q
- Ma, Y., Choi, C.-Y., Thomas, A., and Gibson, L. (2022). Review of contaminant levels and effects in shorebirds: knowledge gaps and conservation priorities. *Ecotoxicol. Environ. Saf.* 242, 113868. doi: 10.1016/j.ecoenv.2022.113868
- Ma, Z., Choi, C. Y., Gan, X., Li, J., Liu, Y., Melville, D. S., et al. (2023). Achievements, challenges, and recommendations for waterbird conservation in China's coastal wetlands. *Avian Res.* 14, 100123. doi: 10.1016/j.avrs.2023.100123
- Mahoney, H., Xie, Y., Brinkmann, M., and Giesy, J. P. (2022). Next generation per- and polyfluoroalkyl substances: status and trends, aquatic toxicity, and risk assessment. *EcoEnviron. Health* 1, 117–131. doi: 10.1016/j.eehl.2022.05.002
- Molina, E. D., Balandier, R., Fitzgerald, S. D., Giesy, J. P., Kannan, K., Mitchell, R., et al. (2006). Effects of air cell injection of perfluorooctane sulfonate before incubation on development of the white leghorn chicken (*Gallus domesticus*) embryo. *Environ. Toxicol. Chem.* 25, 227–232. doi: 10.1897/04-414r.1
- Murray, N. J., Marra, P. P., Fuller, R. A., Clemens, R. S., Dhanjal-Adams, K., Gosbell, K. B., et al. (2018). The large-scale drivers of population declines in a long-distance migratory shorebird. *Ecography* 41, 867–876. doi: 10.1111/ecog.02957
- Newsted, J. L., Beach, S. A., Gallagher, S. P., and Giesy, J. P. (2006). Pharmacokinetics and acute lethality of perfluorooctanesulfonate (PFOS) to juvenile mallard and northern bobwhite. *Arch. Environ. Contam. Toxicol.* 50, 411–420. doi: 10.1007/s00244-005-1137-x
- Olivero-Verbel, J., Tao, L., Johnson-Restrepo, B., Guette-Fernández, J., Baldiris-Avila, R., O'Byrne-Hoyos, I., et al. (2006). Perfluorooctanesulfonate and related fluorochemicals in biological samples from the north coast of Colombia. *Environ. pollut.* 142, 367–372. doi: 10.1016/j.envpol.2005.09.022
- Rajpar, M. N., Ozdemir, I., Zakaria, M., Sheryar, S., and Rab, A. (2018). Seabirds as bioindicators of marine ecosystems. *Seabirds*. London: Intech. ch. 4. doi: 10.5772/intechopen.75458
- Ricolfi, L., Taylor, M. D., Yang, Y., Lagisz, M., and Nakagawa, S. (2024). Maternal transfer of per- and polyfluoroalkyl substances (PFAS) in wild birds: A systematic review and meta-analysis. *Chemosphere* 361, 142346. doi: 10.1016/j.chemosphere.142346

- Robuck, A. R., McCord, J. P., Strynar, M. J., Cantwell, M. G., Wiley, D. N., and Lohmann, R. (2021). Tissue-specific distribution of legacy and novel per- and polyfluoroalkyl substances in juvenile seabirds. *Environ. Sci. Technol. Lett.* 8, 457–462. doi: 10.1021/acs.estlett.1c00222
- Routti, H., Krafft, B. A., Herzke, D., Eisert, R., and Oftedal, O. (2015). Perfluoroalkyl substances detected in the world's southernmost marine mammal, the Weddell seal (*Leptonychotes weddellii*). *Environ. pollut.* 197, 62–67. doi: 10.1016/j.envpol.2014.11.026
- Sonne, C., Desforges, J. P., Gustavson, K., Bossi, R., Bonefeld-Jørgensen, E. C., Long, M., et al. (2023). Assessment of exposure to perfluorinated industrial substances and risk of immune suppression in Greenland and its global context: a mixed-methods study. *Lancet Planet Health* 7, 570–579. doi: 10.1016/S2542-5196(23)00106-7
- Stein, C. R., McGovern, K. J., Pajak, A. M., Maglione, P. J., and Wolff, M. S. (2016). Perfluoroalkyl and polyfluoroalkyl substances and indicators of immune function in children aged 12–19 y. *Pediatr. Res.* 79, 348–357. doi: 10.1038/pr.2015.213
- Sun, J., Fang, R., Wang, H., Xu, D. X., Yang, J., Huang, X., et al. (2022). A review of environmental metabolism disrupting chemicals and effect biomarkers associating disease risks: Where exposomics meets metabolomics. *Environ. Int.* 158, 106941. doi: 10.1016/j.envint.2021.106941
- Sun, J., Xing, L., and Chu, J. (2023). Global ocean contamination of per- and polyfluoroalkyl substances: A review of seabird exposure. *Chemosphere* 330, 138721. doi: 10.1016/j.chemosphere.2023.138721
- Sylvester, F., Weichert, F. G., Lozano, V. L., Groh, K. J., Bálint, M., Baumann, L., et al. (2023). Better integration of chemical pollution research will further our understanding of biodiversity loss. *Nat. Ecol. Evol.* 7, 1552–1555. doi: 10.1038/s41559-023-02117-6
- Verreault, J., Berger, U., and Gabrielsen, G. W. (2007). Trends of perfluorinated alkyl substances in herring gull eggs from two coastal colonies in northern Norway: 1983–2003. *Environ. Sci. Technol.* 41, 6671–6677. doi: 10.1021/es070723j
- Walters, W. J., and Christensen, V. (2018). Ecotracer: analyzing concentration of contaminants and radioisotopes in an aquatic spatial-dynamic food web model. *J. Environ. Radioactivity* 181, 118–127. doi: 10.1016/j.jenvrad.2017.11.008
- Wang, X., Jiang, H. X., Zhang, Y. N., Chen, L. X., Song, C. Z., and Li, Y. X. (2017). Diet composition of Saunders's Gull (*Larus saundersi*) determined using stable isotope analysis at the Shuangtaihekou National Nature Reserve, China. *Acta Ecol. Sin.* 37, 1796–1804. doi: 10.1021/acs.est.9b06379
- Wang, W., Wang, J. J., Zuo, P., Li, Y., and Zou, X. Q. (2019). Analysis of structure and energy flow in southwestern Yellow Sea ecosystem based on Ecopath model. *J. Appl. Oceanogr.* 38, 528–539. doi: 10.1007/s11356-021-16032-5
- Wang, X. L., Zhang, Q. C., Zhao, Z. Y., Song, W. G., Cheng, L., Yang, J. H., et al. (2021). A multi-plug filtration (m-PFC) cleanup method based on carboxylic multi-walled carbon nanotubes for the detection of 14 perfluorinated compounds and dietary risk assessment of chicken, beef, and mutton collected from Shanghai markets. *Food Control* 130, 108330. doi: 10.1016/j.foodcont.2021.108330
- Wee, S. Y., and Aris, A. Z. (2023). Environmental impacts, exposure pathways, and health effects of PFOA and PFOS. *Ecotoxicol. Environ. Saf.* 267, 115663. doi: 10.1016/j.jecoen.2023.115663
- Yang, Z., Lagassé, B. J., Xiao, H., Jackson, M. V., Chiang, C. Y., Melville, D. S., et al. (2020). The southern Jiangsu coast is a critical moulting site for Spoon-billed Sandpiper *Calidris pygmaea* and Nordmann's Greenshank *Tringa guttifer*. *Bird Conserv. Int.* 30, 649–660. doi: 10.1017/S0959270920000210
- Zhong, H., Zheng, M., Liang, Y., Wang, Y., Gao, W., Wang, Y., et al. (2021). Legacy and emerging per- and polyfluoroalkyl substances (PFAS) in sediments from the East China Sea and the Yellow Sea: Occurrence, source apportionment and environmental risk assessment. *Chemosphere* 282, 131042. doi: 10.1016/j.chemosphere.2021.131042



OPEN ACCESS

EDITED BY

Kun Chen,
Jiangsu University, China

REVIEWED BY

Karine Beaugelin-Seiller,
Institut de Radioprotection et de Sûreté
Nucléaire, France
Liwei Chen,
Hefei Normal University, China

*CORRESPONDENCE

Jialin Ni

✉ nijialin@tio.org.cn

RECEIVED 27 January 2024

ACCEPTED 04 October 2024

PUBLISHED 22 October 2024

CITATION

Ni J, Chen D, Qian Z, Lin J, Lin F, Ji J,
Huang D and Yu T (2024) A study on the
transfer of radionuclides and of the resulting
radiation dose assessment for marine
organisms on the eastern coast of Yantai city.
Front. Mar. Sci. 11:1377411.
doi: 10.3389/fmars.2024.1377411

COPYRIGHT

© 2024 Ni, Chen, Qian, Lin, Lin, Ji, Huang and
Yu. This is an open-access article distributed
under the terms of the [Creative Commons
Attribution License \(CC BY\)](#). The use,
distribution or reproduction in other forums
is permitted, provided the original author(s)
and the copyright owner(s) are credited and
that the original publication in this journal is
cited, in accordance with accepted academic
practice. No use, distribution or reproduction
is permitted which does not comply with
these terms.

A study on the transfer of radionuclides and of the resulting radiation dose assessment for marine organisms on the eastern coast of Yantai city

Jialin Ni^{1*}, Dongjun Chen², Zhen Qian², Jing Lin¹, Feng Lin¹,
Jianda Ji¹, Dekun Huang¹ and Tao Yu¹

¹Third Institute of Oceanography, Ministry of Natural Resources, Xiamen, China, ²Radiation Environment Supervision Station of Fujian Province, Fuzhou, China

Oceans are repositories of radionuclides. Radionuclides are transferred through the food chain and cause ionizing radiation hazards for marine organisms. In this study, the transfer characteristics of ²²⁶Ra, ⁴⁰K, ¹⁴C, ³H, ¹³⁷Cs and ⁹⁰Sr in organisms at different trophic levels in the eastern coast of Yantai city were investigated. The risk of ionizing radiation to organisms was assessed using the ERICA Tool 2.0. The results show no significant changes in the concentration of any of the nuclides in the coastal area compared to the preoperation period of the nuclear power plant. The transfer factor of ¹³⁷Cs, ⁴⁰K, ²²⁶Ra, ¹⁴C, ⁹⁰Sr and ³H at the different trophic levels of marine organisms were 2.09, 1.29, 1.17, 1.15, 1.06 and 0.74, respectively. The dose rates of ionizing radiation to organisms from six radionuclides ranged from 32.02 nGy·h⁻¹ to 195.49 nGy·h⁻¹ and had a mean value of 102.86 ± 57.30 nGy·h⁻¹. The main artificial radionuclides (¹⁴C, ³H, ⁹⁰Sr, ¹³⁷Cs) released by nuclear power plants in the study area produced negligible radiation doses to marine organisms. However, other artificial radionuclides present in the effluents of nuclear power plants (⁹⁹Tc, ^{110m}Ag and ¹³¹I) as well as other natural radionuclides (includes ²¹⁰Po, ²¹⁰Pb, etc) were not included, and further evaluation of these is recommended.

KEYWORDS

radionuclides, amplification effects, biotrophic level, ionizing radiation, ERICA tool

1 Introduction

The assessment of the exposure of biota to radiation is part of the environment protection system (Maystrenko and Rybak, 2022). Preventing or reducing the frequency of deleterious radiation effects to a level where they would have a negligible impact on the maintenance of biological diversity, the conservation of species, or the health and status of natural habitats, communities and ecosystems is one of the objectives of the International Commission on Radiological Protection (ICRP) (ICRP, 2008). Oceans are repositories of both naturally occurring and anthropogenic radionuclides (Qiao et al., 2023). Radionuclides present in the marine environment can be transferred in organisms through food chains. The organisms are themselves exposed internally to radiation from radionuclides that have been taken up from the environment and externally to radiation in their habitat (UNSCEAR, 2011). The direct hazards from ionizing radiation have been found to manifest at different levels of organization, from the subcellular level and individual organisms to populations and ecosystems (Sazykina and Kryshev, 2003; Garnier-Laplace et al., 2004). Radiation damage to genetic material can result in far-ranging disasters through genetic variation (ICRP, 1991; UNSCEAR, 2012). A comprehensive understanding of the behavior of radionuclides in the ocean and their radiological impact on the environment is of utmost importance (Lee et al., 2023). Therefore, it is essential to study the transfer of radionuclides in marine organisms and to conduct risk assessments to aid in the protection of marine wildlife and human health.

The large variety of species and radionuclides in the ocean, as well as the different behavior of organisms toward these radionuclides, contribute to multiple combinations of radionuclide transfer in marine organisms. This exacerbates many difficulties in accurately assessing the radiation risk to living species from radionuclides in marine environments (Beaugelin-Seiller et al., 2019). The identification of key radionuclides based on their potential contribution to the radiation dose to marine organisms is one of the key steps in assessing biological radiation risk. ^{226}Ra and ^{40}K are the naturally occurring radionuclides that show the highest specific activity in living organisms (Arogunjo et al., 2009; Lima et al., 2005). ^{14}C and ^3H are the two artificial radionuclides that contribute the most to the total radiation dose that affects wildlife during normal operation of a nuclear power plant (Beaugelin-Seiller et al., 2019; IAEA, 2021; Tani and Ishikawa, 2023). ^{137}Cs and ^{90}Sr are important artificial radionuclides released from nuclear power plants, and they easily accumulate in organisms (Kononov et al., 2016; Pinder et al., 2016). Therefore, ^{226}Ra , ^{40}K , ^{14}C , ^3H , ^{137}Cs , and ^{90}Sr were used as radionuclides of interest in this research.

The general approach to assessing radiation doses to organisms consists on constructing assessment models, including equilibrium and dynamic models. The former applies to chronic exposures under normal conditions, while the latter is more suitable for acute exposures under accidental conditions (Vives I Batlle et al., 2016). The Environmental Risk from Ionizing Contaminants: Assessment and Management (ERICA) Tool, developed by the EU, is an assessment model based on equilibrium conditions (Brown et al.,

2016). In reality, there is no instantaneous equilibrium of radionuclides between organisms and environmental media. Therefore, the dynamic assessment model under accident conditions is close to the real situation. Current models related to dynamic assessment include the BURN-POSEIDON method (Lepicard et al., 2004), the ANL method (Vives I Batlle et al., 2016), the D-DAT method (Vives I Batlle et al., 2008), the ECOMOD method (Sazykina, 2000), the IRSN method (Fiévet et al., 2006), the NRPA method (Brown et al., 2004), and the multicompartment kinetic-allometric (MCKA) model (Bezhenar et al., 2021). The results calculated by the models tend to differ due to the different models and the model parameters, as well as influences from the uncertainties of the parameters being used (Vives I Batlle et al., 2016).

Food chains (webs) are the support of material cycles and energy flows in biological communities and ecosystems and are important mediators of the impacts of marine pollutants on ecosystems (Liu, 2013). Most radionuclides enter the biocenosis from lower levels of the food chain, including those of autotrophic organisms and bacteria, and then move with food to higher levels of the food chain (Fisher et al., 2000; Wang et al., 1996). The trophic level (TL) reflects an organism's position in an ecosystem's food chain/food web and can be used to indicate the energy consumption level of a species, as well as the ability of a particular population to assimilate energy (Bo, 2005). In recent years, it has been recognized that the changes of biological trophic level are influenced by a combination of biotic and abiotic factors (Zhang and Tang, 2004). The study of trophic levels has become an important indicator of the marine environment for assessing and monitoring ecosystem dynamics, biodiversity change and fisheries sustainability (Aydin et al., 2003; Pauly et al., 2001). The accumulation of radionuclides in marine organisms, which is similar to that of metal pollutants, is a complex and dynamic process that is determined by a combination of biological and environmental factors in the habitat and by the nature of the nuclide (Fakhri et al., 2022; Ishii et al., 2020; Suk et al., 2019). Kasamatsu and Ishikawa (1997) analyzed stomach contents of fish samples together with ^{137}Cs concentrations in the stomach contents and demonstrated that the ^{137}Cs concentration in preys of predators increased with their trophic levels (Kasamatsu and Ishikawa, 1997). Currently, carbon and nitrogen isotope components have been widely used to analyze the trophic levels and food sources of marine organisms to identify and determine the processes by which heavy metals or organic pollutants accumulate and flow in biological populations or food chains (Chouvelon et al., 2019; Gao et al., 2021; Liu et al., 2019). However, carbon and nitrogen isotope analysis techniques have not been reported in marine radioactivity studies.

To study the transfer properties of these six radionuclides (^3H , ^{226}Ra , ^{40}K , ^{14}C , ^{137}Cs , and ^{90}Sr) at the different trophic levels, and to assess the contribution of the major artificial radionuclides released from the Haiyang nuclear power plant on the radiation dose to marine species, the following studies were carried out in the surrounding 30km sea area of the Haiyang Nuclear Power Plant. First, the impact of Haiyang nuclear power plant operations on the marine environment was investigated in November 2022 by measuring radionuclide activity concentrations in the

environment and in organisms. Second, through the analysis of carbon and nitrogen isotope contents in organisms, the transfer features of radionuclides in organisms at different trophic levels were investigated. Third, multivariate statistical analyses were performed to determine the correlation between different radionuclide activities in the organism and the trophic level of the organism. Finally, the radiation dose to organisms at different trophic levels in the marine environment was assessed with the ERICA Tool.

2 Materials and methods

2.1 Sampling and analysis

2.1.1 Sample collection

The Haiyang Nuclear Power Plant is located in Yantai city on the Yellow Sea coast of China's Jiaodong Peninsula. It is surrounded by the sea on three sides. The commercial operation of the 2 AP1000 nuclear units in the plant started in October 2018 and January 2019 and have been in operation for more than 4 years. In November 2022, 18 sampling stations were deployed evenly along the direction of the tidal field within the 30 km sea area of the Nuclear Power Plant (Figure 1). A pump was used to collect 60 liters of surface seawater into plastic drums at each sampling station. The seawater was acidified to a pH less than 2 with 8 mol/L nitric acid

and sealed. A 3-kg sample of marine surface sediment was collected with a Peterson grab dredge (sampling volume 5 L, opening area 15 cm × 30 cm) at each sampling station and stored frozen in polyethylene bags. Nine species of marine organisms were collected from small fishing boats at port terminals near the nuclear power plant (Table 1). These fishing boats were limited by power constraints and they could only catch organisms within 30 km of the nuclear power plant which is consistent with the range of our survey stations. For each biological sample, 5 to 10 kg of fresh sample was collected and frozen for preservation. Finally, the samples were sent to the laboratory for further processing.

2.1.2 Sample processing and analysis

2.1.2.1 Sample processing

Seawater samples were decanted in the laboratory for 2-3 days, and the clear liquid was drawn off with a siphon. Afterward, the ^{137}Cs , ^{226}Ra , ^{40}K , ^{90}Sr , ^3H , and ^{14}C content in seawater were determined according to relevant national or industrial standards. Briefly, the ^{137}Cs in the seawater was first adsorbed with ammonium phosphomolybdate (AMP) and then precipitated. Second, clear seawater was aspirated by siphoning, and the AMP after adsorption of ^{137}Cs was filtered and collected (Third Institute Of Oceanography, 2018). ^{226}Ra was processed by coprecipitation with barium sulfate. Afterward, the barium sulfate precipitates were combined with the AMP precipitates and ashed in a muffle furnace at 450°C. The ash samples were compacted and sealed in

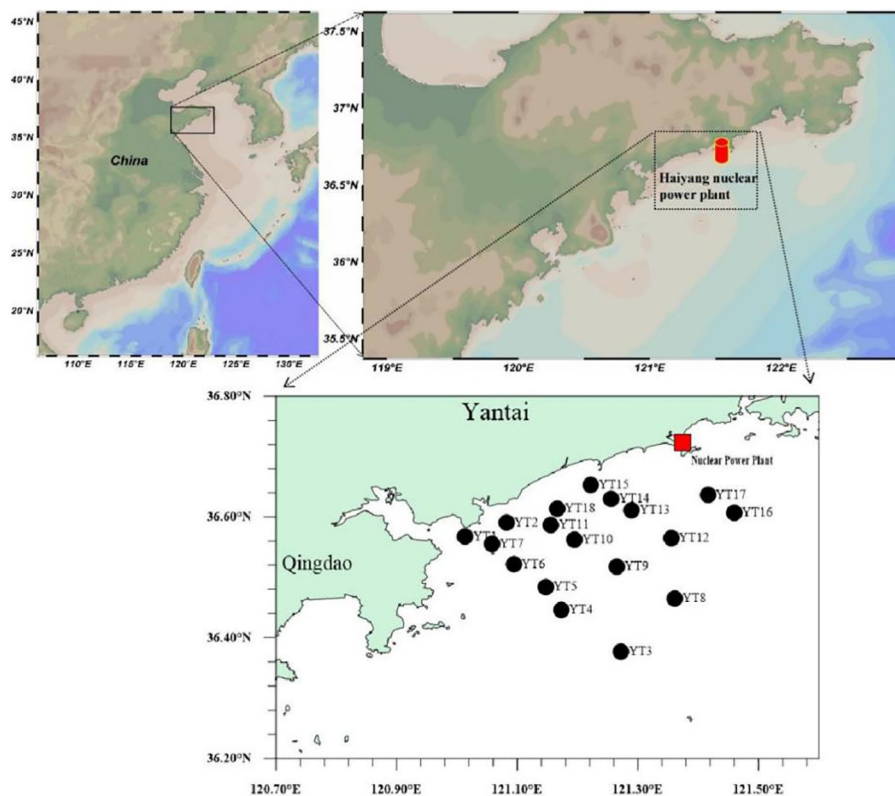


FIGURE 1
Location of the study area and distribution of sampling stations.

TABLE 1 Information on samples of marine organisms.

Organisms	Length(cm)	Width(cm)	Height(cm)	Weight(g)	Habitat
<i>Anomiostrea coraliophila</i> – bivalve mollusks	3.52 ± 0.23	1.85 ± 0.20	2.3 ± 0.14	32.3 ± 0.32	In the Sediment
<i>Loligo beka</i> – Beka squid – cephalopod mollusk	6.89 ± 0.27	1.57 ± 0.07	1.51 ± 0.05	7.89 ± 0.21	In the Water
<i>Octopus variabilis</i> – cephalopod mollusk	14.52 ± 0.23	3.34 ± 0.21	3.27 ± 0.18	27.84 ± 0.48	
<i>Pleuronichthys cornutus</i> - Osteichthyes - Chordata	13.32 ± 0.19	6.55 ± 0.23	2.11 ± 0.08	78.56 ± 0.78	On the Sediment-surface
<i>Cynoglossus semilaevis</i> - Osteichthyes - Chordata	10.05 ± 0.18	3.01 ± 0.05	0.32 ± 0.05	14.89 ± 0.36	
<i>Lepidotrigla micropterus</i> - Osteichthyes - Chordata	15.67 ± 0.36	3.02 ± 0.25	3.17 ± 0.12	34.28 ± 0.63	
<i>Saurida elongata</i> - Osteichthyes - Chordata	21.82 ± 0.29	3.67 ± 0.11	3.89 ± 0.13	64.69 ± 0.64	
<i>Trachypenaeus curvirostris</i> - Crustacea–Arthropoda	7.02 ± 0.17	1.02 ± 0.03	1.01 ± 0.02	5.02 ± 0.18	
<i>Squilla oratoria</i> - Crustacea–Arthropoda	14.03 ± 0.21	2.51 ± 0.14	1.89 ± 0.12	32.21 ± 0.37	

For each organism, 10 samples were taken randomly. The length, width, height and weight of the sample torsos were measured using Vernier calipers and a balance. The mean and standard deviation were then calculated separately.

a $\Phi 75$ mm \times 75-mm cylindrical plastic sample box for 30 days before measurement (Third Institute Of Oceanography, 2018). ^3H content in the seawater was measured by an ultralow-background liquid scintillation counter (Environment, 2020). First, 1 L of seawater was removed and distilled to reduce the conductivity, after which the solution was electrolytically concentrated. Second, 8 mL of sample was mixed with 12 mL of a liquid scintillation cocktail in a plastic vial. Third, the resulting solution was stored in an LSC sample holder for 12 hours in the dark before counting (Feng et al., 2020). ^{90}Sr content in the seawater was measured by the di(2-ethylhexyl) phosphoric acid (HDEHP) extraction- β counting method (Third Institute Of Oceanography, 2018). First, a total of 2.00 mL of 100 mg/mL $\text{Sr}(\text{NO}_3)_2$, 1.00 mL of 20 mg/mL $\text{Y}(\text{NO}_3)_3$, 60 g of NH_4Cl and 400 g of Na_2CO_3 were added to 40 L of seawater and then stirred for 30 minutes. Second, the precipitate was filtered, and then 10 mol/L HNO_3 was used to dissolve the precipitate. The solution was extracted twice using 50 mL of 10% di(2-ethylhexyl) phosphoric acid (HDEHP), and the organic phase was re-extracted twice using 20 mL of 10 mol/L HNO_3 . Third, a total of 5 mL of $\text{C}_2\text{H}_2\text{O}_4$ was added to form a saturated solution, and the solution was adjusted to pH=1.5–2.0 using a 6 mol/L $\text{NH}_3\text{H}_2\text{O}$ solution and 2 mol/L HNO_3 . Finally, the YC_2O_4 sediment was produced. The YC_2O_4 was filtered and placed into an α/β counter to determine the activity of ^{90}Y . The activity of ^{90}Sr was then calculated from the ^{90}Y data. ^{14}C in seawater was measured by a wet oxidation-ultralow background liquid scintillation counter (China, 2019). First, 20 L of seawater was removed and placed in a four-necked flask. FeSO_4 , H_2O_2 and $\text{K}_2\text{S}_2\text{O}_8$ were added, and the flask was subsequently heated. Second, N_2 gas was passed through one side of the flask, and the other side was dried with H_2SO_4 . The dried gas was then absorbed with NaOH solution. Third, 8 mL of CO_2 absorption solution was mixed with 12 mL of a liquid scintillation cocktail in a plastic vial. Finally, the resulting solution was stored in an LSC sample holder for 12 hours in the dark before counting. A total of 1.5 L of filtered seawater was pipetted into the measuring cassette, and the cassette

was subsequently placed on the gamma energy spectrometer to measure ^{40}K (Commission, 2018).

Sediment samples were removed from gravel, larger plant and animal debris, then sequentially dried, ground, and finally sieved through an 80 mesh nylon sieve with a cover. Then, a 300-g prepared sediment sample was compacted and sealed in a $\Phi 75$ mm \times 75 mm cylindrical plastic sample box for 30 days before measurement. The activity of ^{226}Ra was determined based on the gamma ray of ^{214}Pb (351.92keV) and ^{214}Bi (609.31keV). ^{40}K and ^{137}Cs radionuclides activity were determined directly from their respective emission at 1460.81keV and 661.65keV. The activity concentrations were determined by taking into account the net area of the photopeak, the gamma-ray emission probability, the absolute peak efficiency, and the mass of the sample (Patra et al., 2014; Yang et al., 2015). ^{90}Sr in the sediment was also measured by the HDEHP extraction- β counting method, and the sample was counted using the gas-flow proportional alpha/beta counting system (Third Institute Of Oceanography, 2018).

The marine organism samples were dried to constant weight at 60°C in a drum dryer. The pulverized dried biological samples were ashed in a muffle furnace at 450°C for 24–40 hours. The ashed biosamples were then stored in sealed boxes (100 g per sample) for 30 days before analysis (China, 2020). The HDEHP extraction- β counting method and an α/β counter were used for ^{90}Sr analysis (Third Institute Of Oceanography, 2018). A total of 100 g of dried biological sample was weighed, ground into powder form and subsequently placed in a combustion device for slow combustion. The water vapor and CO_2 generated after combustion were collected. The subsequent steps were the same as those for monitoring ^3H and ^{14}C in water samples (Environment, 2020; Lin et al., 2020).

2.1.2.2 Radionuclide measurement

The ^{137}Cs , ^{40}K , and ^{226}Ra activities were measured using a high-purity germanium γ spectrometer (Canberra GR4021, 40% relative efficiency). The following characteristic γ -ray peaks were selected to

calculate the ^{226}Ra (295.21, 351.92, 609.31 keV), ^{40}K (1,460.8 keV), and ^{137}Cs (661.7 keV) activities. To ensure that the data results met the quality control requirements, the instrumentation used in this study was used within the validity period of the calibration. Moreover, the standard materials were analyzed simultaneously with the sample for quality control. The point sources of ^{60}Co (Laboratoire Etalons d'Activite, No-50321), ^{137}Cs (Laboratoire Etalons d'Activite, No-50585), and ^{242}Am (Laboratoire Etalons d'Activite, No-50236) were used for the instrumental scales before the measurements. ^3H and ^{14}C were measured by an ultralow-background liquid scintillation counter (LSC, Quantulus 1220, PerkinElmer). The efficiency of the LSC was measured by preparing standard sources in the same form as the samples to be measured using ^3H standard solution (Physikalisch-Technische Bundesanstalt, 2005-1439) and ^{14}C standard solution (Physikalisch-Technische Bundesanstalt, 2013-1055). ^{90}Sr was counted using the gas-flow proportional alpha/beta counting system (Ortec MPC-9604). The counting efficiency was measured by using the ^{90}Sr - ^{90}Y standard reagent (National Institute of Metrology China, Beijing, China). In addition, the testing programs in this study were approved by inspection and testing organizations. Three replicate measurements were analyzed for each sample.

2.1.2.3 Carbon and nitrogen isotope detection in biological samples

The dorsal fin muscles of fish, abdominal muscles of crustaceans, tentacle muscles of cephalopods, and closed shell muscles of shellfish were rinsed and freeze-dried in a freeze-dryer (SP Scientific FM 25EL). The tissues were then ground into powder in an agate mortar using a pestle. The biological powder was decarbonized and degreased with hydrochloric acid and degreasing solution. After drying, 0.1 mg and 0.5 mg of the sample powder were fed into a stable isotope ratio mass spectrometer (Thermo Fisher Mat 253). The power was turned on, and the samples were combusted at high temperatures to produce CO_2 or N_2 , which was detected and analyzed by an elemental analyzer (Flash 2000HT) and a mass spectrometer (Mat 253) detector inside the instrument. The instrument provides an abundance ratio of $^{13}\text{C}/^{12}\text{C}$ or $^{15}\text{N}/^{14}\text{N}$ in the sample. The carbon and nitrogen stable isotope ratios (δ) in the sample were calculated as in Equation 1 (Yichen, 2021).

$$\delta(\text{‰}) = \left[\frac{R_{\text{Samples}} - R_{\text{Standard}}}{R_{\text{Standard}}} \right] \times 1000 \quad (1)$$

where R_{samples} represent the ratios of carbon and nitrogen isotopes ($^{13}\text{C}/^{12}\text{C}$ or $^{15}\text{N}/^{14}\text{N}$) in the measured samples. R_{standard} is the internationally recognized standard carbon isotope ratio and standard atmospheric nitrogen (N_2) isotope ratio. $\delta^{13}\text{C}$ values were determined with an accuracy of $\pm 0.1\text{‰}$. $\delta^{15}\text{N}$ values were determined with an accuracy of $\pm 0.2\text{‰}$. To improve the stability of the instrument and the credibility of the data and to ensure that the results met the quality control requirements, one additional standard sample was added for calibration after every three samples were measured. Furthermore, three biological replicates were analyzed for each sample.

2.2 Data processing analysis

2.2.1 Bioconcentration factors

The bioaccumulation factor is the specific activity of an element or radionuclide in biological tissue relative to its concentration in the environment. For aquatic ecosystems, most approaches calculate $CR_{\text{wo-media}}$ using water, as shown in Equation 2 (IAEA, 2014):

$$CR_{\text{wo-media}} = \frac{\text{Concentration per unit mass of organism (Bq/kg} \cdot \text{wet weight)}}{\text{Concentration per unit volume of sea water (Bq/L)}} \quad (2)$$

where $CR_{\text{wo-media}}$ represents the bioaccumulation factor in aquatic ecosystems. In this study, $CR_{\text{wo-media}}$ represents the concentration of radionuclides in the whole organism to that in the filtered water.

2.2.2 Biological trophic level calculations

In this study, trophic levels were calculated using the carbon and nitrogen stable isotope contents of collected biological samples. Organisms fractionate carbon and nitrogen stable isotopes through processes such as ingestion, absorption, and metabolism. In general, the ratio of $\delta^{15}\text{N}$ in organisms increases by 2.5‰ to 5‰ from one trophic level to the next. The $\delta^{15}\text{N}$ ratio was used to calculate the trophic level (TL) of the organisms as shown in Equation 3 (Peterson and Fry, 1987):

$$TL = \left[\frac{\delta^{15}\text{N}_{\text{sample}} - \delta^{15}\text{N}_{\text{baseline}}}{\Delta\delta^{15}\text{N}} \right] + 1 \quad (3)$$

where $\delta^{15}\text{N}_{\text{sample}}$ is the N isotope ratio in the measured sample and $\delta^{15}\text{N}_{\text{baseline}}$ represents N isotope baseline values. Nitrogen isotope measurements from mussel bodies (6.05‰) were used as the baseline in this study (Deling et al., 2005). $\Delta\delta^{15}\text{N}$ is the N stable isotope enrichment factor (2.5‰) in the common food web of the Yellow-Bo Sea in China (Qu et al., 2016).

2.2.3 Magnification factors for radionuclides at the different trophic levels

The cumulative magnification or dissolution of radionuclides in the food web is expressed as a magnification factor, TMF (trophic magnification factor), which is calculated as shown in Equations 4 and 5 (Borga et al., 2012).

$$\text{Log}_{10} C_m = b(TL) + a \quad (4)$$

$$\text{TMF} = 10^b \quad (5)$$

where C_m is the specific activity of radionuclides measured in the organism, TL is the biological trophic level, b is the slope of the linear regression equation between Log_{10} (radionuclide-specific activity) and the trophic level (TL), and a is an intercept. TMF is the magnification factor for radionuclides at the trophic level. A $\text{TMF} > 1$ indicates that there is a magnification effect of the radionuclide at the trophic level.

2.2.4 Radiation dose to marine biological species

In this study, the ERICA tool developed by the European Union and the default parameters (radionuclide weighting factors and radiation dose conversion factors) were used to conduct the biological radiation dose assessment. The size (length, width and height) and weight of the investigated biological species were entered into the ERICA Tool 2.0 to construct the assessment model. In the process of calculating the biological radiation dose, the ^3H , ^{226}Ra , ^{40}K , ^{14}C , ^{137}Cs and ^{90}Sr concentrations in seawater entered into the ERICA Tool were the average of 18 survey stations. The ^{226}Ra , ^{40}K , ^{137}Cs and ^{90}Sr concentrations in sediment entered were also averaged over 18 stations, and the default Kd of the ERICA tool was used to calculate the ^3H and ^{14}C concentrations of the sediments. Concentrations of six radionuclides in organisms were used as monitoring results.

2.2.5 Data statistics and analysis

One-way analysis of variance (ANOVA) was performed to analyze radionuclide bioaccumulation factors in different species using SPSS Statistics 26 to determine the significance of radionuclide bioaccumulation factors among species (Liu, 2013). Multifactor redundancy analysis of radionuclide mass activities in organisms and their relation with ash mass to fresh mass of organisms and trophic levels was performed using Origin 2021 (Yichen, 2021). The bioaccumulation and transfer of different types of radionuclides in organisms and their correlation with ash mass to fresh mass of organisms and biological trophic level were subsequently examined (Yichen, 2021). Origin 2021 was used to fit trophic magnification factors for radionuclides at different biological trophic levels to investigate the radionuclide transfer in marine organisms.

3 Results and discussion

3.1 Results for radionuclides in the seawater

The radionuclide data for the study area are shown in Supplementary Tables 1 and 2. The statistical analysis results are shown in Tables 2, 3 and Figure 2. There were no significant differences in ^{226}Ra , ^{40}K , ^{90}Sr , or ^3H at the 18 stations. The YT2,

YT7 and YT8 stations had higher ^{137}Cs activity in seawater than did the other stations. ^{14}C was below the detection limit (1 mBq/L) in the seawater at stations YT10 and YT13. The average activity concentrations of radionuclides in seawater were in the following order: ^{40}K (9.99 ± 0.48 Bq/L) > ^3H (0.66 ± 0.20 Bq/L) > ^{226}Ra (9.30 ± 2.31 mBq/L) > ^{14}C (5.03 ± 1.53 mBq/L) > ^{90}Sr (1.56 ± 0.17 mBq/L) > ^{137}Cs (1.16 ± 0.39 mBq/L).

The activity concentrations of nuclides were at the same level as those in sea areas affected by discharges from nuclear power plants in China, such as the Changjiang nuclear power marine area, Tianwan nuclear power marine area, Yangjiang nuclear power marine area, and Fuqing nuclear power marine area (Shouxin et al., 2022; Xue et al., 2013). Compared to those in 1995–2009, the levels of ^{137}Cs and ^{90}Sr in seawater in the study area decreased (Haiyun et al., 2010). This was probably because ^{137}Cs and ^{90}Sr originate mainly from early nuclear explosion tests. As the nuclides decay, the activity concentrations of the residual components in the seawater gradually decrease. Compared with the radionuclide levels in the sea area before the operation of the nuclear power plant in 2010–2012, there were no significant changes in ^{40}K , ^{226}Ra , ^{137}Cs or ^3H in seawater, and ^{90}Sr was reduced (Xue et al., 2013).

3.2 Results for radionuclides in the sediments

The results of radionuclide detection in the sediments of the sea area are shown in Table 3, and the statistical analysis is shown in Figure 2. The ^{226}Ra , ^{40}K , and ^{137}Cs concentrations at stations YT1 and YT2 were lower than those at the other stations. These differences are probably because of the coarser sediment grain sizes at stations near the river mouth. Moreover, the ^{90}Sr concentrations in the sediments were not significantly different. The average activities of radionuclides in the sediments were in the following order: ^{40}K (650.44 ± 68.85 Bq/kg-dry) > ^{226}Ra (27.04 ± 4.66 Bq/kg-dry) > ^{137}Cs (1.34 ± 0.51 Bq/kg-dry) > ^{90}Sr (0.38 ± 0.15 Bq/kg-dry).

Compared with the radionuclide levels in the period from 2010 to 2012, the levels of ^{40}K , ^{226}Ra , ^{137}Cs , and ^{90}Sr in the sediment did not change significantly and were at the same level as those in other nuclear power sea areas in China, including Daya Bay NPP, Changjiang NPP, and Tianwan NPP (Guiyuan et al., 2019; Konghua et al., 2005; Shouxin et al., 2022; Weirong et al., 2020).

TABLE 2 Results for radionuclides in seawater during different periods in the study area.

Time	Statistical items	^{226}Ra	^{40}K (Bq/L)	^{137}Cs	^{90}Sr	^3H (Bq/L)	^{14}C	Data sources
2022	min.–max.	5.92–13.41	9.2–11	0.63–2.25	1.22–1.85	0.37–1.15	≤ 8.2	This research
	mean \pm SD	9.30 ± 2.31	9.99 ± 0.48	1.16 ± 0.39	1.56 ± 0.17	0.66 ± 0.20	5.03 ± 1.53	
2010–2012	min.–max.	5.3–8.8	8.05–12.80	0.64–2.86	2.49–6.68	0.29–0.75	1.2–5.1	(Shouxin et al., 2022; Xue et al., 2013)
1995–2009	mean \pm SD	np	np	0.01–7.1	0.3–16.1	np	np	(Haiyun et al., 2010)
	mean	np	np	2.5	1.9	np	np	

np, No data provided.
(mBq/L).

TABLE 3 Results for radionuclides in sediments during different periods in the study area (Bq/kg-dry).

Time	Statistical items	^{226}Ra	^{40}K	^{137}Cs	^{90}Sr	Data sources
2022	min.–max.	13.6–32.9	447–763	≤ 1.91	0.12–0.64	This research
	mean \pm SD	27.04 ± 4.66	650.44 ± 68.85	1.34 ± 0.51	0.38 ± 0.15	
2010–2012	min.–max.	29.9–36.8	660–746	1.4–3.3	0.08–0.58	(Shouxin et al., 2022)

The ^{40}K activity in the sediments of the investigated area is slightly greater than the global average (412 Bq/kg-dry) for marine areas. However, it is similar to that in the east coast region of Cyprus (628.1 Bq/kg-dry), Brazil (coast of Rio de Janeiro, 678 Bq/kg-dry), the Aqaba Gulf (641.1 Bq/kg-dry) and the Bay of Bengal (684.4 Bq/kg-dry) (Al-Mur and Gad, 2022; Al-Trabulsy et al., 2011; De Carvalho et al., 2016). The specific activity of ^{226}Ra in sediments near the Haiyang Nuclear Power Plant is comparable to that in Tuban, southern coast of Albania (23 Bq/kg-dry) and Brazil (coast of Rio de Janeiro, 24 Bq/kg-dry) (Aryanti et al., 2021; De Carvalho et al., 2016; Tsabaris et al., 2007), and it is also similar to the world average (32 Bq/kg-dry) (UNSCEAR, 2000). However, the activity of these radionuclides is lower than the value of natural radionuclide activity in various marine areas worldwide, such as close to the Mawan coal-fired power plant (CFPP) in Shenzhen (204 Bq/kg-dry) (Liu et al., 2015). According to the statistical analysis in Figure 2, the specific activities of the natural radionuclides ^{40}K and ^{226}Ra in the sediments near stations YT1 and YT2 were significantly lower than those at the other stations. These differences are probably because of the coarser sediment grain sizes at stations near the river mouth.

organisms are as follows: ^{40}K (74.58 Bq·kg⁻¹·wet) > ^{14}C (22.90 Bq·kg⁻¹·wet) > ^3H (1.05 Bq·kg⁻¹·wet) > ^{226}Ra (0.33 Bq·kg⁻¹·wet) > ^{90}Sr (0.08 Bq·kg⁻¹·wet) > ^{137}Cs (0.02 Bq·kg⁻¹·wet). The specific activities of ^{40}K , ^{226}Ra , ^{90}Sr , and ^{137}Cs in the organisms in the sea area of this study were within the same range as those in the sea areas of the Fuqing NPP, Ningde NPP, and Yangjiang NPP in China and were not significantly different (Li et al., 2021; Sun et al., 2021). There are two chemical forms of ^3H in the ocean (tritiated water and tritiated organic molecules). Tritiated water combines with organic compounds through photosynthesis by primary producers to form organically bound tritium (OBT), which can accumulate in organisms higher up in the food chain (Lin et al., 2020). Tritiated water accounts for a large portion of the dose in the short term, and OBT accounts for a large portion of the dose in the longer term (IAEA, 2014). Therefore, this study measured the OBT activity of the examined organisms. The specific activity of OBT in organisms was comparable to that in organisms inhabiting waters adjacent to the Fangchenggang nuclear power plant and slightly greater than that in the nearshore waters of Zhejiang (Lin et al., 2020). However, it was lower than that in the English Channel (Fievet et al., 2013).

3.3 Radionuclides in organisms

The results for radionuclides in organisms are shown in Supplementary Table 3. The ^{226}Ra , ^{40}K , ^{137}Cs , ^{90}Sr , ^{14}C , and ^3H activities in marine organisms ranged from 0.04 to 0.98 Bq/kg-fresh, 43.1 to 132 Bq/kg-fresh, 0.01 to 0.03 Bq/kg-fresh, 0.02 to 0.20 Bq/kg-fresh, 14.37 to 30.65 Bq/kg-fresh, and 0.41 to 2.21 Bq/kg-fresh, respectively. The mean specific activities of the radionuclides in

3.4 Carbon and nitrogen isotope contents of organisms and at different trophic levels

The results of the carbon and nitrogen isotope detection in marine organisms and calculations for different trophic levels in this study are shown in Supplementary Table A3 and in Figure 3. The $\delta^{13}\text{C}$ content of the organisms ranged from -14.4‰ to -19.34‰, with a total span of 4.94‰ and a mean value of (-17.18 \pm 1.43)‰. The $\delta^{15}\text{N}$ content of the

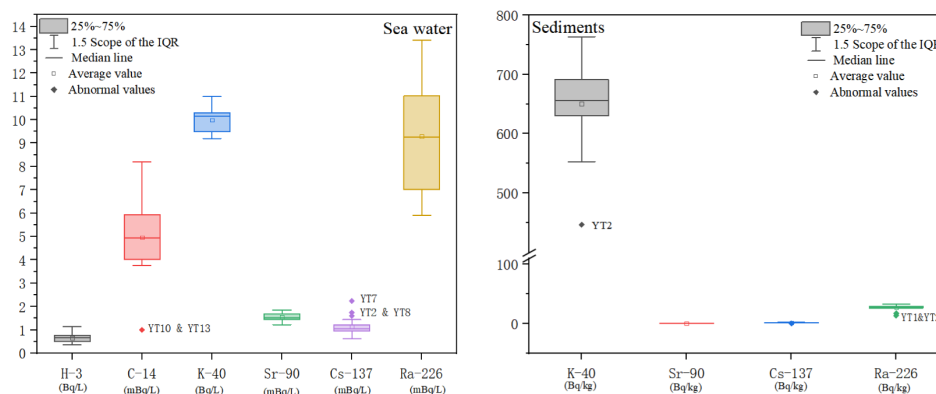


FIGURE 2 Statistical analysis of radionuclides activity concentrations in seawater and sediments.

organisms ranged from 8.48‰ to 12.89‰, with a total span of 4.41‰ and a mean value of 11.44 ± 1.46 ‰. The carbon and nitrogen isotope contents of the organisms were similar as those reported in previous investigations and studies in this marine area (Huaiyu et al., 2021; Yichen, 2021). The $\delta^{13}\text{C}$ contents of the different living species in descending order were as follows: *Loligo beka* > *Octopus variabilis* > *Cynoglossus semilaevis* > *Squilla oratoria* > *Anomiostrea coraliophila* > *Saurida elongata* > *Lepidotrigla micropterus* > *Trachypenaeus curvirostris* > *Pleuronichthys cornutus*. The $\delta^{15}\text{N}$ content in the organisms, in descending order, was as follows: *Saurida elongata* > *Squilla oratoria* > *Loligo beka* > *Cynoglossus semilaevis* > *Lepidotrigla micropterus* > *Octopus variabilis* > *Trachypenaeus curvirostris* > *Pleuronichthys cornutus* > *Anomiostrea coraliophila*. The order of carbon and nitrogen isotope contents among living species showed some variability.

The trophic level range of the organisms in this study ranged from 1.97 to 3.74, with a total span of 1.77 and a mean value of 3.16 ± 0.59 . The results were similar to the coastal waters of Jiangsu Province in 2017 (1.52 ~ 4.28) and Xiaoqing River Estuary adjacent sea area in 2020 (1.65 ~ 3.54) in 2017 (Chuanxin et al., 2022; Nan et al., 2022). It has been shown that if the difference in stable carbon isotopes between 2 species in the same ecosystem is less than 0.60‰, the two species are not in a predatory relationship and may be at the same trophic level. When stable carbon isotopes are greater than 1.5‰, it is also assumed that the two species are not predatory but rather that at least 1 trophic level exists between them (Yukun, 2016). The total span of $\delta^{13}\text{C}$ in the nine marine organisms in this study was 4.94‰, indicating they belonged to multiple trophic levels, which is consistent with their known trophic levels.

3.5 Bioconcentration factor and multivariate statistical analysis

The radionuclide concentration factors of marine organisms are shown in Table 4. As ^{226}Ra and ^{40}K are natural radionuclides, they

are in dynamic equilibrium in the marine environment and in organisms. The average concentration factors of ^{226}Ra and ^{40}K in mollusks, fish and crustaceans in the study area were 4.86 and 4.89, 24.73 and 10.5, and 100.54 and 5.31, respectively. These findings showed that these organisms have a certain bioconcentration effect on the above radionuclides. The concentration factors of ^{226}Ra in fish and mollusks were consistent with the IAEA report (IAEA, 2004, 2014). However, crustaceans had a lower concentration factor for ^{226}Ra than that reported by the IAEA (IAEA, 2004, 2014). ^3H , ^{14}C , ^{90}Sr and ^{137}Cs might not reach equilibrium in the study area due to the discharge of nuclear power plants, and the concentration factors of these nuclides in organisms might also not reach equilibrium either. Therefore, the bioconcentration factor coefficients for ^{14}C , ^{90}Sr and ^{137}Cs in organisms were somewhat different from those in the IAEA report. However, due to the high mobility of ^3H in water, ^3H can quickly reach equilibrium in organisms (IAEA, 2014). The concentration factor of ^3H in organisms was the same as that reported by IAEA.

The results from the one-way ANOVA showed that the significance levels for radionuclide bioaccumulation factors among species of ^{226}Ra and ^{40}K were 0.0001 and 0.015, respectively, showing there was a significant difference in bioaccumulation factors for these radionuclides between the different species. The significance levels for ^{137}Cs , ^{14}C , and ^3H were 0.32, 0.06, 0.08, and 0.80, respectively, between the different species, showing the differences were not significant.

Multivariate statistical analyses (MSAs) were performed to analyze the correlation of the radionuclides with respect to the ash-to-fresh weight ratio and trophic level of the organisms, and the results are shown in Figure 4. The cumulative inertia of the two constraint axes reached 91.38%, which meant that the variability of radionuclides in organisms can be well explained by ash mass to fresh mass of organisms and the trophic level. As shown in Figure 4, ^{40}K , ^{137}Cs , ^{14}C , and ^{90}Sr were strongly positively correlated with the biological trophic level and ash mass to fresh mass of organisms,

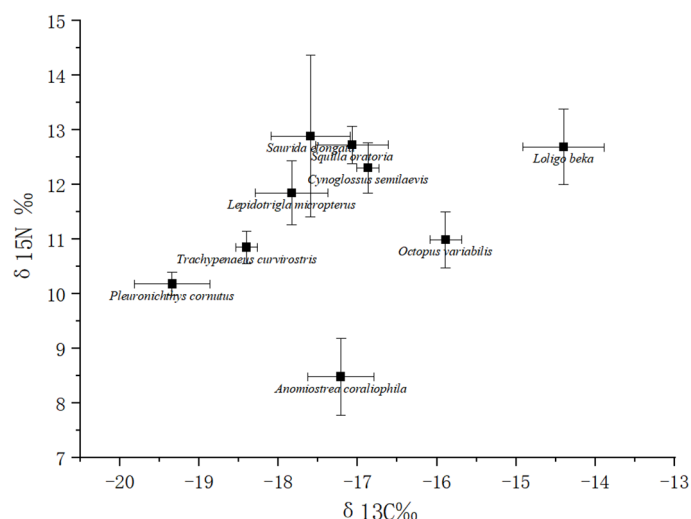


FIGURE 3
Results for carbon and nitrogen isotope distributions in marine organisms.

TABLE 4 Bioconcentration factor (CR_{wo-water}) for wildlife groups in marine ecosystems (Bq/kg, fresh weight whole organism: Bq/L water, min–max, mean \pm SD).

Species	Statistical items	^{137}Cs	^{226}Ra	^{40}K	^3H	^{14}C	^{90}Sr
Mollusks:	min–max	4.31–9.48	4.30–7.53	4.31–5.58	0.94–1.62	2856.86–4833	14.1–29.49
	mean \pm sd	6.32 \pm 2.77	4.86 \pm 0.65	4.89 \pm 0.65	1.33 \pm 0.35	3703.11 \pm 1018.14	20.73 \pm 7.91
	IAEA-2004 (Recommended value)	60	100	np	1.0	20000	10
	IAEA-2014 (Geometric mean)	35	47	np	np	np	110
Fish: benthic feeding	min–max	7.76–28.45	13.98–44.09	7.06–13.21	0.62–2.82	4648.11–6093.44	20.51–62.18
	mean \pm sd	19.18 \pm 8.89	24.73 \pm 13.37	10.50 \pm 2.58	1.60 \pm 1.01	5364.81 \pm 782.41	44.55 \pm 18.99
	IAEA-2004 (Recommended value)	100	100	np	1	20000	3
	IAEA-2014 (Geometric mean)	31	75	np	1.0	np	7.4
Crustaceans	min–max	20.69–23.28	95.7–105.38	4.75–5.87	0.65–3.33	4000–4401.59	103.21–125
	mean \pm sd	21.99 \pm 1.83	100.54 \pm 6.84	5.31 \pm 0.79	2.00 \pm 1.90	4200.8 \pm 283.97	114.11 \pm 15.41
	IAEA-2004 (Recommended value)	50	100	np	1	20000	5
	IAEA (Geometric mean)	21	73	np	1.0	np	45
TMF		2.09	1.17	1.29	0.74	1.15	1.06

np, No data provided.

with correlation sizes changing in the following order: $^{40}\text{K} > ^{90}\text{Sr} > ^{137}\text{Cs} > ^{14}\text{C}$. This may be because K and C are the major elements of biological proteins, and Cs and K belong to the same group in the periodic system. They have similar chemical properties related to easy absorption by living organisms (Pentreath, 2019). The ^{226}Ra and ^{90}Sr concentrations in the organisms were strongly correlated and strongly positively correlated with ash mass to fresh mass of organisms. This may be because Ca is one of the main elements of organism bones, and Ra and Sr belong to the same group in the periodic system as Ca and both are osteophilic. Correlation analysis of the biological species revealed that *Octopus variabilis* and *Loligo beka* were strongly correlated. *Lepidotrigla*

and *Saurida elongata* were more strongly correlated, and *Trachypenaeus curvirostris* and *Squilla oratoria* were even more strongly correlated. This was consistent with the morphological structures, and physiological habits of organisms.

3.6 Cumulative transfer of radionuclides at the different trophic levels of marine organisms

Referring to the methodology of Gao et al. in 2021 (Gao et al., 2021), the trophic magnification factors (TMFs) for different types of

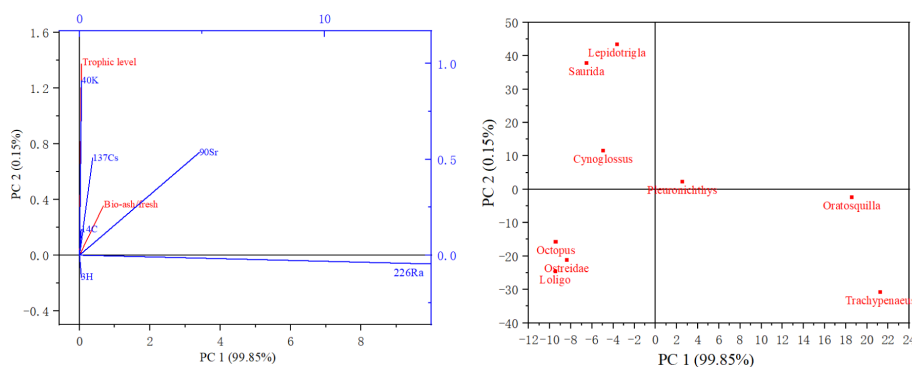


FIGURE 4

Multivariate statistical analysis of radionuclides versus biological carbon and nitrogen content and ash mass to fresh mass of organisms.

radionuclides at different biological trophic levels were fitted. The fitting results are shown in [Supplementary Figure 1](#), and the results from the magnification factor (TMF) calculation are shown in [Supplementary Table 4](#). The TMF for ^3H was less than 1.0, indicating that the increase in trophic level has a diluting effect on the activity of ^3H . This result was similar to that for the heavy metals Co, Mn, Cd, Cu, and Zn in trophic level accumulation transfer in marine organisms ([Bezhenar et al., 2021](#); [Zheng et al., 2023](#)). TMFs greater than 1.0 for ^{137}Cs , ^{226}Ra , ^{40}K , ^{14}C , and ^{90}Sr suggested amplification of these radionuclides through the trophic levels of marine organisms. This result was similar to the transfer of the heavy metals Hg and Cr at marine trophic levels ([Liu et al., 2019](#)). The magnitudes of the cumulative transfer coefficients of radionuclides through the trophic levels of marine organisms were in the following order: ^{137}Cs (2.09) > ^{40}K (1.29) > ^{14}C (1.15) > ^{226}Ra (1.17) > ^{90}Sr (1.06) > ^3H (0.74). There is a wide variety of marine organisms, and the study is only based on radionuclide detections in nine different marine organisms. It is recommended that more detection data be used in the future to further optimize the fitting results. Using assimilation efficiency simulations, [Bezhenar et al. \(2021\)](#) calculated that concentrations of ^{137}Cs increase with trophic level of marine organisms ([Bezhenar et al., 2021](#)). The magnification factor for ^{137}Cs in the present study was equal to that used (TMF = 2.0) by [Kasamatsu and Ishikawa \(1997\)](#), who analyzed the concentration of ^{137}Cs in the stomach and gastric contents of fish ([Kasamatsu and Ishikawa, 1997](#)).

The differences in the cumulative delivery of radionuclides at different marine trophic levels may be related to the feeding ecology of the different species and the variability in uptake efficiency by the digestive system ([Konovalenko et al., 2016](#); [Nakata and Sugisaki, 2015](#)). When radionuclides are highly concentrated in prey organisms and when the intestinal transfer coefficient of the radionuclide to the predator is high, then the predator organisms are enriched in radionuclides mainly through the digestive absorption pathway ([Carvalho, 2018](#)). In addition, differences in the physicochemical properties of nuclides influence the mechanism of internal stabilization regulation of bioconcentrated radionuclides ([Fowler and Carvalho, 1985](#)). Some radioisotopes are chemically similar to certain life-essential elements, such as ^{137}Cs and K, ^{90}Sr , ^{226}Ra , and Ca; therefore, they may be passed through the food chain once they are enriched in organisms ([Rainbow, 1998](#)). Equilibrium between tissue free water tritium and water is achieved in less than a day due to regulation of the water balance by respiration and osmoregulatory processes; thus, the differences in tritium in organisms are mainly due to differences in organically bound tritium (OBT) ([Calmon and Garnier-Laplace, 2001](#)). This is because OBT levels in aquatic biota are affected by a combination of different physicochemical forms of organic tritium present in the ecosystem, different uptake pathways and different transfer rates ([Ferreira et al., 2023](#)).

3.7 Assessment of radiation dose to marine species

The dose rates of ionizing radiation to the sampled organisms by the six radionuclides (^3H , ^{226}Ra , ^{40}K , ^{14}C , ^{137}Cs and ^{90}Sr) ranged from 32.02 nGy/h to 195.49 nGy/h, with a mean value of 102.86 ± 57.30

nGy/h. The dose rates to organisms from the six radionuclides in this study were about two orders of magnitude below the recommended value by ERICA tool (10 $\mu\text{Gy/h}$). The ionizing radiation risk quotient was in the range of 0.003 to 0.019. The results of the assessment indicated that the ionizing radiation hazard to organisms from the investigated radionuclides were negligible. *Trachypena curvirostris*, *Squilla oratoria* and *Pleuronichthys cornutus* received the highest doses of ionizing radiation. The doses of ionizing radiation to organisms from artificial radionuclides (^{14}C , ^3H , ^{90}Sr , ^{137}Cs) ranged from 0.45–1.08 nGy/h, with an average value of 0.86 ± 0.19 nGy/h. ^{226}Ra and ^{40}K produced approximately 99.16% of the total dose of ionizing radiation to organisms from these six radionuclides.

Many studies have been carried out on the assessment of radiation doses from radionuclides to marine organisms ([Al-Mur and Gad, 2022](#); [Keum et al., 2013](#)). Based on monitoring data from Daya Bay from 2011–2017, [Yue Yu et al. \(2023\)](#) showed that the total dose rates of ^{137}Cs , ^{90}Sr , ^{40}K , ^{226}Ra , ^{232}Th , ^{238}U , and ^{210}Po to the marine ecosystem of Daya Bay ranged from 230.5 to 853.9 nGy/h. ^{210}Po , ^{226}Ra , and ^{232}Th were the main dose contributors. ^{137}Cs and ^{90}Sr accounted for approximately 0.01%–0.06% of the total radiation dose ([Yu et al., 2023](#)). [Jiang Sun et al. \(2021\)](#) showed that the total radiation dose rates of ^{210}Po , ^{210}Pb , ^{137}Cs , ^{90}Sr , ^{238}U , ^{226}Ra , and ^{40}K to 12 marine organisms in the sea areas of the Fuqing NPP and Ningde NPP ranged from 37 to 1531 nGy/h. The dose contributions of ^{137}Cs and ^{90}Sr were <0.13% ([Sun et al., 2021](#)), and it's similar to the results of the present study (0.03%–0.35%). A large contribution to the radiation dose received by marine fauna comes from members of the naturally occurring uranium series that accumulate in the body, especially polonium, such as ^{210}Po ([Carvalho, 1988](#); [Cherry et al., 1994](#)). Compared with the results from the above studies, the radiation doses generated by artificial radionuclides in this study were similar. Therefore, the proportion of radiation doses to organisms from the four artificial radionuclides (^{14}C , ^3H , ^{90}Sr , ^{137}Cs) would be further reduced if other natural radionuclides (including ^{210}Po , ^{210}Pb , ^{238}U) were accounted for in the study area.

4 Conclusions

The activity concentrations of radionuclides (^3H , ^{226}Ra , ^{40}K , ^{14}C , ^{137}Cs and ^{90}Sr) in both the environment and organisms did not change significantly compared to those in the preoperational period.

Mollusks, fish and crustaceans showed bioaccumulative effects on ^{137}Cs , ^{226}Ra , ^{40}K , ^{14}C , ^3H , and ^{90}Sr . The bioaccumulation factors for ^{137}Cs , ^{226}Ra , and ^{40}K in mollusks, fish, and crustaceans were different. This showed that there is some variability in the uptake of these three nuclides by different biological species. The results from the magnification factor (TMF) calculation in [Supplementary Table A.4](#) showed that ^3H dilution occurred with increasing trophic level. ^{137}Cs , ^{226}Ra , ^{40}K , ^{14}C , and ^{90}Sr had amplification effects through the trophic levels. The cumulative magnification factors of radionuclides at the different trophic levels are in the following order: ^{137}Cs (2.09) > ^{40}K (1.29) > ^{14}C (1.15) > ^{226}Ra (1.17) > ^{90}Sr (1.06) > ^3H (0.74).

The dose rates of ionizing radiation from six radionuclides, ^3H , ^{226}Ra , ^{40}K , ^{14}C , ^{137}Cs and ^{90}Sr , ranged from 32.02 nGy·h⁻¹ to 195.49 nGy·h⁻¹, with a mean value of 102.86 ± 57.30 nGy·h⁻¹ for different

species in the study area. The dose rates to organisms from the six radionuclides in this study were about two orders of magnitude below the standard limit of radiation dose (10 $\mu\text{Gy/h}$). Compared to the biological radiation dose from natural radionuclides (^{226}Ra , ^{40}K), the percentage of radiation dose rate (0.84%) from the main artificial radionuclides (^{14}C , ^3H , ^{90}Sr , ^{137}Cs) released by the nuclear power plant in the marine environment was negligible in our study.

Data availability statement

The datasets presented in this study can be found in online repositories. The names of the repository/repositories and accession number(s) can be found in the article/[Supplementary Material](#).

Author contributions

JN: Methodology, Writing – original draft. DC: Data curation, Validation, Writing – review & editing. ZQ: Data curation, Validation, Writing – review & editing. JL: Investigation, Writing – review & editing. FL: Investigation, Validation, Writing – review & editing. JJ: Investigation, Validation, Writing – review & editing. DH: Investigation, Writing – review & editing. TY: Funding acquisition, Validation, Writing – review & editing.

Funding

The author(s) declare that financial support was received for the research, authorship, and/or publication of this article. This

project is supported by Natural Science Foundation of Fujian Province (2023J011370), Science and Technology Project of Fujian Province (Grant No.2019Y0073), the Marine Environment Radioactivity Monitoring and Early Warning Project (LSKJ202202903) and the Fundamental Research Funds of the Third Institute of Oceanology, Ministry of Natural Resources of China (Haisanke 2019001).

Conflict of interest

The authors declare that the research was conducted in the absence of any commercial or financial relationships that could be construed as a potential conflict of interest.

Publisher's note

All claims expressed in this article are solely those of the authors and do not necessarily represent those of their affiliated organizations, or those of the publisher, the editors and the reviewers. Any product that may be evaluated in this article, or claim that may be made by its manufacturer, is not guaranteed or endorsed by the publisher.

Supplementary material

The Supplementary Material for this article can be found online at: <https://www.frontiersin.org/articles/10.3389/fmars.2024.1377411/full#supplementary-material>

References

- Al-Mur, B. A., and Gad, A. (2022). Radiation hazard from natural radioactivity in the marine sediment of jeddah coast, red sea, Saudi Arabia. *J. Mar. Sci. Eng.* 10, 1145. doi: 10.3390/jmse10081145
- Al-Tabulsi, H. A., Khater, A. E. M., and Habbani, F. I. (2011). Radioactivity levels and radiological hazard indices at the saudi coastline of the gulf of aqaba. *Radiat. Phys. Chem. Oxf. Engl.* 1993, 80 (3), 343–348. doi: 10.1016/j.radphyschem.2010.09.002
- Arogunjo, A. M., Hoellriegel, V., Giussani, A., Leopold, K., Gerstmann, U., Veronese, L., et al. (2009). Uranium and thorium in soils, mineral sands, water and food samples in a tin mining area in Nigeria with elevated activity. *J. Environ. Radioact.* 99, 232–240. doi: 10.1016/j.jenvrad.2008.12.004
- Aryanti, C. A., Suseno, H., Muslim, Prihatiningsih, W. R., and Yahya, M. N. (2021). Concentration of natural radionuclide and potential radiological dose of ^{226}Ra to marine organism in tanjung awar-awar, tuban coal-fired power plant. *Jurnal. Segara.* 17 (3), 195–206. doi: 10.15578/segara.v17i3.10555
- Aydin, K. Y., McFarlane, G. A., King, J. R., and Megrey, B. A. (2003). *The BASS/Model Report on Trophic Models of theSubarctic Pacific Basin Ecosystems* (Sidney, B.C., Canada: North Pacific Marine Science Organization (PICES), 93.
- Beaugelin-Seiller, K., Howard, B. J., and Garnier-Laplace, J. (2019). An approach to identifying the relative importance of different radionuclides in ecological radiological risk assessment: application to nuclear power plant releases. *J. Environ. Radioact.* 197, 116–126. doi: 10.1016/j.jenvrad.2018.11.011
- Bezhenar, R., Kim, K. O., Maderich, V., de With, G., and Jung, K. T. (2021). Multi-compartment kinetic-allometric (mcka) model of radionuclide bioaccumulation in marine fish. *Biogeosciences* 18, 2591–2607. doi: 10.5194/bg-18-2591-2021
- Bo, Z. (2005). *Preliminary studies on marine food web and trophodynamics in China coastal seas* (Qing Dao: Ocean University of China).
- Borga, K., Kidd, K. A., Muir, D. C., Berglund, O., Conder, J. M., Gobas, F. A., et al. (2012). Trophic magnification factors: considerations of ecology, ecosystems, and study design. *Integr. Environ. Assess. Manag.* 8, 64–84. doi: 10.1002/ieam.v8.1
- Brown, J. E., Alfonso, B., Avila, R., Beresford, N. A., Copplestone, D., and Hosseini, A. (2016). A new version of the erica tool to facilitate impact assessments of radioactivity on wild plants and animals. *J. Environ. Radioact.* 153, 141–148. doi: 10.1016/j.jenvrad.2015.12.011
- Brown, J., Børretzen, P., Dowdall, M., Sazykina, T., and Kryshev, I. (2004). The derivation of transfer parameters in the assessment of radiological impacts on arctic marine biota. *Arctic* 57, 279–289. doi: 10.14430/arctic505
- Calmon, P., and Garnier-Laplace, J. (2001). *Tritium and the environment* (Paris: IRSN).
- Carvalho, F. P. (1988). ^{210}Po in marine organisms: a wide range of natural radiation dose domains. *Radiat. Prot. Dosimetry.* 24, 113–117. doi: 10.1093/rpd/24.1-4.113
- Carvalho, F. P. (2018). Radionuclide concentration processes in marine organisms: a comprehensive review. *J. Environ. Radioact.* 186, 124–130. doi: 10.1016/j.jenvrad.2017.11.002
- Cherry, R., Heyraud, M., and Rindfuss, R. (1994). Polonium-210 in teleost fish and in marine mammals: interfamilial differences and a possible association between polonium-210 and red muscle content. *J. Environ. Radioact.* 24, 273–291. doi: 10.1016/0265-931X(94)90044-2
- China, H. M. O. E. (2019). *Analytical method of ^{14}C in liquid effluent of nuclear of power plant-wet oxidation* (Beijing: China Environment Publishing Group Press).
- China, N. H. C. O. (2020). *Gamma spectrometry method of analyzing radionuclides in biological samples* (Beijing: Standards Press of China).
- Chouvelon, T., Strady, E., Harmelin-Vivien, M., Radakovitch, O., Brach-Papa, C., Crochet, S., et al. (2019). Patterns of trace metal bioaccumulation and trophic transfer

in a phytoplankton-zooplankton-small pelagic fish marine food web. *Mar. pollut. Bull.* 146, 1013–1030. doi: 10.1016/j.marpolbul.2019.07.047

Chuanxin, Z., Jing, C., Yinglu, J., Linlin, C., Haihui, L., Quanchao, W., et al. (2022). Benthic food web structure of xiaoqing river estuary adjacent sea area revealed by carbon and nitrogen stable isotope analysis. *Acta Oceanol. Sin.* 44 (1), 89–100. doi: 10.12284/hyxb2022016

Commission, N. H. A. F. (2018). *Determination of radionuclides in water by gamma spectrometry* (Beijing: Standards Press of China).

De Carvalho, F. M., Da Costa Lauria, D., Ribeiro, F. C. A., Fonseca, R. T., Da Silva, P. S., and Martins, N. S. F. (2016). Natural and man-made radionuclides in sediments of an inlet in Rio de Janeiro state, Brazil. *Mar. pollut. Bull.* 107, 269–276. doi: 10.1016/j.marpolbul.2016.03.059

Deling, C., Hongyan, L., Qisheng, T., and Yao, S. (2005). Establishment of trophic continuum in the food web of the yellow sea and east China sea ecosystem: insight from carbon and nitrogen stable isotopes. *Sci. China* 2, 123–130.

Environment, R. M. T. C. (2020). *Analysis method for tritium in water, HJ 1126-2020* (Beijing: China Environment Publishing group).

Fakhri, Y., Sarafraz, M., Pilevar, Z., and Khaneghah, A. M. (2022). The concentration and health risk assessment of radionuclides in the muscle of tuna fish: a worldwide systematic review and meta-analysis. *Chemosphere.* 389, 133–149. doi: 10.1016/j.chemosphere.2021.133149

Feng, L., Tao, Y., Wen, Y., Jialin, N., and Lin, L. (2020). Electrolytic enrichment method for tritium determination in the arctic ocean using liquid scintillation counter. *Acta Oceanol. Sin.* 39, 73–77. doi: 10.1007/s13131-020-1647-4

Ferreira, M. F., Turner, A., Vernon, E. L., Grisolia, C., Lebaron-Jacobs, L., Malard, V., et al. (2023). Tritium: its relevance, sources and impacts on non-human biota. *Sci. Total. Environ.* 867, (162816). doi: 10.1016/j.scitotenv.2023.162816

Fievet, B., Pommier, J., Voiseux, C., Bois, P. B. D., Laguionie, P., Cossonnet, C., et al. (2013). Transfer of tritium released into the marine environment by french nuclear facilities bordering the english channel. *Environ. Sci. Technol.* 47, 6696–6703. doi: 10.1021/es400896t

Fiévet, B., Voiseux, C., Rozet, M., Masson, M., and du Bois, P. B. (2006). Transfer of radiocarbon liquid releases from the areva la hague spent fuel reprocessing plant in the english channel. *J. Environ. Radioact.* 90, 173–196. doi: 10.1016/j.jenvrad.2006.06.014

Fisher, N. S., Stupakoff, I., Sañudo-Wilhelmy, S., Wang, W. X., and Crusius, J. (2000). Trace metals in marine copepods: a field test of a bioaccumulation model coupled to laboratory uptake kinetics data. *Mar. Ecol. Prog.* 194, 211–218. doi: 10.3354/meps194211

Fowler, S. W., and Carvalho, F. P. (1985). Americium biokinetics in benthic organisms as a function of feeding mode. *Bull. Environ. Contamination. Toxicol.* 35, 826–834. doi: 10.1007/BF01636594

Gao, Y., Wang, R., Li, Y., Ding, X., Jiang, Y., Feng, J., et al. (2021). Trophic transfer of heavy metals in the marine food web based on tissue residuals. *Sci. Total. Environ.* 772, 145064. doi: 10.1016/j.scitotenv.2021.145064

Garnier-Laplace, J., Gilek, M., Sundell-Bergman, S., and Larsson, C. (2004). Assessing ecological effects of radionuclides: data gaps and extrapolation issues. *J. Radiol. Prot.* 24, 139–155. doi: 10.1088/0952-4746/24/4A/009

Guiyuan, L., Fei, D., Wanliang, C., Guibiao, W., and Wentao, C. (2019). Levels of radioactivity in marine sediments around the daya bay nuclear power plants site. *Nucl. Saf.* 18, 5.

Haiyun, Y., Ling, Z., Yan, Z., Fei, S., Meiyan, L., Zhonggang, C., et al. (2010). Monitoring of radioactivity levels of sea water in near coast marine environment in China during 1995–2009. *Radiat. Prot. Bull.* 35, 13–16.

Huaiyu, B., Yukun, W., Tingting, Z., Lingfeng, H., and Yao, S. (2021). Trophic levels and feeding characters of marine fishes in the yellow sea and northern east China sea based on stable isotope analysis. *Prog. Fishery. Sci.* 42, 10–17.

IAEA (2004). *Sediment distribution coefficients and concentration factors for biota in the marine environment*, TECHNICAL REPORTS SERIES No 422 (VIENNA).

IAEA (2014). *Handbook of parameter values for the prediction of radionuclide transfer to wildlife*, TECHNICAL REPORTS SERIES No. 479 (VIENNA).

IAEA (2021). *Approaches for modelling of radioecological data to identify key radionuclides and associated parameter values for human and wildlife exposure assessments*, IAEA TECDOC SERIES (VIENNA).

ICRP (1991). “Risk estimates for carcinogenic effects of radiation,” in *Annals of the ICRP* (New York: Annals of the ICRP).

ICRP (2008). *Recommendations of the international commission on radiological protection. 2008. Environmental protection: the concept and use of reference animals and plants* (New York: Annals of the ICRP).

Ishii, Y., Matsuzaki, S. I. S., and Hayashi, S. (2020). Different factors determine 137 cs concentration factors of freshwater fish and aquatic organisms in lake and river ecosystems. *J. Environ. Radioact.* 213, (106102). doi: 10.1016/j.jenvrad.2019.106102

Kasamatsu, F., and Ishikawa, Y. (1997). Natural variation of radionuclide 137cs concentration in marine organisms with special reference to the effect of food habits and trophic level. *Mar. Ecol. Prog. Ser.* 160, 109–120. doi: 10.3354/meps160109

Keum, D. K., Jun, I. N., Lim, K. M., and Choi, Y. H. (2013). Radiation dose to human and non-human biota in the republic of Korea resulting from the Fukushima nuclear accident. *Nucl. Eng. Technol.: Int. J. Korean. Nucl. Soc.* 45 (1), 1–12. doi: 10.5516/NET.03.2011.063

Konghua, J., Qing, T., Quanlu, G., and Zhigang, C. (2005). Tnps environmental monitoring in 2004 (pre-operation). *Radiat. Prot.* 25, 321–333.

Kononenko, L., Bradshaw, C., Andersson, E., Lindqvist, D., and Kautsky, U. (2016). Evaluation of factors influencing accumulation of stable sr and cs in lake and coastal fish. *J. Environ. Radioact.* 160, 64–79. doi: 10.1016/j.jenvrad.2016.04.022

Lee, J., Yi, S. C., and Ko, M. J. (2023). Monitoring of 137cs, 239 + 240pu, and 90sr in the marine environment of South Korea and their impact on marine biota: 10 years after the Fukushima accident. *Sci. Total. Environ.* 905, (167077). doi: 10.1016/j.scitotenv.2023.167077

Lepicard, S., Heling, R., and Maderich, V. (2004). Poseidon/rodos models for radiological assessment of marine environment after accidental releases: application to coastal areas of the baltic, black and north seas. *J. Environ. Radioact.* 72, 153–161. doi: 10.1016/S0265-931X(03)00197-8

Li, D., Jiang, Z., Zhao, L., Zhao, F., and Zhou, P. (2021). Assessment of radioactivity level in the terrestrial and marine organisms in yangjiang and its adjacent areas (China). *Int. J. Environ. Res. Public Health* 18, (16). doi: 10.3390/ijerph18168767

Lima, A., Albanese, S., and Cicchella, D. (2005). Geochemical baselines for the radioelements k, u, and th in the campania region, Italy: a comparison of stream-sediment geochemistry and gamma-ray surveys. *Appl. Geochem.* 20, 611–625. doi: 10.1016/j.apgeochem.2004.09.017

Lin, F., Yu, W., Guo, J., Liao, H., and Wang, Y. (2020). A method for the determination of organically bound tritium in marine biota based on an improved tubular-combustion system. *J. Environ. Radioact.* 211, 106084. doi: 10.1016/j.jenvrad.2019.106084

Liu, J. (2013). *Accumulation of heavy metals in multi-phase media and their transfer and biomagnification in food web of laizhou bay* (Qingdao: Institute of Oceanology of Chinese Academy of Sciences).

Liu, J., Cao, L., and Dou, S. (2019). Trophic transfer, biomagnification and risk assessments of four common heavy metals in the food web of laizhou bay, the bohai sea. *Sci. Total. Environ.* 670, 508–522. doi: 10.1016/j.scitotenv.2019.03.140

Liu, G., Luo, Q., Ding, M., and Feng, J. (2015). Natural radionuclides in soil near a coal-fired power plant in the high background radiation area, south China. *Environ. Monit. Assess.* 187, 356. doi: 10.1007/s10661-015-4501-y

Maystrenko, T., and Rybak, A. (2022). Radiation exposure and risk assessment to earthworms in areas contaminated with naturally occurring radionuclides. *Environ. Monit. Assess.* 194, (10). doi: 10.1007/s10661-022-10382-4

Nakata, K., and Sugisaki, H. (2015). “Impacts of the Fukushima nuclear accident on fish and fishing grounds,” in *Impacts of the Fukushima Nuclear Accident on Fish and Fishing Grounds*. (Yokohama, Kanagawa, Japan: Fisheries Research Agency).

Nan, L. Y., Rui, Z., Hu, Z., Shuo, Z., and Shike, G. (2022). Seasonal variation in the trophic structure of food webs in coastal waters of Jiangsu province based on stable isotope techniques. *Acta Oceanol. Sin.* 44, 1–10.

Patra, A. C., Mohapatra, S., Sahoo, S. K., Lenka, P., Dubey, J. S., Thakur, V. K., et al. (2014). Assessment of ingestion dose due to radioactivity in selected food matrices and water near Vizag, India. *J. Radioanal. Nucl. Chem.* 300, 903–910. doi: 10.1007/s10967-014-3097-y

Pauly, D., Palomares, M. L., Froese, R., Sa-A, P., Vakily, M., Preikshot, D., et al. (2001). Fishing down Canadian aquatic food webs. *Can. J. Fisheries. Aquat. Sci.* 58, 51–62. doi: 10.1139/f00-193

Pentreath, R. J. (2019). *Nuclear Power, Man and the Environment* (London: Routledge), 266.

Peterson, B. J., and Fry, B. (1987). Stable isotopes in ecosystem studies. *Annu. Rev. Ecol. Syst.* 1, 293–320. doi: 10.1146/annurev.es.18.110187.001453

Pinder, J. E., Rowan, D. J., and Smith, J. T. (2016). Development and evaluation of a regression-based model to predict cesium-137 concentration ratios for saltwater fish. *J. Environ. Radioact.* 152, 101–111. doi: 10.1016/j.jenvrad.2015.11.004

Qiao, J., Casacuberta, N., and Ginnity, P. M. (2023). Editorial: natural and artificial radionuclides as tracers of ocean processes. *Front. Mar. Sci.* 10. doi: 10.3389/fmars.2023.1170408

Qu, P., Wang, Q., Pang, M., Zhang, Z., Liu, C., and Tang, X. (2016). Trophic structure of common marine species in the bohai strait, north China sea, based on carbon and nitrogen stable isotope ratios. *Ecol. Indic.* 66, 405–415. doi: 10.1016/j.ecolind.2016.01.036

Rainbow, P. S. (1998). “Phylogeny of trace metal accumulation in crustaceans,” in *Metal metabolism in aquatic environments*. Eds. W. J. Langston and M. Bebianno (Boston, MA: Springer). doi: 10.1007/978-1-4757-2761-6_9

Sazykina, T. G. (2000). Ecomod — an ecological approach to radioecological modelling. *J. Environ. Radioact.* 50 (3), 207–220. doi: 10.1016/S0265-931X(99)00119-8

Sazykina, T. G., and Kryshev, A. I. (2003). EPIC database on the effects of chronic radiation in fish: Russian/FSU data. *J. Environ. Radioact.* 68, 65–87. doi: 10.1016/S0265-931X(03)00030-4

Shouxin, C., Honghai, Z., and Wu, M. (2022). Marine environmental radioactive levels in the waters adjacent to Xiamen and environmental quality assessment. *J. Appl. Oceanogr.* 41, 443–453. doi: 10.3969/j.issn.2095-4972.2022.03.009

Suk, H., Kim, H., Lee, S. H., and Intae, (2019). Distribution and accumulation of artificial radionuclides in marine products around Korean peninsula. *Mar. pollut. Bull.* 146, 521–531. doi: 10.1016/j.marpolbul.2019.06.082

- Sun, J., Men, W., Wang, F., and Wu, J. (2021). Activity levels of ^{210}Po , ^{210}Pb and other radionuclides (^{134}Cs , ^{137}Cs , ^{90}Sr , ^{110}mAg , ^{238}U , ^{226}Ra and ^{40}K) in marine organisms from coastal waters adjacent to fuqing and ningde nuclear power plants (China) and radiation dose assessment. *Front. Mar. Sci.* 8. doi: 10.3389/fmars.2021.702124
- Tani, T., and Ishikawa, Y. (2023). A deuterium tracer experiment for simulating accumulation and elimination of organically bound tritium in an edible flatfish, olive flounder. *Sci. Total. Environ.* 903, 166792. doi: 10.1016/j.scitotenv.2023.166792
- Third Institute Of Oceanography, S. O. A. (2018). *Technical specification for marine environmental radionuclide monitoring, HY/T 235-2018* (Beijing: Standards Press of China).
- Tsabarlis, C., Eleftheriou, G., Kapsimalis, V., Anagnostou, C., Vlastou, R., Durmishi, C., et al. (2007). Radioactivity levels of recent sediments in the butrint lagoon and the adjacent coast of Albania. *Appl. Radiat. Isot.* 65, 445–453. doi: 10.1016/j.apradiso.2006.11.006
- UNSCEAR. (2000). Sources and effects of ionizing radiation. In: *UNSCEAR 2000 report to the General Assembly, with scientific annexes. v. 1: Sources.-v. 2: Effects*. (New York).
- UNSCEAR. (2011). UNSCEAR 2008 Report to the General Assembly with Scientific Annexes. In: *Source and effects of ionizing radiation. In: Source and effects of ionizing radiation*. (New York).
- UNSCEAR. (2012). Biological Mechanisms of Radiation Actions At Low Doses (United Nations), 1–45. Available online at: <http://www.unscear.org/docs/reports/>. (New York).
- Vives I Batlle, J., Wilson, R. C., Watts, S. J., Jones, S. R., McDonald, P., Vives-Lynch, S., et al. (2008). Dynamic model for the assessment of radiological exposure to marine biota. *J. Environ. Radioact.* 99 (11), 1711–1730. doi: 10.1016/j.jenvrad.2007.11.002
- Vives I Batlle, J., Beresford, N. A., Beaugelin-Seiller, K., Bezhenar, R., Brown, J., Cheng, J. J., et al. (2016). Inter-comparison of dynamic models for radionuclide transfer to marine biota in a Fukushima accident scenario. *J. Environ. Radioact.* 153, 31–50. doi: 10.1016/j.jenvrad.2015.12.006
- Wang, W. X., Reinfelder, J. R., Lee, B. G., and Fisher, N. S. (1996). Assimilation and regeneration of trace elements by marine copepods. *Limnol. Oceanogr.* 1, 70–81. doi: 10.4319/lo.1996.41.1.0070
- Weirong, L., Yuhong, Q., Feng, L., Wei, Z., and Xin, W. (2020). Results analysis of two marine radioactivity surveys in the adjacent water of hainan changjiang npp. *J. Appl. Oceanogr.* 39, 64–71.
- Xue, W., Chengpeng, H., and Chunlei, W. (2013). *Shandong haiyang nuclear power project unit 3&4project environmental impact report* (Shanghai: Shanghai Nuclear Engineering Research and Design Institute Co., Ltd).
- Yang, B., Ha, Y., and Jin, J. (2015). Assessment of radiological risk for marine biota and human consumers of seafood in the coast of Qingdao, China. *Chemosphere* 135, 363–369. doi: 10.1016/j.chemosphere.2015.04.097
- Yichen, L. (2021). *Bioaccumulation and influential mechanisms of heavy metals in offshore seafood* (Qingdao: Chinese Academy of Sciences).
- Yu, Y., Zhou, P., and Men, W. (2023). Impact of long-term operation of nuclear power plants on the marine ecosystem of daya bay. *Mar. pollut. Bull.* 193, (115146). doi: 10.1016/j.marpolbul.2023.115146
- Yukun, W. (2016). *Preliminary studies on the population ecology based on fish otolith microstructure and microchemistry* (Qingdao: Ocean University of China).
- Zhang, B., and Tang, Q. (2004). Study on trophic level of important resources species at high trophic levels in the bohai sea, yellow sea and east China sea. *Adv. Mar. Sci.* 22, 393–404.
- Zheng, R., Liu, Y., and Zhang, Z. (2023). Trophic transfer of heavy metals through aquatic food web in the largest mangrove reserve of China. *Sci. Total. Environ.* 899 (165655). doi: 10.1016/j.scitotenv.2023.165655



OPEN ACCESS

EDITED BY

Xuchun Qiu,
Jiangsu University, China

REVIEWED BY

Manu Soto,
University of the Basque Country, Spain
Dario Savoca,
University of Palermo, Palermo, Italy

*CORRESPONDENCE

Matthias Brenner
✉ Matthias.Brenner@awi.de

RECEIVED 28 June 2024

ACCEPTED 03 April 2025

PUBLISHED 17 June 2025

CITATION

Binder FI, Bünning LTH, Strehse JS,
Van Haelst S, De Rijcke M, Maser E and
Brenner M (2025) Biological effects of
munition left on sunken war ships in the
North Sea: a multi-biomarker study using
caged blue mussels and fish caught at
WWII wreck sites at the Belgian coast.
Front. Mar. Sci. 12:1456409.
doi: 10.3389/fmars.2025.1456409

COPYRIGHT

© 2025 Binder, Bünning, Strehse, Van Haelst,
De Rijcke, Maser and Brenner. This is an open-
access article distributed under the terms of
the [Creative Commons Attribution License \(CC BY\)](#). The use, distribution or reproduction
in other forums is permitted, provided the
original author(s) and the copyright owner(s)
are credited and that the original publication
in this journal is cited, in accordance with
accepted academic practice. No use,
distribution or reproduction is permitted
which does not comply with these terms.

Biological effects of munition left on sunken war ships in the North Sea: a multi-biomarker study using caged blue mussels and fish caught at WWII wreck sites at the Belgian coast

Franziska Isabell Binder^{1,2}, Lillian Tabea Hannah Bünning³,
Jennifer Susanne Strehse³, Sven Van Haelst⁴,
Maarten De Rijcke⁴, Edmund Maser³ and Matthias Brenner^{2*}

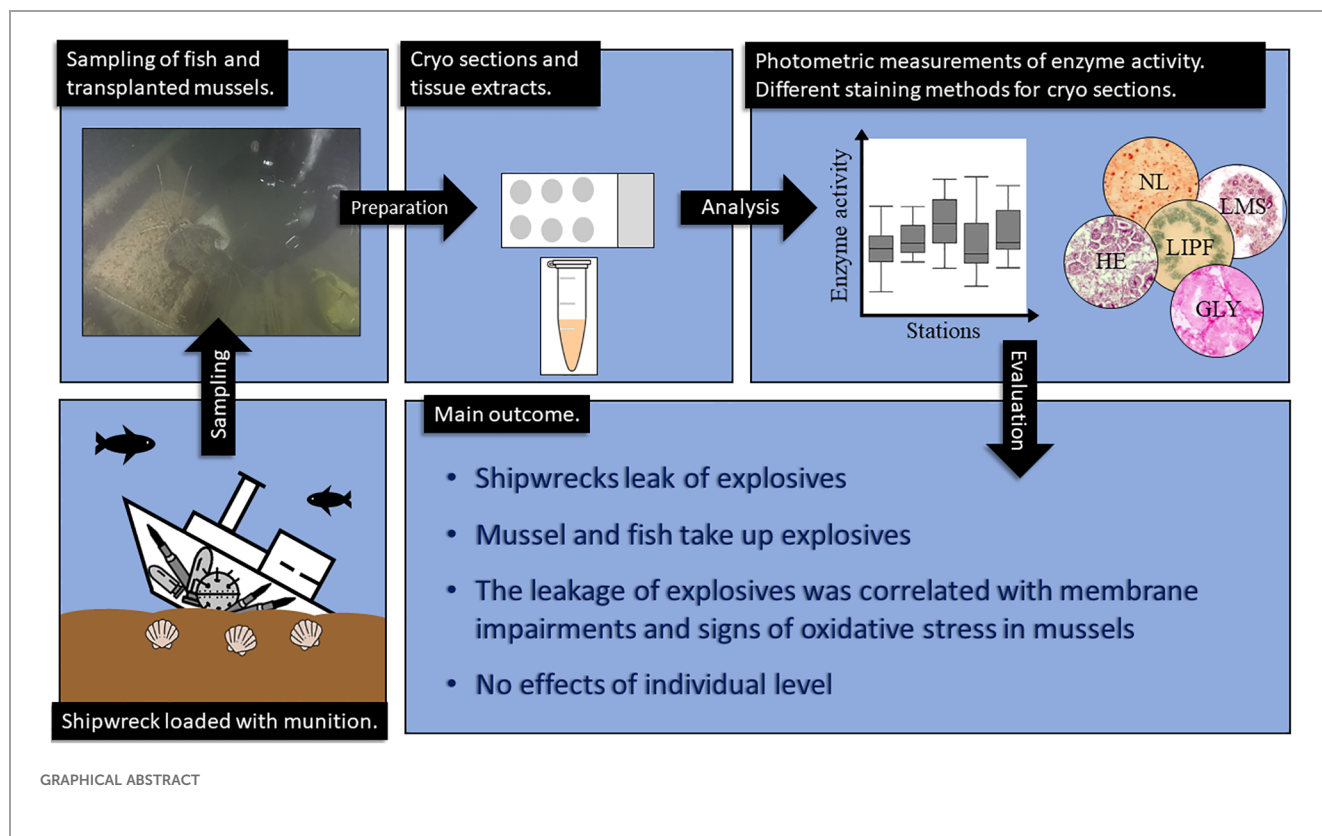
¹Institute for Chemistry and Biology of the Marine Environment (ICBM), Oldenburg, Germany,

²Department of Ecological Chemistry, Alfred Wegener Institute Helmholtz Centre for Polar and Marine Research, Bremerhaven, Germany, ³Institute of Toxicology and Pharmacology for Natural Scientists, University Medical School Schleswig-Holstein, Kiel, Germany, ⁴Flanders Marine Institute (VLIZ), Oostende, Belgium

The environmental risks associated with dumped munitions, unexploded ordnance (UXO) and sunken war ships is gaining more and more attention nowadays, since these warfare materials may start leaking, posing a threat to marine wildlife. This study aims to assess the effects of pollution by explosives for marine fauna associated with sunken war ships still loaded with munitions at the time of sinking. *For this purpose*, transplanted blue mussels (*Mytilus edulis*) and passive samplers were exposed for several weeks on two WWII warship wrecks (*HMS Basilisk* and *V1302*, formerly named *John Mahn*) to detect leakage of explosives and to characterize the effects of those substances on mussel health. In addition, fish (*Trisopterus luscus*) dwelling at *V1302* were caught and investigated following the same approach as used with the mussels. The hazardous potential of dissolved explosives was assessed using multi-biomarker analysis, which includes the enzyme activity of catalase (CAT), glutathione S-transferase (GST) and acetylcholinesterase (AChE), as well as histochemical biomarkers like lysosomal membrane stability (LMS), lipofuscin (LIPF), neutral lipids (NL) and glycogen (GLY) as an indicator of mussel's energy reserve. Chemical analysis of passive samplers as well as mussel and fish tissue indicated leakage of explosives at both wrecks and a subsequent uptake by exposed organisms. The leakage of explosives was correlated with membrane impairments and signs of oxidative stress measured in exposed mussels and fish.

KEYWORDS

multi-biomarker approach, enzyme activity, dissolved TNT, biological effects, warship wrecks



Highlights

- Investigated wrecks are leaking energetic compounds from corroding munition.
- Blue mussels and fish take up energetic compounds.
- Concentrations of munition compounds are in the order of nanograms per gram tissue.
- Mussels respond to concentrations of dissolved explosive showing signs of oxidative stress.

1 Introduction

Since World War I (WWI) the production of conventional munitions and chemical warfare agents (CWA) increased significantly (Beldowski et al., 2014), as well as their entry into marine waters (Beddington and Kinloch, 2005). There were two main ways of how warfare materials got into the oceans: (1) By war activities including training, mine laying, failed detonations, emergency launches and sunken wrecks loaded with warfare materials (Böttcher et al., 2011) and (2) by intentional dumping operations especially after World War II (WWII) (Böttcher et al., 2011; HELCOM, 2013), chosen as fast and cheap method of demilitarization (HELCOM, 2013).

Throughout WWII, the world experienced the single, largest loss of shipping in any period of time (Gilbert, 2005). For instance, in the East Asian Pacific alone more than 3,800 vessels were sunk during WWII, and it is likely that many of these ships were still

loaded with munitions at the time of sinking (Monfils et al., 2006). Also the North Sea was a so-called watery grave for many ships (Bellamy, 1991). Data from the German Maritime Agency, Hamburg record approx. 120 military shipwrecks (Grassel et al., 2021) from WWI and II within the German Exclusive Economic Zones (EEZ) alone. In the Belgian part of the North Sea (BPNS) there are 140 known and identified wrecks that were sunk during war activities. About one hundred of these shipwrecks may still contain munitions (Deutsches Schifffahrtsmuseum, n.d).

Shipwrecks may pose severe risks to the aquatic environment due to their remaining fuel, their cargo or both. Especially military wrecks may contain considerable amounts of munition shells, mines, depth charges and other explosives, as well as chemical warfare agents (Gilbert, 2005). Hence, shipwrecks are of particular importance for environmental risk assessments. For the present study two identified wrecks, the *HMS Basilisk* and the *V1302* formerly named *John Mahn*, were selected. Main reasons for selection were the confirmation of remaining munitions onboard, the existence of archive information regarding the type of munition and the accessibility of the wrecks for scientific divers. Further information about the ships and their sinking scenarios are provided in the supplement of this study (chapter S.1 and Supplementary Figure S1).

Lost or dumped underwater munitions of the World Wars still endanger the marine environment and human health nowadays. This threat can be divided into three categories: (1) risk of spontaneous detonation and the spreading of unexploded material e.g. during underwater works or when washed onshore

(Appel et al., 2019; Beddington and Kinloch, 2005; Böttcher et al., 2011); (2) direct physical contact with toxic chemicals or munitions and the resulting health risks (Beddington and Kinloch, 2005) and (3) contamination of the marine environment by leaking chemicals through corroded munition shells (Appel et al., 2018; Beck et al., 2019; Beddington and Kinloch, 2005; Böttcher et al., 2011; Strehse et al., 2017). Since both CWAs and explosives are bio-available for organisms (Beck et al., 2022; Höher et al., 2019; Schuster et al., 2021; Strehse et al., 2017) there is also a risk that the released chemicals enter the marine food web (Böttcher et al., 2011; Ek et al., 2006, 2008; Maser and Strehse, 2021).

One of the most commonly used explosives is the nitroaromatic compound 2,4,6-trinitrotoluene (TNT) (Juhasz and Naidu, 2007; Lotufo et al., 2013). TNT and other munition constituents are known to be metabolized in the marine environment: The main metabolic pathway of TNT is the reduction to 2-amino-4,6-dinitrotoluol (2-ADNT) and 4-amino-2,6-dinitrotoluol (4-ADNT) via biotic processes, mainly by bacteria or enzymes of or within marine organisms (Beck et al., 2018; Juhasz and Naidu, 2007). During the manufacturing of TNT, several other nitroaromatic compounds are created as by-products. Most of them get removed or destroyed by the purification processes but some of them remain as contaminants in the munitions (Wellington and Mitchell, 1991). This includes 2,4-dinitrotoluene (2,4-DNT) and 1,3-dinitrobenzene (1,3-DNB), which are only slowly biodegradable (Wexler, 2014). The chemical structure of the mentioned explosives is shown in Figure 1.

TNT, its metabolites 2-ADNT and 4-ADNT, as well as the impurities 2,4-DNT and 1,3-DNB all cause adverse health effects, and are harmful to the aquatic environment (Wexler, 2014). The toxic effects of TNT and other explosives have been shown in several studies using different toxicological endpoints (e.g. Nipper et al., 2001, 2009). However, there is still a scientific controversy whether TNT is more or less toxic than its metabolites (Sims and Steevens, 2008).

To assess the effects of pollutants, mussels have often been used as test organisms (Strehse and Maser, 2020). Blue mussels have several properties which make them suitable bioindicators as summarized by Beyer et al. (2017) and Farrington and Quinn (1973) (e.g. potential of bioconcentrating chemicals, robust organisms, abundant in all world oceans, common prey species, represent the environmental conditions of a specific area due to sessile lifestyle, can be easily transplanted) Mussels, especially

Mytilus spp., are well established bioindicators which have already been used to monitor dissolved energetic compounds (Strehse et al., 2017) or to detect effects of dumped CWAs (Lastumäki et al., 2020).

In addition to mussels, fish have also been used as bioindicators, because these organisms fulfil the general requirements of a bioindicator as reviewed by Kuklina et al. (2013): they are ecologically relevant because they play an important role in the marine food web, they are generally sensitive to stressors, and fish have a wide distribution, etc. Fish are also known to bioaccumulate toxic substances (de Andrade et al., 2003) and may be especially suitable to assess the toxic effects of TNT, as it has been shown that they are sensitive to TNT exposure with LC₅₀-values ranging from 0.8 to 3.7 mg/L (Talmage et al., 1999). For the present study, pout (*Trisopterus luscus*) was chosen as fish model, since the species is known to live around hard substrates like reef structures, stones and wrecks (Mallefet et al., 2007; Zintzen et al., 2006).

TNT and its metabolites are suspected to cause oxidative stress in cells and tissues of exposed organisms (Adomako-Bonsu et al., 2024). In addition, pre-investigations at the wreck sites revealed low exposure concentrations for dissolved TNT. Therefore, biomarkers were chosen which proved already their response to dissolved TNT in lab studies (Schuster et al., 2021) and are capable to function as early warning markers, showing their effects or endpoints on sub-cellular or cellular levels. Further, preference was given to biomarker which can be applied using both fish and mussels as bioindicators. At the conclusion, for the present study the following biomarkers were selected: Lysosomal membrane stability (LMS), enzyme activity of Catalase (CAT), glutathione S-transferase (GST) and acetylcholinesterase (AChE), as well as the biomarkers lipofuscin (LIPF), neutral lipids (NL) and glycogen (GLY). Further information about the biomarkers is available in the [Supplementary Material](#) (chapter S.2).

The aim of the present study was to assess the hazard potential of pollution by explosives and its ecological effects on exposed fauna at two World War II shipwrecks located near the Belgian coast, the British Destroyer *HMS Basilisk* and the patrol boat *V1302*. The objectives were to determine (1) whether the selected shipwrecks emit hazardous energetic compounds and, if so, (2) whether this contamination affects the health condition of the transplanted mussels of the species *Mytilus edulis* and the health of caught fish (*Trisopterus luscus*) by using a multi-biomarker approach including enzyme activities.

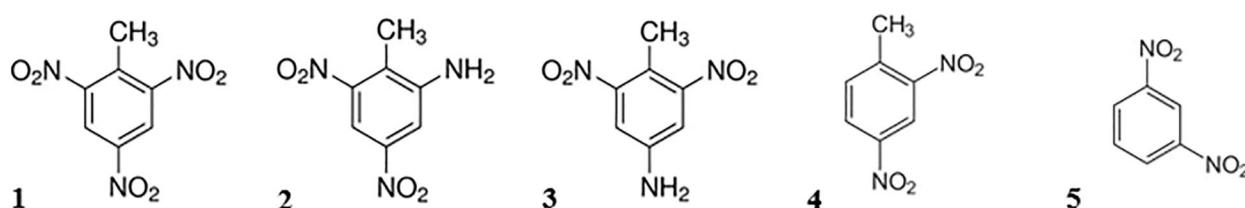


FIGURE 1

Chemical structure of selected explosives. (1) 2,4,6-trinitrotoluene (TNT), (2) 2-amino-4,6-dinitrotoluene (2-ADNT), (3) 4-amino-2,6-dinitrotoluene (4-ADNT), (4) 2,4-dinitrotoluene (2,4-DNT) and (5) 1,3-dinitrobenzene (1,3-DNB).

2 Material and methods

2.1 Study areas

Subjects of the present study were the two wrecks *V1302* (formally named *John Mahn*) and the *HMS Basilisk* (also known as *H11*), as well as the wind park *Belwind* which served as a reference area. All three stations are located in the Belgian part of the North Sea (BPNS), in front of the Belgian coast near the cities Nieuwpoort, Ostend and Zeebrugge (Figures 2, 3).

The BPNS is criss-crossed by several sandbanks (Figure 3). The current in this area can be highly variable due to the tidal cycles, but two main currents can be identified: Near the coast there is a north-easterly current coming from the English Channel into the North Sea. The other current flows further away from the coast in south south-westerly direction parallel to the Westhinder Bank (Maes et al., 2005). Within the BPNS there is a tidal range from approximately 2 to 5 m, with the highest tidal action near the English Channel (Sündermann and Pohlmann, 2011).

The two wrecks are located in different geographical and hydrographical locations. *HMS Basilisk* lies in 10 m depth at 51° 8' 16" N, 2° 35' 6" E, on the Trapegeer sandbank in front of the Belgian coast (Figure 3). The seabed near the shore consists mostly of fine sand (Maes et al., 2005). The front part of the wreck was separated from the main part close to the engine room and lies to port side (Figure 4).

The *V1302* lies approx. 37 km northwest of Zeebrugge at 51° 28' 42" N; 2° 43' 18" E (Figure 3) in 35 meter depth (Gröner et al., 1993; Lettens, 2002). The wreck is positioned on its keel with a slight slope to starboard side (25°) in east-west direction (Figure 5). Below the former water line close to the bridge a big hole from one of the bomb impacts is visible. Depth charges can be found on the

stern. The wreck is entangled with nets, trawls and fishing lines (Lettens, 2002).

The offshore wind park *Belwind* is located in the BPNS on top of the Bligh Bank (51° 39' 36" N, 2° 48' 0" E) and is one of several wind farms operated by *Parkwind*. It covers a surface area of 17 km² and is located 46 km off the coast of Zeebrugge (Figure 3). Water depth at the site is between 20 and 37 m. The wind farm contains 56 turbines at distances of 500 to 650 m and has been operating since 2010 (Belwind, 2017; BOP, n.d.).

2.2 Experimental design

The investigation was conducted during two cruises of the RV Simon Stevin: One cruise in 2019 (labelled as SS1019) to both wrecks, and a second in 2020 (labelled as SS0720) to the *V1302*, during which the main investigation took place. The cruise SS1019 served as test for the feasibility of the experimental setup and to investigate whether any leakage of explosive chemicals occurs at one of the wrecks. For the main investigation the *V1302* was chosen because the wreck is easier to access by divers, since it is further outside the tidal zone and the water is less turbid. During the main experiment, mussels were exposed and fish were caught to determine any potential biological effects as a response to the exposure with dissolved explosives from the wreck. A tabular overview about the experimental setup can be seen in Table 1.

Mussels (*Mytilus edulis*) for transplantation on the wrecks were collected by divers from pylons at the reference area *Belwind* from approx. 10 m depth. Collected mussels were measured and only mussels with a shell length of 6 to 8 cm were kept for the experiment. Nylon net bags were filled with mussels and a set of two passive samplers (Chemcatcher®) to detect energetic



FIGURE 2

Southern part of the North Sea including the economic zones. The area enclosed by green lines represent the Southern Bight. The white shaded area marked with "B" represents the Belgian economic zone (Maes et al., 2005 modified).

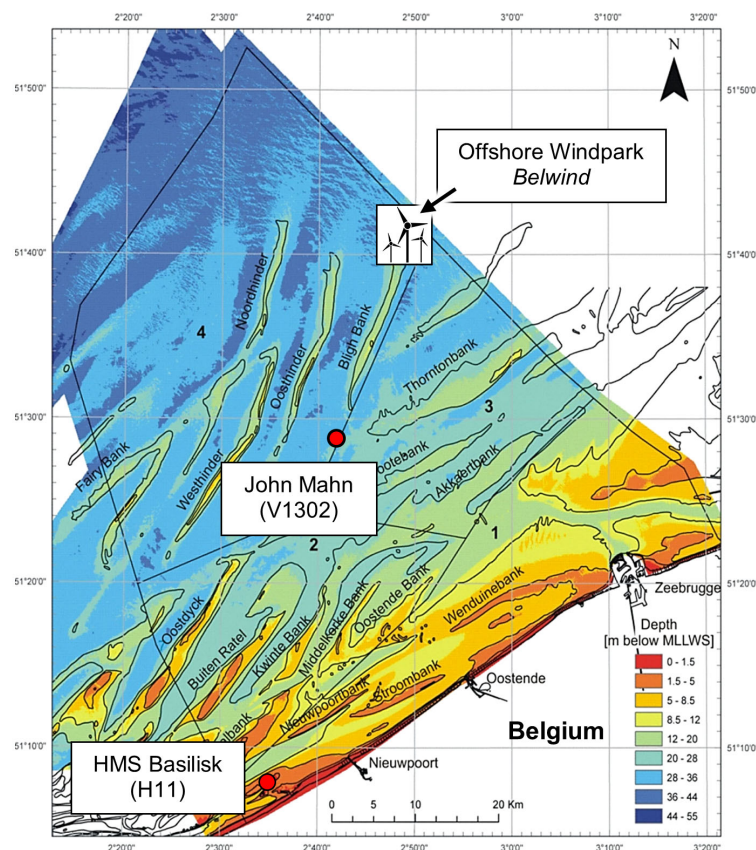


FIGURE 3

Map of the Belgian coast. Positions of the shipwrecks *John Mahn/V1302* and *HMS Basilisk* are indicated by red dots. The wind park reference area *Belwind* is indicated by windmills. The colour code represents depth in m below mean lower low water spring tides (MLLWS) (Mathys, 2009 modified).

compounds during the exposure. The use of passive samplers allows a qualitative detection of energetic compounds within the water column as well as the estimation of their ratio. Transplantation and retrieval of the mussels were conducted by scientific divers.

Mussels at the *HMS Basilisk* were placed at 8 m depth. Due to this wreck's deeper location, mussels at the *V1302* were placed at 30 m depth. During both field experiments passive samplers were also installed at the reference site *Belwind*. In addition, reference mussels

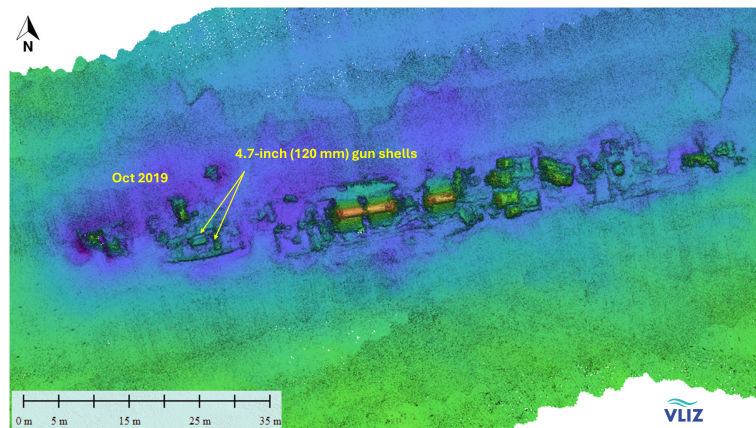


FIGURE 4

Multibeam image of *HMS Basilisk* including the location where mussels were transplanted in 2019.

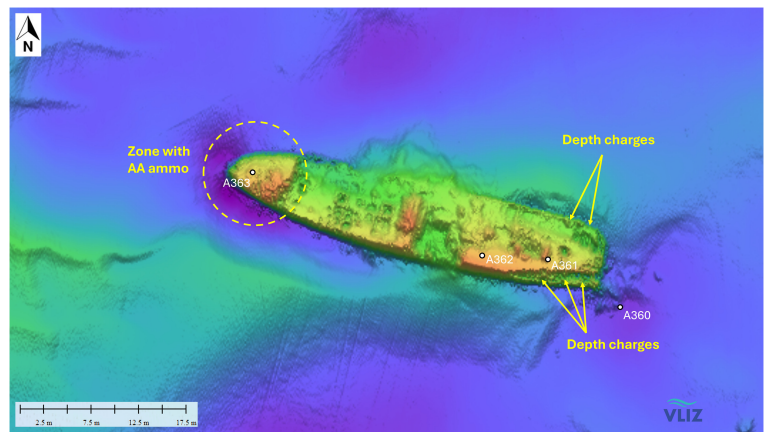


FIGURE 5
Multibeam image of munitions onboard the V1302 and the locations for the transplanted mussels (A360–A363).

were also obtained from the pylons at 10 m depth at the end of the experiments.

During the field experiment in 2019 (cruise SS1019) mussels were exposed at both wrecks: For each wreck one site was chosen close to munition items where mussels were exposed for 3 months (from August until October) together with passive samplers.

The main experiment was conducted in 2020 (cruise SS0720). Here, only the V1302 was investigated, and the mussel nets were placed along the entire length of the wreck (Figure 5). The different stations were labelled A360, A361, A362 and A363. At each station 30 mussels (20 mussel for biomarker analysis, 3 for chemical analysis and the rest as reserve) were exposed for 4 months (from March 13th 2020 until July 30th 2020).

2.3 Mussel and fish sampling, dissection, and morphometric measurements

After the exposure phase mussels were collected and directly processed in the wet lab of the research vessel. Shell length was measured using a Vernier calliper (± 0.1 mm). Total wet weight and shell wet weight were determined using a laboratory scale to calculate the condition index (CI) (Equation 1).

CI = (weight of soft body [g]/weight of shell[g]) * 100 (1)

To prepare the dissection of mussels, the posterior adductor muscle was first cut. Then gill, mantle and digestive gland tissue

were dissected and transferred to cryo-vials. Tissues were snap frozen in liquid nitrogen and stored in nitrogen vapour on board. Back on land, samples were kept at -80°C until further processing. 20 mussels per station were used for biomarker analysis. Three additional mussels per station were used for the chemical analysis of tissues. For chemical tissue analysis the whole soft body was used, which were also snap frozen and subsequently stored at -20°C. Since more than half of the mussels at station A363 had died, only 9 mussels were available for biomarker analysis, and 1 mussel for chemical tissue analysis.

Pouting (*T. luscus*) were caught directly above the wreck at slack water using commercially available sports fishing gear. Twenty specimens of a length above 25 cm were caught at the wreck and the reference site. Caught fish were processed directly on board. Fish were weighed (wet weight), the total length measured and anesthetized by a blow on the head, followed by decapitation prior to the subsequent dissection. The bile was collected by puncture of the gall bladder with needles (0.15 mm × 35 mm) and disposable syringes (1 mL) and transferred into a cryo-vial before snap frozen in liquid nitrogen. In addition, fish livers were investigated macroscopically for nodules and tumours. Pieces of liver were dissected for anti-oxidative-defence measurement and cryo-sectioning, placed in cryo-vials and snap frozen as described above. Another piece of liver was placed in aluminium foil and frozen at -20°C for chemical analysis. Finally, approx. 20 g of skin free muscle tissue from the fish’s filet was dissected and stored in a 15 mL Falcon tube kept at -20°C for chemical analysis. The

TABLE 1 Tabular overview about the experimental setup.

Kind of investigation	Year (cruise)	Study area	Samples	Analysis
Test	2019 (SS1019)	<ul style="list-style-type: none">HMS BasiliskV1302Belwind	<ul style="list-style-type: none">MusselsPassive samplers	<ul style="list-style-type: none">Chemical analysis
Main Investigation	2020 (SS0720)	<ul style="list-style-type: none">V1302Belwind	<ul style="list-style-type: none">MusselsFishPassive samplers	<ul style="list-style-type: none">Chemical analysisHistochemical biomarkerBiochemical biomarker

biometric data were used to determine the Fulton's condition factor (K) as an indicator of the general fish fitness status (Equation 2).

$$K = (\text{total weight [g]} / \text{length [cm]}^3) * 100 \quad (2)$$

2.4 Chemical analysis

The preparation of passive samplers as well as chemical analyses by GC-MS/MS were performed according to Bünning et al. (2021) and Maser et al. (2023). In brief: The PES and HLB membranes of the passive samplers were freeze-dried separately, extracted with acetonitrile, and the extracts were analyzed using GC-MS/MS, consisting of a TSQ 8000 Evo mass spectrometer and a Trace 1310 gas chromatograph with a TG-5MS Amine column (15 m * 0.25 mm * 0.25 µm) (Thermo Fisher Scientific Inc., Waltham, MA, USA). Mussels and fish muscle were freeze-dried, ground, extracted with ACN, purified using 3 mL SPE columns, eluted with ACN, and also analyzed using GC-MS/MS. The bile samples were incubated with glucuronidase for 20 hours, extracted using 1 mL SPE columns, eluted with ACN, and analyzed using GC-MS/MS. All measurements were performed with splitless injections and quantified using external calibration curves.

Detailed descriptions of the methodology, instrument parameters and detection limits used for the GC-MS/MS measurements of the samples from the *V1302* are published in Maser et al. (2023). Sample preparation and analysis of the samples from the *HMS Basilisk* and the reference site are carried out in the same way as described in Maser et al. (2023).

2.5 Biomarker analysis

2.5.1 Biochemical biomarkers

2.5.1.1 Homogenisation of mussel digestive gland, mussel gill tissue and fish liver

Homogenisation of mussel digestive gland tissue and fish liver was conducted using a modified version of the method described by Ahvo (2020a). Samples were individually homogenised in 100 mM potassium phosphate buffer with a pH of 7.0. Mussel digestive gland tissue was diluted at a ratio of 1:10 (tissue in mg, buffer in µL) in 2 mL vials for soft tissue homogenisation and kept on ice. Samples of fish liver were diluted in a ratio of 1:20 (tissue in mg, buffer in µL). Homogenisation of mussel gill tissue was conducted as described by Ahvo (2020d) using a 20 mM sodium phosphate buffer with a pH of 7.0. Buffer used for gill tissue was freshly mixed with 0.1% Triton-X100 on each day. Tissue samples of gill were diluted at a ratio of 1:3 (tissue in mg, buffer in µL) in 2 mL vials for soft tissue homogenisation and kept on ice. Homogenisation of tissue samples was executed using the precellys lysing kit Tissue homogenizing CK Mix (Cat.: P000918-LYSK0-A) and the Precellys® 24 homogenizer (Bertin Technology) by 5000 rpm, 2 x 15 sec with 15 sec break between shakings. To keep temperature at 4°C during homogenisation, a Cryolys® (Bertin Technology) was used and (re)

filled with liquid nitrogen. Samples were then centrifuged with an Eppendorf centrifuge 5430R for 20 min at 4°C at 10000 g. Supernatants were transferred into 1.5 mL Eppendorf tubes and kept on ice until subsequent enzyme analysis.

Enzyme activity measurements for catalase (CAT) and glutathioneS-transferase (GST) activity were conducted using 96-well UV microplates. Acetylcholinesterase (AChE) activity was measured by using non-UV 96-well microplates. Measurements were done with a microplate reader (Infinite 200, TECAN) and analysed with i-control software 2.0. The volume of supernatants, reaction buffer and reagents in the wells for photometric measurements were adjusted to the used tissue samples in the present study. Samples were measured directly after homogenisation. Leftover extracts were frozen at -20°C for the determination of total proteins. Enzyme activity was adjusted to protein concentration in samples according to Bradford (1976). Protein analyses were conducted using the same microplate reader and non-UV 96-well microplates.

2.5.1.2 Catalase activity

Catalase (CAT) activity was determined by measuring the decrease in absorbance at 240 nm. The used method was based on Claiborne (1985/2018) and modified for mussel and fish tissue by Ahvo (2020b). CAT activity was measured with a final concentration of 10 mM H₂O₂.

2.5.1.3 Glutathione S-transferase activity

Glutathione S-transferase (GST) activity was measured using the method based on Habig et al. (1974) and modified for mussel and fish samples by Ahvo (2020c). GST was measured at 340 nm as increase in absorbance when adding a mixture of GSH (glutathione), CDNB (1-chloro-2,4 dinitrobenzene) and Dulbecco's buffer with a final concentration of 2 mM GSH and 1 mM CDNB.

2.5.1.4 Acetylcholinesterase activity

The method used for determining acetylcholinesterase (AChE) activity was based on Bocquené and Galgani (1998) and modified by Ahvo (2020d) for microplates. AChE was measured as increase in absorbance at 412 nm in a mixture containing 0.57 mM DTNB (5,5'-dithiobis 2-nitrobenzoic acid) and 2.86 mM ACTC (acetylthiocholine) in phosphate buffer.

2.5.1.5 Determination of proteins in extract and calculation of activity per protein

Enzyme activity was determined as activity per protein (Equations 3–5). To do so total protein content in extracts were defined according to Bradford (1976) using a bovine serum albumin standard (BSA, Sigma A-6003). Protein analyses were executed by measuring the absorbance at 590 nm. Enzyme activity per protein [U/mg protein] was calculated using the following formulas (used molar coefficients ε: H₂O₂: 43,6 M⁻¹cm⁻¹, CDNB: 9.6 M⁻¹ cm⁻¹, DTNB: 1.36 * 10⁴ M⁻¹ cm⁻¹):

Activity in extract :

$$\left[\frac{U}{ml} \right] = \frac{-\text{slope} \left[\frac{1}{min} \right] * \text{vol well} [mL]}{\text{molar coefficient} \epsilon \left[\frac{1}{mol * cm} \right] * d [cm] * \text{vol sample} [mL]} \quad (3)$$

Activity per fresh weight :

$$\left[\frac{U}{g \cdot fw.} \right] = \text{activity in extract} \left[\frac{U}{mL} \right] * \frac{\text{vol homo-buffer} [mL]}{\text{fresh weight} [g \cdot fw.]} \quad (4)$$

Activity per protein :

$$\left[\frac{U}{mg \text{ protein}} \right] = \frac{\text{activity in extract} \left[\frac{U}{mL} \right]}{\text{protein content} [mg/mL]} \quad (5)$$

2.5.2 Histochemical biomarkers

2.5.2.1 Tissue preparation for histochemical biomarkers

For determination of sex and gonad status of mussels, as well as for lysosomal membrane stability (LMS) and histochemical biomarker analysis, cryostat sections were prepared by gluing (Thermo ScientificTM Richard-Allan ScientificTM Neg-50TM) frozen samples of mussel digestive gland and mantle on pre-frozen aluminium chucks for cryostat sectioning (three samples on one chuck). Tissue sections of 10 µm were obtained using a cryotome (Thermo ScientificTM, Cryo Star NX70) with chamber/knife temperature of -25/-23°C. Per chuck a duplicate section was made. The sections were stored at -80°C until further processing for LMS, lipofuscin, glycogen, and neutral lipid staining (only digestive gland tissue) as well as for sex and gonad status determination (digestive gland and mantle tissue). Sections for LMS analysis were stored for a maximum of 24 h by -20°C before treatment.

2.5.2.2 Determination of sex and gonad status

Cryostat sections of mussel digestive gland and mantle were stained with Gill's Hematoxylin and counterstained using an Eosine-Phloxin solution (HE method) as described e.g. in Brenner et al. (2014). First, cryo-sections were fixed 5 min in Baker's Formalin, rinsed with Milli-Q water for 1-2 min and stained in Gill's Hematoxylin for 15 sec. Sections were then counterstained in Eosine-Phloxin solution for 30 sec. Finally, the stained samples were dipped 6 times in 80% ethanol and dried briefly before mounted with Euparal.

2.5.2.3 Lysosomal membrane stability

The lysosomal membrane stability test was performed according to Moore et al. (2004). First, serial cryostat sections were treated at 37°C for increasing time intervals (2 to 50 min) using a mixture of 0.1 M citrate buffer with a pH of 4.5 and containing 3% NaCl to destabilize the membrane. Subsequently section incubation took place for 15 min at 37°C in a solution containing Naphthol AS-BI Nacetyl b-D-glucosamide (Sigma) dissolved in 2-methoxy ethanol and low-viscosity polypeptide (Polypep, Sigma) dissolved in 0.1 M citrate buffer, pH 4.5 with 3% NaCl. Then sections were treated with Fast Violet B (Sigma) dissolved in 0.1 phosphate buffer with a pH of 7.4 to alter a post-coupling reaction resulting in a violet colour

change. After 10 min samples were rinsed with running tap water and fixed in Baker's Formalin. Finally, slides dried overnight in the dark at room temperature and were then mounted with Kaiser's glycerine-gelatine.

2.5.2.4 Glycogen

The glycogen (GLY) content was used to assess mussel fitness and nutritional status. To determine GLY quantities, duplicate sections were stained using the Perjod-Acid-Schiff-Method (PAS) based on Culling (1974). Duplicate sections were fixed 10 min in Carnoy's fixative rinsed with Milli-Q water, placed in 1% periodic acid, and again rinsed in Milli-Q water. Sections were then stained for 5 min in Schiff's reagent and rinsed with Milli-Q water again. Stained sections were rinsed in a series of different ethanol solutions (50%, 70%, 80%, 96%, 100%) for 1 min each and cleaned with Appliclear until no more colours arises in the water. After a short period of drying, the stained sections were mounted with Permount.

2.5.2.5 Lipofuscin

Lipofuscin (LIPF) accumulation in the lysosomes served as indicator for oxidative stress and was determined using the Schmorl's reaction after Pearse (1985), and modified by Brenner et al. (2014). Duplicate cryostat sections were fixed for 15 min in 4% Baker's formalin, rinsed in Milli-Q water and then stained in a 1% hydrous ferric chloride/potassium ferricyanide (1:1) solution. Afterwards, stained sections were washed in 1% acetic acid for 2 min and rinsed under tap water for 10 min. Finally, sections were rinsed 3 times in Milli-Q water and mounted with Euparal after a short drying period.

2.5.2.6 Neutral lipids

The accumulation of neutral lipids (NL) was determined using the Oil-Red-O method (ORO) after Lillie and Ashburn (1943) modified by Brenner et al. (2014). First, duplicated sections were fixed in Baker's formalin for 15 min, and dipped 15 times in Milli-Q water, followed by washing in 60% Triethylphosphate for 1 min. Afterwards, the sections were stained for 15 min in Oil-Red-O solution containing 1% Oil Red O and 60% Triethylphosphate (solution was pre-cooked for 5 min and filtered hot and cold once) and rinsed again for 30 sec in 60% Triethylphosphate. Finally, the stained sections were rinsed with Milli-Q water, dried and mounted using Kaiser's glycerine-gelatine.

2.5.2.7 Microscopic image analyses

To determine lysosomal membrane stability as well as the lipofuscin, glycogen, and neutral lipid amount in the digestive gland of mussel tissue, a computer assisted image analysis program (camera: MRc, ZEISS; software: AxioVision SE64 Rel. 4.9, ZEISS) combined with a light microscope (Zeiss, Axioskop) at 400-fold magnification were used. For each staining method and sample, three black and white pictures were taken and analysed (3 measurements per individual).

To assess the lysosomal membrane stability the staining intensity of lysosomes was measured. The time needed for

destabilisation of the membrane is reflected by the maximal staining intensity in the lysosomes represented by a “peak”. In general two peaks are present which represent different membrane properties of two sub-populations of lysosomes (Moore et al., 2004). The earlier the peaks occur, the more unstable the membrane was which indicates pre-damage. To determine the labilisation period only the first peak is used (Moore et al., 2004).

For lipofuscin and neutral lipids, image analysis was conducted on selected areas of the image, using the microscope-camera system described above. Suitable areas for image analyses were areas with intact tissue and visible tubules. Within this selected image the areas containing the respective staining was chosen. For glycogen the entire images were analysed because tubules were hard to identify.

Sex and gonadal status were determined using the same light microscope and camera like described earlier at 100-fold magnification. Gonadal status was separated into 3 categories according to Brenner et al. (2014): (1) Recovering (non-discriminable), (2) premature (discriminable) and (3) mature gonads (discriminable). Pictures showing examples of the different categories are given in Supplementary Figure S2 in the supplementary chapter S.3. Numbers of individuals assigned to a specific category were counted and displayed as percentages.

2.6 Statistics

Data was arranged using Microsoft Excel 365, and visualized as well as analysed using R (Version 4.1.0, The R Foundation for Statistical Computing). Data is mostly presented as boxplot. A boxplot visualises the data distribution using quantiles including the median, minimum and maximum values and also outliers. The

Shapiro-Wilk test and Levene’s test were used to test the data for normal distribution and homogeneity of variance. To determine significant differences between the mussel stations a one-way ANOVA was performed, and the Tukey Test was applied as *post hoc* test when data was normally distributed and showed homogeneity in variances. If this was not the case the Kruskal-Wallis ANOVA and the Dunn’s Test were used as non-parametric alternatives. Fish samples were tested with the independent t-test when data were normally distributed and homogenic in variances. As non-parametric alternative the Mann-Whitney U-test was used. Significant levels were set to $p < 0.05$, $p < 0.005$ and $p < 0.0005$. In each graphic, significance levels of wreck station compared to the reference are displayed with stars ($p < 0.05 = *$, $p < 0.005 = **$ and $p < 0.0005 = ***$).

3 Results

3.1 Cruise 2019 – chemical analysis

For the cruise in 2019 passive samplers, TNT, 4-ADNT and 2-ADNT were targeted (Figure 6). Results revealed the presence of explosives at both the *V1302/John Mahn* (JM) and the *HMS Basilisk* (BA) in the order of ng per sampler. The passive samplers at *V1302* had a higher total concentration of explosives (JM: Average concentration of 22.5 ng/sampler. BA: Average concentration of 16.5 ng/sampler). In general, TNT was found at the highest concentration (JM S1: 8.2 ng/sampler, JM S2: 15.1 ng/sampler, BA S1: 5.2 ng/sampler, BA S2: 7.9 ng/sampler), followed by 2-ADNT (JM S1: 5.2 ng/sampler, JM S2: 6.8 ng/sampler, BA S1: 3.1 ng/sampler, BA S2: 9.1 ng/sampler) and 4-ADNT (JM S1: 4.5 ng/sampler, JM S2: 5.2 ng/sampler, BA S1: 2.5 ng/sampler, BA S2: 5.2 ng/sampler).

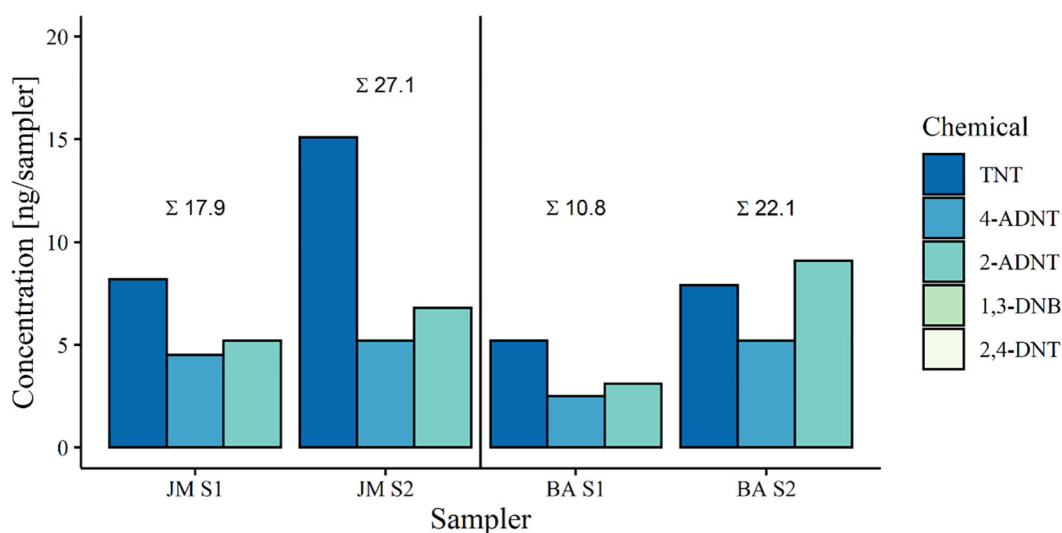


FIGURE 6

Energetic compounds detected in passive samplers during the exposure phase in 2019. Targeted chemicals were TNT (2,4,6-trinitrotoluene), 4-ADNT (4-amino-2,6-dinitrotoluene) and 2-ADNT (2-amino-4,6-dinitrotoluene). JM = *V1302/John Mahn*, BA = *HMS Basilisk*.

3.2 Cruise 2020

3.2.1 Chemical analysis

Concentration of energetic compounds measured within passive samplers at the different stations revealed the presence of explosive chemicals within the water column in the order of ng per sampler (Table 2). Dissolved explosives were not only detected at the wreck sites of the *V1302* (average explosive concentration 28.6 ng/sampler. A361: 25.4 ng/sampler, A362: 50.7 ng/sampler, A363: 9.6 ng/sampler) but also at the reference site (average explosive concentration: 16.1 ng/sampler). Except for station A362, TNT concentrations were highest at the exposure locations. The highest TNT concentration was detected at station A361 with 19.1 ng/sampler, followed by A362 with 17.3 ng/sampler, the reference area with 8.7 ng/sampler and the lowest concentration was found at A363 with 7.6 ng/sampler. At station A362, 1,3-DNB showed the highest concentration (28.7 ng/sampler), whereas this chemical was not detectable at the other stations. For station A360, no data were available because the passive samplers vanished during the exposure. It should be noted here that passive sampler data give only a rough indication on the leakage of explosives from corroding munitions.

The concentrations of explosives in freeze-dried mussel tissues were an order of magnitude lower relative to the concentrations found in the passive samplers (Table 2). The overall amount of energetic compounds within mussel tissue was similar at the different stations at the *V1302* wreck site (Table 2). The highest amount of energetic compounds was measured in mussels collected at station A362 with 5.1 ng/g dry weight (d. w.) followed by A360 (4.7 ng/g d. w.), A361 (4.3 ng/g d. w.) and A363 (2.3 ng/g d. w.). Results from the reference site are not available as no samples were taken for chemical analysis. At all stations, TNT concentration was consistently highest (A360: 2.9 ng/g d. w., A361: 1.9 ng/g d. w., A362: 2.9 ng/g d. w., A363: 1.2 ng/g d. w.). Concentration of other chemicals were comparable with a level of < 1 ng/g d. w.

3.2.2 Biomarker studies at the *V1302* using blue mussels

3.2.2.1 Condition index

Condition indices (CI) of mussels at the wreck and the reference area did not show significant differences ($p = 0.117$), although the CI of mussels at the reference site was generally slightly lower (72.08 ± 21.78) compared to the CI of the wreck (88.63 ± 26.78) (Figure 7). CI of mussels collected at the wreck were similar (A360: 83.26 ± 24.1 , A361: 91.45 ± 26.2 , A362: 91.81 ± 27.74 , A363: 87.48 ± 33.89).

3.2.2.2 Glycogen content

Glycogen (GLY) contents in the mussel digestive gland cells were similar between the different stations except for station A362

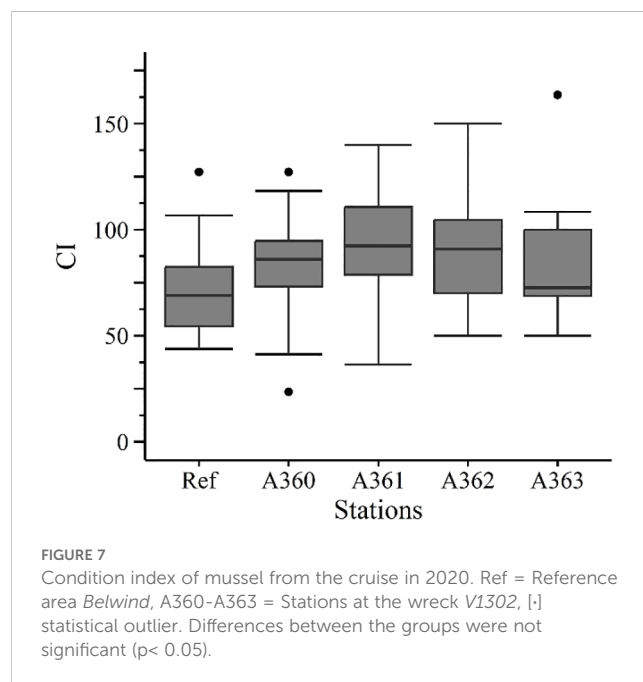


TABLE 2 Mussel and passive sampler chemical analysis of the 2020 cruise to *V1302* (Maser et al., 2023).

Mussel sample	1,3-DNB [ng/g d.w.]	2,4-DNT [ng/g d.w.]	TNT [ng/g d.w.]	4-ADNT [ng/g d.w.]	2-ADNT [ng/g d.w.]
A360	0.6	<LOD	2.9	0.7	0.5
A361	0.9	<LOD	1.9	0.5	1.0
A362	0.8	<LOD	2.9	0.7	0.7
A363	0.6	<LOD	1.2	0.3	0.5
Passive Sampler	1,3-DNB [ng/PS]	2,4-DNT [ng/PS]	TNT [ng/PS]	4-ADNT [ng/PS]	2-ADNT [ng/PS]
Belwind (ref. site)	<LOD	<LOD	8.7	5.0	2.4
A361*	0.6	0.3	19.1	2.7	2.7
A362**	28.7	1.7	17.3	1.4	1.6
A363***	<LOD	<LOD	7.6	1.2	0.8

*A361 Only 1 PS on the position. Both membranes were intact.

**A362: PS 1 approx. 25% of the membrane area was missing. PS 2 had no membrane left at all.

***A363: In one PS the membrane was completely missing, in the other only the pinched edge of both membranes was present, rest was missing. LOD was in the order of fg/μL.

(Figure 8): Station A362 had a GLY level of $19 \pm 3.52\%$ whereas the other stations had a similar GLY level of 13.02 up to 13.96% (A360: $13.36 \pm 1.69\%$, A361: $13.06 \pm 1.74\%$, A363: $13.02 \pm 1.46\%$, Ref: $13.96 \pm 1.83\%$). Mussels at station A362 showed significant higher values than at station A360 ($p = 0.011$) and A361 ($p = 0.013$).

3.2.2.3 Gonad status

Gonad status between the stations showed no significant differences (Figure 9). Most of the mussels were immature or recovering (45 to 65%), followed by premature (22 to 40%) and mature (5 to 33%). In general, half of the collected mussels had

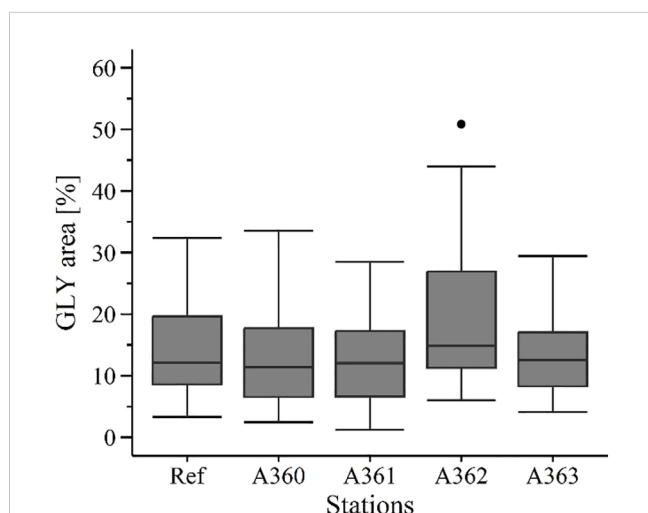


FIGURE 8
Glycogen content [%] in digestive gland tissue of mussels from the cruise in 2020. Ref = Reference area Belwind, A360-A363 = Stations at the wreck V1302, [-] statistical outlier. Differences between the groups were not significant ($p < 0.05$).

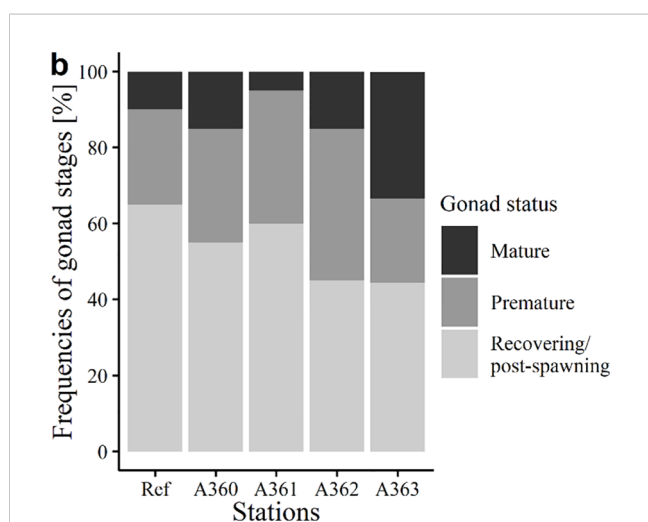


FIGURE 9
Gonad status of mussels [%] from the cruise in 2020. Ref = Reference area Belwind, A360-A363 = Stations at the wreck V1302.

differentiable gonads (premature + mature) while the other half of mussel individuals could not be determined sexually.

3.2.2.4 Biochemical biomarkers

Catalase (CAT) activity was higher in mussel tissue of the wreck sites (average: 25.72 ± 9.24 U/mg protein) in comparison to the reference area (20.74 ± 7.87 U/mg protein) but only station A361 showed significance over the reference ($p = 0.017$) with an activity of 29.79 ± 9.87 U/mg protein (Figure 10a).

Activity of glutathione S-transferase (GST) was generally lower than CAT activity. GST activity showed similar levels for mussels at wreck sites (average: 6.16 ± 3.63 U/mg protein) and the reference site (7 ± 3.76 U/mg protein) (Figure 10b). Activity levels were ranging from 5.36 ± 4.23 U/mg protein (A360) up to 7.16 ± 4.09 U/mg protein (A363) with no significances.

Acetylcholinesterase (AChE) activity was in general one dimension lower than CAT and GST activity (Figure 10c). It must be noted that AChE activity was measured in gill tissue and not in digestive gland as the other enzymes. AChE in mussel tissue of the wreck sites had only slightly lower activity (average of all wreck stations: 17.16 ± 8.53 mU/mg protein) compared to the reference (19.53 ± 13.14 mU/mg protein). Station A360 had the lowest activity with 14.67 ± 7.11 mU/mg protein. However, differences were not significant.

3.2.2.5 Histochemical biomarkers

Results of the lysosomal membrane stability (LMS) analysis showed a similar pattern for peak 1 and 2 (Figure 11). For both, the peaks of the reference mussels occurred significantly later than compared to wreck mussels. The first peak of LMS in reference mussels and mussels from station A362 occurred mainly after 20 min, whereas mussels of the other stations showed the first peak between 10 and 15 min. Also, for the second peak reference mussels and mussels from station A362 showed a later response with a peak after 40 min compared to the other station which had a peak after 35 min. Furthermore, both peaks showed significant differences between the stations (first peak: Ref vs A360: $p < 0.0005$, Ref vs A361: $p < 0.005$, Ref vs A363: $p < 0.05$, A360 vs A362: $p < 0.005$, A361 vs A362: $p < 0.005$, A362 vs A363: $p = 0.04$; Second peak: Ref vs A360: $p < 0.005$, Ref vs A361: $p < 0.0005$, Ref vs A363: $p < 0.005$, A361 vs A362: $p = 0.01$).

Lipofuscin (LIPF) level in digestive gland cells was measured between 8 and 12.5% with significant differences between stations ($p < 0.0005$) (Figure 12a). Significant differences were detected between reference and A361 ($p = 0.033$) as well as between reference and A362 ($p < 0.0005$). Further, differences with statistical significance could also be detected between station A360 and A361 ($p = 0.006$), A362 ($p < 0.0005$) and A363 ($p = 0.031$). The highest LIPF content in average could be detected in mussels from the station A360 ($12.53 \pm 0.65\%$) and from the reference ($12.20 \pm 1.10\%$). The lowest content was found in mussels from station A362 ($8.63 \pm 0.75\%$).

Neutral lipid (NL) content in mussel tissue was slightly lower in mussels of the reference (2.63 ± 1.42) compared to wreck mussels (average of wreck: $5.54 \pm 1.43\%$). (Figure 12b). Significant

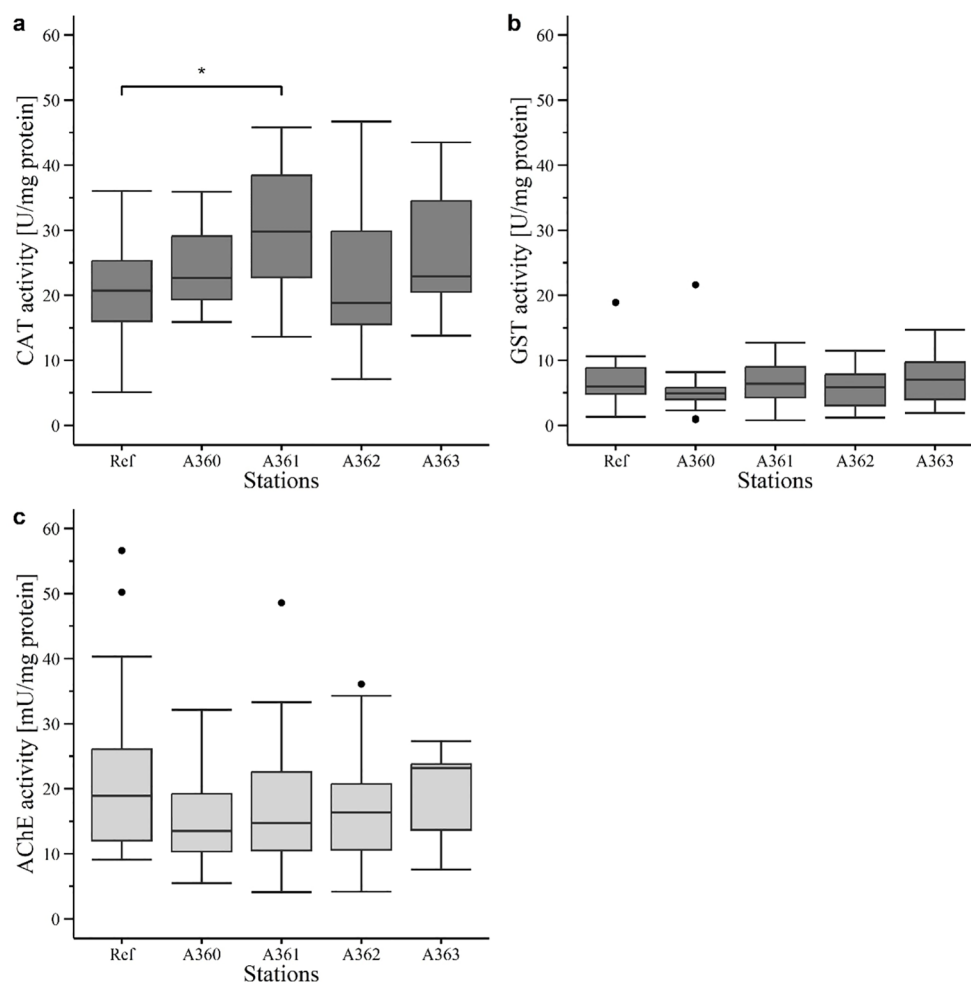


FIGURE 10

Enzyme activity in digestive gland (dark grey) and gill tissue (light grey) of mussels in 2020: **(a)** Catalase (CAT) activity (U/mg protein). **(b)** Glutathione S-transferase (GST) activity (U/mg protein). **(c)** Acetylcholinesterase (AChE) activity (mU/mg protein). Ref = Reference area *Belwind*, A360 – A363 = Stations at V1302, [-] statistical outlier. Significant differences to the reference are displayed with stars ($p < 0.05 = *$).

differences were detected for reference compared with station A360 ($p = 0.0006$), A361 ($p = 0.0015$) and A362 ($p = 0.014$).

3.2.3 Exposed fish

Fish liver samples were taken from both the V1302 wreck and the reference site to assess the biomarker response within these tissues according to the exposure to dissolved TNT and its metabolites deriving from corroding munition onboard the wreck. However, the fat content of the liver samples was relatively high. Hence, samples remained soft and smeary even after being stored at -80°C , making it impossible to cut and process the samples with a cryotome. Therefore, no LMS and histochemical biomarker analysis could be conducted. The remaining tissues were used for the assessment of enzyme activities (see below).

3.2.3.1 Chemical analysis

Chemical analysis of the fish filets revealed the presence of TNT and its degradation products within fish (Table 3). The average detected TNT concentration was 4.2 ng/g d.w. Two individuals

showed a clearly higher concentration, up to 3 times higher than average (12.8 and 10.3 ng/g d.w.). The lowest TNT concentration was 1.7 ng/g d.w. In general, the average detected TNT concentration was 4 times higher than the degradation products 4-ADNT and 2-ADNT, whereas 2-ADNT was slightly higher than 4-ADNT (average 2-ADNT: 1.6 ng/g d.w. 4-ADNT: 1.1 ng/g d.w.). 2-ADNT concentrations ranged from 0.7 up to 2.1 ng/g d.w. and 4-ADNT ranged from 0.9 up to 3.2 ng/g d.w. 1,3-DNB and 2,4-DNT were mostly beneath the limit of detection. 1,3-DNB (0.2 ng/g d.w.) and 2,4-DNT (0.6 ng/g d.w.) were only detected in the filet with the highest TNT concentration. 2,4-DNT could also be detected in one additional filet with a concentration of 1.1 ng/g d.w. The fish bile contained only very low concentrations of 2-ADNT (up to 0.5 ng/g d.w.) and 4-ADNT (up to 0.6 ng/g d.w.) whereas TNT could not be detected.

3.2.3.2 Fulton's condition factor

The condition factor (K) between caught fish at the reference site (1.49 ± 0.26) and at the V1302 wreck (1.54 ± 0.17) showed no significant differences.

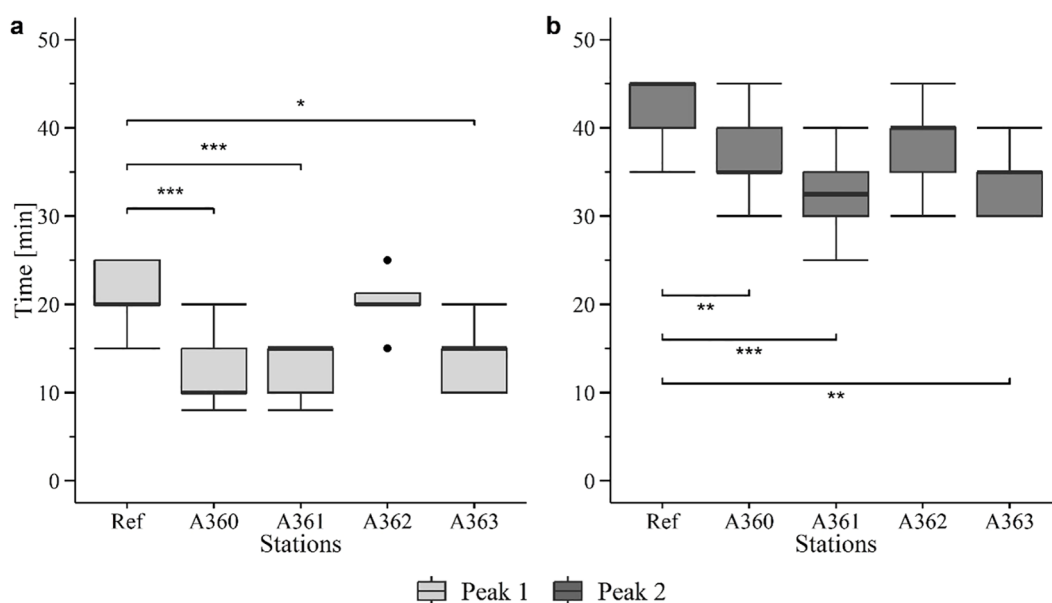


FIGURE 11

Boxplots of lysosomal membrane stability (LMS) of peak 1 (a) and peak 2 (b) in cells of mussel digestive gland tissue from the cruise in 2020. Ref = Reference area Belwind, A360 – A363 = Stations at V1302, [-] statistical outlier. Significant differences to the reference are displayed with stars ($p < 0.05 = *$, $p < 0.005 = **$ and $p < 0.0005 = ***$).

3.2.3.3 Biochemical biomarkers

Catalase (CAT) activity in fish liver were very similar between the fish caught at the reference area (165 ± 78.85 U/mg protein in average) and the wreck site (165.1 ± 62.52 U/mg protein in average)

(Figure 13a). Therefore, no significant differences could be detected between the stations. The glutathione S-transferase (GST) activity also showed no significant differences between the reference and wreck sites (Figure 13b), even though the fish caught at the wreck

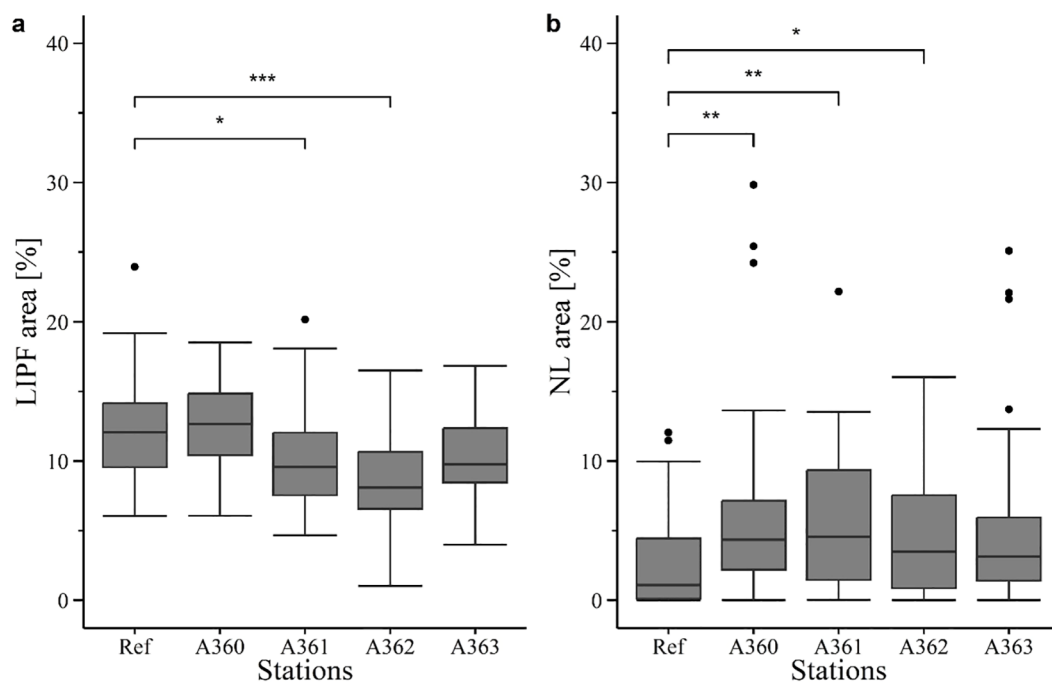


FIGURE 12

Histochemical biomarkers determined in tissue cells of digestive gland in mussels in 2020. Ref = Reference area at Belwind, A360 – A363 = Stations at V1302, [-] statistical outlier. Significant Differences to the reference are displayed with stars ($p < 0.05 = *$, $p < 0.005 = **$ and $p < 0.0005 = ***$) Used biomarkers were (a) lipofuscin content (LIPF) and (b) neutral lipids (NL).

TABLE 3 Chemical analysis of fish file samples and bile caught during the 2020 cruise at V1302 (Maser et al., 2023).

Filet	1,3-DNB [ng/g d.w.]	2,4-DNT [ng/g d.w.]	TNT [ng/g d.w.]	4-ADNT [ng/g d.w.]	2-ADNT [ng/g d.w.]
Filet 1	<LOD	<LOD	4.8	0.7	0.9
Filet 2	0.2	0.6	12.8	1.8	3.2
Filet 3	<LOD	<LOD	3.8	0.9	1.4
Filet 4	<LOD	<LOD	6.8	2.1	2.6
Filet 5	<LOD	1.1	5.6	1.4	1.8
Filet 6	<LOD	<LOD	10.3	1.9	2.8
Filet 7	<LOD	<LOD	5.4	1.4	2.0
Filet 8	<LOD	<LOD	5.0	1.1	1.5
Filet 9	<LOD	<LOD	4.0	0.8	1.2
Filet 10	<LOD	<LOD	4.7	1.1	1.5
Filet 11	<LOD	<LOD	4.3	1.3	1.9
Filet 12	<LOD	<LOD	3.6	1.1	1.7
Filet 13	<LOD	<LOD	4.0	1.1	2.0
Filet 14	<LOD	<LOD	3.6	1.0	1.7
Filet 15	<LOD	<LOD	2.6	0.9	1.4
Filet 16	<LOD	<LOD	2.3	0.8	1.1
Filet 17	<LOD	<LOD	2.6	0.9	1.4
Filet 18	<LOD	<LOD	1.8	0.7	1.1
Filet 19	<LOD	<LOD	2.0	0.8	1.2
Filet 20	<LOD	<LOD	1.9	0.7	0.9
Filet 21	<LOD	<LOD	2.0	0.9	1.2
Filet 22	<LOD	<LOD	1.8	0.8	1.1
Filet 23	<LOD	<LOD	1.7	0.9	1.0
Bile	1,3-DNB [ng/mL]	2,4-DNT [ng/mL]	TNT [ng/mL]	4-ADNT [ng/mL]	2-ADNT [ng/mL]
Bile 18	<LOD	<LOD	<LOD	<LOD	<LOD
Bile 20	<LOD	<LOD	<LOD	0.6	0.5
Bile Pool 1*	<LOD	<LOD	<LOD	0.4	0.4

*Contains 32 μ L bile of fish 5 and 53 μ L of fish 6.

LOD was in the order of fg/ μ L.

had a general higher enzyme activity (110.41 ± 51.98 U/mg protein in average) than the reference fish (87.77 ± 40.33 U/mg protein in average).

4 Discussion

Wrecks can be a source of many pollutants depending of their cargo, armament and the vessel's propulsion. The wrecks investigated for this study were coal or fuel-oil driven. To keep the engine running also lubricants and smears sometimes based on mineral oil derivatives were used. In addition, steel ships were

protected against sea water driven corrosion by covering the hull with lead containing coatings. Finally, the ships were loaded with munition filled with toxic explosives. Thus, making the wrecks a point source of a pollutant mixtures most probably unique for a specific wreck. For remaining munition investigations using archive information and battle reports were done to estimate amount of munition still on the wrecks at least until the time of sinking. Further, in case of V1302 and HMS Basilisk the remaining munition was visually confirmed by divers. Overall, munition is assumed to be the prominent source of pollutants on the investigated wrecks, knowing, that other pollutants may add to the responses of biomarker analysed for this study.

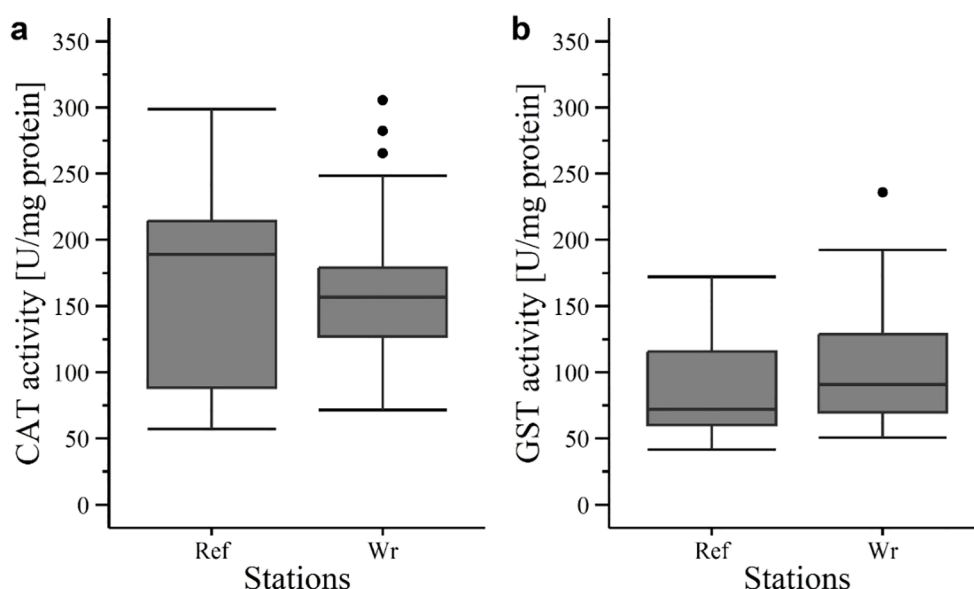


FIGURE 13

Enzyme activity in liver tissue of fish in 2020 at V1302: (a) Catalase (CAT) and (b) glutathione S-transferase (GST) activity. Ref, reference; Wr, wreck; [·] statistical outlier. Differences between the groups were not significant ($p < 0.05$).

It is well established that explosives are taken up, metabolized and accumulated in marine organisms of different types (Ballentine et al., 2015; Lotufo et al., 2009; Rosen and Lotufo, 2007b). Several studies have shown that exposure to explosives poses a threat to a variety of marine species. For instance, Nipper et al. (2001) showed negative effects of TNT, tetryl and hexogen on different marine species like algae, polychaetes, opossum shrimps and redfish, with a lowest effective concentration ranging from 0.26 to 7.6 mg/L. It is also known that exposure to munition compounds has varying degrees of effects on different life stages. Rosen and Lotufo (2007a), for instance, showed a higher sensitivity of juvenile mussels (*Mytilus galloprovincialis*) against exposure to explosives compared to adults. Exposure can also trigger a change in behaviour as reported by Schuster et al. (2021). They found higher numbers of mussels with closed valves when Baltic blue mussels of the *Mytilus* family were exposed to higher TNT concentrations. They also reported effects of TNT exposure on different stress biomarkers. Most of the available studies are laboratory experiments using concentrations of munitions compounds that are much higher than those found in the environment. Knowledge about effects of dissolved explosives under field conditions is still scarce, but studies are now being published that show a response of organisms and benthic communities to dissolved explosives from dump and wreck sites of conventional munitions (Van Landuyt et al., 2022; Vedenin et al., 2023).

To assess the environmental risks of sunken warships and their cargo, two research expeditions to preselected wrecks were conducted, one in October 2019 (SS1019) and one in July 2020 (SS0720). The aim of the cruise SS1019 was to determine if the wrecks exhibit leakage of chemicals, and whether the exposure setup and sampling methods were suitable for the planned experiments. It

turned out that both wrecks showed leakage of dissolved explosives. The V1302 was finally selected as the main research site in 2020, because the wreck site of the *HMS Basilisk* is under strong tidal influence. This results in high current velocities and turbid water, restricting the diver-based operations necessary to transplant and retrieve the mussels.

Due to the relatively short exposure time of 4 months possible responses of mussels were expected to be on low organisational levels, e.g. on subcellular, cellular and tissue levels. Therefore, the present study used several biomarkers which are known for potential alternation at low concentrations of pollutants. This includes histochemical biomarkers and the measurements of the energy status as well as the assessment of enzyme activities of the Anti-Ox-Defence-System. The same biomarker approach was then used to assess also the fish caught at the wreck and reference area.

4.1 Bioavailability of warfare chemical substances in the marine environment

Chemical analyses revealed leakage of explosives at the V1302 and *HMS Basilisk* as well as uptake by transplanted mussels and wild fish. Traces of explosives could be detected within the water and sediment, as well as mussel and fish tissue (for results of water and sediment samples, see Maser et al. (2023)). Detected explosives within the various samples were on the order of ng per unit. This fits with the usually detected concentrations of munition compounds within environmental samples which is on the order of ng/L or $\mu\text{g/kg}$ as reviewed by Beck et al. (2018). Recent studies already showed the potential of explosive leakage through corroded munition shells. For instance, Strehse et al. (2017) detected leakage of munition compounds at a bulk of explosives and Appel

et al. (2018) near a pile of corroded mines in Kiel Bight, Baltic Sea. Both studies used transplanted mussels for assessing the leakage. Dissolved TNT leaking out of the munition shells can be metabolised, mainly by bacteria (Juhász and Naidu, 2007; Rosen and Lotufo, 2007b) or by enzymes within the marine biota (Koske et al., 2020). Munition compounds as well as their metabolites are taken up and further metabolized by mussels (e.g. Appel et al., 2018; Schuster et al., 2021; Strehse et al., 2017). For instance, Appel et al. (2018) and Strehse et al. (2017) could detect explosive concentrations within mussel tissue in the order of ng/g mussel tissue. This is in accordance with the findings of the present study where mussel tissue also contained explosive concentrations in the order of ng/g mussel tissue. It is known that *M. edulis* contains several enzyme systems like cytochrome P-450 monooxygenase which may play a role in TNT metabolism (Livingstone and Pipe, 1992). Lab exposure experiments using blue mussels provided further evidence for the ability of mussels to metabolise TNT, since after the exposure to dissolved TNT mostly TNT metabolites were found in the investigated mussel tissues (Schuster et al., 2021).

4.2 Comparability of physiological status of mussel individuals

Species reproduction is an energy consuming and stressful process. Mussels also invest a lot of energy into their gametes and into spawning (Mredul et al., 2024). Individuals which have recently spawned are most probably not comparable, regarding their energy and stress level, to individuals that are still developing their gonads. To ensure that mussels used in the experiments were in a similar physical condition, the gonad status was determined. Further, also the condition index of all investigated mussels was tested for differences. As result no significant differences between mussel from the two different sites were detectable, suggesting that site specific geo- and hydrographical conditions did not influence mussel condition.

Mussels transplanted to the *V1302* and *HMS Basilisk* were first collected from the reference area and pre-sorted according to their size before caged and transplanted. After the exposure mantle tissue of all exposed specimen was analysed for the gonad status. The results show that mussels from the different exposure stations of the *V1302* and from the reference site were in a comparable physiological state as indicated by a similar gonad status. Approximately, half of the mussels had mature/premature gonads and the other half were still developing, which fits with the seasonal time of mussel sampling. The general spawning period of *Mytilus edulis* extends from April until the end of June and in Autumn gonads begin to build up again (Sprung, 1983).

4.3 Effects of leaked explosives on mussels and fish

Leaked munition compounds show a slow dissolution (Beck et al., 2018) and are usually found in ng/L concentrations in the

aquatic environment (Beck et al., 2019; Kammann et al., 2024; Koske et al., 2020). It has therefore been suggested that those compounds are unlikely to cause acute toxicity or even lethal effects in organisms living at or in the vicinity from munition dumping sites (Beck et al., 2018, 2019). This appears to be true for the present study. Lethal concentrations of dissolved TNT are in the range of mg/L for many marine organisms, but at the two wreck sites investigated here measured concentrations in the water column were in the range of ng/L. This means that the caged mussels were exposed to concentrations of dissolved TNT reflecting a chronic toxicity level.

To measure the effects of chronic toxicity a multi-biomarker approach focussing on early warning marker on sub-cellular and cellular levels was used. Enzymes of the Anti-Ox-Defence system, such as catalase (CAT) and glutathione S-transferase (GST) were tested in both exposed fish and mussels. In mussels, CAT activity tended to be higher in individuals exposed at the wreck site. However, there was only a single, low significant difference detected for one wreck station (A361) relative to the reference site. This is in line with findings from Schuster et al. (2021) who conducted an exposure experiment under laboratory conditions in which mussels (*Mytilus* spp.) were exposed for 96 h to 10 mg TNT/L (acute exposure experiment) and 21 d to 2.5 mg TNT/L (chronic exposure). In this study, the authors could not detect significant increased CAT activity during the acute exposure. During the chronic exposure experiment CAT activity was only increased in gill tissue but not in the digestive gland. It has been suggested that CAT activity in gill tissue is more sensitive to environmental pollutants than other tissues due to their physiological role in respiration (Regoli and Principato, 1995). For future studies, it might be of interest to detect CAT activity in mussel gills as well.

GST activity in mussels of the present study was similar between wreck stations and the reference area and showed no significant differences. This is in line with another study conducted by Höher et al. (2019) who exposed *M. trossulus* for 96 h hours to CWA's in the order of µg/L in a lab-controlled experiment. In this study the chemical concentration used was too low to trigger GST adaptation. TNT exposure has previously been shown to increase GST activity in mussels, as reported by Schuster et al. (2021). The authors could detect a significant increase of GST activity in the chronic exposure experiment in mussels exposed to 1.25 and 2.5 mg/L TNT. Combined, these studies suggest that the exposure concentrations of dissolved TNT in our study were too low to induce significant GST activity.

Results of the neurotoxic biomarker acetylcholinesterase (AChE) exhibited a lower activity in mussel tissue of the wreck sites than those found in the reference area. In general, a lowered AChE activity is a sign of reaction to pollution, but the differences in AChE activity were not significant. This finding matches the results found by Lastumäki et al. (2020) and Schuster et al. (2021). Both, the field experiment conducted by Lastumäki et al. (2020) and the two laboratory experiments conducted by Schuster et al. (2021) did not reveal a significant increase in AChE when mussels were exposed to munition compounds. Further, it is suggested that AChE inhibition and the alteration of antioxidant enzymes like

CAT are reversely correlated as reviewed by Lionetto et al. (2011). However, this phenomenon could not be observed in the present study.

Results of the lysosome membrane stability (LMS) in mussels show a clear pattern. Membrane stability was significantly higher in cells of the digestive gland tissue at the reference site than at all exposed mussels except for station A362. This is true for both peak 1 and 2. A possible explanation is that labialisation of membranes is caused by oxyradicals, developed due to the presence of TNT and its metabolites within the cells. Other studies showed that low LMS values are negatively correlated with high values of neutral lipids (NL) and lipofuscin (LIPF) (Krishnakumar et al., 1994, 1997; Lastumäki et al., 2020). In the present study, the results showed an increase in NL in tissue of wreck mussels but a decrease in LIPF.

LIPF content in wreck mussels were generally lower compared to reference mussels, but only two stations showed significant differences (A361 and A362). In addition, the significant level of station A361 was only on low level. In general, a downregulation of biomarkers could indicate a bell-shaped response (Regoli, 2000; Viarengo et al., 2007). If that would be the case for our data, then LIPF of all wreck stations should be significant lower compared to the reference and CAT activity should show a significant negative correlation to LIPF. Since these trends were not observed, a bell-shaped response seems unlikely. However, the exposure concentration might be too low to trigger a response. For instance, Lastumäki et al. (2020) conducted a field experiment with transplanted mussels (*Mytilus trossulus*) were mussels were exposed 2.5 month at dumping sites of chemical warfare agents (CWA) in the Baltic Sea. The concentrations of munition compounds found in mussel tissue was on the order of ng/L and they could not detect an increase in LIPF content either. In contrast, an increase in LIPF content can be observed when mussels are exposed to high TNT concentrations (10 mg/L conducted over 96 h), as shown by the laboratory exposure experiment conducted by Schuster et al. (2021).

An accumulation of NL in digestive gland cells of mussels is associated with stress induced by toxic chemicals indicating lipidosis (Krishnakumar et al., 1994; Lowe, 1988; Viarengo et al., 2007). In the present study significantly higher NL levels were found in wreck mussels compared to the reference. Accordingly, Schuster et al. (2021) could detect an increase in NL when mussels were exposed to higher TNT concentration up to 2.5 mg/L during the chronic exposure experiment. In the present study the detected explosive concentrations at the sampling sites were only on the order of ng/L, but there is still an effect visible. It should, however, be noted that the highest NL content was not necessarily found at stations where mussels had the highest TNT concentration in their tissues.

Glycogen (GLY) is the primary energy reserve in most bivalves (Patterson et al., 1999). The GLY storage is affected by various environmental factors including chemical pollution which induces stress in the organisms. This often leads to an increased metabolism and a reduced GLY storage. Therefore, in the present study a lower amount of GLY was expected in mussels located near to munition due to the increased energy requirements caused by increased stress.

However, this could not be observed. All stations showed a similar GLY level with exception of station A362 which had an increased GLY content compared to the other wreck stations A360 and A363 but not to the reference site. Schuster et al. (2021) also, could not detect a decrease in GLY of digestive gland cells when mussels were exposed to TNT, despite using a much higher concentration than what was detected at the wreck stations of the present study. Even though some of the tested biomarkers in the present study showed a response to chemical pollution, the effects were not prominent enough to change the energy storage of mussels. This is also true for the individual level, since the Condition Index CI did not differ between mussels exposed at the wrecks site and those from the reference. However, considering the available literature, this seems to be plausible given the low exposure concentrations and the relatively short time of exposure.

In addition to the mussel caging experiment, wild fish were also caught at the wreck and reference sites and tested for biomarker responses. Fish samples showed no significant alteration in Fulton's Condition Factor (K) and enzyme activity when exposed to dissolved explosives at the wreck site compared to the reference area. Only GST activity showed an increasing trend in fish from the wreck site, although the difference was not statistically significant. In contrast, Ek et al. (2005) already proofed that TNT can have an influence on GST activity in fish: They could detect a significant higher GST activity in fish (*Oncorhynchus mykiss*) intraperitoneally injected with TNT when compared to a control. Della Torre et al. (2008) also found increased GST activity in European eel (*Anguilla anguilla*) when exposed to higher TNT concentrations in a laboratory experiment. Further, Niemikoski et al. (2020) could detect a significant change in CAT and GST activity in Atlantic cod (*Gadus morhua*) from chemical munition dumpsites in the Baltic Sea when exposed to CWAs. However, the test organisms used in those studies were exposed to higher concentrations of munition compounds (lab studies) or to different chemicals (Niemikoski et al., 2020).

The acute and chronic toxicity of TNT and its metabolites has, nevertheless, already been reported for many fish species by older studies like those reviewed by Talmage et al. (1999). Recent studies also proved that fish take up TNT (Maser et al., 2023) and CWA (Niemikoski et al., 2020). While Koske et al. (2020) and Kammann et al. (2024) found munition compounds in the bile of common dab (*Limanda limanda*, L.) living near dump sites in the North and Baltic Sea, Maser et al. (2023) and Maser et al. (in press) could even show that TNT and its metabolites occurred in the edible part (fillet) of fish (pouting: *Trisopterus luscus*) living at a wreck site in the Belgian North Sea, as well as in flounders (*Platichthys flesus*) caught in the German North Sea at the coast of Lower Saxony, respectively.

Overall, the comparison of the biomarker results of the present study with findings of former studies is difficult, since most existing knowledge is derived from laboratory studies, where higher concentrations of explosives were used or different chemicals like CWAs were applied. For instance, in comparison with Schuster et al. (2021), there is a difference in exposure

concentration of ng/L detected in the present study whereas Schuster et al. (2021) used mg/L in the laboratory experiment with mussels. Even though they used much higher explosive concentration, not all biomarkers were significantly increased during exposure to higher TNT concentration. The same is true for fish. Studies referring to the enzyme activity as a response to higher TNT exposure concentrations used much higher concentrations of explosives than the present study (Della Torre et al., 2008; Ek et al., 2005).

Another problem regarding the assessment of the biomarker results is the fact that also traces of dissolved TNT were found at the reference site. Concentrations measured in the passive sampler from the reference site are lower than those from two wreck stations (A361 & A362) but comparable to the values measured at A360. As the area has been cleared of lost explosives before the construction phase of the windmill farm, we had assumed that no TNT would be present at this site. At a true reference area, however, the background concentrations of the target chemical used as exposure agent should of course be zero or close to zero. In our study, the tested biomarkers have probably also responded to the TNT traces at the reference site levelling the expected responses between exposure and reference sites. Future studies should put more effort in pre-investigations of the planned reference area, to make sure that the area is free of dissolved explosives.

In addition, there is increasing evidence of sublethal and chronic effects of marine organisms when exposed to munition compounds, especially for immobile organisms living in or on the sediment (Juhasz and Naidu, 2007; Lotufo et al., 2013; Talmage et al., 1999). Those chronic effects can manifest in various forms, including reduced growth and reproduction, impaired development, and damage to the nervous, immune and blood systems (Gong et al., 2007). However, such investigations would need extended exposure times. Alternatively, histological investigations of organs, such as the liver of long-living non-migrating fish could help to assess chronic effects of low concentrated chemicals, such as dissolved explosives.

5 Conclusion

Results of the present study proved the leakage of energetic chemicals at the wrecks of *HMS Basilisk* and the *V1302/John Mahn*, as well as the uptake of those compounds by investigated mussels and fish. In mussels, the leakage of explosives is correlated with membrane impairments of cell organelles and signs of oxidative stress. However, in fish no correlation between uptake of explosives and biomarker response could be detected. If responses of a biomarker occurred, they were restricted to the sub-cellular and cellular levels. No effects on the individual level were visible. However, as corrosion of munition shells and the leakage of explosives proceeds, the situation may worsen, since more TNT will get dissolved. Therefore, further monitoring is recommended.

Data availability statement

The datasets presented in this study can be found in online repositories. The names of the repository/repositories and accession number(s) can be found below: Binder et al., 2023; <https://doi.org/10.1594/PANGAEA.962697>.

Ethics statement

The animal study was approved by Prof. Dr. Thomas Brey, E-Mail: Thomas.Brey@awi.de, Phone: +49 471 48 31 1300. The study was conducted in accordance with the local legislation and institutional requirements.

Author contributions

FB: Formal Analysis, Investigation, Methodology, Validation, Visualization, Writing – original draft. LB: Formal Analysis, Investigation, Methodology, Validation, Writing – original draft. JS: Formal Analysis, Investigation, Methodology, Writing – original draft. SV: Conceptualization, Investigation, Methodology, Writing – original draft. MD: Conceptualization, Investigation, Methodology, Writing – original draft. EM: Funding acquisition, Resources, Supervision, Writing – original draft. MB: Funding acquisition, Investigation, Methodology, Project administration, Supervision, Writing – review & editing.

Funding

The author(s) declare that financial support was received for the research and/or publication of this article. The research was co-funded by the European Union (European Regional Development Fund) under the North Sea Interreg Programme 2014-2020. Research was conducted, within the framework of the project “North Sea Wrecks -An Opportunity for Blue Growth: Healthy Environment, Shipping, Energy Production and -transmission (NSW). Publication costs were financed by the Alfred Wegener Institute’s Open Access Fund.

Acknowledgments

We would like to thank the captain and the crew of the RV Simon Stevin for all the support during the two expeditions for the North Sea Wrecks project. In addition, we would like to thank the scientific divers from VLIIZ, Oostende, for their support in placing and recovering the mussels at the wreck sites. Last but not least we thank the reviewers for their valuable comments, which helped to improve the present publication.

Conflict of interest

The authors declare that the research was conducted in the absence of any commercial or financial relationships that could be construed as a potential conflict of interest.

Publisher's note

All claims expressed in this article are solely those of the authors and do not necessarily represent those of their affiliated

organizations, or those of the publisher, the editors and the reviewers. Any product that may be evaluated in this article, or claim that may be made by its manufacturer, is not guaranteed or endorsed by the publisher.

Supplementary material

The Supplementary Material for this article can be found online at: <https://www.frontiersin.org/articles/10.3389/fmars.2025.1456409/full#supplementary-material>

References

- Adomako-Bonsu, A. G., Jacobsen, J., and Maser, E. (2024). Metabolic activation of 2,4,6-trinitrotoluene; a case for ROS-induced cell damage. *Redox Biol.* 72, 103082. doi: 10.1016/j.redox.2024.103082
- Ahvo, A. (2020a). DAIMON 2 PROJECT SOPs: Homogenisation of fish liver and mussel digestive gland tissues. version 1.1. (SYKE) (Finland: F. E. I. Helsinki).
- Ahvo, A. (2020b). DAIMON 2 PROJECT SOPs: Catalase activity. version 1.1. (SYKE) (Helsinki: F. E. I. Finland).
- Ahvo, A. (2020c). DAIMON 2 PROJECT SOPs: Glutathione-S-transferase activity. version 1.1. (SYKE) (Helsinki: F. E. I. Finland).
- Ahvo, A. (2020d). DAIMON 2 PROJECT SOPs: Acetylcholinesterase. version 1.1. (SYKE) (Helsinki: F. E. I. Finland).
- Appel, D., Beck, A. J., Eggert, A., Gräwe, U., Kampmeier, M., Martin, H.-J., et al. (2019). *Practical Guide for Environmental Monitoring of Conventional Munitions in the Seas - Results from the BMBF funded project UDEMM "Umweltmonitoring für die Delaboration von Munition im Meer" Version 1.1.* Ed. J. Greinert (Kiel, Germany: GEOMAR Helmholtz-Zentrum für Ozeanforschung).
- Appel, D., Strehse, J. S., Martin, H. J., and Maser, E. (2018). Bioaccumulation of 2,4,6-trinitrotoluene (TNT) and its metabolites leaking from corroded munition in transplanted blue mussels (*M. edulis*). *Mar. pollut. Bull.* 135, 1072–1078. doi: 10.1016/j.marpolbul.2018.08.028
- Ballentine, M., Tobias, C., Vlahos, P., Smith, R., and Cooper, C. (2015). Bioconcentration of TNT and RDX in coastal marine biota. *Arch. Environ. Contamination Toxicol.* 68, 718–728. doi: 10.1007/s00244-014-0104-9
- Beck, A. J., Gledhill, M., Kampmeier, M., Feng, C., Schlosser, C., Greinert, J., et al. (2022). Explosives compounds from sea-dumped relic munitions accumulate in marine biota. *Sci. Total Environ.* 806, 151266. doi: 10.1016/j.scitotenv.2021.151266
- Beck, A. J., Gledhill, M., Schlosser, C., Stamer, B., Böttcher, C., Sternheim, J., et al. (2018). Spread, behavior, and ecosystem consequences of conventional munitions compounds in coastal marine waters. *Front. Mar. Sci.* 5, doi: 10.3389/fmars.2018.00141
- Beck, A. J., van der Lee, E. M., Eggert, A., Stamer, B., Gledhill, M., Schlosser, C., et al. (2019). *In situ* measurements of explosive compound dissolution fluxes from exposed munition material in the Baltic Sea. *Environ. Sci. Technol.* 53, 5652–5660. doi: 10.1021/acs.est.8b06974
- Beddington, J., and Kinloch, A. J. (2005). *Munitions dumped at sea: A literature review* (London: Imperial College London Consultants).
- Beldowski, J., Potrykus, J., Szubska, M., Klusek, Z., Anu, L., Lehtonen, K. K., et al. (2014). *CHEMSEA Findings: Results from the CHEMSEA project - Chemical munitions search and assessment* (Sopot, Poland: Institute of Oceanology of the Polish Academy of Sciences).
- Bellamy, C. (1991). The military uses of the North Sea. *Ocean Shoreline Manag.* 16 (3–4), 275–289. doi: 10.1016/0951-8312(91)90008-P
- Belwind (2017). Belwind - Wind farm in the North Sea Press Information. Available online at: https://arquivo.pt/wayback/20160118141207/http://www.belwind.eu/files/604739_belwind%20persdossier_ENG.pdf (Accessed May 25, 2021).
- Beyer, J., Green, N. W., Brooks, S., Allan, I. J., Ruus, A., Gome, T., et al. (2017). Blue mussels (*Mytilus edulis* spp.) as sentinel organisms in coastal pollution monitoring: A review. *Mar. Environ. Res.* 130, 338–365. doi: 10.1016/j.marenvres.2017.07.024
- Binder, F. I., Marx, U., De Rijcke, M., Van Haelst, S., and Brenner, M. (2023). *Enzyme activity and histochemical biomarkers of mussels and fish caught at two shipwrecks at the Belgian coast* (PANGAEA). doi: 10.1594/PANGAEA.962697
- Bocquené, G., and Galgani, F. (1998). *Biological Effects of Contaminants: Cholinesterase Inhibition by Organophosphate and Carbamate Compounds* Vol. 22 (Denmark: Copenhagen International Council for the Exploration of the Sea Copenhagen).
- BOP The Belwind offshore wind project. Available online at: <https://www.belgianoffshoreplatform.be/en/projects/belwind/> (Accessed May 25 2021).
- Böttcher, C., Knobloch, T., Rühl, N.-P., Sternheim, J., Wichert, U., and Wöhler, J. (2011). *Munitionsbelastung der deutschen Meeresgewässer - Bestandsaufnahme und Empfehlungen (Stand 2011)* (Hamburg: Bundesamt für Seeschifffahrt und Hydrographie).
- Bradford, M. M. (1976). A rapid and sensitive method for the quantitation of microgram quantities of protein utilizing the principle of protein-dye binding. *Analytical Biochem.* 72, 248–254. doi: 10.1016/0003-2697(76)90527-3
- Brenner, M., Broeg, K., Frickenhaus, S., Buck, B. H., and Koehler, A. (2014). Multi-biomarker approach using the blue mussel (*Mytilus edulis* L.) to assess the quality of marine environments: season and habitat-related impacts. *Mar. Environ. Res.* 95, 13–27. doi: 10.1016/j.marenvres.2013.12.009
- Bünning, T. H., Strehse, J. S., Hollmann, A. C., Böttcher, T., and Maser, E. (2021). A toolbox for the determination of nitroaromatic explosives in marine water, sediment, and biota samples on femtogram levels by GC-MS/MS. *Toxics* 9. doi: 10.3390/toxics9030060
- Claiborne, A. (1985/2018). "Catalase activity," in *Handbook of methods for oxygen radical research*. Ed. R. A. Greenwald (CRC Press, Boca Raton), 283–284.
- Culling, C. F. A. (1974). *Handbook of Histopathological and Histochemical Techniques. 3rd ed* (Butterworth, London: Including Museum Techniques).
- de Andrade, V. M., da Silva, J., da Silva, F. R., Heuser, V. D., Dias, J. F., Yoneama, M. L., et al. (2003). Fish as bioindicators to assess the effects of pollution in two southern Brazilian rivers using the comet assay and micronucleus test. *Environ. Mol. Mutagenesis* 44, 459–468. doi: 10.1002/em.20070
- Della Torre, C., Corsi, I., Arukwe, A., Valoti, M., and Focardi, S. (2008). Interactions of 2,4,6-trinitrotoluene (TNT) with xenobiotic biotransformation system in European eel *Anguilla Anguilla* (Linnaeus 1758). *Ecotoxicology Environ. Saf.* 71, 798–805. doi: 10.1016/j.ecoenv.2008.03.003
- Deutsches Schifffahrtsmuseum *Toxic Legacies of War - North Sea Wrecks*. Available online at: <https://www.dsm.museum/ausstellung/ausstellungen/toxic-legacies-of-war-north-sea-wrecks> (Accessed August 27 2021).
- Ek, H., Dave, G., Nilsson, E., Sturve, J., and Birgersson, G. (2006). Fate and effects of 2,4,6-trinitrotoluene (TNT) from dumped ammunition in a field study with fish and invertebrates. *Arch. Environ. Contamination Toxicol.* 51, 244–252. doi: 10.1007/s00244-005-0117-5
- Ek, H., Dave, G., Sturve, J., Almroth, B. C., Stephensen, E., Forlin, L., et al. (2005). Tentative biomarkers for 2,4,6-trinitrotoluene (TNT) in fish (*Oncorhynchus mykiss*). *Aquat. Toxicol.* 72, 221–230. doi: 10.1016/j.aquatox.2005.01.001
- Ek, H., Nilsson, E., and Dave, G. (2008). Effects of TNT leakage from dumped ammunition on fish and invertebrates in static brackish water systems. *Ecotoxicology Environ. Saf.* 69, 104–111. doi: 10.1016/j.ecoenv.2006.12.016
- Farrington, J. W., and Quinn, J. G. (1973). Petroleum hydrocarbons in Narragansett Bay. 1. Survey of hydrocarbons in sediments and clams (*Mercenaria mercenaria*). *Estuar. Coast. Mar. Sci.* 1, 71–79. doi: 10.1016/0302-3524(73)90059-5
- Gilbert, R. (2005). The global risk of marine pollution from WWII shipwrecks: examples from the seven seas. *Int. Oil Spill Conf. Proc.* 1, 1049–1054. doi: 10.7901/2169-3358-2005-1-1049
- Gong, P., Guan, X., Inouye, L. S., Pirooznia, M., Indest, K. J., Athow, R. S., et al. (2007). Toxicogenomic analysis provides new insights into molecular mechanisms of the sublethal toxicity of 2,4,6-trinitrotoluene in *Eisenia fetida*. *Environmental Sci. Technol.* 41, 8195–8202. doi: 10.1021/es0716352
- Grassel, P., Otte, F., and Bergmann, S. (2021). "Militärische Altlasten im Meer: ein gefährliches Erbe. Das Projekt North Sea Wrecks," in *Nachrichten des Marschenrates*,

vol. 58, (Wilhelmshaven, Germany: Marschenrat zur Förderung der Forschung im Küstengebiet der Nordsee e. V.), 13–17.

Gröner, E., Maass, J., and Maas, M. (1993). “Flußfahrzeuge, u-jäger, vorpostenboote, hilfminensucher, küstenschutzverbände (Teil 1),” in *Die deutschen Kriegsschiffe 1815–1945*, vol. 8/1. (Bernard & Graef Verlag, Bonn), 611.

Habig, W. H., Pabst, M. J., and Jakoby, W. B. (1974). Glutathione S-transferases. *J. Biol. Chem.* 249, 7130–7139. doi: 10.1016/s0021-9258(19)42083-8

HELCOM (2013). “Chemical munitions dumped in the Baltic Sea,” in *Report of the ad hoc Expert Group to Update and Review the Existing Information on Dumped Chemical Munitions in the Baltic Sea* Baltic Sea Environment Proceeding (BSEP) (Helsinki, Finland: Baltic Marine Environment Protection Commission (HELCOM) HELCOM), vol. 142, 128.

Höher, N., Turja, R., Brenner, M., Nyholm, J. R., Ostin, A., Leffler, P., et al. (2019). Toxic effects of chemical warfare agent mixtures on the mussel *Mytilus trossulus* in the Baltic Sea: A laboratory exposure study. *Mar. Environ. Res.* 145, 112–122. doi: 10.1016/j.marenvres.2019.02.001

Juhasz, A. L., and Naidu, R. (2007). Explosives: Fate, dynamics, and ecological impact in terrestrial and marine environments. *Rev. Environ. Contamination Toxicol.* 191, 163–215. doi: 10.1007/978-0-387-69163-3_6

Kammann, U., Topker, V., Schmidt, N., Rodiger, M., Aust, M.-O., Gabel, M., et al. (2024). Explosives leaking from dumped munition contaminate fish from German coastal waters: a reason for chronic effects? *Environ. Sci. Europe* 36, 116. doi: 10.1186/s12302-024-00942-5

Koske, D., Straumer, K., Goldenstein, N. I., Hanel, R., Lang, T., and Kammann, U. (2020). First evidence of explosives and their degradation products in dab (*Limanda limanda* L.) from a munition dumpsite in the Baltic Sea. *Mar. pollut. Bull.* 155, 111131. doi: 10.1016/j.marpolbul.2020.111131

Krishnakumar, P. K., Casillas, E., and Varanasi, U. (1997). Cytochemical responses in the digestive tissue of *Mytilus edulis* complex exposed to microencapsulated PAHs or PCBs. *Part C Pharmacol. Toxicol. Endocrinol. Comp. Biochem. Physiol.* 118C, 11–18. doi: 10.1016/S0742-8413(97)00076-5

Kuklina, I., Kouba, A., and Kozák, P. (2013). Real-time monitoring of water quality using fish and crayfish as bio-indicators: a review. *Environ. Monit. Assess.* 185, 5043–5053. doi: 10.1007/s10661-012-2924-2

Lastumäki, A., Turja, R., Brenner, M., Vanninen, P., Niemikoski, H., Butrimavičienė, L., et al. (2020). Biological effects of dumped chemical weapons in the Baltic Sea: A multi-biomarker study using caged mussels at the Bornholm main dumping site. *Mar. Environ. Res.* 161, 105036. doi: 10.1016/j.marenvres.2020.105036

Letzens, J. (2002). V-1302 (John Mahr) [1942]. Available online at: <https://www.wrecksite.eu/wreck.aspx?20> (Accessed May 21 21).

Lillie, R. D., and Ashburn, L. L. (1943). Supersaturated solutions of fat stains in dilute isopropanol for demonstration of acute fatty degeneration not shown by Herxheimer's technique. *Arch. Pathol.* 36, 432–440.

Lionetto, M. G., Caricato, R., Calisi, A., and Schettino, T. (2011). “Acetylcholinesterase inhibition as a relevant biomarker in environmental biomonitoring: New insights and perspectives,” in *Ecotoxicology around the globe*. Ed. J. E. Visser (Nova Science Publisher Inc, New York, United States), 87–115.

Livingstone, D. R., and Pipe, R. K. (1992). “Mussels and environmental contaminants: molecular and cellular aspects,” in *The mussel Mytilus; ecology, physiology, genetics, and culture*. Ed. E. G. Gosling (Elsevier, Amsterdam), 425–464.

Lotufo, G. R., Lydy, M., Rorrer, G. L., Cruz-Urbe, O., and Cheney, D. P. (2009). “Bioconcentration, bioaccumulation, and biotransformation of explosives and related compounds in aquatic organisms,” in *Ecotoxicology of Explosives*. Eds. G. I. Sunahara, G. Lotufo, R. G. Kuperman and J. Hawari (CRC Press, Boca Raton, London, New York), 135–155.

G. R. Lotufo, G. Rosen, W. Wild and G. Carton (Eds.) (2013). *Summary Review of the Aquatic Toxicology of Munitions Constituents* (Vicksburg, Mississippi, USA: Environmental Laboratory, U.S. Army Engineer Research and Development Cente).

Lowe, D. M. (1988). Alterations in cellular structure of *Mytilus edulis* resulting from exposure to environmental contaminants under field and experimental conditions. *Mar. Ecol. - Prog. Ser.* 46, 91–100. doi: 10.3354/meps046091

Maes, F., Schrijvers, J., Van Lancker, V., Verfaillie, E., Degraer, S., Deros, S., et al. (2005). “Towards a spatial structure plan for sustainable management of the sea,” in *Research in the framework of the BSP programme “Sustainable Management of the Sea” – PODO II* (Brussels, Belgium: Belgian Science Policy (BELSPO)), 539.

Mallefet, J., Zintzen, V., Massin, C., Norro, A., Vincx, M., De Maerschalck, V., et al. (2007). *Belgian Shipwreck: Hotspots for Marine Biodiversity (BEWREMABI)* (Brüssel: Belgian Science Policy Office).

Maser, E., Bünning, T. H., Brenner, M., Van Haelst, S., De Rijcke, M., Müller, P., et al. (2023). Warship wrecks and their munition cargos as a threat to the marine environment and humans: The V 1302 “JOHN MAHR” from World War II. *Sci. Total Environ.* 857, 159324. doi: 10.1016/j.scitotenv.2022.159324

Maser, E., Bünning, T. H., and Strehse, J. S. (2024). How contaminated is flatfish living near World Wars’ munition dumping sites with energetic compounds. *Arch. Toxicol.* 98, 3825–3836. doi: 10.1007/s00204-024-03834-y

Maser, E., and Strehse, J. S. (2021). Can seafood from marine sites of dumped World War relics be eaten? *Arch. Toxicol.* 95, 2255–2261. doi: 10.1007/s00204-021-03045-9

Mathys, M. (2009). *The Quaternary geological evolution of the Belgian Continental Shelf, southern North Sea* (Gent, Belgium: (PhD thesis), University Gent).

Monfils, R., Gilbert, T., and Nawadra, S. (2006). Sunken WWII shipwrecks of the Pacific and East Asia: the need for regional collaboration to address the potential marine pollution threat. *Ocean Coast. Manage.* 49, 779–788. doi: 10.1016/j.ocecoaman.2006.06.011

Moore, M. N., Lowe, D., and Köhler, A. (2004). “Biological effects of contaminants: Measurement of lysosomal membrane stability,” in *ICES Techniques in Marine Environmental Sciences (TIMES)* Copenhagen: ICES, vol. 36. (ICES, Copenhagen), 31.

Mredul, M. M. H., Sokolov, E. P., Kong, H., and Sokolova, I. M. (2024). Spawning acts as a metabolic stressor enhanced by hypoxia and independent of sex in a broadcast marine spawner. *Sci. Total Environ.* 909, 168419. doi: 10.1016/j.scitotenv.2023.168419

Niemikoski, H., Straumer, K., Ahvo, A., Turja, R., Brenner, M., Rautanen, T., et al. (2020). Detection of chemical warfare agent related phenylarsenic compounds and multibiomarker responses in cod (*Gadus morhua*) from munition dumpsites. *Mar. Environ. Res.* 162, 105160. doi: 10.1016/j.marenvres.2020.105160

Nipper, M., Carr, R. S., Biedenbach, J. M., Hooten, R. L., Miller, K., and Saepoff, S. (2001). Development of marine toxicity data for ordnance compounds. *Arch. Environ. Contamination Toxicol.* 41, 308–318. doi: 10.1007/s002440010253

Nipper, M., Carr, R. S., and Lotufo, G. R. (2009). “Aquatic toxicology of explosives,” in *Ecotoxicology of Explosives*. Eds. G. I. Sunahara, G. Lotufo, R. G. Kuperman and J. Hawari (CRC Press, Boca Raton, London, New York), 77–115.

Patterson, M. A., Parker, B. C., and Neves, R. J. (1999). Glycogen concentration in the mantle tissue of freshwater mussels (*Bivalvia: Unionidae*) during starvation and controlled feeding. *Am. Malacological Bull.* 15, 47–50.

Pearse, A. G. E. (1985). “Histochemistry: theoretical and applied,” in *Analytical Technology, 4th ed*, vol. 2. (Churchill, Livingstone, Edinburgh, London, Melbourne and New York).

Regoli, F. (2000). Total oxyradical scavenging capacity (TOSC) in polluted and translocated mussels: a predictive biomarker of oxidative stress. *Aquat. Toxicol.* 50, 351–361. doi: 10.1016/S0166-445X(00)00091-6

Regoli, F., and Principato, G. (1995). Glutathione, glutathione-dependent and antioxidant enzymes in mussel, *Mytilus galloprovincialis*, exposed to metals under field and laboratory conditions: implications for the use of biochemical biomarkers. *Aquat. Toxicol.* 31, 143–164. doi: 10.1016/0166-445X(94)00064-W

Rosen, G., and Lotufo, G. R. (2007a). Toxicity of explosive compounds to the marine mussel, *Mytilus galloprovincialis*, in aqueous exposures. *Ecotoxicology Environ. Saf.* 68, 228–236. doi: 10.1016/j.ecoenv.2007.03.006

Rosen, G., and Lotufo, G. R. (2007b). Bioaccumulation of explosive compounds in the marine mussel, *Mytilus galloprovincialis*. *Ecotoxicology Environ. Saf.* 68, 237–245. doi: 10.1016/j.ecoenv.2007.04.009

Schuster, R., Strehse, J. S., Ahvo, A., Turja, R., Maser, E., Bickmeyer, U., et al. (2021). Exposure to dissolved TNT causes multilevel biological effects in Baltic mussels (*Mytilus* spp.). *Mar. Environ. Res.* 167, 105264. doi: 10.1016/j.marenvres.2021.105264

Sims, J. G., and Steevens, J. A. (2008). The role of metabolism in the toxicity of 2,4,6-trinitrotoluene and its degradation products to the aquatic amphipod *Hyalella azteca*. *Ecotoxicology Environ. Saf.* 70, 38–46. doi: 10.1016/j.ecoenv.2007.08.019

Sprung, M. (1983). Reproduction and fecundity of the mussel *Mytilus edulis* at Helgoland (North Sea). *Helgoländer Meeresuntersuchungen* 36, 243–255. doi: 10.1007/BF01983629

Strehse, J. S., Appel, D., Geist, C., Martin, H. J., and Maser, E. (2017). Biomonitoring of 2,4,6-trinitrotoluene and degradation products in the marine environment with transplanted blue mussels (*M. edulis*). *Toxicology* 390, 117–123. doi: 10.1016/j.tox.2017.09.004

Strehse, J. S., and Maser, E. (2020). Marine bivalves as bioindicators for environmental pollutants with focus on dumped munitions in the sea: A review. *Mar. Environ. Res.* 158, 105006. doi: 10.1016/j.marenvres.2020.105006

Sündermann, J., and Pohlmann, T. (2011). A brief analysis of North Sea physics. *Oceanologia* 53, 663–689. doi: 10.5697/oc.53.3.663

Talmage, S. S., Opresko, D. M., Maxwell, C. J., Welsh, C. J., Cretella, F. M., Reno, P. H., et al. (1999). Nitroaromatic munition compounds: environmental effects and screening values. *Rev. Environ. Contamination Toxicol.* 161, 1–156. doi: 10.1007/978-1-4757-6427-7_1

Van Landuyt, J., Kundu, K., Van Haelst, S., Neyts, M., Parmentier, K., De Rijcke, M., et al. (2022). 80 years later: Marine sediments still influenced by an old war ship. *Front. Mar. Sci.* 9, 1017136. doi: 10.3389/fmars.2022.1017136

Vedenin, A., Kröncke, I., and Greinert, J. (2023). *Impact of munition dumpsites on the benthic macrofauna in the western Baltic Sea* (Vienna, Austria: Paper presented at the EGU General Assembly 2023).

Viarengo, A., Lowe, D., Bolognesi, C., Fabbri, E., and Koehler, A. (2007). The use of biomarkers in biomonitoring: a 2-tier approach assessing the level of pollutant-induced stress syndrome in sentinel organisms. *Comp. Biochem. Physiology Part C* 146, 281–300. doi: 10.1016/j.cbpc.2007.04.011

Wellington, D. R., and Mitchell, W. R. (1991). *In vitro* cytotoxicity of certain munition nitroaromatic compounds. *Chemosphere* 23, 363–373. doi: 10.1016/0045-6535(91)90190-O

Wexler, P. (2014). *Encyclopedia of toxicology*, 3 ed Vol. 1 (San Diego, USA: Academic Press).

Zintzen, V., Massin, C., Norro, A., and Mallefet, J. (2006). Epifaunal inventory of two shipwrecks from the Belgian Continental Shelf. *Hydrobiologia* 555, 207–219. doi: 10.1007/s10750-005-1117-1

Frontiers in Marine Science

Explores ocean-based solutions for emerging global challenges

The third most-cited marine and freshwater biology journal, advancing our understanding of marine systems and addressing global challenges including overfishing, pollution, and climate change.

Discover the latest Research Topics

[See more →](#)

Frontiers

Avenue du Tribunal-Fédéral 34
1005 Lausanne, Switzerland
frontiersin.org

Contact us

+41 (0)21 510 17 00
frontiersin.org/about/contact

